Doctoral Programme in Neuroscience

Instituto de Neurociencias

Neuroimmune interactions in the cornea: effects of resident dendritic cell depletion on cold nerve terminal activity, basal tearing, and pain

Laura Frutos Rincón

Thesis director

Dr. Juana Gallar Martínez

Thesis co-director

Dr. Mª del Carmen Acosta Boj

Universidad Miguel Hernández de Elche

- 2022 -

INSTITUTO DE NEUROCIENCIAS

The Doctoral Thesis entitled "Neuroimmune interactions in the cornea: effects of resident dendritic cell depletion on cold nerve terminal activity, basal tearing, and pain" is presented as a compendium of the following publications:

- **Frutos-Rincón L**, Gómez-Sánchez JA, Íñigo-Portugués A, Acosta MC, Gallar J. An Experimental Model of Neuro-Immune Interactions in the Eye: Corneal Sensory Nerves and Resident Dendritic Cells. Int J Mol Sci. 2022 Mar 10; 23(6):2997. doi: 10.3390/ijms23062997.

  International Journal of Molecular Sciences, IF 2021: 6.208; (Q1, Biochemistry & Molecular Biology).

INSTITUTO DE NEUROCIENCIAS

INSTITUTO DE NEUROCIENCIAS

Dr. Juana Gallar Martínez, Director, and Dr. Ma del Carmen Acosta Boj, co-director of the doctoral thesis entitled "Neuroimmune interactions in the cornea: effects of resident dendritic cell depletion on cold nerve terminal activity, basal tearing, and pain",

INFORM

That Mrs. Laura Frutos Rincón has carried out, under our supervision, the above-mentioned work accomplishing the terms and conditions defined in her PhD Research Plan, and agreeing with the Code of Good Practice in Research of the Universidad Miguel Hernández de Elche, satisfactorily fulfilling the requirements for its public defense as a doctoral thesis.

Signed in Sant Joan d'Alacant on the date indicated below.

Thesis director   Thesis co-director

Dr. Juana Gallar Martínez   Dr. Mª del Carmen Acosta Boj

Dr. Elvira Mª de la Peña García, Coordinator of the Neuroscience PhD programme at the Institute of Neuroscience, a joint centre of the Miguel Hernández University (UMH) and the Spanish National Research Council (CSIC),

INFORMS:

That Mrs Laura Frutos Rincón has carried out under the supervision of our PhD Programme the work entitled "Neuroimmune interactions in the cornea: effects of resident dendritic cell depletion on cold nerve terminal activity, basal tearing, and pain" in accordance with the terms and conditions defined in its Research Plan and in accordance with the Code of Good Practice of the University Miguel Hernández de Elche, fulfilling the objectives satisfactorily for its public defence as a doctoral thesis.

Which I sign for the appropriate purposes, in Sant Joan d'Alacant on July, 2022

Dr. Elvira Mª de la Peña García

Coordinator of the PhD Programme in Neuroscience

Av Ramón y Cajal s/n

elvirap@umh.es   Tel: +34 965 919533   SANT JOAN CAMPUS

                        Fax: +34 965 919549   550 SANT JOAN D'ALACANT- SPAIN

INDEX

LIST OF ABBREVIATIONS

APC: antigen presenting cell

BATF3: basic-leucine zipper ATF-like

BDCA: blood dendritic cell antigen

CADM1: cell adhesion molecule 1

CCL: C-C motif chemokine ligand

CD: cluster of differentiation

cDC: conventional dendritic cell

CDP: common dendritic cell precursor

CGRP: calcitonin gene-related peptide

CLEC9A: C-type lectin domain containing 9A

CNTF: ciliary neurotrophic factor

DAPI: 4',6-diamidino-2-phenylindole, dihydrochloride

DC: dendritic cell

DED: dry eye disease

dLN: draining lymph nodes

DT: diphtheria toxin

DTR: diphtheria toxin receptor

ECM: extracellular matrix

ENT: epithelial nerve terminals

EPCAM: epithelial cell adhesion molecule

FasL: FasLigand

GFP: green fluorescent protein

GM-CSF: granulocyte-macrophage colony-stimulating factor

HB-LT: High background-low threshold cold thermoreceptor

HSC: hematopoietic stem cell

HSV: herpes simplex virus

ID2: inhibitor of DNA binding 2

IFN: interferon

IL: interleukin

IRF: interferon regulatory factor

IVCM: in vivo confocal microscopy

LB-HT: low background-high threshold cold thermoreceptor

LC: Langerhans cell

LNP: limbal nerve plexus

LP: lymphoid precursor

LTDT: long-term DT injections

LTPBS: long-term PBS injections

MC: monocyte-derived dendritic cell

MDP: monocyte and dendritic cell precursor

MHC-II: major histocompatibility complex II

MMP: matrix metalloproteases

MP: myeloid precursor

MTC: mixed-type cold thermoreceptor

MUC: mucin

NFIL3: nuclear factor IL-3 regulated

NK: natural killer cell

NTI: nerve terminal impulse

PBS: phosphate-buffered saline

pDC: plasmacytoid dendritic cell

PDL-1: programmed death ligand-1

RC: recovery of DCs

SEP: subepithelial plexus

SIRPa: signal-regulatory protein alpha

SN: stromal nerve trunks

SS: Sjögren's syndrome

STDT: short-term DT injections

STPBS: short-term PBS injections

TA: Transient amplifying cells

TF: transcription factor

TG: trigeminal ganglion

Th: helper T cell

TLR: toll-like receptor

Tregs: regulatory T cells

TRPM8: Transient receptor potential channel subfamily M (melastatin) member 8

VIP: vasoactive intestinal polypeptide

XCR1: chemokine receptor for XCL1

LIST OF FIGURES

ABSTRACT

The cornea is an avascular connective tissue that is crucial, not only as the primary barrier of the eye, but also as a proper transparent refractive structure. The avascular, immune-privileged tissue of the cornea is an ideal model to study the interactions between its well-characterised and dense sensory nerves (easily accessible for both focal electrophysiological recording and morphological studies) and its low number of resident immune cell types, distinguished from those cells migrating from blood vessels. The various functions of resident immune cells have been assessed in corneal pathological conditions and diseases, however, their contribution to the maintenance of homeostasis remains elusive.

The objective of the present Thesis was to determine the functional interaction between corneal dendritic cells (DCs) and corneal sensory nerves at basal conditions (that is, in absence of any corneal inflammation or damage) and its possible consequences in protective processes of the ocular surface such as tearing or nociceptive behaviour.

For this purpose, short-term and long-term resident DC depletion was induced in the cornea of CD11c-DTR+ transgenic mice (5 month s, both sexes) by diphtheria toxin (DT) subconjunctival injections to determine the effects of the corneal DC absence on corneal cold sensory nerve activity, basal tearing and pain. Sensory nerve activity was studied by *ex vivo* electrophysiological recordings; basal tearing rate was measured with commercial phenol red threads and spontaneous pain behaviour was monitored by measuring the eye closure ratio. Finally, to assess corneal DC morphology and distribution in the cornea, we used endogenous fluorescence whole-mount corneas.

Local DC depletion altered cold thermoreceptors nerve terminal impulse (NTI) activity in response to temperature changes: while short-term DC depletion sensitised cold thermoreceptors, especially in their response to heat, long-term DC depletion desensitised cold thermoreceptors in their response to cold and had an impact in NTI shape. Moreover, the absence of DCs produced pain in both short-term and long-term depletion conditions, although this pain was higher in acute conditions in which, in addition, the basal tearing rate was significantly reduced to almost half.

Corneal DC repopulation produced almost a full recovery of naïve cold thermoreceptor's NTI activity and shape, although we still observed signs of spontaneous pain.

Finally, when we analysed the effect of the subconjunctival injection itself by using PBS instead of DT, we observed an increase in cooling responses and some changes in NTI shape, suggesting a mild lesion due to the injection procedure. However, these changes were the opposite than those observed under DC depletion conditions and basal tearing and pain behaviour were unaffected in these animals.

In conclusion, our experimental data show that there is a functional interplay between DCs and nerves at basal conditions and this suggests a crucial role of DC in corneal nerve activity and in ocular surface homeostasis maintenance.

RESUMEN

La córnea es un tejido conectivo avascular que resulta crucial, no sólo como barrera primaria del ojo, sino también como transparente estructura refractiva. Este tejido avascular y con privilegio inmune resulta un modelo ideal para estudiar las interacciones que se producen entre sus densos nervios sensoriales (fácilmente accesibles tanto para su registro electrofisiológico focal como para su estudio morfológico) y sus pocos tipos de tipos de células inmunes residentes, que se distinguen de las que migran desde los vasos sanguíneos circundantes. Las diferentes funciones de las células inmunes residentes en la córnea se han evaluado en condiciones de enfermedad y patología corneales, sin embargo, su contribución al mantenimiento de la homeostasis sigue por determinar.

El objetivo de la presente Tesis fue demostrar la posible interacción funcional entre las células dendríticas (CD) y los nervios sensoriales de la córnea en condiciones basales (es decir, en ausencia de cualquier inflamación o daño) y sus posibles consecuencias en los procesos protectores de la superficie ocular, como son el lagrimeo o el comportamiento nociceptivo.

Para ello, se indujo una depleción de las CD residentes a corto y largo plazo en la córnea de ratones transgénicos CD11c-DTR+ (5 meses, ambos sexos) mediante inyecciones subconjuntivales de toxina diftérica (TD) para determinar los efectos de la ausencia de las CD en la actividad de los nervios sensoriales de frío corneales, el lagrimeo basal y el dolor. La actividad de los nervios sensoriales se estudió mediante registros electrofisiológicos *ex vivo*; la tasa de lagrimeo basal se midió con hilos comerciales de rojo de fenol y el dolor espontáneo se monitorizó midiendo la ratio de cierre del ojo. Por último, para evaluar la morfología y la distribución de las CD en la córnea, se llevaron a cabo montajes de córnea completa en las que se observaba la fluorescencia endógena de las células.

La depleción local de las CD alteró la actividad de los impulsos nerviosos de las terminaciones (INT) de los termorreceptores de frío en respuesta a los cambios de temperatura: mientras que la depleción de las CD a corto plazo producía una sensibilización de los termorreceptores de frío, especialmente en su respuesta al calor, la depleción de CD a largo plazo producía una desensibilización de los termorreceptores de frío en su respuesta al frío y tuvo un impacto en la forma del INT. Además, la ausencia

de las CD produjo dolor tanto a corto como a largo plazo, siendo este dolor mayor en condiciones agudas en las que, además, la tasa de lagrimeo basal se redujo significativamente hasta casi la mitad.

La repoblación de las CD en la córnea produjo una recuperación casi total de la actividad y la forma de los INT de los termorreceptores de frío en condiciones naif, aunque todavía se observaron signos de dolor espontáneo.

Por último, cuando analizamos el efecto de la propia inyección subconjuntival utilizando solución salina tamponada con fosfato en lugar de TD, observamos un aumento de las respuestas al frío y algunos cambios en la forma del INT, lo que sugiere una lesión leve debida al procedimiento de inyección. Sin embargo, estos cambios fueron opuestos a los observados en condiciones de depleción de las CD y ni la tasa de lagrimeo basal ni el dolor se vieron afectados en estos animales.

En conclusión, nuestros datos experimentales demuestran que existe una interacción funcional entre las CD residentes y los nervios sensoriales corneales en condiciones basales. Esto sugiere un papel crucial de las CD en la actividad de los nervios corneales y en el mantenimiento de la homeostasis de la superficie ocular.

I.INTRODUCTION

1-The cornea

The cornea and the conjunctiva constitute the eye tissues exposed to the environment. The cornea is an avascular connective tissue that is crucial, not only as the primary barrier of the eye, but also as a powerful refractive structure. As a barrier, the cornea provides structural integrity to the ocular globe and protects its inner components from infectious agents and physical injury or chemical insults. On the other hand, as a refractive structure, it has two key properties: refractive power (for light refraction) and transparency (for light transmission) (Dawson, Ubels and Edelhauser, 2011).

The shape of the human cornea is prolate, which creates an aspheric optical system (DelMonte and Kim, 2011). The human cornea has a refractive index of 1.376 and a dioptric power higher than 40 dioptres, about 2/3 of the total ocular power (Saude, 1993). It is 540-700 μm thick, being thinner in the centre and thicker in the periphery (Dawson, Ubels and Edelhauser, 2011). The human cornea measures about 11 mm vertically and 12 mm horizontally (Rüfer et al., 2005) covering the anterior 1/6th of the ocular surface and is organised into 5 layers (**Figure 1**): epithelium, Bowman's layer, stroma, Descemet's membrane, and endothelium. Among species, the cornea keeps the same general structure, with differences in thickness and presence or absence of Bowman's layer.

Transparency of all ocular structures is crucial for vision. Transparency of the cornea is the result of many factors including its highly organised anatomical structure, the physiology of its cellular components, the lack of myelination of nerves inside the cornea, its tightly controlled (de)hydration state and the absence of blood and lymphatic vessels, among others. Since vision plays a critical role in obtaining information from the external environment, the cornea also has specific characteristics that ensure its own protection against injury. One of the most important features in this regard is the high sensitivity of the cornea to external insults provided by its extremely rich sensory innervation.

Taking all the corneal characteristics into account, it is clear that the cornea is an ideal model for studying the interactions between corneal nerves and the few cell types

present in this quite simple structure. Particularly, the cornea represents a perfect scenario to study neuro-immune interactions because of different reasons: the cornea is densely innervated (Müller et al., 2003; Belmonte and Gallar, 2011) with sensory nerves easily accessible for electrophysiological recordings whose functional properties have been described in detail (Belmonte et al., 2004b; González-González et al., 2017); the cornea is fully transparent (Maurice, 1957; Hassell and Birk, 2010), which means that fluorescence data could be gathered at high resolution for both *in vivo* and *ex vivo* experiments, and finally, the cornea is avascular (Ambati et al., 2006; Cursiefen et al., 2006), which allows distinguishing the contribution of resident immune cells from that of immune cells migrating from blood vessels.
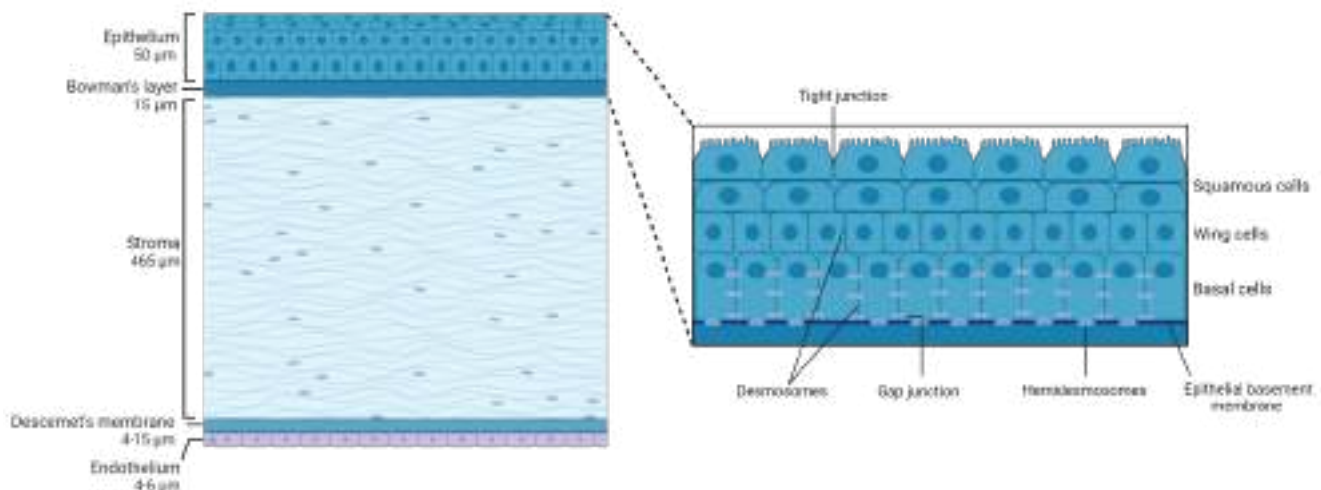
Figure 1. Schematic representation of the corneal structure, showing its five main layers and their thickness. Inset: diagram of the corneal epithelium, showing its different cell layers and details on the different types of cell-cell junctions contributing to corneal epithelium impermeability.

1.1 Corneal structure

1.1.1 Epithelium

The corneal epithelium, composed by a single layer of basal cells and several stratified and non-keratinized cell layers (**Figure 1, inset**), constitutes the first protective

ocular barrier against external threats. In humans, it is 50µm thick, representing around 8% of the total thickness of the cornea (Almubrad and Akhtar, 2011).

The outermost corneal epithelium is constituted by 2-3 layers of squamous cells (DelMonte and Kim, 2011) (**Figure 1, inset**). These cells are flat and polygonal and have apical microvilli which in turn are covered by a fine glycocalyx consisting of membrane-associated mucins including MUC1, MUC4, and MUC16 (Argüeso and Gipson, 2001). These squamous cells maintain tight junctions with their neighbours, which is essential for their function as a barrier to prevent large molecules or microbes from entering the deeper corneal layers. Beneath the superficial layers of squamous cells are the mid-epithelial layers of wing cells (**Figure 1, inset**). Wing cells are less flattened but have tight lateral junctions with their neighbours very similar to those observed in the squamous cells (DelMonte and Kim, 2011). Finally, basal cells constitute the deepest cell layer of the corneal epithelium (**Figure 1, inset**). This layer around 20 µm thick is constituted by a single layer of columnar epithelial cells that are connected through gap junctions and desmosomes and are attached to the underlying basement membrane by hemidesmosomes, preventing epithelium from separating from the other corneal layers (DelMonte and Kim, 2011).

In mice, the epithelium contributes approximately 30% to the total corneal thickness. The stratified layout of the murine corneal epithelium is consistent with the description of this epithelium in the mammalian cornea. However, the mouse corneal epithelium consists of approximately twice the layers of cells compared with the human epithelium, with a higher number of squamous cells (Henriksson et al., 2009).

Corneal epithelial cell layers turn over every 7-10 days (Hanna et al., 1961) following a delicate balance between superficial cell shedding and cell proliferation and migration from basal cells. Basal progenitor epithelial cells from the limbus (limbal stem cells) migrate towards the centre of the cornea where they differentiate into transient amplifying cells (TA). TA basal cells, which are two horizontal progenies from the stem cells, migrate from the limbus to the periphery of the cornea to reach the centre and undergo mixed proliferation (one daughter cell is retained in the basal cell layer and the other moves into the middle layers of the epithelium). Once TA cells reach the end of their proliferative capacity, they become basal epithelial cells. Basal epithelial cells undergo vertical proliferation in two daughter cells resulting in two wing cells and

eventually into two squamous cells that will be later shed by blinking **(Figure 2)**. This concept was coined the X, Y, Z hypothesis of Thoft and Friend (Thoft and Friend, 1983) where X is the basal corneal epithelial cell horizontal migration and vertical terminal proliferation, Y is the limbal cell proliferation and migration and Z is the squamous corneal epithelial cell shedding.
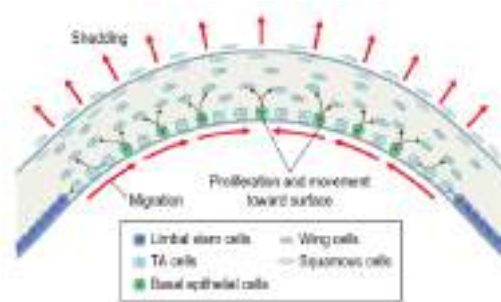
Figure 2. Corneal epithelial cell layers renewal diagram. Taken and modified from Adler's Physiology of the Eye, 11th edition, Elsevier.

Between corneal epithelium and the next corneal layer, the stroma, there is the epithelial basement membrane synthesised by epithelium basal cells. This membrane, also called basal lamina, is approximately 0.05 μm thick and comprises laminin, type IV collagen, heparan sulphate, and fibronectin. Basal lamina serves as a scaffold for epithelial cell movement and attachment, and it is composed by two distinct layers when observed by electron microscopy: the more external *lamina lucida* and a thicker more internal *lamina densa* (Dawson, Ubels and Edelhauser, 2011).

1.1.2 Bowman's layer

Bowman's layer in the human cornea is an acellular condensate of collagens type IV, V, VI and VII arranged randomly (Saude, 1993) **(Figure 3)** that helps the cornea to maintain its shape (DelMonte and Kim, 2011). This layer is approximately 15 μm thick and associated with the basal lamina of the epithelium and continues with the stroma.

It is worth mentioning that in mice, subepithelial collagen fibres are also arranged randomly forming what would be a thin Bowman's layer. However, some authors believe

that this is not a true layer (Hazlett, 1993; Rehbinder, 1978), but an adaptation of the stromal tissue (Henriksson et al., 2009).

Figure 3. Bowman's layer. Transmission electron micrograph (×72,500) of the acellular Bowman's membrane in cross-section (main photo) and tangential section (inset). Taken from Adler's Physiology of the Eye, 11th edition, Elsevier.

1.1.3 Stroma

Corneal stroma comprises 90% of the total corneal thickness (Dawson, Ubels and Edelhauser, 2011). It is mainly composed of water (78%), an organised structural network of types I and V collagen fibres (80% of corneal stroma's dry weight), keratocytes and extracellular matrix.

The stromal collagen fibres are arranged in parallel bundles (fibrils) that are packed in parallel arranged layers (lamellae) **(Figure 4)**. In turn, each of these layers is arranged at right angles relative to fibres in adjacent lamellae and this precise organisation results in stromal transparency as it reduces forward light scatter (Maurice, 1970).

Keratocytes, the major cell type of corneal stroma, are sandwiched between collagenous lamellae, mostly in the anterior stroma. These stellate-shaped cells are connected to each other through gap junctions present on their numerous dendritic processes (Watsky, 1995). Keratocytes are involved in maintaining the extracellular matrix environment and stromal composition as they are able to synthesise glycosaminoglycans, collagen molecules and matrix metalloproteases (MMPs) (DelMonte and Kim, 2011). As a first response to stromal injury, keratocytes are activated and migrate taking on a fibroblast-like appearance (Stramer et al., 2003) and within 1-2 weeks of the initial insult, myofibroblasts enter the injured area and become involved in

the stromal remodelling which can take months or even years to complete (DelMonte and Kim, 2011).

In mice, the corneal stroma accounts for two thirds of the total corneal thickness. In these animals, stromal collagen fibres have a diameter of 29±4 nm (Haustein, 1983) with keratocytes arranged parallel to the collagen bundles.

Figure 4. Corneal stroma. Transmission electron micrograph (×72,500) of the posterior third of the stroma in cross-section (main photomicrograph) and tangential section (inset). Taken from Adler's Physiology of the Eye, 11th edition, Elsevier.

1.1.4 Descemet's membrane

Descemet's membrane is primarily composed of type IV and VIII collagen fibrils as well as the glycoproteins fibronectin, laminin, and thrombospondin (Dawson, Ubels and Edelhauser, 2011). It is less strong and stiff than the posterior stroma and is secreted by endothelial cells since the 8th gestation week (DelMonte and Kim, 2011). Descement's membrane has a thickening rate of approximately 1 μm per decade of life: its thickness is around 4 μm at birth, while at the end of the normal lifespan Descement's membrane is around 10–15 μm thick (Dawson, Ubels and Edelhauser, 2011). Besides, this thickness can also increase focally or diffusely with injury (trauma or surgery) or disease, due to abnormal collagen deposition.

Descemet's membrane in mice is more homogeneous and granular on the anterior chamber side, resembling a typical basal lamina, and it also becomes thicker with age (Smith, 2002).

<u>1.1.5 Endothelium</u>

The corneal endothelium is a monolayer of hexagonal cells whose density and topography change continuously throughout life (DelMonte and Kim, 2011). At birth, corneal endothelium is 10 μm thick and its cell density is approximately 3500 cells/mm^2, however, this number decreases at approximately 0.6% per year (DelMonte and Kim, 2011). Corneal endothelium maintains its continuity by migration and expansion of survival cells to cover the defect surface, so the percentage of hexagonal cells decreases (*pleomorphism*, that is, endothelial cells become different from each other in shape) while the coefficient of variation of cell area increases (*polymegathism*, that is, endothelial cells become different from each other in size, appearing large cells) (Dawson, Ubels and Edelhauser, 2011).

The main function of corneal endothelium is to maintain corneal transparency and health by regulating its hydration and nutrition (Dawson, Ubels and Edelhauser, 2011). Adjacent endothelial cells share extensive lateral interdigitations and possess tight and gap junctions along their apical and lateral borders respectively, forming an incomplete barrier with a preference to the diffusion of small molecules (Dawson, Ubels and Edelhauser, 2011). The endothelium acts as a "leaky" barrier that allows passive fluid flow from the hypotonic corneal stroma to hypertonic aqueous humour through the osmotic gradient, maintaining the relative dehydrated state of the stroma. Nevertheless, although this passive movement does not require energy, endothelial cells maintain the osmotic gradient by active transport of ions. In this context, the major transport protein found to be essential is Na$^+$/K$^+$-ATPase, present in the basolateral membranes of endothelial cells.

1.2 Corneal Innervation

The cornea is supplied by both sensory and autonomic nerves, being one of the most densely innervated tissues in the body (Müller et al., 2003). The trigeminal nerve, the major sensory nerve of the head, have three different sensory branches: ophthalmic (V1), maxillary (V2), and mandibular (V3) (Al-Aqaba et al., 2019; Belmonte, Tervo, and Gallar, 2011). Most nerves supplying the cornea are sensory nerves, and most of them have their origin in the ophthalmic branch of the trigeminal ganglion (TG). Besides, a

little innervation from the maxillary branch has also been reported in the inferior cornea and the conjunctiva (Vonderahe, 1928; Ruskell, 1974).

V1 branches into the frontal, the lachrymal and the nasociliary nerves (**Figure 5**). In turn, the nasociliary nerve branches into two long ciliary nerves (**Figure 5**) and a connecting branch with the ciliary ganglion (**Figure 5**), a parasympathetic ganglion that sends 5-10 short ciliary nerves carrying both trigeminal sensory nerve fibres from the nasociliary nerve and parasympathetic and sympathetic axons, the last from the superior cervical ganglion. The density of the sympathetic nerves varies a lot among different species (Marfurt and Ellis, 1993), being higher in the cat and rabbit cornea (Ehinger, 1966; Morgan et al., 1987; Marfurt et al., 1989) and very sparse in humans and other primates (Ehinger, 1966; Toivanen et al., 1987).

Short and long ciliary nerves enter the posterior globe medially and laterally to the optic nerve (Marfurt et al., 2010; Belmonte, Tervo, and Gallar, 2011), penetrating the sclera. After that, they form a ring around the optic nerve and travel anteriorly in the suprachoroidal space towards the anterior segment of the eye (Belmonte, Tervo, and Gallar, 2011) undergoing repetitive branching. When reaching the limbal area, some fibres innervate the ciliary body and the iris, while most fibres form a dense ring-like network that encircle the limbus around the cornea, giving rise to the limbal plexus (He et al., 2010). The majority of nerve fibres in this plexus are believed to be vasomotor nerves innervating limbal blood vessels, while a variable number of nerve trunks enter the corneal stroma unrelated to blood vessels (Marfurt, C.F., 2000).
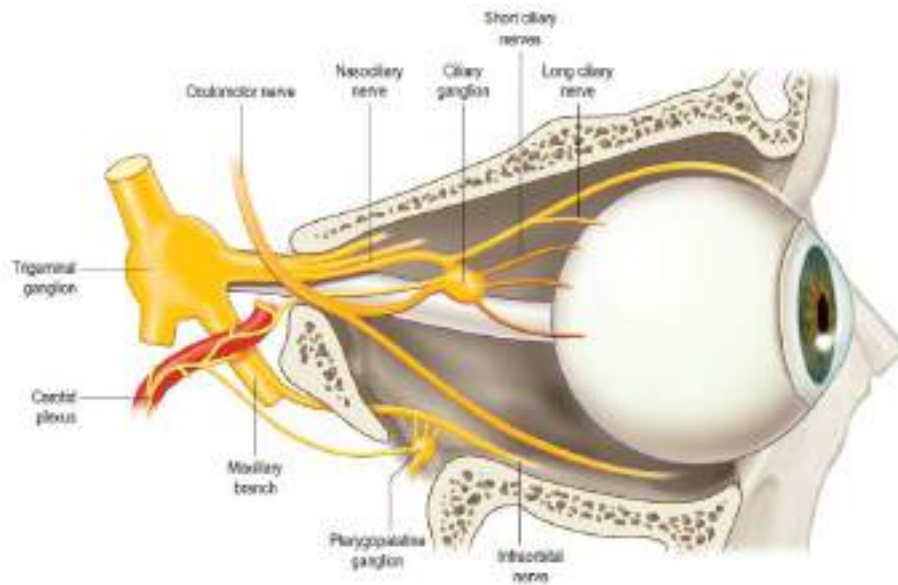
Figure 5. Innervation of the eye. Medial view of the orbit showing the sensory and autonomic nerves directed to the eye. Frontal and lachrymal nerves are not shown. Taken from Adler's Physiology of the Eye, 11th edition, Elsevier, Belmonte 2011.

1.2.1 Corneal nerve architecture

The architecture of corneal innervation has been studied for many years by a wide variety of methods, including light and electron microscopy, immunohistochemistry, and IVCM, among others. Besides, it has been described among different species such as human (Müller et al., 2003; Marfurt et al., 2010), cat (Chan-Ling, 1989; Marfurt et al., 1989), guinea pig (Zander and Weddell, 1951; Ivanusic et al., 2013) and mouse (Mckenna and Lwigale, 2011; Wang et al., 2012). Corneal innervation is anatomically organised in four levels from the penetrating stromal nerve trunks to the nerve terminals in the epithelium (**Figure 6**).
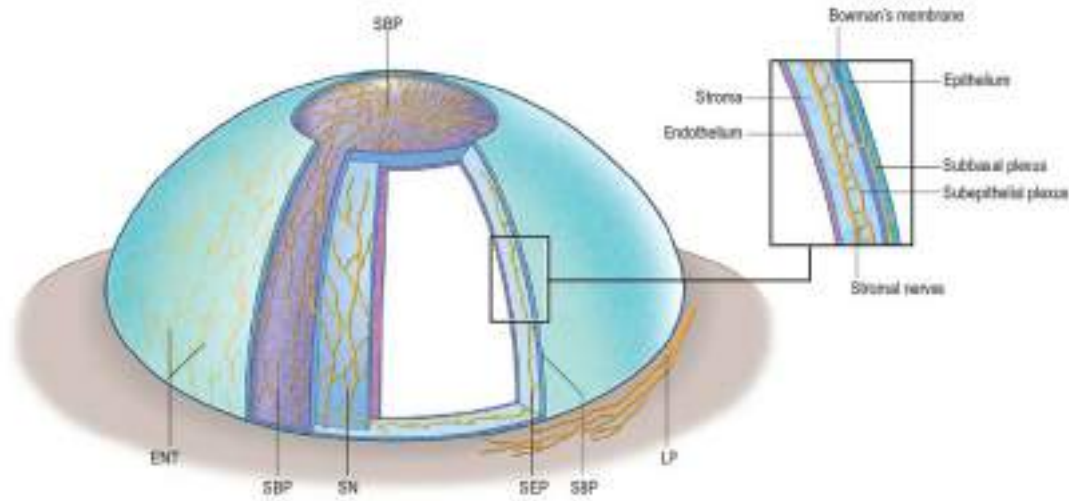
Figure 6. Schematic distribution of nerves in the cornea. From the limbal nerve plexus (LNP), stromal nerve trunks (SN) penetrate the stroma radially and divide dichotomously to form the subepithelial plexus (SEP). Branches of this plexus ascend towards the epithelium, traverse Bowman's membrane and form the sub-basal plexus (SBP) between the epithelium basal layer and its basal lamina, where nerve branches run horizontally as families of long parallel nerves (leashes) which in turn give rise to intraepithelial nerve terminals (ENT). Taken from Adler's Physiology of the Eye, 11th edition, Elsevier, Belmonte 2011.

1.2.1.1 Stromal nerves

Corneal stromal nerves enter the cornea radially through the corneoscleral limbus in the middle third of the stroma. Besides, other small nerve bundles enter the cornea more superficially in the episcleral and conjunctival planes, innervating the superficial stroma and the periphery of the corneal epithelium respectively (Zander and Weddell, 1951; Chan-Ling, 1989; He et al., 2010).

When entering the stroma at a depth of approximately 293 μm, myelinated axons (about 20%) lose their perineurium and myelin sheath (Müller et al., 2003) and run within the stroma as fascicles enclosed by a basal lamina and Remak Schwann cells (the non-myelinating Schwann cells) (Belmonte, Tervo, and Gallar, 2011). The distal branches of this arborization anastomose extensively forming the anterior stromal nerve plexus (Marfurt et al., 2010), a complex network of nerve bundles and individual axons. The posterior half of the stroma and endothelium, on the contrary, are devoid of sensory nerve fibres (Belmonte, Tervo, and Gallar, 2011).

In mice, stromal nerves do not enter the cornea radially at regular intervals as in humans. Stromal innervation is provided by nerve bundles entering into the cornea from four quadrants and branching irregularly to cover the entire cornea (Mckenna and Lwigale, 2011) (**Figure 7A,B**).
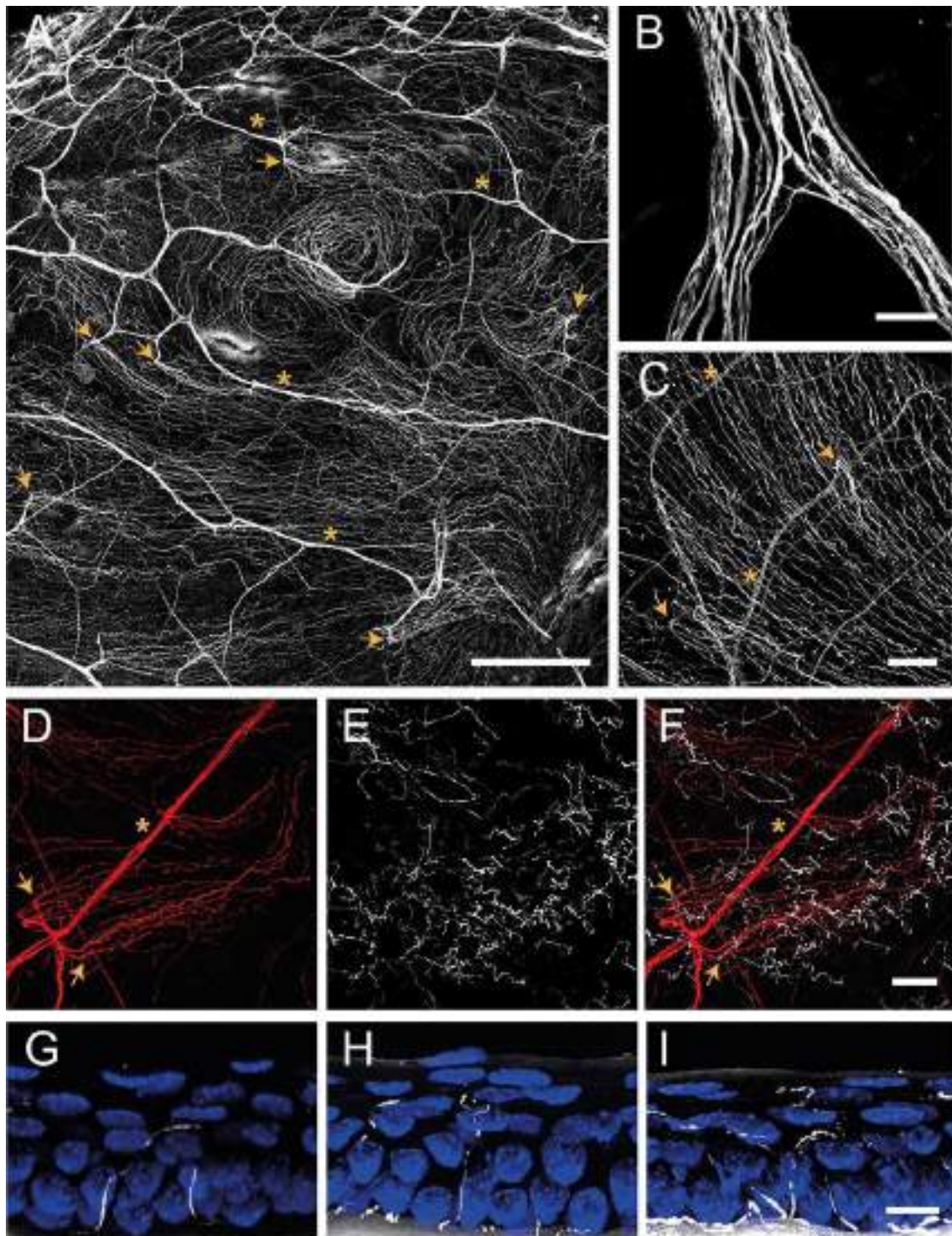
Figure 7. Confocal images of sensory nerves immunostained with anti-☐ tubulin III antibody in the mouse cornea. (A) Sensory nerve trunks enter from the limbus into the stroma of the cornea where they ramify giving rise to a dense subepithelial plexus (asterisks). **(B)** Detail of a stromal nerve trunk branching. **(C-D)** From the stroma, nerve fibres penetrate through the basal lamina (arrowheads) and form the subbasal plexus. Subbasal nerve fibres run parallel for a long distance within the epithelium basal cell layer. **E-I.** Subbasal nerves give rise to terminal branches that ascend along their trajectory through the epithelial cells. According to the number of branches, three morphological types of corneal nerve terminals are identified: simple **(G)**, ramified **(H)** and complex **(I)** nerve terminals. Scale bars: A, 250 μm; B, 25 μm; C-F, 50 μm; G-I, 10 μm.

1.2.1.2 Subepithelial nerve plexus

In humans and higher mammals, the most superficial layer of the anterior stromal nerve plexus, immediately beneath Bowman's layer, is referred to as the corneal subepithelial nerve plexus. Subepithelial plexus has a very high nerve density, but in general, it is denser in the peripheral and intermediate cornea, and less dense in the central cornea (Marfurt et al., 2010).

Anatomically, in the subepithelial plexus there are two distinct types of nerve bundles (Marfurt et al., 2010; Belmonte, Tervo, and Gallar, 2011). One form a complex anastomotic meshwork of single axons and thin tortuous fascicles that do not penetrate Bowman's membrane, while the second type consists of about 400-500 medium-sized, curvilinear bundles that turn 90º and penetrate Bowman's layer and basal lamina mainly in the peripheral and intermediate cornea (Müller et al., 2003; Marfurt et al., 2010). These nerve bundles terminate in bulb-like structures and divide into smaller ones in groups up to 20 subbasal nerve fibres, known as epithelial leashes (Müller et al., 2003; Marfurt et al., 2010). These leashes, that are parallel to the ocular surface, anastomose extensively to form a dense subbasal nerve plexus (see below).

It is worth mentioning that while unmyelinated nerves maintain their Remak Schwann cell coating in the stroma, they shed them before penetrating the basal lamina. In this regard, it has been suggested that corneal epithelial cells function as surrogate Schwann cells for the sub-basal and intraepithelial nerves in health conditions and after injury (Stepp et al., 2017).

1.2.1.3 Subbasal nerve plexus

The corneal epithelium receives sensory nerve fibres either from the subepithelial plexus or directly from the conjunctival nerves (He et al., 2010; Marfurt, 2000). The subbasal nerve plexus is constituted by epithelial leashes from subepithelial nerves that anastomose extensively and interconnect repeatedly with one another such that they are no longer recognizable as individual leashes (**Figure 7C,D**), although leashes are less numerous and separated in the periphery (Marfurt et al., 2010). The term "epithelial leash" was defined as a group of subbasal nerves that derives from the same parent anterior stromal nerve trunk (Rózsa and Beuerman, 1982; Schimmelpfennig, 1982; Chan-Ling, 1989), being a unique neuroanatomical structure only found in the cornea of most species, including humans.

The subbasal nerve plexus is a dense, homogenous nerve plexus situated between the basal epithelial cells and the basal lamina. In humans, it is formed by 5,000-7,000 nerve fascicles in an area of about 90 mm^2 (Belmonte at al., 1997), with a total number of axons estimated to vary between 20,000 and 44,000 (Müller et al., 2003). Morphologically, each leash consists of a variable number of straight nerve fibres, each containing 3-10 individual axons travelling up to several millimetres. Subbasal nerve fibres converge on a spiral whose centre is called the vortex (Dua et al., 1993; Al-Aqaba et al., 2010). This vortex is also present in other species including mice (Mckenna and Lwigale, 2011; Ivanusic et al., 2013) and rats (Dvorscak and Marfurt, 2008) and the mechanisms underlying its formation remain unclear. The most extended hypothesis is that nerves and basal epithelial cells advance in the same direction and velocity in a whorl-like pattern in response to a chemotropic guidance, to electromagnetic cues, and/or to population pressures (Nagasaki and Zhao, 2003; Patel and McGhee, 2005).

1.2.1.4 Intraepithelial nerve terminals

Single nerve fibres arising from the subbasal plexus split off and turn 90° vertically as a profusion of terminal axons ascending between the epithelial cells, often with a modest amount of additional branching (**Figure 7E-I**) (Belmonte, Tervo, and Gallar, 2011). The term intraepithelial nerve terminal was defined by Carl Marfurt as the

entire epithelial axon distal to its point of origin from a subbasal nerve and all its collateral branches and terminal expansions (the so-called *nerve endings*) (Marfurt et al., 2010). Corneal epithelium innervation is extremely dense. It is estimated that the human central cornea contains around 3.500-7,000 nerve terminals per square millimetre, although this number changes throughout life and in ocular pathologies.

The intraepithelial nerve terminals innervate the corneal epithelium through all its layers. Those running between the basal and wing epithelium cells run in a horizontal direction and branch relatively infrequently (Marfurt et al., 2010) while intraepithelial nerve terminals that terminate within the more superficial cell layers are generally more complex (**Figure 7E, G-I**). Intraepithelial nerve terminals can be classified into three different types: simple, ramifying, and complex (Al-Aqaba et al., 2019). *Simple terminals* do not branch after leaving the subbasal plexus and end with a bulbar swelling within or below the superficial squamous cells (Ivanusic et al., 2013; Al-Aqaba et al., 2019) (**Figure 7G**). Simple terminals are more abundant in the central cornea. *Ramifying terminals* branch within the squamous cell layer into 3-4 branches that run horizontally for a hundred of microns and that end in a single bulbar swelling like the simple terminals (Ivanusic et al., 2013; Al-Aqaba et al., 2019) (**Figure 7H)** being more numerous in the peripheral cornea (Ivanusic et al., 2013). Finally, axons forming the *complex terminals* start to branch within the wing cells layer and terminate with multiple larger bulbous endings within the wing and squamous cell layers **(Figure 7I)**. Complex terminals are found in the central and the peripheral cornea, but their complexity and size are higher in the periphery (Ivanusic et al., 2013).

Intraepithelial nerve terminals seem to be functionally different as immunocytochemical staining reveals differences in the expression of neuropeptides and neurotransmitters. In mice and guinea pig, nerves that terminate in the basal epithelium and the outermost cell layers have simple endings immunopositive for Calcitonin Gene Related Peptide (CGRP) and substance P (SP), suggesting that peptidergic simple nerve terminals correspond functionally to polymodal nociceptor nerve terminals (Ivanusic et al., 2013). On the other hand, complex nerve terminals are immunoreactive to TRPM8 (Transient receptor potential channel subfamily M member 8) supporting the idea that complex terminals correspond to cold thermoreceptor terminals (Ivanusic et al., 2013). More recent studies in guinea pig corneas also suggest that these intraepithelial nerve

terminals can be distinguished morphologically as TRPM8-positive terminals are more complex than TRPV1-positive terminals (Alamri et al., 2018).

1.2.2 Functional types of corneal nerves

Electrophysiological recordings of sensory nerve fibres innervating the cornea have revealed the existence of different functional types of ocular sensory nerves, classically classified depending on the modality of stimulus by which they are activated (Belmonte et al., 2004a; Belmonte and Gallar, 2011). Most corneal sensory nerves are the peripheral branches of medium or small trigeminal neurons with thin myelinated (A-delta) or unmyelinated (C) axons (Belmonte et al., 2004a). The external stimuli are transduced by their intraepithelial nerve terminals into a discharge of nerve impulses that encode the stimulus' spatial and temporal characteristics. The impulse discharge is conducted by trigeminal neurons to the central nervous system, where sensory input is processed to finally evoke a sensation and is also used to regulate protective functions such as tearing and blinking. Depending on the variable activation of the different classes of corneal sensory neurons, different sensations are evoked (Acosta et al., 2001; Belmonte and Gallar, 2011).

1.2.2.1 Mechanonociceptors

About 15% of corneal nerve fibres are mechanonociceptors, which express Piezo2 channels (Bron et al., 2014; Fernández-Trillo et al., 2020) and are activated exclusively by mechanical forces (**Figure 8**). Mechanonociceptors are usually A-delta fibres and produce a short-lasting impulse discharge in response to a sustained mechanical stimulus, therefore signalling the presence and velocity of change of the mechanical force, rather than its intensity or duration (Belmonte and Giraldez, 1981; Belmonte et al., 1991). These relatively rapidly adapting mechanosensitive fibres contribute to the pain experienced when a foreign body touches the ocular surface (Acosta et al 2001).

1.2.2.2 Polymodal nociceptors

The majority of corneal sensory fibres (around a 70%) are polymodal nociceptors, which express in their nerve terminals a diversity of transducing ion channels, such as TRPA1, TRPV1, ASIC and Piezo2 that allow them to be activated by noxious mechanical forces, heat (temperatures over 39ºC) and a wide variety of exogenous and endogenous chemicals (protons, ATP, prostaglandins, cytokines, etc.) (Chen et al., 1997; Belmonte et al., 2004b) (**Figure 8**).

Polymodal nociceptors produce an irregular and repetitive discharge as long as the stimulus is maintained that is proportional to its intensity (Gallar et al, 1993; Belmonte et al., 2004b). Moreover, under certain circumstances, polymodal nociceptors can be sensitised, developing an irregular low frequency long after the stimulus has disappeared (Gallar et al., 2007). Besides, sensitization produces a decrease in threshold and an increase in the firing frequency in response to a new stimulus (Bessou and Perl, 1969; Belmonte and Giraldez, 1981). Most corneal polymodal nociceptors are slow-conducting C-type fibres and are the origin of the ocular discomfort and pain sensations developed under pathological conditions, local inflammation, or injury (Gallar et al., 2007; Meyer, R.A., Ringkamp, M., Campbell, J.N., and Raja, S.N., 2008).

1.2.2.3 Cold thermoreceptors

The third class of corneal sensory fibres are cold thermoreceptors (10-15%), associated with A-delta and C nerve fibres. Cold thermoreceptors have spontaneous discharge and increase their firing rate in response to temperature reduction and to osmolality increases (Gallar et al., 1993; Carr et al., 2003; Parra et al., 2014) (**Figure 8**). Cold thermoreceptors are transiently silenced upon warming, although some of them restart firing in response to high temperatures (paradoxical response to heat) (Belmonte and Gallar, 2011; Acosta et al., 2013). Cold thermoreceptors firing increases proportionally to the speed and magnitude of the corneal temperature reduction, as well as to the final static temperature (Belmonte and Gallar, 2011). When enough cold thermoreceptors are recruited with an augmented tear evaporation, a conscious sensation of dryness is expected (Belmonte et al., 2004a). Cooling sensations with temperature

reductions are increasingly unpleasant when higher temperature decreases are applied (Acosta et al., 2001).

The activity of corneal cold thermoreceptors expressing TRPM8 is crucial in different mechanisms protecting the eye, such as lacrimation and blinking (Acosta et al., 2004, 2014; Parra et al., 2010; Belmonte and Gallar, 2011; Quallo et al., 2015). The deletion of TRPM8 channels produces both a decrease in basal tearing (Parra et al., 2010) and blinking (Quallo et al., 2015) in mice, supporting the idea that sensory input of cold thermoreceptors is used by the CNS to regulate blinking and tearing. Ageing induces changes in TRPM8 expression and activity, which correlates with the changes in tearing developed with age (Alcalde et al., 2018).
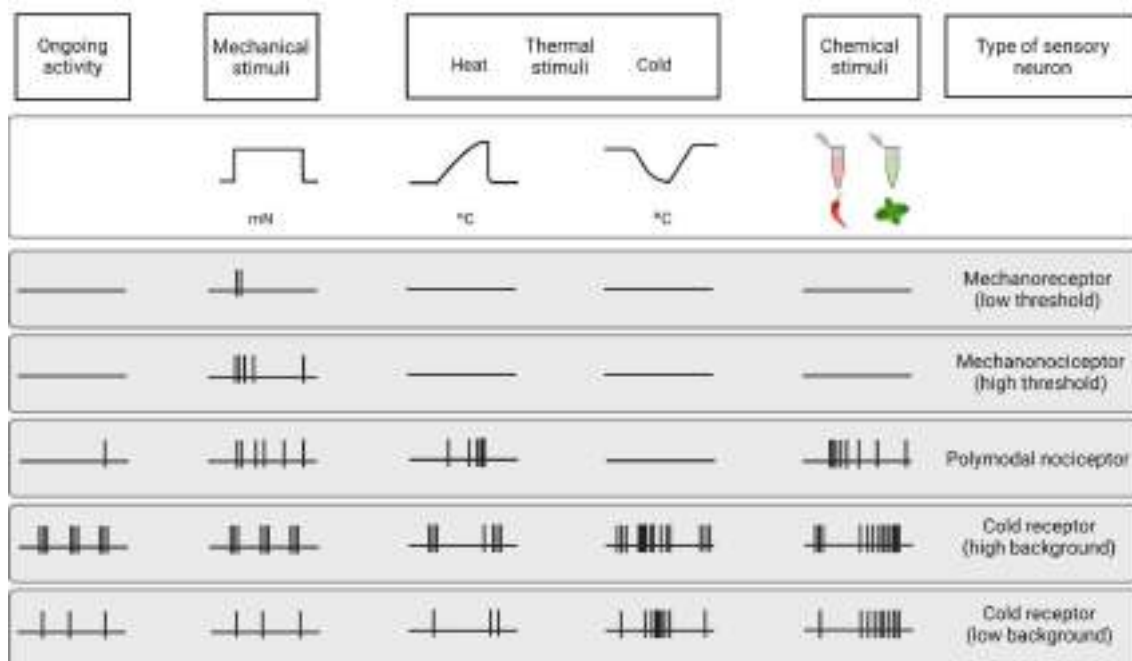
Figure 8. Functional types of sensory neurons innervating the cornea. Schematic representation of the spontaneous and stimulus-evoked impulse activity of the different functional types of sensory nerves innervating the cornea. Based on the characteristics of the impulse discharge in absence of intended stimulation (ongoing activity) and in response to different types of stimuli (upper part of the figure), the peripheral terminals of primary sensory neurons innervating the cornea are classified into five different functional types of sensory neurons.

1.2.3 Changes of nerve activity under inflammation and after injury.

After inflammation or lesion, corneal sensory nerve activity is altered. Like in other tissues, corneal nociceptors (specially polymodal nociceptors) are sensitised (Gallar et al., 2004, 2007; Acosta et al., 2013, 2014; Kovács et al., 2016; Belmonte, 2019; Luna et al., 2021), a functional state characterised by an increase in spontaneous activity, a reduction of the response threshold and an increased response to stimulation (Schaible and Schmidt, 1985). Sensitization constitutes the basis of *spontaneous pain* and *hyperalgesia* experienced during inflammation. Additionally, corneal nociceptors also contribute to the inflammatory processes of the ocular surface (a process known as *neurogenic inflammation*) (Gonzalez et al., 1993; Vitar et al., 2021) by releasing pro-inflammatory neuropeptides as SP and CGRP (Müller et al., 2003; Murata and Masuko, 2006; Yang et al., 2021). After injury, regenerating nociceptors present increased spontaneous activity due to the increased expression of specific types of Na+ channels by regenerating neurons (Luna et al, 2021).

Contrarily, cold thermoreceptors' activity is decreased under inflammation (Acosta et al., 2013, 2014) because the activity of TRPM8 channels is inhibited by inflammatory mediators as bradykinin through a G-protein (Zhang et al., 2012). During chronic tear deficiency, activity of cold thermoreceptors is increased due to the increase of Na+ currents and the decrease of K+ currents (Kovács et al., 2016).

1.3 The cornea: an immune-privileged tissue

The ocular surface is a mucosal surface in which the optical properties are critically important and where immune-mediated inflammation should not cause collateral damage (Foulsham et al., 2018). Most of our current knowledge about the ocular surface immune-privilege arises from studies with corneal allografts, whose benefits have been widely described (Taylor, 2016; Niederkorn, 2019). The cornea should perform an important balance between fighting infections and maintaining transparency in order to preserve vision. This immune-privilege tissue can be exposed to antigens, allergens, and pathogens without eliciting significant immune responses. The concept of '*immune privilege*' was first coined by Medawar decades ago (Medawar, 1948), however, it has been extensively reviewed since its initial conception, 2009; Hori et al., 2010).

Traditionally, corneal immune privilege was ascribed to the lack of lymphatic and blood vessels and lack of resident antigen presenting cells (APCs) at basal conditions. Nevertheless, until today, different studies have demonstrated that the cornea is endowed with a significant number of resident APCs such as macrophages and dendritic cells (DCs) (Brissette-Storkus et al., 2002; Hamrah et al., 2002, 2003c, 2003a; Jamali et al., 2020). In this regard, immune privilege means that even if immune cell activity is present, it is driven towards anti-inflammatory and tolerogenic immune responses (Taylor, 2016).

Cells in the cornea, mostly epithelial cells, express and secrete different molecules that confer a tolerogenic profile upon DCs (Foulsham et al., 2018) or that promote regulatory activity or apoptosis in the T cells (Taylor, 2016). Among these molecules, the immunoregulatory factor Decay Accelerating Factor (DAF, also known as CD55) (Forrester and Xu, 2012) or the apoptosis-inducing ligands FasL (FasLigand) and Programmed Death Ligand-1 (PDL-1) (Foulsham et al., 2018) seem to be crucial. In addition to suppress T cell effector responses by producing their apoptosis, these ligands also allow regulatory T cells (Tregs) to function since Tregs are more resistant to FasL-induced apoptosis (Weiss et al., 2011) and are activated by PDL-1 (Francisco et al., 2010; Lee and Taylor, 2013).

Along with the previously described mechanisms that contribute to the cornea's immune privilege, there is also a neuroregulation of ocular surface immunity by corneal nerves (Foulsham et al., 2018). Different neuropeptides released by corneal nerves are involved in this process. Vasoactive intestinal polypeptide (VIP) downregulates TLRs, inhibit chemokine expression, induce tolerogenic DCs and limit the release of pro-inflammatory cytokines (Delgado and Ganea, 2013) while CGRP inhibits the production of inflammatory cytokines by macrophages and also the maturation of DCs (Springer et al., 2003).

2- Dendritic Cells

2.1 An overview of dendritic cells

First discovered in mouse spleen in the 1970s (Steinman and Cohn, 1973), DCs are a heterogeneous group of professional APCs that induce naïve T cell activation and T

effector differentiation (Hamrah et al., 2003a; Patente et al., 2019) playing an important role between innate and adaptive immune responses. DCs include members of different lineages that can be found in two different functional states: mature and immature (Hamrah et al., 2003a; Patente et al., 2019) (**Figure 9**). Immature DCs are characterised by a high antigen capture ability due to their high endocytic capacity, but a low T cell-stimulatory capability due to their low surface expression of co-stimulatory molecules and chemokine receptors (Steinman and Swanson, 1995; Trombetta and Mellman, 2005). DC maturation, which is triggered by tissue disturbances, leads to a decrease in their endocytic activity but an increase in the expression of major histocompatibility complex class II (MHC-II) and co-stimulatory molecules, such as CD40, CD80 and CD86 (Banchereau et al., 2000; Trombetta and Mellman, 2005; Reis E Sousa, 2006; Steinman, 2012), becoming powerful T cell stimulators in secondary lymphoid organs (Hawiger et al., 2001; Worbs et al., 2017).

Mature DCs can induce specific CD8+ and CD4+ T cell responses (O'Keeffe et al., 2015). When interacting with CD4+ T cells, DCs can induce their differentiation into different T helper (Th) subsets such as Th1, required for immunity against intracellular pathogens and cancer (Constant et al., 1995; Amsen et al., 2004; Kadowaki, 2007; O'Keeffe et al., 2015; Patente et al., 2019), Th2, essential for driving immune responses against parasitic infections (Constant et al., 1995; Soumelis et al., 2002; Jenkins et al., 2007; O'Keeffe et al., 2015) or Th17, important for neutralising bacterial and fungal pathogens (Bailey et al., 2007; Huang et al., 2012). T cell differentiation in each subtype is a complex phenomenon that can be influenced by the cytokines in the DC tissue of origin (Rescigno, 2014) or their maturation state (Reis E Sousa, 2006).

In addition to their role in inducing specific CD8+ and CD4+ T cells responses, DCs are also able to induce and maintain immune tolerance at basal conditions (Steinman et al., 2003; Liu and Cao, 2015; Raker et al., 2015; Patente et al., 2019). These "tolerogenic DCs" are immature DCs that express less co-stimulatory molecules, upregulate the expression of inhibitory molecules and secrete anti-inflammatory cytokines (Morelli and Thomson, 2007; Manicassamy and Pulendran, 2011), being essential to prevent responses against healthy tissues (Hawiger et al., 2001; Steinman et al., 2003; Yates et al., 2007).
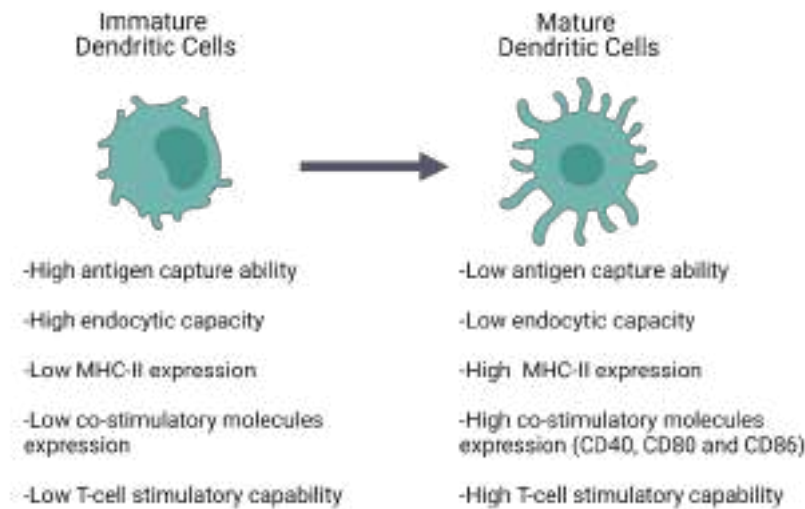
Figure 9. DC maturation triggered by tissue homeostasis disturbances.

In both humans and mice, DCs are identified by their high expression of MHC-II and CD11c (Patente et al., 2019). However, DCs express other molecules that allow their classification into different subtypes that differ from their phenotypic markers and genetic profile. Overall, these subtypes are type 1 and 2 conventional DCs (cDCs), plasmacytoid DCs (pDCs), Langerhans cells (LCs) and monocyte-derived DCs (MCs).

DCs arise from CD34+ hematopoietic stem cells (HSCs) that give rise to lymphoid (LPs) and myeloid precursors (MPs) (**Figure 10**). MPs differentiate into monocyte and DC precursors (MDPs), which in turn give rise to monocytes and to the common DC precursors (CDPs). CDPs can differentiate into the preclassical DCs (pre-cDCs), which are the progenitors of the two major cDC subpopulations cDC1 and cDC2, or into pDCs (Geissmann et al., 2010; Patente et al., 2019) (**Figure 10**), although recent studies suggest that mouse pDCs predominantly originate from a distinct progenitor from cDCs (O'Keeffe et al., 2015; Wang et al., 2017). LPs can also give rise to pDCs, however, this ontogenic pathway is not completely elucidated (**Figure 10**). Once in the blood, pDCs and cDCs can migrate to lymphoid and nonlymphoid tissues.

LCs derive primarily from foetal liver monocytes that colonise the skin during embryogenesis (Halim et al., 2016) and maintain themselves by local proliferation in response to macrophage growth factors and IL-32 (Hawiger et al., 2001).

Finally, MCs are cells with DC-like features that can be generated by mouse monocytes during steady state in skin and mucosal tissues (Varol et al., 2007; Tamoutounour et al., 2013) and during inflammation (Plantinga et al., 2013; Tamoutounour et al., 2013). In vitro, mouse MCs can be also produced by bone marrow precursor stimulation with granulocyte-macrophage colony-stimulating factor (GM-CSF) (Inaba et al., 1992). Human MCs are produced in vitro by culturing human monocytes in the presence of GM-CSF and IL-4 (Sallusto and Lanzavecchi, 1994).
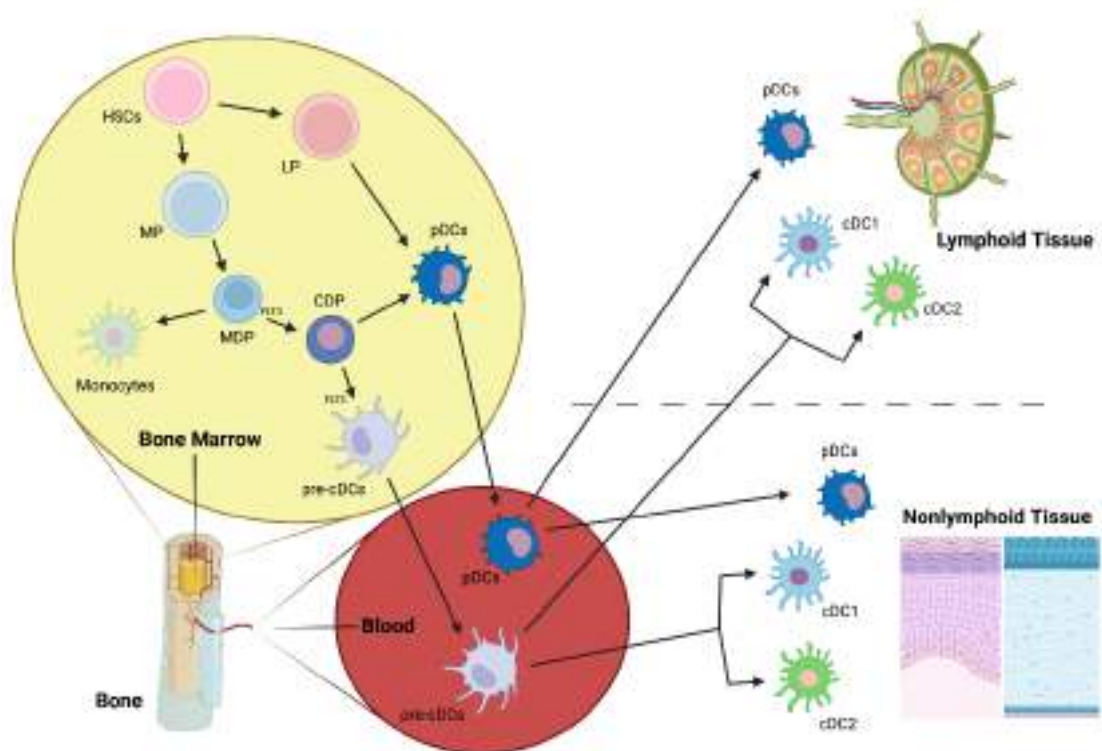
Figure 10. Simplified scheme of DC ontogeny. cDC1 and cDC2, main conventional dendritic cell subtypes; CDP, common DC precursor; FLT3, Fms-Related Tyrosine Kinase 3; HSCs, hematopoietic stem cells; LP, lymphoid precursor; MDP, macrophage-DC precursor; MP, myeloid precursor; pre-cDCs, pre-classical dendritic cells; pDCs, plasmacytoid dendritic cells.

2.2 Dendritic cell subpopulations

2.2.1 Conventional DC (cDC)

2.2.1.1 cDC1

cDC1 is a cDC subpopulation that efficiently prime CD8+ T cells by performing antigen cross-presentation (Bachem et al., 2010). cDC1can be found both in the periphery (where they represent 30% of cDC) and in lymphoid organs (where they account for 40%).

In humans and mice, cDC1s express CD141, the chemokine receptor XCR1, C-type lectin CLEC9A and the cell adhesion molecule CADM1 (Reynolds and Haniffa, 2015) (**Figure 11**). Moreover, in mice, cDC1s are identified by the expression of CD8α in the spleen and CD103 in non-lymphoid tissues (Reynolds and Haniffa, 2015) (**Figure 11**) and can be also characterised by the expression of other C-type lectin receptors like CD205 and CD207 (Cabeza-Cabrerizo et al., 2021).

For the generation of cDC1s, the main transcription factors (TFs) are the basic leucine zipper transcriptional factor ATF-like 3 (BATF3) (Hildner et al., 2008) and IFN-regulatory factor 8 (IRF8) (Schiavoni et al., 2002). In mice, besides BATF3 and IRF8, other TFs are also essential for cDC1s generation (Hacker et al., 2003; Kashiwada et al., 2011; Reynolds and Haniffa, 2015) like DNA binding protein inhibitor ID2 and nuclear factor interleukin-3-regulated protein (NFIL3).

2.2.1.2 cDC2

cDC2 is a more heterogeneous DC subset than cDC1 that has been shown to induce Th1, Th2, and Th17 responses from CD4+ helper T cells (Th) (Segura et al., 2012; Leal Rojas et al., 2017) and that has different regulatory roles by inducing regulatory T cells (Tregs) in some tissues like intestine or liver (Bamboat et al., 2009; Watchmaker et al., 2014). cDC2s can be found in lymphoid, non-lymphoid tissues and in blood (Haniffa et al., 2013; Patente et al., 2019) where they are more abundant than cDC1s.

This subpopulation is characterised by the expression of SIRPα in both human and mice and CD1c or CD11b in human or mice respectively (O'Keeffe et al., 2015; Reynolds and Haniffa, 2015) (**Figure 11**). Moreover, cDC2s can express other markers according to their location which produces their great heterogeneity (Patente et al., 2019).

For cDC2 differentiation, different TFs are involved, with IRF4 traditionally considered the most important one (Schlitzer et al., 2013). However, more recent studies suggest that IRF4 is more essential for cDC2 function regulation rather than for cDC2 development (Murphy et al., 2016). Other TFs shown to be associated with cDC2 differentiation are PU.1 and RelB (Wu et al., 1998; Zhu et al., 2012) in mice and IRF8 (Hambleton et al., 2011) in humans.

2.2.2 Plasmacytoid DC (pDC)

pDC1 is a DC subpopulation that secrete high levels of IFN-α after TLR7/9 stimulation and has a pivotal role in viral infections (Reizis et al., 2011). In addition, these cells have also been associated with immune tolerance (Jamali et al., 2021). pDC are continuously generated in the bone marrow and subsequently enter the bloodstream (where they constitute less than 1% of mononuclear cells) (Sawai et al., 2013; Chistiakov et al., 2014) to then home primary and secondary lymphoid tissues in steady state (Bendriss-Vermare et al., 2001; Nakano et al., 2001; Contractor et al., 2007; Boor et al., 2019). During microbial infections or autoimmune diseases, these cells are recruited to peripheral tissues where they are typically absent (Nestle et al., 2005; Sozzani et al., 2010). However, and although in low densities, few peripheral tissues host pDC during steady state like the lung or the vagina (Donnenberg and Donnenberg, 2003; Lund et al., 2006).

Phenotypically, pDCs are distinct in mice and humans. In humans, pDCs are identified by their expression of CD123, CD303 (BDCA2) and CD304, while in mice, pDCs express CD307, B220 and SiglecH (Reynolds and Haniffa, 2015) (**Figure 11**). Importantly, human pDCs do not express CD11c (Facchetti et al., 1988; Jamali et al., 2021) and can be divided into two subsets based on their levels of DC2 expression (Matsui et al., 2009).

Regarding TFs for pDC generation, in both humans and mice, E2.2 seems to be the most important one (O'Keeffe et al., 2015; Reynolds and Haniffa, 2015; Patente et al., 2019).

2.2.3 Langherhans cells (LC)

LCs are a subset of cells located in epidermal surfaces, being the most numerous antigen-presenting cells in human skin (O'Keeffe et al., 2015; Reynolds and Haniffa, 2015). LCs can induce several immune responses by stimulating CD4+ T cell proliferation and polarisation towards Th2 phenotype (Klechevsky et al., 2008; O'Keeffe et al., 2015), and particularly in humans, these cells can also stimulate naïve CD8+T cells (Klechevsky et al., 2008).

Human and murine LCs express EPCAM, low CD11c and langerin, that acts as a receptor for microbial pathogens (Reynolds and Haniffa, 2015) (**Figure 11**). Besides, in both humans and mice, LCs present Birbeck granules (Birbeck et al., 1961), a type of organelles whose function still remains unclear. Additionally, in humans, LCs are also CD1a+ and CD1c+ (Haniffa et al., 2012; Reynolds and Haniffa, 2015).

The development of LCs is mainly dependent on Runx3 and PU.1 (Fainaru et al., 2004; Chopin et al., 2013).

2.2.4 Monocyte-derived DC (MC)

MCs have contributed a lot to the knowledge about DCs in humans. Due to their potential, they are currently being studied for the treatment and monitoring of different human diseases, mainly cancer (Patente et al., 2019).

Ontogeny data suggest that inflammatory DCs (another DC subpopulation that expresses high levels of CD11c and MHC-II) are the in vivo counterparts of MCs (Segura et al., 2013; Reynolds and Haniffa, 2015) (**Figure 11**).

PU.1 and IRF4 act as TFs for human monocyte differentiation into MCs in vitro (Bakri et al., 2005; Lehtonen et al., 2005).

Conventional DC type 1 (cDC1)
Human: CD141/XCR1/CLEC9A/CADM1
Mouse:CD8α/CD103/CD141/XCR1/CLEC9A/CADM1

Conventional DC type 2 (cDC2)
Human: CD1c/SIRPα
Mouse:CD11b/SIRPα

Langerhans cell (LC)
Human: EPCAM/Langerin/CD1a/CD1c
Mouse: EPCAM/Langerin

Plasmacytoid DC (pDC)
Human: CD123/CD303/CD304
Mouse:CD317/B220/SiglecH

Monocyte-derived DC (MC)
Human: High CD11c/MHC-II
Mouse: High CD11c/MHC-II

Figure 11. Specific surface markers expressed by the different DC subtypes in humans and mice.

2.3 Distribution of resident dendritic cells in the cornea

Traditionally, the cornea has been considered a tissue devoid of resident immune cells. However, heretofore many studies in humans and mice have shown the presence of macrophages (Brissette-Storkus et al., 2002; Hamrah et al., 2003a, 2003b) and the major DC subsets (**Figure 12**) in this tissue (Yamagami et al., 2005; Hattori et al., 2016). In addition, other immune cells such as γδ T lymphocytes (Li et al., 2007) or NK cells (Liu et al., 2012) have been reported in the limbus.

The density of DCs decreases from the limbus towards the centre of the cornea (Yamagami et al., 2005; Hattori et al., 2016) and correlates with ocular inflammation (Hamrah et al., 2003b). DC localization throughout corneal layers depends on DC subpopulation (Hamrah et al., 2002, 2003c, 2003b) (**Figure 12**). cDCs were traditionally thought to be confined to the peripheral cornea and the limbus, nevertheless, it was later demonstrated that these cells are also located in the central corneal epithelium and stroma, especially during inflammation (Hamrah et al., 2003b). Immature cDCs are more numerous in the periphery, but in response to an inflammatory stimulus they increase and mature throughout the cornea, with higher levels MHC-II and co-stimulatory molecules (Hamrah et al., 2003b; Foulsham et al., 2018). LCs have been reported only in the peripheral epithelium (Hamrah et al., 2002) with a distribution pattern very similar to that in skin (Mayer et al., 2007) and pDC are located in the anterior stroma, immediately below the basal epithelium both in the central and peripheral cornea (Jamali et al., 2021).
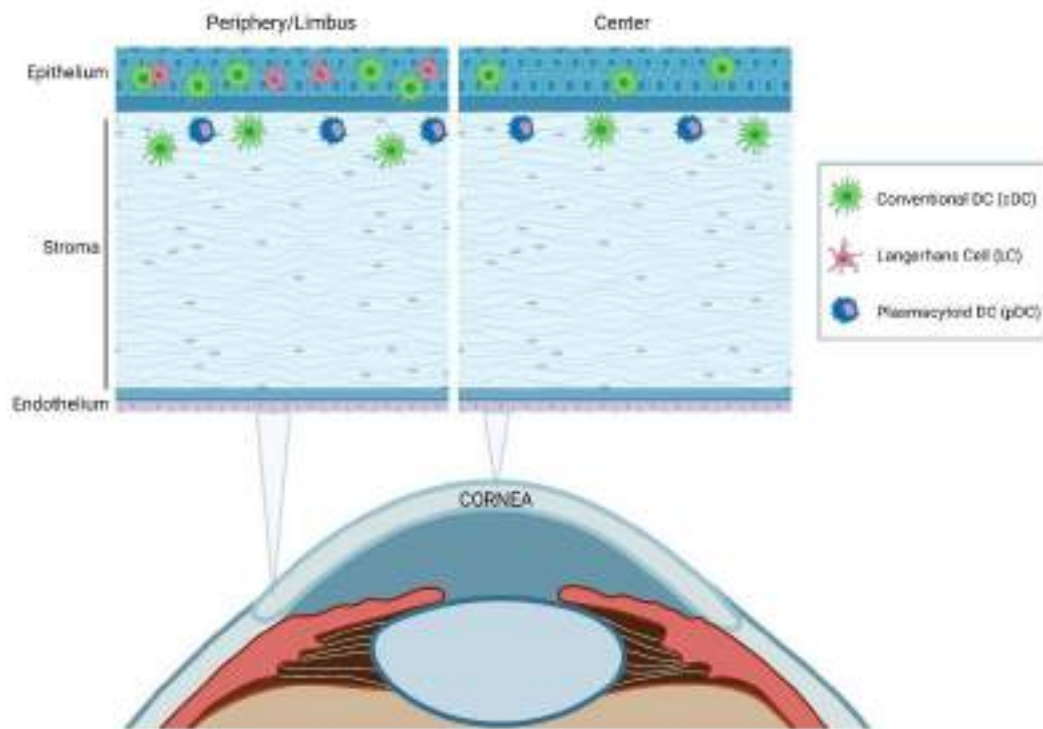
Figure 12. Schematic illustration of the distribution of resident DCs in the cornea at steady state. Most of DC subtypes are preferentially distributed in the epithelium and the anterior stroma and are more abundant in the peripheral cornea and limbal area than in the central cornea.

2.4 Dendritic cells in ocular diseases

2.4.1 Humans

DCs are the major immune cells involved in the most common ocular surface diseases (Palomar et al., 2019). In humans, most of the current investigations on corneal DCs are done by using In Vivo Confocal Microscopy (IVCM), which allows the study of subbasal and stromal corneal nerves. IVCM has been more and more used for the diagnosis and management of different corneal diseases because it is minimally invasive and has a high resolution (Villani et al., 2014). In this context, the in vivo dynamic assessment of corneal inflammatory cell density seems to be a good indicator of the disease severity. An inverse correlation between corneal nerve density and density of

DCs has been described in patients with infectious keratitis including fungal, bacterial and Acanthamoeba keratitis (Cruzat et al., 2011). Moreover, the reduction of corneal nerves and the increase in DC density was bilateral even after unilateral infectious keratitis (Cruzat et al., 2015). Along the same lines, an increase in corneal DC density has

also been observed by IVCM in patients with herpetic uveitis and juvenile idiopathic uveitis (Postole et al., 2016), aqueous-deficient dry eye disease (DED) (Lin et al., 2010), Sjögren's syndrome (SS) (Tuisku et al., 2008) and in contact lens wearers (Zhivov et al., 2007).

In this vein, other clinical studies have postulated a connection between the patient's tear cytokines and corneal DCs. Significant correlation between proinflammatory cytokines and increased DC density, and reduction in corneal subbasal nerve density has been described in bacterial keratitis (Yamaguchi et al., 2014). Significantly higher levels of IL-1β, IL-6 and IL-8 cytokines were found in tears of the affected eyes compared with healthy controls, as well as higher levels of CCL-2, IL-10 and IL-17a cytokines in the contralateral eyes (Yamaguchi et al., 2014). However, this is not the only study that correlates proinflammatory tear cytokines with corneal DC density. In patients with rheumatoid arthritis after systemic therapy (Villani et al., 2013) a decrease in tear IL-1 and IL-6 levels is accompanied with a decrease in DC density.

2.4.2 Mice

Most of the current knowledge in the pathophysiology of DCs in ocular diseases arises from studies performed in mice. The implication of DCs in infectious keratitis and, particularly, in herpes simplex virus (HSV) keratitis, is one of the most characterised in models. As early as one day after HSV-1 inoculation, pDCs are increased in both peripheral and central cornea, and this increase progresses until 6 days post-inoculation (Hu et al., 2013). Moreover, following HSV-1 inoculation, pDCs also increase in the draining lymph nodes (dLNs), with a major shift towards mature pDCs (Sendra et al., 2016). During primary herpes simplex keratitis, there is a neuro-invasion of sensory corneal nerves by HSV that remains latent in the TG. If there is a virus reactivation, that leads to chronic recurrent herpes stromal keratitis (Miranda-Saksena et al., 2000) and may eventually produce severe corneal scarring. In this context, it has been shown that pDC depletion prior to HSV-1 inoculation produces increased virus titers in the cornea and increased viral transmission to TG and dLNs (Hu et al., 2013; Sendra et al., 2017), suggesting a protective role of these cells. This is the opposite of what is observed in local depletion of cDCs, which produces a decreased corneal nerve infection and a decreased

and delayed systemic viral transmission in TG and dLNs (Hu et al., 2015). Nevertheless, in both cDC and pDC depleted-mice, a higher clinical keratitis severity was observed compared to sham-depleted animals, maybe due to the major influx of immune cells to the cornea. Further, depletion of corneal pDCs in BDCA-2-DTR mice prior to HSV-1 inoculation is accompanied by alterations in the dLN cytokine milieu, leading to decreased density of Tregs (Sendra et al., 2017) as well as increased recruitment of ex-Tregs to the cornea and dLN in vivo (Jamali et al., 2021).

DC immune responses in the cornea have been also widely studied in sterile models of inflammation. In ocular tissues, this sterile inflammation occurs in response to chemical and mechanical traumas, contact lens wear or allergens. It has been shown that depletion of corneal pDCs prior to suture placement is accompanied by enhanced clinical opacity of the cornea, as well as augmented influx of inflammatory immune CD45+ cells (Sendra et al. 2014, 2017). Moreover, in a mouse model of ocular allergy, CD11b+ DC subset seems to play a dominant role in secondary allergic immune responses (Khandelwal et al., 2013).

The implication of DCs in ocular diseases has also been described in diabetic sensory neuropathy in the cornea and in DED. Sensory nerve density and DC populations were dramatically decreased in diabetic mice and DC decrease during wound healing results in the reduction of tissue levels of CNTF, which in turn impairs sensory nerve innervation and regeneration (Gao et al., 2016b). Besides, in an experimental model of DED induced by subcutaneous injections of scopolamine, DCs in dLNs were shown to be more activated than in control mice, suggesting that they may stimulate the T cells that participate in the onset and progression of the disease (Maruoka et al., 2018).

These examples are only a part of the huge number of results that are currently being obtained regarding the involvement of DCs in the pathophysiology of ocular diseases. However, we still have limited knowledge in many aspects of the immune response of DCs. Further studies need to be done to define the molecular mechanisms behind DC immune responses and to elucidate the contribution of DCs in other ocular diseases.

II. OBJECTIVES

Previous studies have determined the influence of the nervous system on the immune system, but conversely, the influence of immune cells on the nervous system, apart from the general protective role, has not been so widely studied. The various functions of resident immune cells have been assessed in corneal pathological conditions and diseases, however, their contribution to the maintenance of homeostasis remains elusive. Corneal DC depletion during steady state reduces the density of nerve endings in the centre of the cornea and causes epithelial defects and delayed post-wound nerve regeneration (Gao et al., 2016a). Although these results suggest that intraepithelial DC and sensory nerves may have intimate connections and are functionally interdependent, no functional or behavioural studies have been done to confirm this functional neuro-immune interaction.

The **general objective** of the present thesis is to determine the functional interaction between corneal DC and corneal nerves at steady-state conditions (that is, in absence of any corneal inflammation or damage) and its possible consequences in protective processes of the ocular surface such as nociceptive behaviour or tearing. For this purpose, short-term and long-term resident DC depletion was induced in the cornea of this mice model with the following **specific objectives**:

1. To determine the effects of the absence of corneal DC on corneal cold sensory nerve activity, analysing the changes in nerve terminal impulse (NTI) frequency and shape with *ex vivo* electrophysiological recordings;

2. To establish if the changes of corneal nerve activity are translated into a spontaneous behaviour of pain, monitoring the eye closure ratio in awake mice;

3. To study the effects of corneal DC depletion in basal tearing, by measuring tearing rate in superficially anaesthetized mice, and

4. To assess corneal DC distribution and morphology in the cornea under the different experimental conditions, by analysing the endogenous and/or immunostained fluorescence of whole-mount corneas.

Different studies have shown that the morphological association between corneal nerves and APCs seems to have a potential role on corneal health and disease, with a reduced association under injury or pathological conditions (Seyed-Razavi et al., 2014; Jamali et al., 2020). In order to further analyse this potential neuro-immune interaction morphologically, another objective of the thesis was to develop a mouse model in which DC and nerves were endogenously labelled with GFP (DCs) and tdTomato (nerves).

III. MATERIALS AND METHODS

1. Animals

CD11c-DTR transgenic mice (4–6 months-old) were used. Either male or female animals were included. CD11c-DTR mice carry a transgene encoding for a simian diphtheria toxin (DT) receptor (DTR) plus a green fluorescent protein (GFP) fusion protein under the control of the murine CD11c promoter, which makes CD11c+ cells sensitive to DT leading to DC depletion (Jung et al., 2002) (**Figure 13**). All the experiments were conducted in accordance with the institutional animal care guidelines and according to the Spanish Biomedical Research Act and the European Union Directive 2010/63/EU on the protection of animals used for scientific purposes. All experimental procedures were carried out according to the Spanish Royal Decree 53/2013 and followed a protocol approved by the Ethics Committee of the Universidad Miguel Hernández and the Generalitat Valenciana.
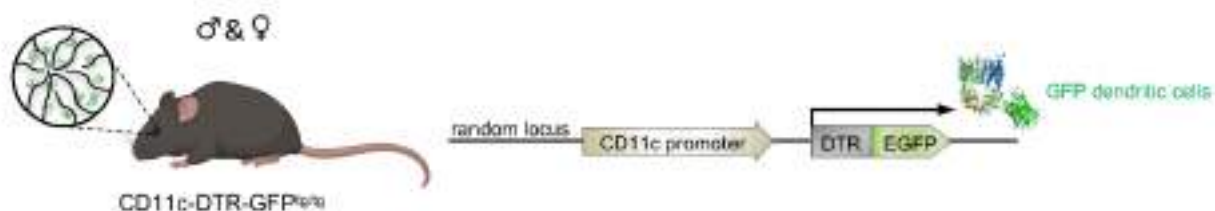
Figure 13. Schematic representation of the transgenic mice used in this study.

2. Diphtheria toxin solution

DT (Sigma-Aldrich, St Louis, MO) was prepared as a 1 mg/mL stock in sterile Phosphate-Buffered Saline 1x (PBS; Sigma-Aldrich, St Louis, MO) and stored at -80ºC. The day of injection, DT was thaw and then diluted with sterile PBS to a final concentration of 3 ng/μL for subconjunctival injections (sc).

3. Corneal DC depletion

The effects of short-term (ST) and long-term (LT) resident DC depletion on corneal sensory nerves were studied in eyes following bilateral subconjunctival injections of 30 ng of DT in 10 µl of PBS (5 µl nasal and 5 µl temporal), once (STDT) or repeated every two days for 8 days (LTDT) respectively, under 1-2% isoflurane anaesthesia (**Figure 14**). The reason behind DT injections every two days for 8 days was to avoid a possible DC repopulation from limbal vessels during this period of time. Besides, the effects of ST and LT effects of PBS injection were also tested with bilateral temporal and nasal subconjunctival injections of 10µl PBS following the same procedure (STPBS and LTPBS) (**Figure 14**). Controls were naïve (not receiving DT or PBS injections) CD11c-DTR mice. Additionally, CD11c-DTR mice 8 days after a single DT injection (DC recovery group, RC) were also studied (**Figure 14**). Corneal DC depletion or recovery was confirmed *in vivo* imaging (confocal/multiphoton microscope Leica SP5) performed prior to the electrophysiological recordings.
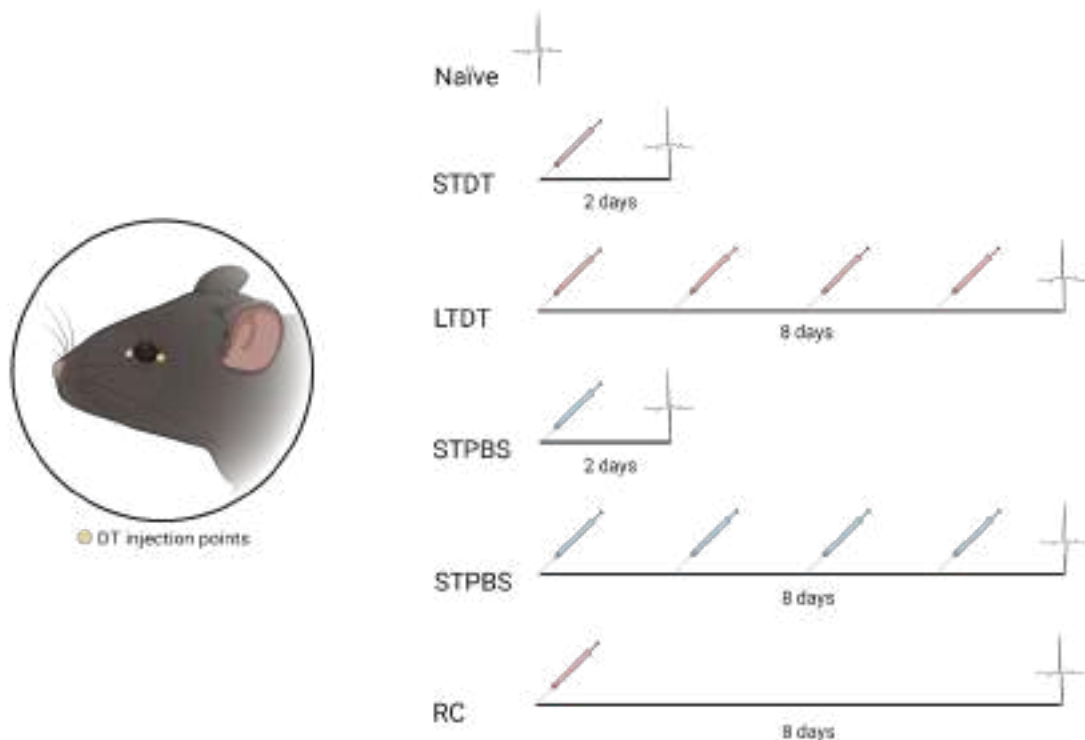
Figure 14. Experimental groups of animals included in this study. Number and time of injections are represented by the syringe drawings (red: DT, blue: PBS). Spike symbols at the end of each line represent

the day when electrophysiological recordings are carried out. Naïve: no injections. ST: short-term. LT: long-term. RC: DC recovery.

4. Electrophysiological recording of corneal nerve activity

Recordings of single corneal nerve terminal activity were performed *in vitro* as described in previous studies (Brock et al., 1998; Parra et al., 2010, 2014; González-González et al., 2017). In brief, mice were sacrificed with an overdose of sodium pentobarbitone (Dolethal®, Vetoquinol, France) injected intraperitoneally and both eyes were enucleated along with a short length of the optic nerve and surrounding tissues. The excised eyes were then pinned to the bottom of a silicone-coated (Sylgard 154®, Dow Corning. MI, USA) chamber and secured in place by continuous suction. The eye was continuously superfused with physiological saline solution of the following composition (in mM): NaCl (128), KCl (5), NaH_2PO_4 (1), $NaHCO_3$ (26), $CaCl_2$ (2.4), $MgCl_2$ (1.3) and glucose (10). The solution was gassed with carbogen (5% CO_2 and 95% O_2) to pH 7.4 and maintained at the desired temperature (basal temperature ~34°C) with a home-made Peltier device.

A borosilicate glass micropipette electrode with a tip diameter of about 50 μm filled with the physiological saline solution was gently placed in contact with the corneal surface using a micromanipulator (**Figure 15A, B**). Light suction was then applied through the pipette to produce a high-resistance seal with the corneal surface, allowing the recording of nerve impulses generated at single nerve terminals located beneath the electrode tip. Electrical signals were recorded with respect to an Ag/AgCl pellet placed inside the recording chamber (**Figure 15A,B**).

Nerve terminal impulses (NTIs) were amplified with an AC amplifier (Neurolog NL104, Digitimer, Welwyn, UK), filtered (high pass 9 Hz, low pass 5 kHz; Neurolog filter module NL124, Digitimer, Welwyn, UK) and stored at 25 kHz into a computer, using a CED micro-1401 interface and Spike2 v.8.02 software (both from Cambridge Electronic Design, Cambridge, UK). Only recordings containing NTIs originating from a single nerve terminal were analysed.

4.1. Experimental protocol

The recording pipette was placed at sequential points on the corneal surface until a site in which spontaneous or stimuli-evoked activity of a single nerve terminal was detected (**Figure 15B**). Responses to cold or mechanical stimuli were assessed, and if no spontaneous or stimulus-evoked activity was obtained, the electrode was moved to the next recording point. The eye was rotated as necessary to explore the whole corneal surface.

The same experimental protocol was applied to all cold thermoreceptor terminals. First, cold stimulation was performed by decreasing the perfusion solution temperature from 34º to 20ºC at a ~0.25ºC/s rate. When the peak temperature fall was attained, warming was applied to return to basal temperature. After a resting period of 3 minutes, a heating ramp from 34ºC to 48ºC was carried out (at ~0.25ºC/s rate), followed by cooling back to 34ºC. Three min afterwards, another heating stimulation ramp was performed. Finally, after 3 min of resting period, mechanical stimulation was made by gentle displacement of the recording pipette with the micromanipulator for 2 seconds.
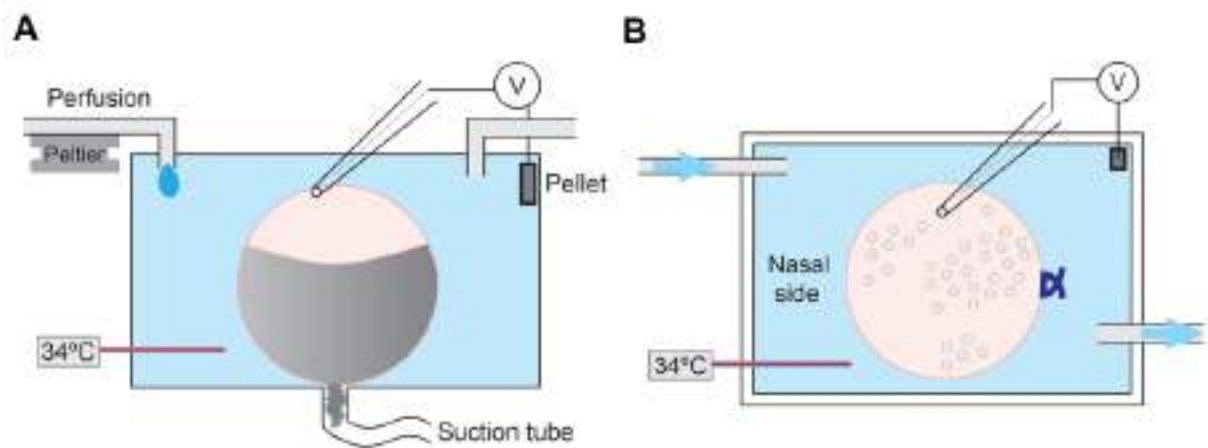
Figure 15. Experimental set-up used for extracellular recording of single nerve terminals. A. Schematic diagram of the lateral view of the chamber. **B.** Schematic diagram of the chamber showing the superior view of the cornea and the different points at which the recording electrode is placed during the experiment.

4.2 Analysis of electrical activity of cold thermoreceptors

The offline analysis of the electrophysiological recordings was done using Spike2 v.8.02 software (Cambridge Electronic Design, Cambridge, UK). NTIs detected during acquisition were filtered using a threshold-based criterion to distinguish them from noise. Although only single unit recordings were studied, some changes in the amplitude of NTIs were observed along the recording time, particularly associated with changes in temperature (Carr et al., 2003). The software was used to separate spikes with similar amplitudes and waveform shape, which were grouped in the same cluster (**Figure 16**).
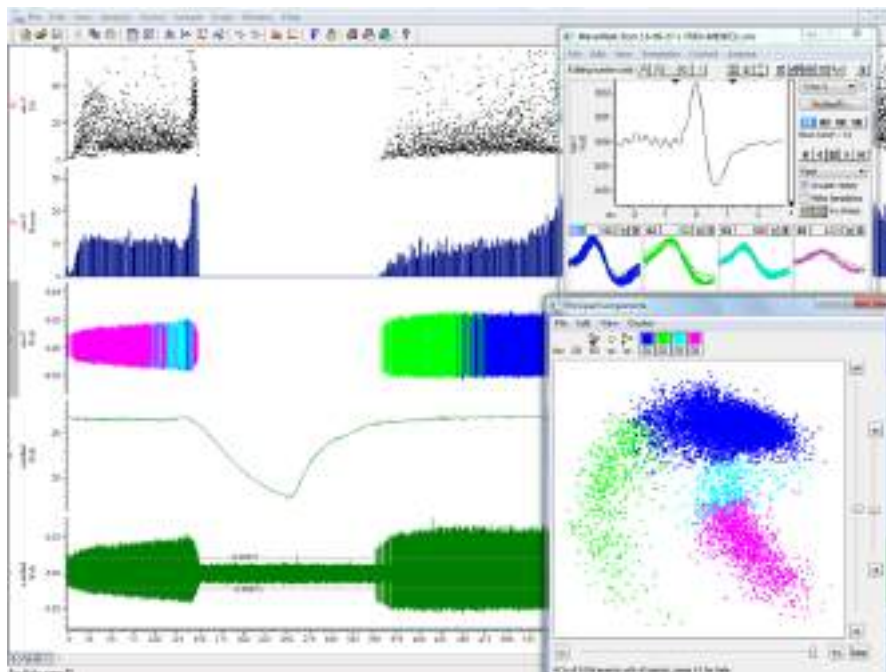
Figure 16. Use of Spike2 software to analyse the electrophysiological recordings. In the large window, NTI activity of a cold-sensitive terminal recorded from 10 min is shown. Traces from top to bottom are: instantaneous frequency (Hz); NTI mean firing rate (impulses per second); filtered NTI activity (μV); temperature of the perfusion solution near the eye (°C) and raw data of recorded NTI activity (μV). The small windows show the different groups of spikes generated with the threshold-based criterion. Based on the waveform shown in the upper window, all the spikes originated from the same sensory nerve ending, although its amplitude changes along the recording time. The different colours represent the different amplitudes of the spike during the recording. Principal components tool was used in order to improve the sorting.

Different parameters of the NTI activity were analysed (**Figure 17**): a) **background activity**: mean basal ongoing frequency in impulses per second (imp/s) at the basal temperature (~34°C) 60s before the onset of a stimulus; b) **Cooling threshold**:

temperature value (ºC) during a cooling ramp at which NTI frequency increased to a value 25% greater than the background activity; c) **Cooling response**: mean discharge rate (imp/s) in response to the cooling ramp; d) **Peak frequency** (PF): maximal firing frequency reached during the cooling ramp (imp/s); e)**Temperature at the peak frequency**: temperature at which PF occurs; f and h) **Heating Threshold**: the temperature (ºC) required to evoke firing in a heating ramp if the cold thermoreceptor has a response to heat; g and i) **Heating response**: mean discharge rate (imp/s) in response to the heating ramp if the cold thermoreceptor has a response to heat; j) **Qualitative mechanical response** (yes/no).
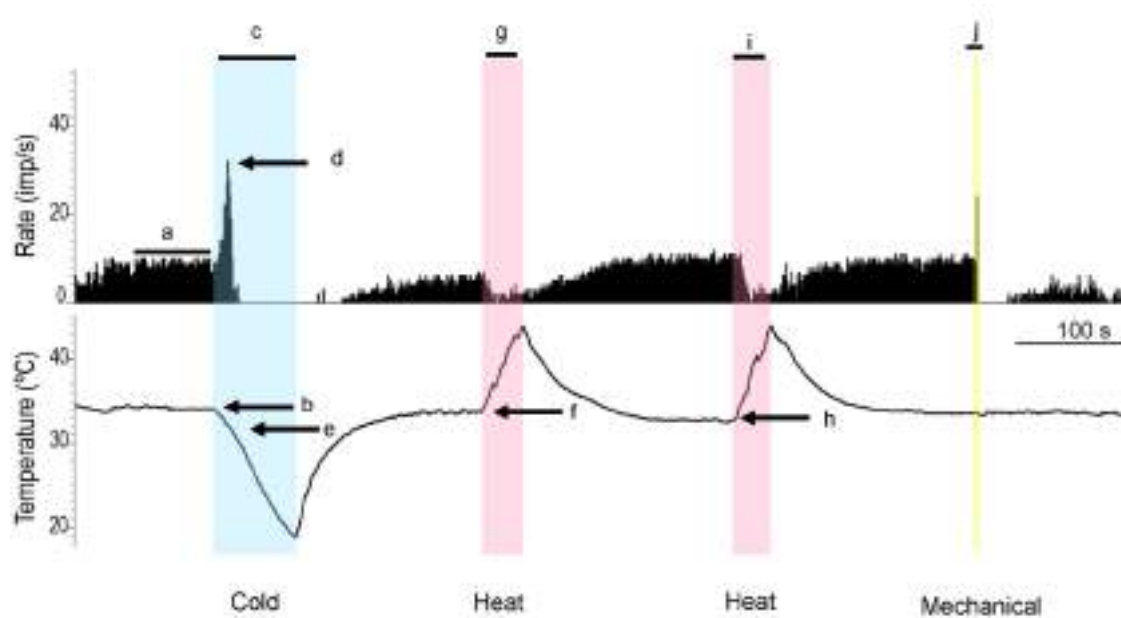
Figure 17. Experimental protocol and example of the change in NTI activity in a corneal nerve terminal evoked by different stimuli. Upper trace: Histogram of the firing frequency in impulses per second. Lower trace: Recording of the temperature of the perfusion solution in °C. The parameters used to quantify the responses to the stimuli were: (a) background activity, (b) cooling threshold, (c) cooling response, (d) peak frequency, (e) temperature at the peak frequency temperature, (f) heating threshold 1, (g) heating response 1, (h) heating threshold 2, (i) heating response 2 and (j) qualitative mechanical response. Each stimulus is represented in a different colour.

4.3 Analysis of cold thermoreceptor nerve impulse shape

Besides, we also analysed the shape of the NTIs recorded from cold thermoreceptors firing spontaneously at the basal temperature of 34ºC (ongoing activity). Based on a previous study (Brock et al., 2001), the following parameters were used for

that purpose (**Figure 18**): the positive peak amplitude (+peak, V), the negative peak amplitude (–peak, V), the maximum rate of voltage change during the initial upstroke and the downstroke of the NTI (+dV/ dt max and -dV/ dt max, V/s), the ratio between them (ratio), the total duration of the NTI (width, ms), and the depolarization (T1, ms) and repolarization times (T2, ms). Because the amplitude varied a lot in and between experiments, the maximum rate of voltage change during the initial upstroke and downstroke were normalised with respect to the NTI positive peak amplitude.
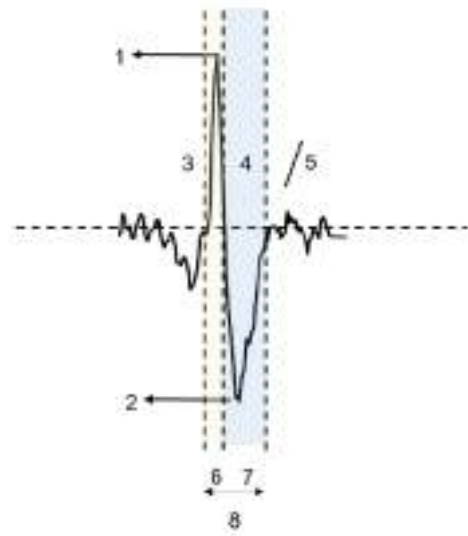
Figure 18. Basal NTI shape analysis. The parameters used to analyse the NTI shape were: **(1)** +peak (mV), **(2)** –peak (mV), **(3)** maximum rate of voltage change during the initial upstroke, +dV/ dt max, **(4)** maximum rate of voltage change during the downstroke, -dV/ dt max, **(5)** ratio between the maximum rate of voltage during the initial upstroke and downstroke, **(6)** depolarization time, T1, **(7)** repolarization time, T2 and **(8)** width (s).

5. Eye closure ratio

Spontaneous eye closure is a good index for monitoring eye pain. Its measurement was performed as previously described by other authors (Fakih et al., 2019, 2021). In photographs taken before and at different time points after DT or PBS injections in awake animals, the eye closure ratio was calculated by dividing the height by the width of the palpebral fissure measured with ImageJ software (NIH, Bethesda, MD, USA) (**Figure 19**).
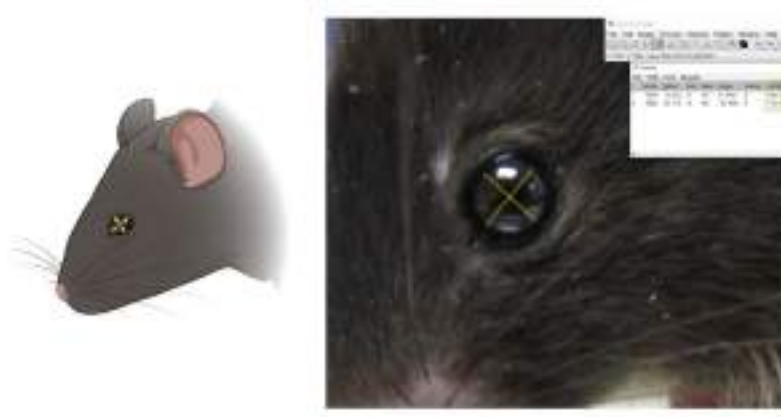
Figure 19. Use of ImageJ to measure spontaneous eye closure ratio.

6. Basal tearing rate measurement

Basal tearing rate was measured before and at different time points after DT or PBS injections. Mice were anaesthetised with isoflurane (1.5-2%; ISOFLO®, Esteve, S.A) and then the tearing rate was measured using commercial phenol red threads (Zone-Quick®, Menicon, Magoya, Japan) placed between the lower lid and the bulbar conjunctiva in the temporally side of the eye for 30s (**Figure 20**). These threads are yellow and change to red colour when wetted in contact with tears; thus, the length of red colour thread reflects the amount of tears (**Figure 20**). Tear rate is expressed as the entire length of the red portion of the thread in mm, measured with a calibrated scale under a stereomicroscope immediately after removal from the lid.
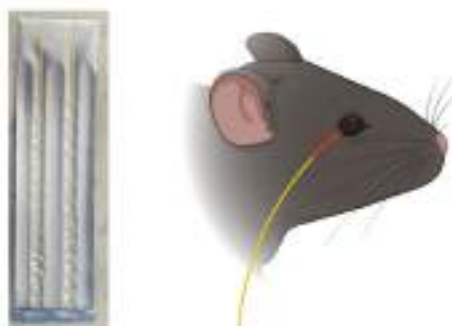
Figure 20. Scheme of basal tear rate measurement using a phenol red thread.

7. Whole-mount corneal tissue preparation

Mice were euthanized with cervical dislocation and the entire eyeball was enucleated and fixed in 4% paraformaldehyde for 2 hours at 4ºC by making a small hole in the limbus. Afterwards, 3 washes with PBS1x (10 minutes each) were carried out. Corneas with a small amount of limbus were excised under microscope. Cell nuclei were stained with 1 mM 4',6-diamidino-2-phenylindole, dihydrochloride (DAPI; ThermoFisher, Waltham, MA, USA) for 10 minutes and, after that, the tissue was rinsed with PBS1x (3 washes of 10 minutes). Different incisions were made to allow the tissue to lay flat and mounted with Fluoromount G mounting medium (Southern Biotech, Birmingham, AL, USA) in glass slides and coverslipped (#1.5 thickness). Finally, the corneas were examined using Leica THUNDER Imager Tissue with x10 and x40 objectives, visualising the DC endogenous GFP fluorescence. Afterwards, Imaris 9.3 software (Bitplane, Belfast, United Kingdom) was used to process the images.

8. Statistical analysis

Data was collected and processed for statistical analysis using SigmaStat software (SigmaStat v3.5; Systat Software Inc, Point Richmond, CA, USA). Values are expressed as mean ± SEM or as median ± interquartile range, as indicated, with n denoting the number of terminals.

Differences between two groups were compared with t-test or its non-parametric equivalent, the Mann-Whitney Rank Sum test. For more than two experimental groups, one-way analysis of variance (ANOVA) or Kruskal-Wallis on ranks test were used depending on the data distribution, and post-hoc comparisons were done by using Dunnett or Dunn's tests to find differences from naïve animals. Before and after differences were compared by using paired t-test, Wilcoxon signed-rank test or Repeated-Measures ANOVA, depending on the data distribution and the experimental group.

To analyse frequency distributions Chi- square or Fisher exact tests were used. $P=0.05$ or below was considered significant.

IV. RESULTS

1. Corneal cold thermoreceptor nerve terminal activity

1.1 Effects of DC depletion

1.1.1 In vivo visual confirmation of DC depletion after DT injections

Before testing the effect of DC absence on corneal cold sensory nerve activity, the local DC depletion in the cornea was ascertained by *in vivo* confocal imaging of the mouse cornea under isoflurane anaesthesia (**Figure 21**).
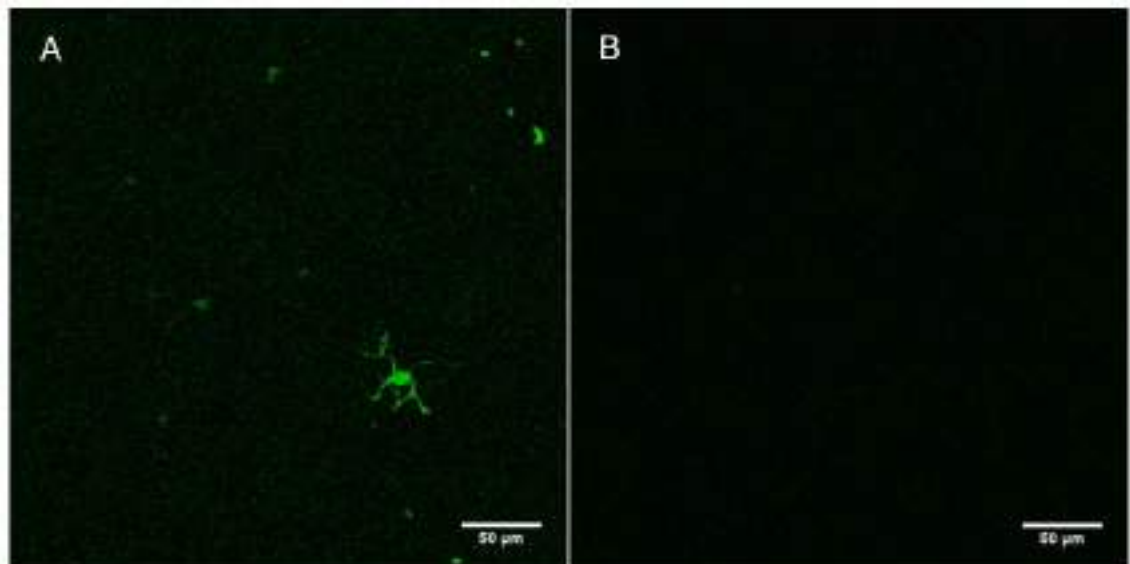
Figure 21. In vivo confocal images of a mouse cornea before and after local DC depletion induced by subconjunctival injection of DT.

1.1.2 Location of active cold thermoreceptor terminals in DC-depleted corneas

In naïve corneas, active cold nerve terminals can be found anywhere on the corneal surface, although the distribution of the different types of functional cold thermoreceptors varies from the centre to the periphery of the cornea in some species, being low background cold thermoreceptors more frequently found in the central cornea

than in the peripheral cornea (Gallar et al., 1993). Similarly, there are differences in the density of DCs, being more abundant in the limbal area than in the central cornea (Mastropasqua et al., 2006).

We first determined if the depletion of DC affected or not the distribution of active cold thermoreceptor nerve terminals within the cornea. We defined three different locations on the cornea: centre, middle periphery and periphery to define the position of the recorded terminals (**Figure 22**).

Figure 22. Defined anatomical locations of nerve terminals recorded in the mouse cornea. C: centre, M: middle periphery, P: periphery

The distribution of cold nerve endings was similar in naïve and short-term DC depletion conditions (**Table 1**). Regarding long-term DC depleted corneas, we observed that the percentage of cold thermosensitive terminals found in the central cornea was slightly lower than expected (LTDT: 23.5%; Naïve: 55%) while the percentage of cold terminals found in the peripheral cornea was slightly higher (LTDT: 35.3%; Naïve: 10%, **Table 1**). However, these percentages were not statistically different (p=0.08, Chi-Square).

1.1.3 Functional types of corneal cold thermoreceptors recorded in DC-depleted corneas

Cold thermoreceptors have been classified based on their background activity and cooling threshold into three different subpopulations: high background-low threshold (HB-LT), low background-high threshold (LB-HT) and mixed type (MTC) cold

thermoreceptors (Gallar et al, 1993; González-González et al., 2017; Bech et al., 2018). Based on that classification, our next step was to determine if the proportion of different functional types of cold nerve terminals (HB-LT, LB-HT and MTC), classified according to their background activity, cooling threshold, and cooling response, changed or not during the absence of DC.

In short-term DT depleted corneas, most cold thermoreceptor terminals were classified as HB-LT. Overall, cold thermoreceptors in short-term DC-depleted corneas had slightly higher background activity and cooling responses, and slightly lower cooling threshold (**Figure 23**). On the contrary, long-term DC depletion produced an increase in the proportion of LB-HT cold thermoreceptors. Under long-term DC depletion conditions, a slightly higher proportion of terminals presented low background activity, high threshold, and low impulse response to cooling ramps (**Figure 23**). Nevertheless, the observed proportions were not statistically significant (p=0.27, Chi-Square).
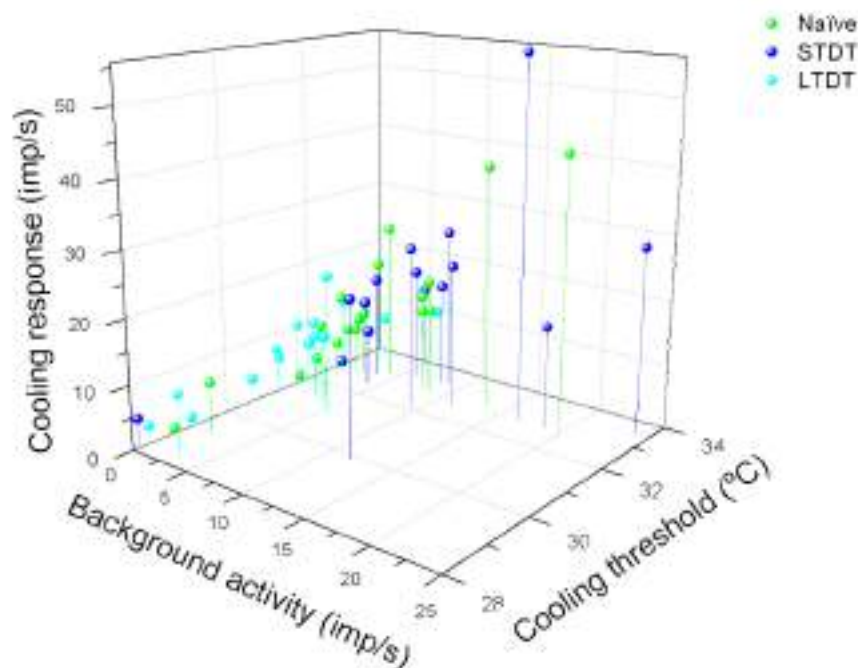
Figure 23. Cold thermoreceptor terminals under short-term and long-term corneal DC depletion. Each dot represents the values of background activity (in impulses/s), cooling threshold (in ºC) and mean discharge rate during the cooling ramp (cooling response, in impulses/s) of a single nerve terminal recorded in naïve cornas and DC-depleted corneas. STDT: short-term DC depletion. LTDT: long-term DC depletion.

1.1.4 Nerve activity of cold thermoreceptor terminals in DC-depleted corneas

We calculated the percentage of successful attempts to record an active terminal regarding the total number of attempts (success, %) in the different experimental groups. We observed that the percentage was very similar between all of them (naïve= 19%; STDT: 14%, p=0.14 and LTDT: 14.5%, p=0.23, Fisher exact test).

The activity of 54 cold thermoreceptors was studied (naïve, n=20, **Figure 24**; STDT, n=17, **Figure 25** and LTDT, n=17, **Figure 26**).

Figure 24. Example of a corneal cold nerve terminal recording in a naïve cornea. Upper trace: Histogram of the firing frequency at rest and in response to thermal and mechanical stimuli (asterisk) in impulses per second (Hz). Lower trace: Recording of the perfusion solution temperature in °C.
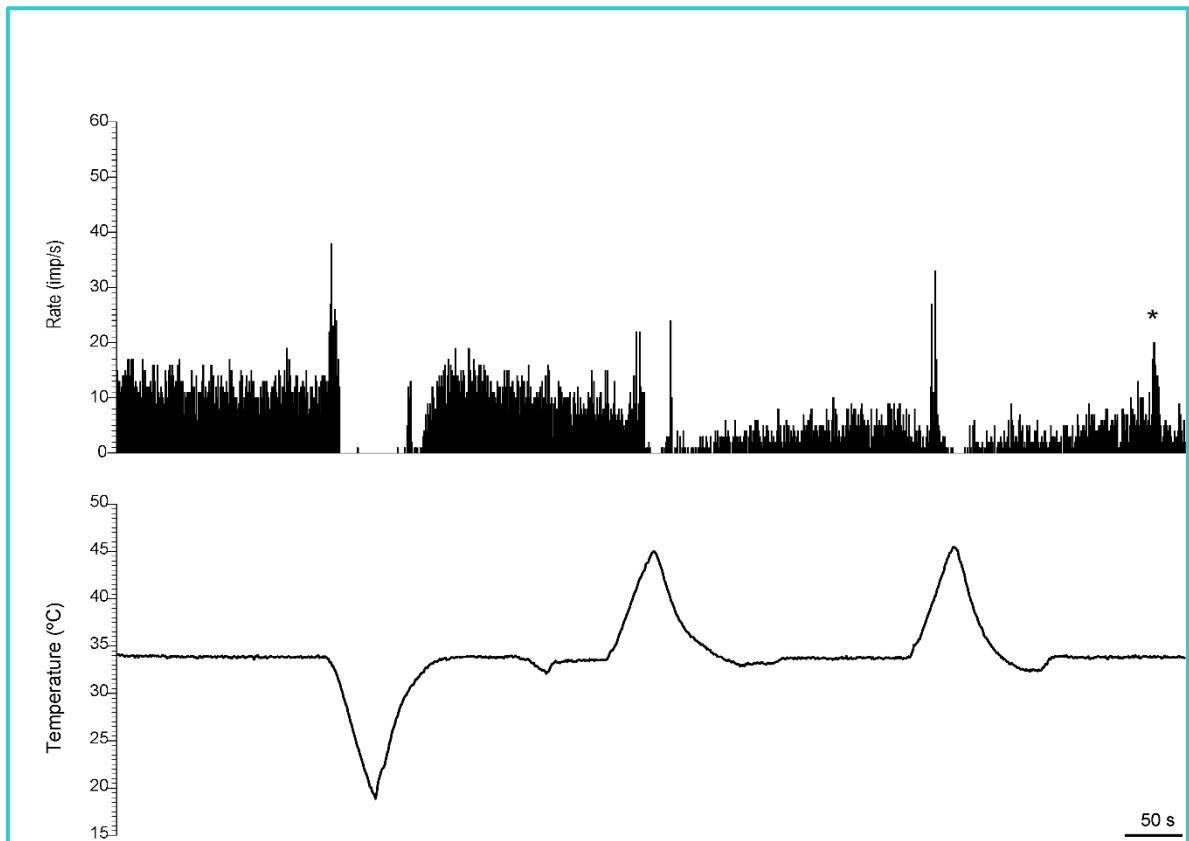
Figure 25. Example of a corneal cold nerve terminal recording under short-term DC depletion conditions. Upper trace: Histogram of the firing frequency at rest and in response to thermal and mechanical stimuli (asterisk) in impulses per second (Hz). Lower trace: Recording of the perfusion solution temperature in °C.

Figure 26. Example of a corneal cold nerve terminal recording under long-term DC depletion conditions. Upper trace: Histogram of the firing frequency at rest and in response to thermal and mechanical stimuli (asterisk) in impulses per second (Hz). Lower trace: Recording of the perfusion solution temperature in °C.

NTI activity analysis showed that short-term DC depletion produced a slight increase in background activity and in the mean discharge and maximum firing frequency during the cooling response (peak frequency) (**Table 1**). However, no significant differences were found neither in the cooling threshold or in the temperature at the peak frequency (**Table 1**).

On the other hand, the proportion of terminals responding to heat under short-term DC depletion conditions was significantly higher (58.82% STDT; 20% naïve; p=0.021, Fisher exact test; **Table 1**) and heating threshold during both heating ramps were significantly lower compared to naïve corneas (p=0.003 heating threshold 1; p=0.003 heating threshold 2; **Table 1**, **Figure 27A, B**), although no significant changes were found in the mean response rate to heat in none of the heating ramps.

When we quantified the proportion of terminals responding to mechanical stimulation, we found that it was significantly lower under short-term DC depletion conditions (30% short-term DC depletion; 75% naïve; p=0.045; Fisher exact test, **Table 1**).
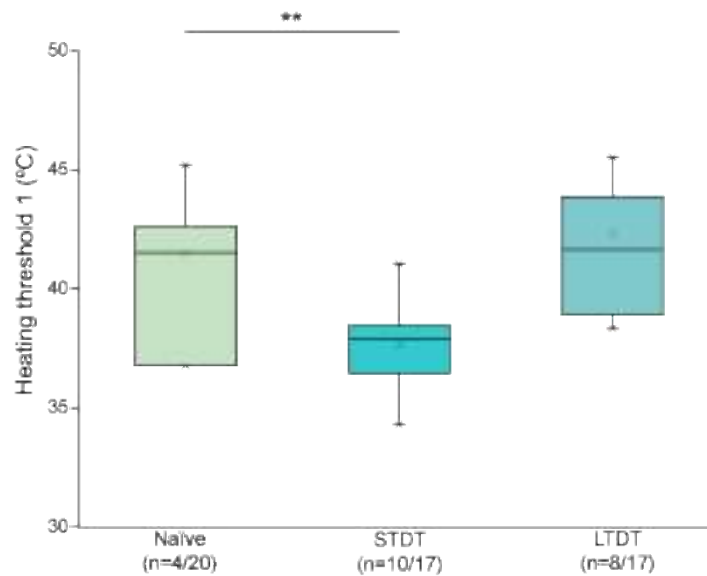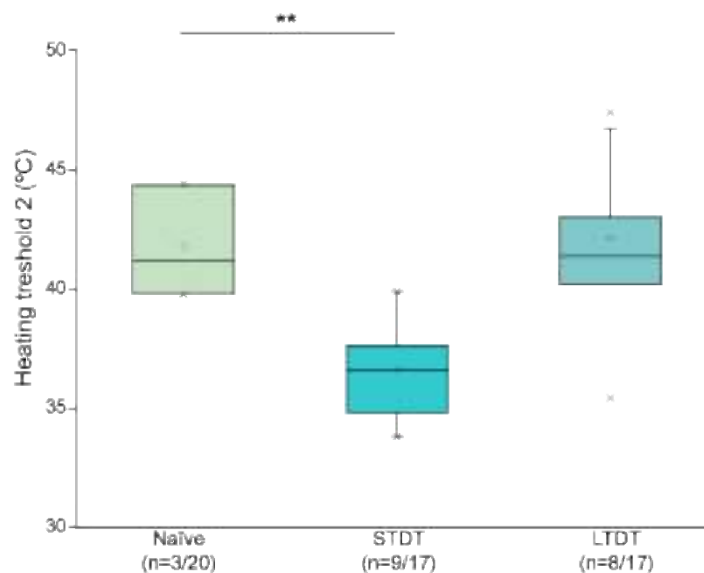
Figure 27. Heating threshold of cold thermoreceptor terminals measured during heating ramps in naïve and DC-depleted corneas. Heating threshold 1 (**A**), heating threshold 2 (**B**). STDT: short-term DC depletion, LTDT: long-term DC depletion. **$p \leq 0.005$; One Way Analysis of Variance and post-hoc comparisons using Dunnett test, differences from naïve.

Long-term DC depletion produced a significant increase in the cooling threshold (p=0.006) and in the temperature at the peak frequency during the cooling ramp (p=0.003), being necessary big drops of temperature to elicit cooling responses (**Table 1**; **Figure 28A, B**). However, no differences were found in the mean discharge or in the maximum firing frequency during the cooling response (peak frequency) (**Table 1**) compared to naïve.

Under long-term DC depletion conditions, the heating thresholds and responses were very similar to those in naïve animals. Besides, the proportion of terminals responding to heat was not statistically different (47.06% LTDT; 20% Naïve; p=0.16, Fisher exact test) and neither was the proportion of cold terminals responding to mechanical stimulation (69% long-term DC depletion; 75% naïve; p=1, Fisher exact test, **Table 1**).
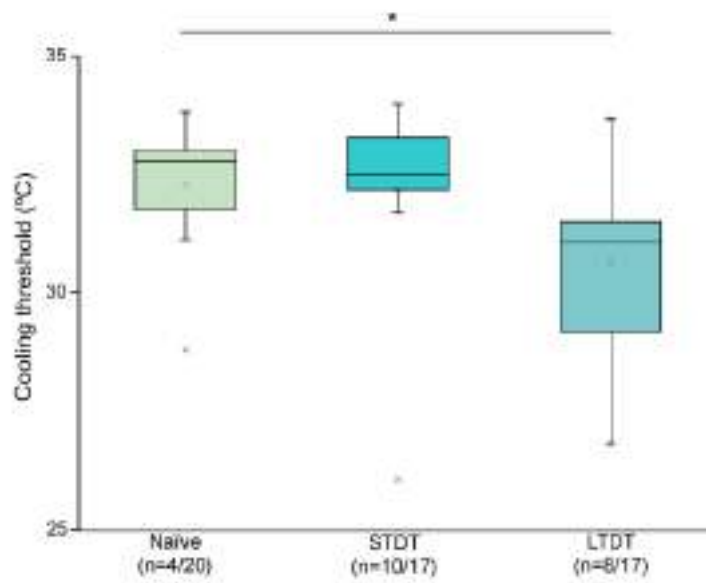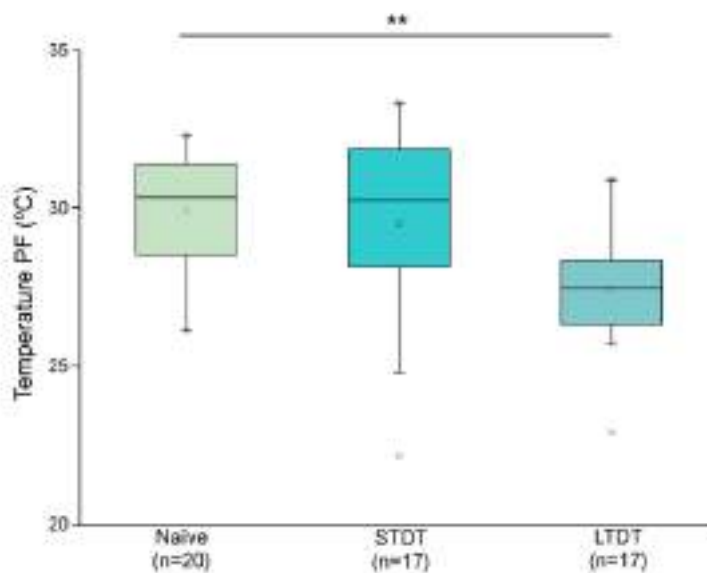
Figure 28. Cooling threshold (A) and temperature to reach the peak frequency (PF; B) in naïve and DC-depleted corneas. STDT: short-term DC depletion, LTDT: long-term DC depletion. *p≤0.05, **p≤0.005; Kruskal-Wallis One Way Analysis of Variance on Ranks and post-hoc comparisons using Dunn's test, differences from naïve.

1.1.5 Changes in nerve terminal impulse shape in DC-depleted corneas

The shape configuration of the ongoing NTIs in naïve, short-term and long-term DC-depleted corneas was biphasic in all the cases (**Figure 29A,B,C**). There were some

differences in the NTI time course under long-term DC depletion conditions. The normalised maximum rate of voltage change during the initial upstroke (+dV/dt max) was slightly slower (**Table 2**; **Figure 29C**) and the maximum rate of voltage change during the downstroke (-dV/dt max) was significantly slower in LTDT conditions than in naïve corneas (p=0.025: **Table 2**; **Figure 29C**).

The ratio between the maximum rate of voltage change during the initial upstroke and the downstroke reflected that in naïve corneas the rate of voltage change during the downstroke was faster than that during the upstroke, and that in short-term and long-term DC depleted corneas both rates were more similar to each other (**Table 2**).

Besides, in long-term DC depletion conditions, duration of NTIs (width) was significantly increased compared with naïve corneas (p=0.009; **Table 2**), having both significantly longer depolarization (T1) and repolarization times (T2) (p=0.035 and p=0.01 respectively; **Table 2**).
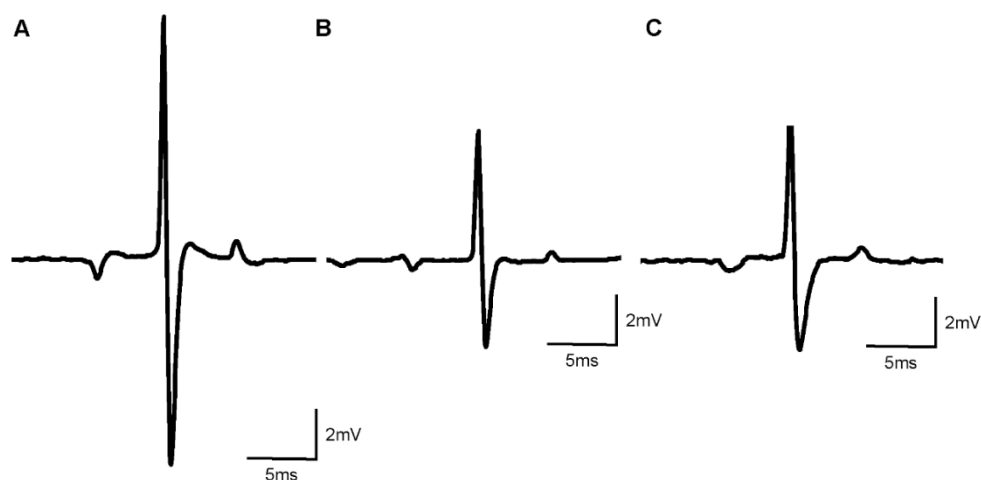
Figure 29. Representative NTIs recorded from cold thermoreceptors at basal temperature (34°C) in naïve and DC-depleted corneas. A. Naïve. **B**. Short-term DC depletion (STDT). **C.** Long-term DC depletion (LTDT). The amplitude of the NTI changed a lot in and between experimental groups. Because of that, the maximum rate of voltage change during the initial upstroke and downstroke were normalised with respect to the NTI positive amplitude of each recorded unit.

1.2 Effects of saline injection (sham group)

To exclude the possibility that the changes observed in nerve activity were not due to DC depletion but to the subconjunctival injection procedure, we injected two different

groups of animals in the same conditions as in STDT and LTDT but injecting PBS instead of DT. These groups were named short-term PBS (STPBS) and long-term PBS (LTPBS). PBS injections had no effects on the presence of DC in the cornea.

1.2.1 Location of active cold thermoreceptor terminals in PBS injected eyes

We defined the same three different corneal anatomical locations as in DC depletion conditions (see **Figure 22**).

We did not find significant differences in cold thermoreceptors anatomical distribution on the cornea (p=0.249, Chi-Square), although most activity found in PBS-injected animals were found in the periphery (peripheral units: STPBS 42.86%; LTPBS 37.5%; naïve 10%; **Table 1**).

1.2.2 Functional types of cold thermoreceptor recorded in PBS injected eyes

The functional distribution of cold thermoreceptors into HB-LT, LB-HT and MTC in both short-term and long-term PBS injection conditions was similar in all experimental groups (p=0.116, Chi-Square; **Figure 30**).
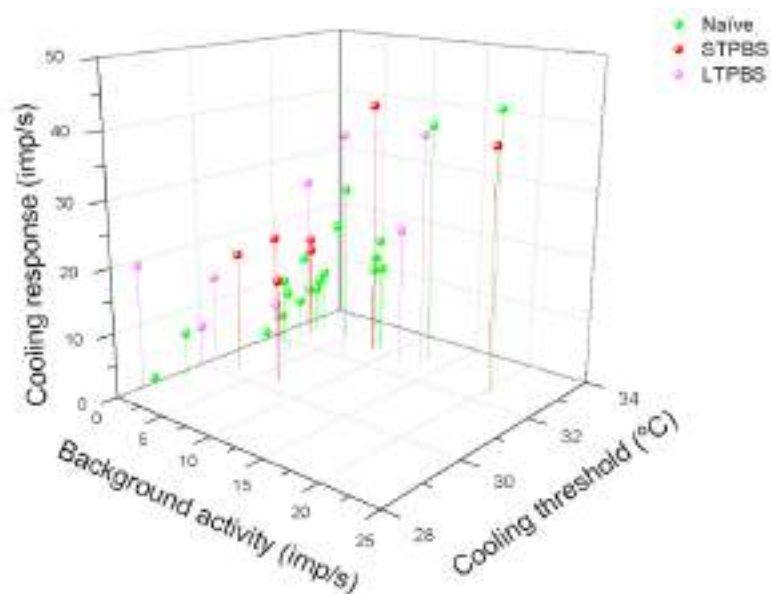
Figure 30. Cold thermoreceptor terminals recorded under short-term and long-term PBS injection conditions. STPBS: short-term PBS injections. LTPBS: long-term PBS injections.

1.2.3 Nerve activity of cold thermoreceptor terminals in PBS-injected eyes

The success in recording active terminals was lower in PBS injected corneas, being only 9.35% in the case of STPBS (p=0.02, Fisher exact test) and 8.07% in LTPBS corneas (p=0.0002, Fisher exact test).

The activity of 35 cold thermoreceptors was studied (naïve, n=20, **Figure 24**; STPBS, n=7, **Figure 31** and LTPBS, n=8, **Figure 32**).
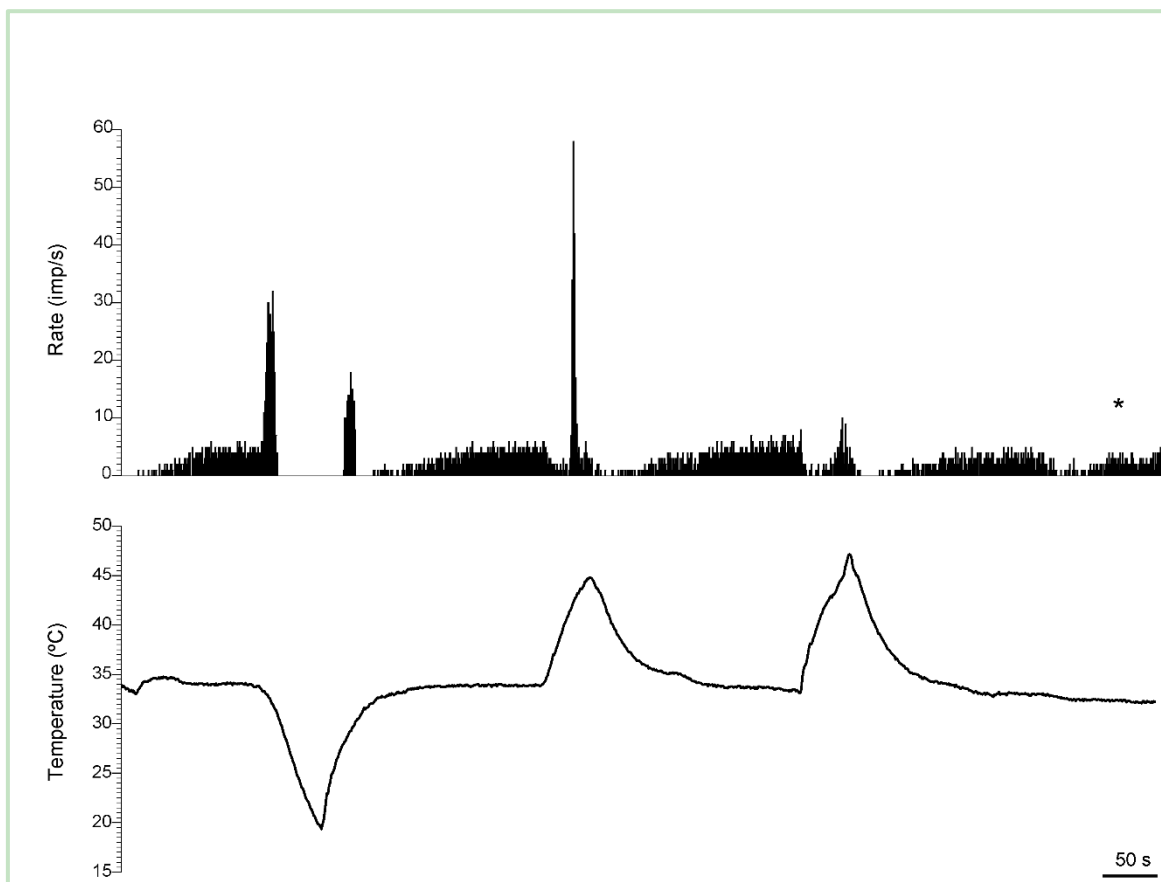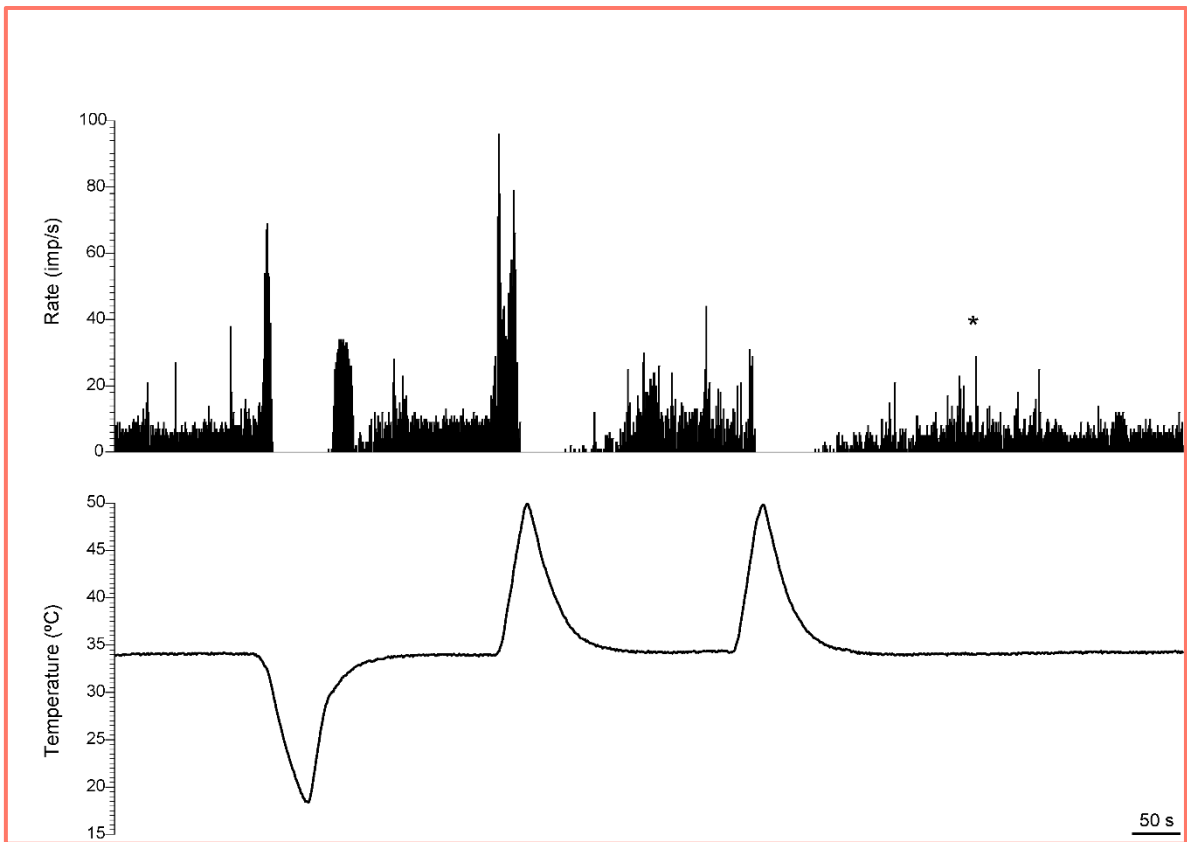

Figure 31. Example of a corneal cold nerve terminal recording under short-term PBS injection conditions. Upper trace: Histogram of the firing frequency at rest and in response to thermal and mechanical stimuli (asterisk) in impulses per second (Hz). Lower trace: Recording of the perfusion solution temperature in °C.
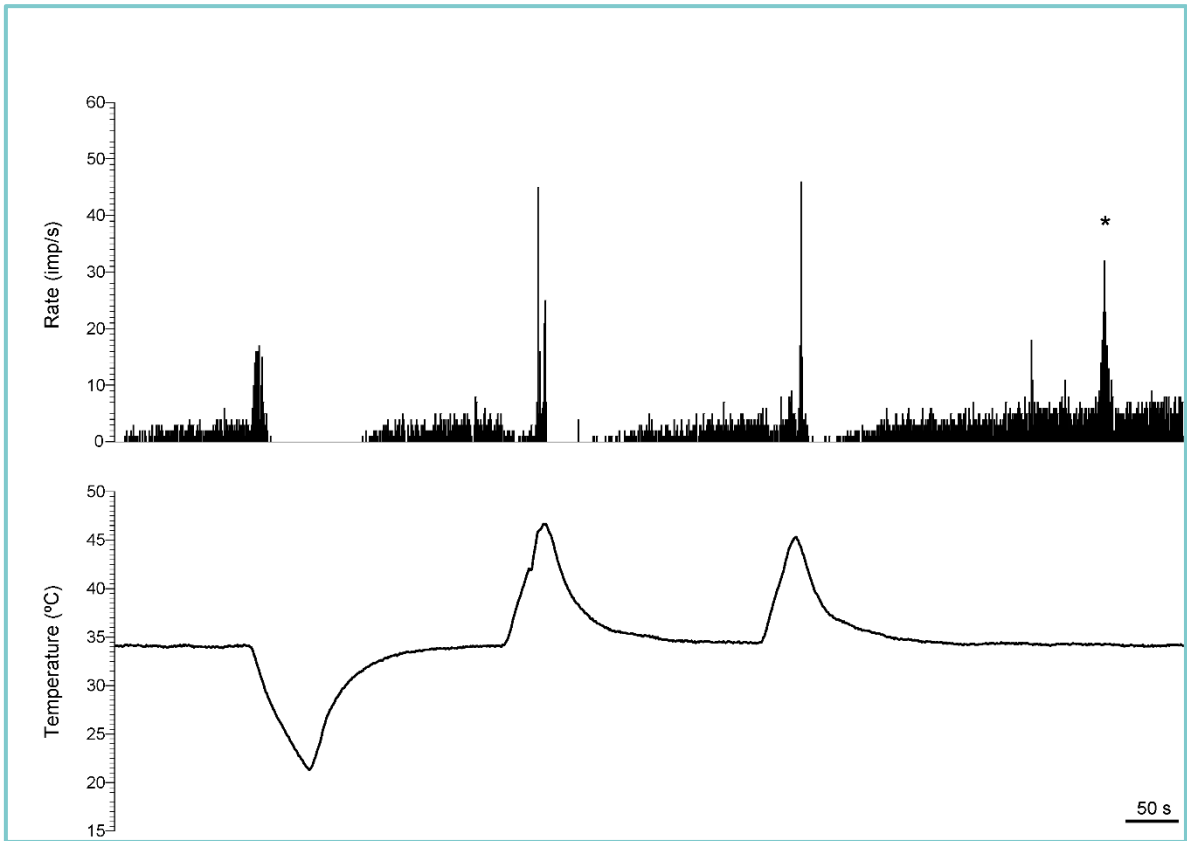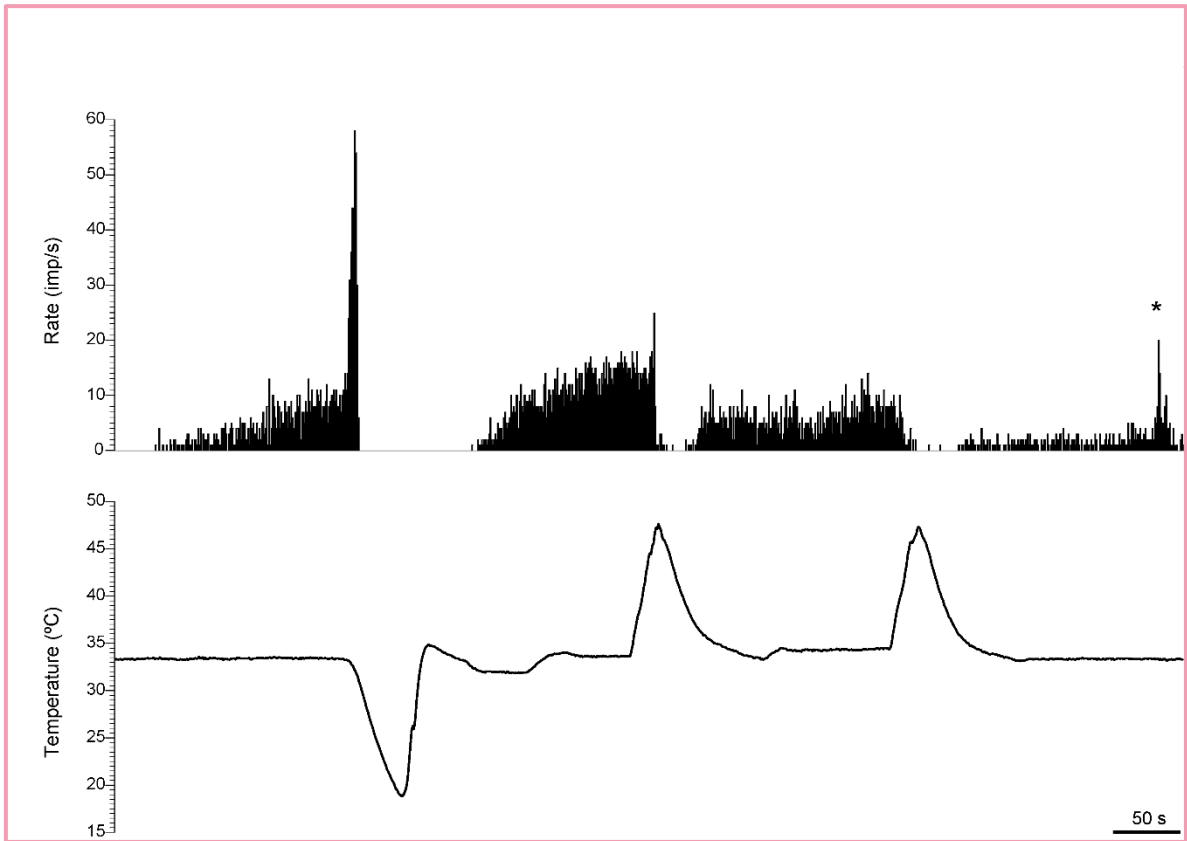
Figure 32. Example of a corneal cold nerve terminal recording under long-term PBS injection conditions. Upper trace: Histogram of the firing frequency at rest and in response to thermal and mechanical stimuli (asterisk) in impulses per second (Hz). Lower trace: Recording of the perfusion solution temperature in °C.

The NTI activity analysis of sham groups showed that the cooling response and the peak frequency during the cooling ramp were significantly higher in STPBS than in naïve corneas (cooling response, p=0.022; peak frequency, p=0.024; **Table 1**, **Figure 33A, B**), although the background activity, cooling threshold and temperature at the peak frequency were similar in STPBS and naïve corneas (**Table 1**). Regarding heating responses, a slight increase in the heating responses and no changes in heating thresholds were observed in STPBS group (**Table 1**). Similarly, the proportion of cold terminals responding to mechanical stimulation in STPBS corneas was not statistically different (66,67% STPBS and 75% naïve, p= 0.138; Fisher exact test, **Table 1**).
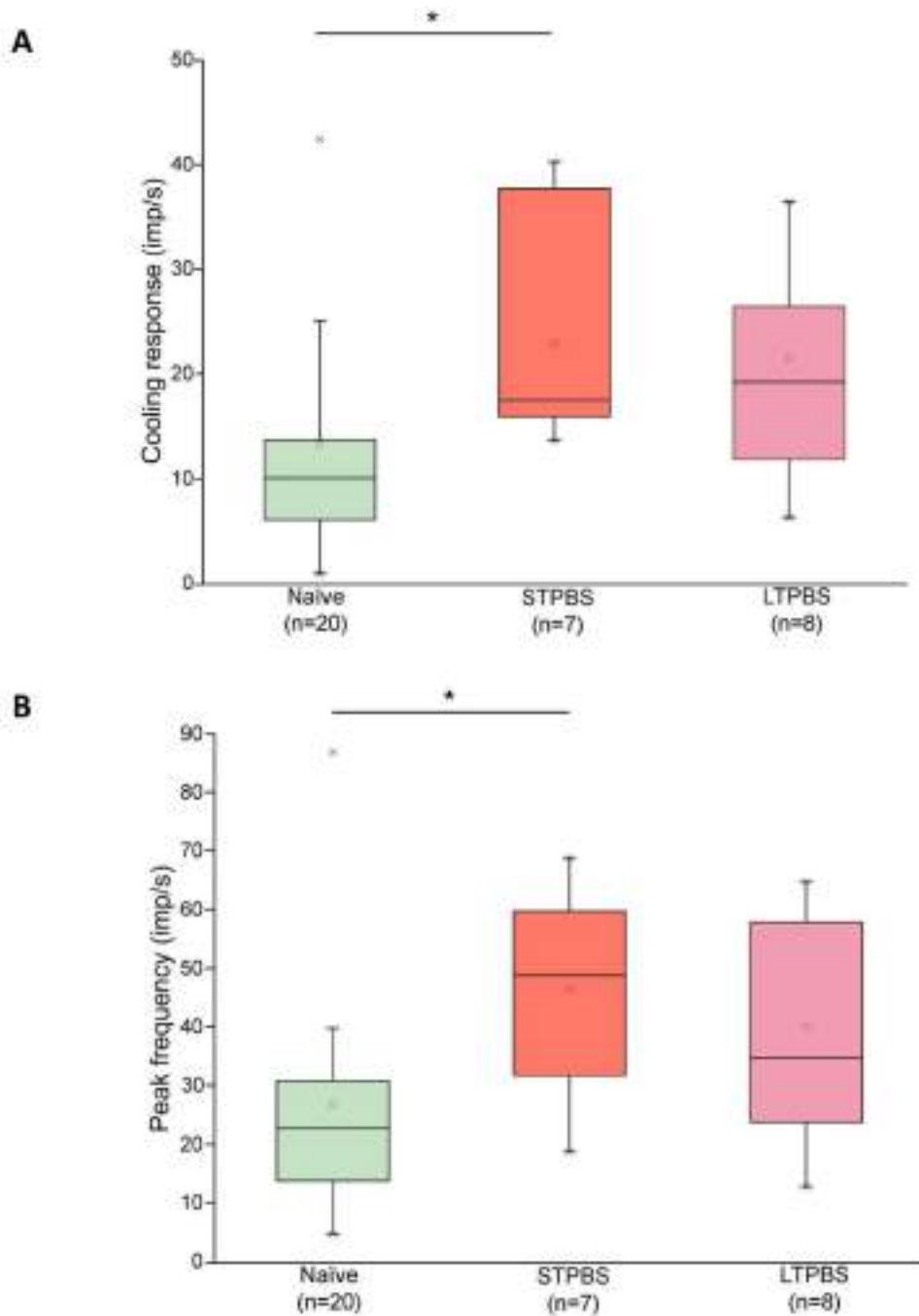
Figure 33. Mean discharge rate (A) and peak frequency (B) during the cooling ramp in naïve and after PBS injection. Cooling response (mean discharge rate, in impulses/s), Peak frequency (PF, in Hz). STPBS: short-term PBS injection, LTPBS: long-term PBS injection. *p≤0.05; Kruskal-Wallis One Way Analysis of Variance on Ranks and post-hoc comparisons using Dunn's test, differences from naïve.

When we analysed the NTI activity under long-term PBS injection conditions and naïve corneas, we found no significant differences in the values of the analysed

parameters, although we observed a slight decrease in the proportion of terminals responding to mechanical stimulation (25% LTPBS; 75% naïve, p=1, Fisher exact test).

Overall, results showed that the effects produced just by the subconjunctival injection of PBS were not the same as those produced by DC depletion induced by DT exposure.

1.2.4 Changes in Nerve Terminal Impulse shape in PBS-injected eyes

The shape configuration of the NTIs recorded at basal temperature (34ºC) in STPBS and LTPBS was also biphasic in all the cases (**Figure 34A, B,C**).

In PBS-injected eyes there were no differences in the normalised maximum rate of voltage change during the initial upstroke (+dV/dt max) or during the downstroke (-dV/dt max) compared to naïve (**Table 2**).

The ratios between the maximum rate of voltage change during the initial upstroke and downstroke reflected that mainly in short-term PBS injection conditions, the rate of voltage change during the downstroke was faster than that in the upstroke, although this ratio was not statistically significant compared to naïve (**Table 2**).

Nevertheless, in STPBS corneas, duration of NTIs (width) was significantly increased (p=0.018; **Table 2**, **Figure 34B**), as well as the repolarization time (t2) (p=0.005; **Table 2**, **Figure 34B**).
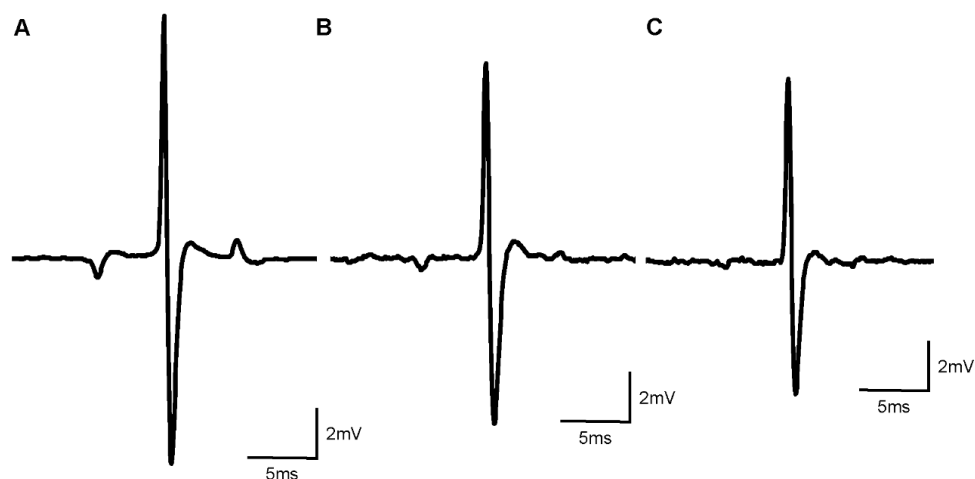
Figure 34. Representative basal NTIs of cold thermoreceptors recorded in naïve and PBS-injected conditions.: A. Naïve. **B**. Short-term PBS injection (STPBS). **C.** Long-term PBS injection (LTPBS). The amplitude of the NTI varied a lot in and between experimental groups. Because of that, the maximum rate of voltage change during the initial upstroke and downstroke were normalised with respect to the NTI positive amplitude in all the cases.

1.3 DC repopulation

1.3.1 In vivo visual confirmation of corneal DC repopulation

We sought to investigate the effects of DC repopulation of previously DC-depleted corneas on cold thermoreceptors. For that purpose, 8 days after a single DT injection, we ascertained the recovery of DCs repopulating both the centre and the periphery of the cornea by *in vivo* confocal microscopy. We then recorded cold NTI activity of this DC recovery group (RC) and compared it with that of cold thermoreceptors in naïve animals.

1.3.2 Location of cold thermoreceptor terminals in DC repopulated corneas

The anatomical distribution of cold thermoreceptors within the cornea was similar to that found in naïve animals. (p=0.97; Chi-Square, **Table 1**).

1.3.3 Functional types of corneal cold thermoreceptors recorded in DC repopulated corneas

As it was the case for the location, the functional distribution of cold thermoreceptors was not significantly different in RC animals (p=0.436, Chi-Square). However, it should be mentioned that no cold thermoreceptors with the specific functional characteristics of LB-HT were found in RC corneas (**Figure 35**).
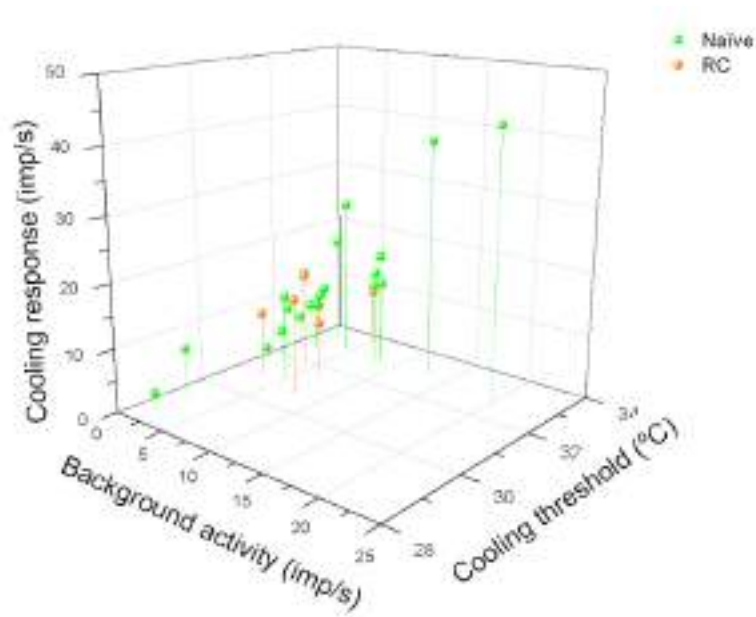
Figure 35. Functional distribution of cold thermoreceptors after corneal DC repopulation. RC: Recovery of corneal DCs after DC depletion.

1.3.4 Nerve activity of cold thermoreceptor terminals in DC repopulated corneas

The proportion of active terminals under DC recovery conditions, and therefore the success in recording them, was 12.87%, similar to naïve corneas (p=0.2, Fisher exact test). The activity of 28 cold thermoreceptor terminals was compared (Naïve: n=20, **Figure 24**; RC: n=8, **Figure 36**).
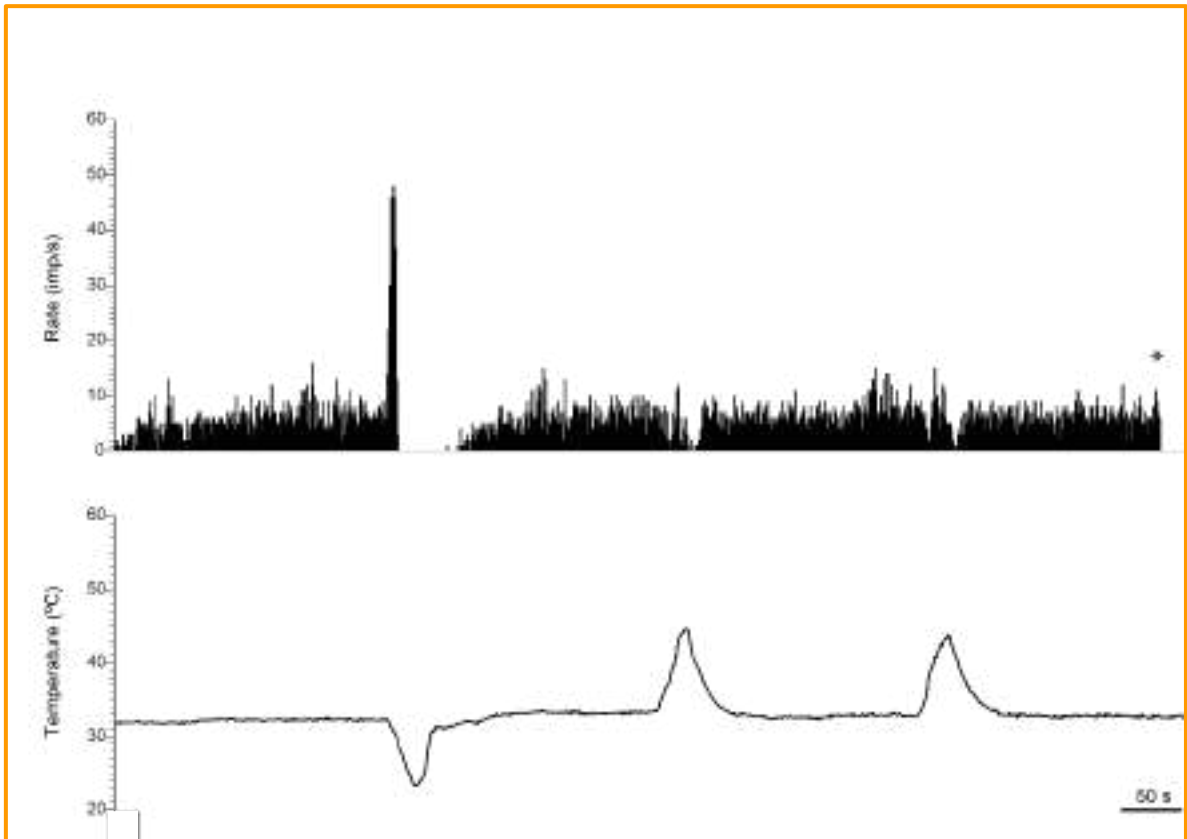
Figure 36. Example of a corneal cold nerve terminal recorded under DC recovery conditions. Upper trace: Histogram of the firing frequency at rest and in response to thermal and mechanical stimuli (asterisk) in impulses per second (Hz). Lower trace: Recording of the perfusion solution temperature in °C.

There were no significant differences in none of the analysed parameters of NTI activity in RC compared to naïve corneas (**Table 1**). In RC cold thermoreceptors had slightly higher background activity at the basal temperature of 34ºC, but in general cooling and heating responses were similar to those in naïve animals.

We observed that under DC recovery conditions, heating thresholds were slightly lower compared to naïve (**Table 1**), but this decrease was not statistically significant. Similarly, the proportion of cold terminals responding to mechanical stimulation was not significantly different (50% recovery; 75% naïve; p=0.33, Fisher exact test, **Table 1**).

In the light of these results, corneal DC repopulation seemed to produce almost a functional recovery of the nerve activity, being the spontaneous and stimulus-evoked activity similar to that of naïve corneas.

1.3.5 Changes in cold nerve terminal impulse shape in DC repopulated corneas

The shape of the NTIs recorded at the basal temperature of 34ºC in RC corneas was also biphasic (**Figure 37A,B**). The maximum rate of voltage change during the initial upstroke and downstroke, and the ratio between them were very similar to those in naïve conditions (**Table 2**).

A slight increase in the width and in depolarization (t1) and repolarization times (t2) was observed, but the differences were not statistically significant (**Table 2**).
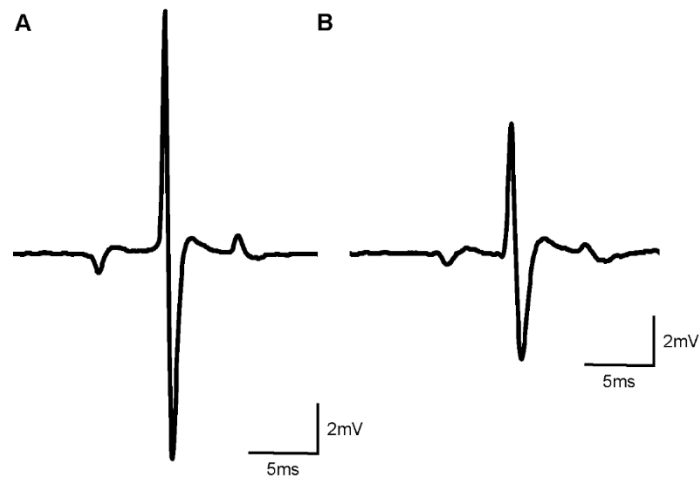
Figure 37. Representative basal NTIs recorded from cold thermoreceptor terminals in naïve and DC recovery conditions. A. Naïve. **B**. DC repopulated cornea after DC depletion (RC). The amplitude of the NTI changed a lot in and between experimental groups. Because of that, the maximum rate of voltage change during the initial upstroke and downstroke were normalised with respect to the NTI positive amplitude in all the cases.

Table 1. Cold thermoreceptor responses to thermal and mechanical stimulation in naïve corneas, under short-term (STDT) and long-term (LTDT) DC depletion, after short-term (STPBS) and long-term (LTPBS) PBS injections, and under DC repopulation of DC-depleted corneas (RC).

	Naïve	STDT	LTDT	STPBS	LTPBS	RC
No. of terminals	20	17	17	7	8	8
Location (% of units)						
Central cornea	55.00	47.06	23.50	42.86	25.00	50.00
Middle peripheral cornea	35.00	47.06	41.20	14.28	37.50	37.50
Peripheral cornea	10.00	05.88	35.30	42.86	37.50	12.50
Ongoing activity at 34°C (imp/s)	4.4±1.1	9.0±1.8	2.7±0.6	6.1±2.7	5.2±1.8	8.6±3.4
Response to cooling ramp from 34°C to 15°C						
Cooling threshold (°C)	32.3±0.3	32.2±0.4	30.7±0.5*	31.9±0.4	31.2±0.6	31.9±0.4
Cooling response (imp/s)	13.4±2.4	18.9±3.2	09.0±1.1	23.0±4.2*	21.6±3.9	17.5±3.4
Peak frequency (imp/s)	27.1±4.2	40.3±7.4	19.8±2.5	46.7±6.8*	40.3±7.0	33.8±5.9
Temperature at the peak frequency (°C)	30.0±0.4	29.6±0.8	27.5±0.5**	29.3±1.2	29.3±0.4	23.3±1.4
Response to heating ramp 1 from 34°C to 50°C						
No. of responding terminals	4/20	10/17	8/17	4/7	5/8	5/8
Heating threshold (°C)	41.6±1.8	37.7±0.7**	42.3±1.0	41.25±1.9	44.5±1.5	38.00±2.1
Heating response (imp/s)	9.3±4.5	7.9±1.4	6.4±2.9	37.6±12.0	21.2±7.4	8.3±2.6
Response to heating ramp 2 from 34°C to 50°C						
No. of responding terminal	3/20	9/17	8/17	3/7	3/8	4/8
Heating threshold (°C)	41.8±1.4	36.6±0.7**	42.1±1.3	42.5±0.9	44.8±1.5	38.9±1.7
Heating response (imp/s)	21.6±13.9	11.3±4.6	08.00±3.5	35.7±15.2	27.1±11.3	09.8±3.0

Response to mechanical stimulation	15/20	3/10	9/13	4/6	2/8	3/6

Data are mean ± SEM, *p≤0.05, **p≤0.005; One Way ANOVA or Kruskal-Wallis One Way Analysis of Variance on Ranks, post-hoc comparisons using Dunnett or Dunn's test, differences from naïve.

Table 2. Shape of NTIs recorded at basal temperature of 34ºCs in naïve corneas and under different DC depletion conditions.

	Naïve	STDT	LTDT	STPBS	LTPBS	RC
n	18	11	16	9	7	7
+peak (mV)	10.8 ± 0.89	5.7 ± 0.50	8.1 ± 0. 60	10.7 ± 0.80	9.3 ±1.10	5.2 ± 0.80
-peak (mV)	-7.8 ± 0.90	-3.5 ± 0.50	-5.9 ± 0.60	-8.4 ± 0.70	-6.5 ± 0.60	-3.9 ± 0.70
+dV/dt max (norm, V/s)	2557.4 ± 135.84	2574.7 ± 192.84	2210.1 ± 140.49	1937.2 ± 243.91	2506.4 ± 91.99	2190.4 ± 204.75
-dV/dt max (norm, V/s)	-3391.1 ± 153.86	-2971.1 ± 130.22	-2813.9 ± 165.27*	-2913.6 ± 225.48	-3338.8 ± 190.42	-3026.3± 225.68
Ratio	-0.7643 ± 0.0356	-0.8718 ± 0.0421	-0.8098 ± 0.0609	-0.6636 ± 0.0711	-0.7756 ± 0.0757	-0.7257 ± 0.0541
Width (ms)	1.5 ± 0.07	1.7 ± 0.12	1.9 ± 0.10*	2.0 ± 0.18*	1.5 ± 0.05	1.8 ± 0.16
T1 (ms)	0.6 ± 0.03	0.6 ± 0.04	0.7 ± 0.04*	0.8 ± 0.10	0.6 ± 0.10	0.7 ± 0.07
T2 (ms)	0.9 ± 0.04	1.1 ± 0.09	1.2 ± 0.07*	1.2 ± 0.08**	0.9 ± 0.04	1.1 ± 0.09

Data are mean ± SEM, *$p \leq 0.05$, **$p \leq 0.005$; One Way ANOVA or Kruskal-Wallis One Way Analysis of Variance on Ranks, post-hoc comparisons using Dunnett or Dunn's test, differences from naïve. STDT: short-term DC depletion, LTDT: long-term DC depletion, STPBS: short-term PBS injections, LT-PBS: long-term PBS injections, RC: DC repopulation of previously DC-depleted corneas.

2. Pain behaviour in awake mice

2.1 Signs of pain under DC depletion conditions

To quantify the spontaneous pain experienced by awake mice under the different DC depletion conditions, we measured the eye closure ratio in DT injected animals.

Signs of spontaneous pain were observed under both STDT and LTDT conditions (**Figure 38**), being the eye closure ratio significantly lower than before DT-injections (STDT: 0.99 ± 0.02 before DT *vs.* 0.21 ± 0.03 at 48h after DT, n=23, p≤0.001, Wilcoxon signed rank test, **Figure 39**; LTDT: 0.92 ± 0.02 before DT *vs.* 0.18 ± 0.02 at 48h *vs* 0.45 ± 0.04 at day 8, n=5, p≤0.001, One way repeated measures ANOVA; **Figure 40**). Besides, other signs of pain such as changes in the ear position or the presence of a bulge on top of the nose were observed in most of the DT injected animals. After 8 days of repetitive DT injections, the eye closure ratio was significantly higher than at 48h after the first DT injection (p=0.004, **Figure 40**), which suggests that in acute conditions pain is more prominent and that there is a reduction of pain under chronic conditions, although not recovering basal eye closure ratio values.
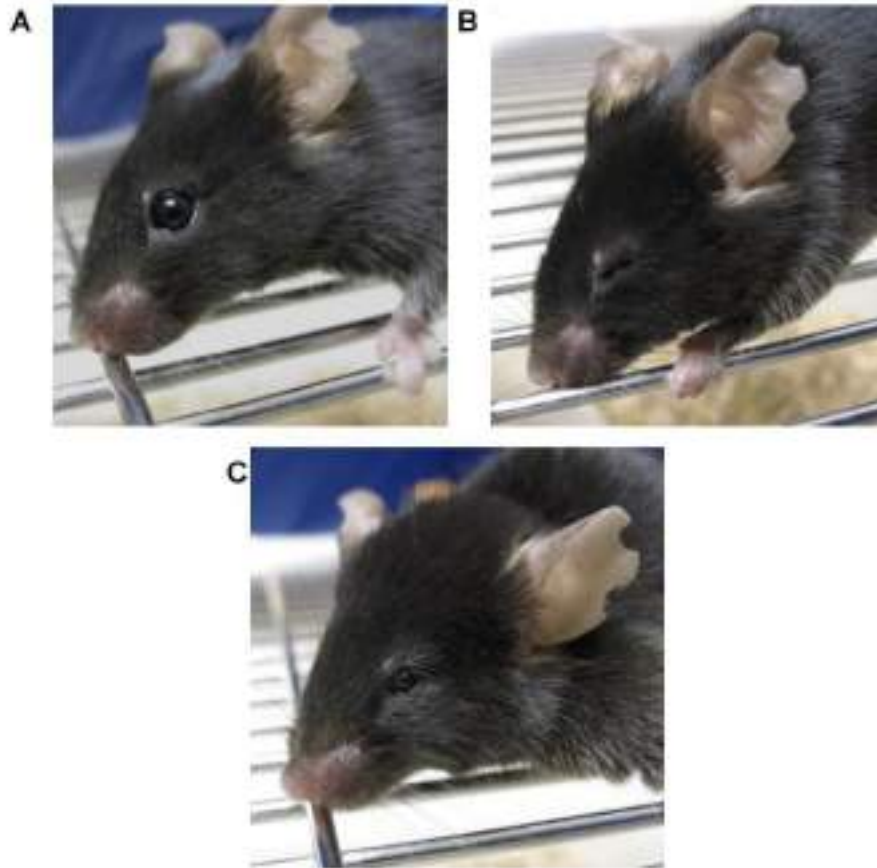
Figure 38. Representative images of spontaneous eye closure in a CD11c-DTR mouse before (A) and at 2 days (B) and 8 days (C) after subconjunctival injection of diphtheria toxin.
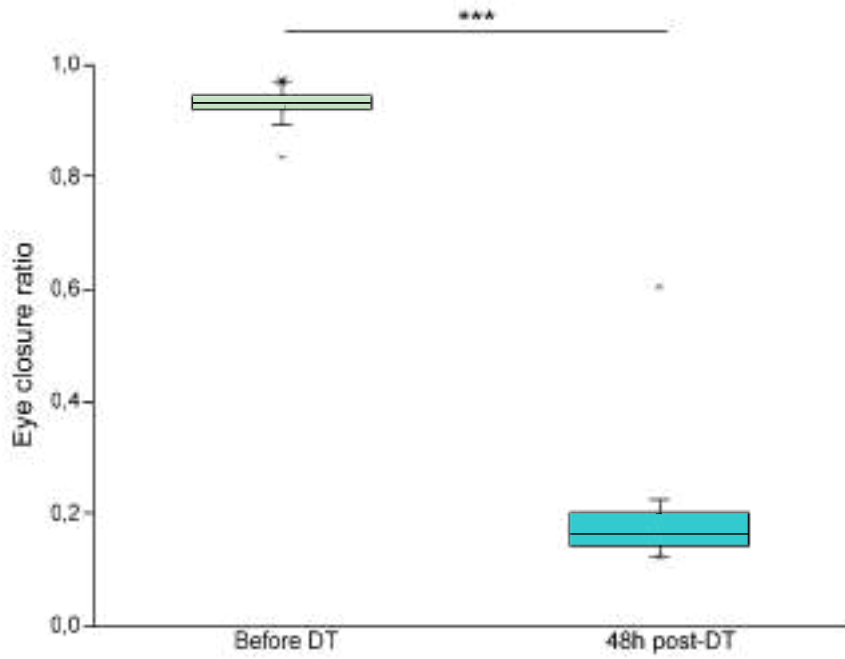
Figure 39. Eye closure ratio before and 48h after DC depletion. N=23 mice, ***p≤0.001. Before and after differences using Wilcoxon Signed Rank Test.
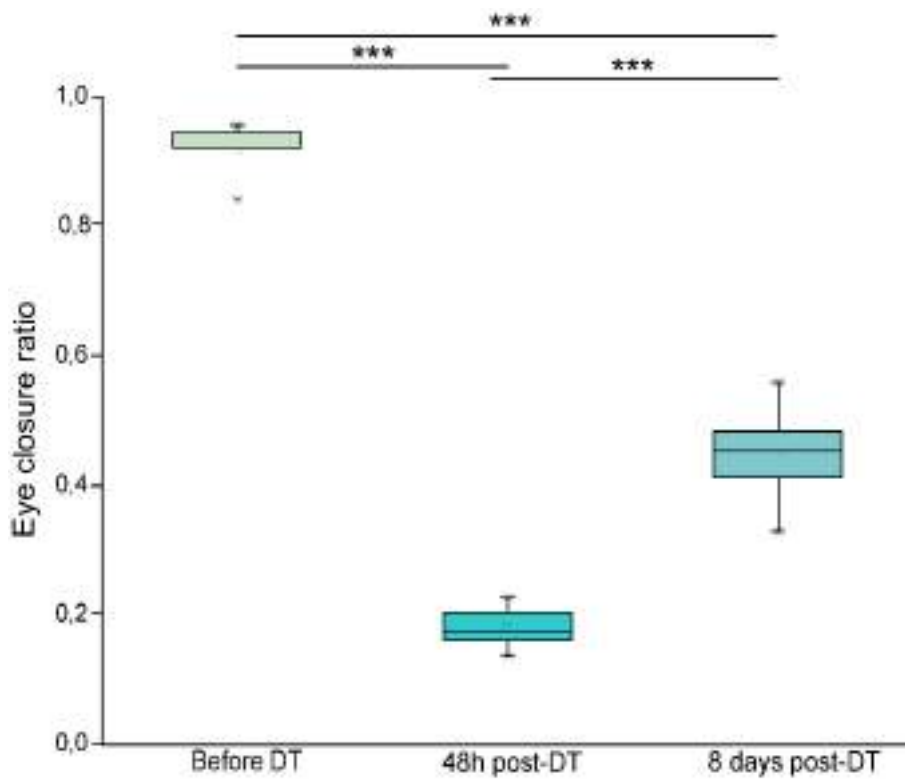
Figure 40. Eye closure ratio before, and 2 days and 8 days after subconjunctival injection of diphtheria toxin. N=5 mice, ***p≤0.001, One Way Repeated Measures ANOVA.

2.2 Signs of pain after subconjunctival saline injection

We measured eye closure ratio before and after injecting PBS instead of DT to test if the subconjunctival injection procedure itself was the cause of the spontaneous pain observed in DT injected animals. We observed that neither short-term nor long-term PBS injections produced pain behaviour (STPBS: 0.93 ± 0.01 before PBS *vs*. 0.92 ± 0.01 at 2 days, n=11, p=0.614, paired t-test, **Figures 41,42**; LTPBS: 0.94 ± 0.01 before PBS *vs*. 0.92 ± 0.02 at 2 days *vs*. 0.93 ± 0.02 at 8 days after repetitive injections, n=6, p=0.477, One way Repeated Measures ANOVA, **Figures 43,44**), thus excluding the injection procedure as the cause of the observed pain.
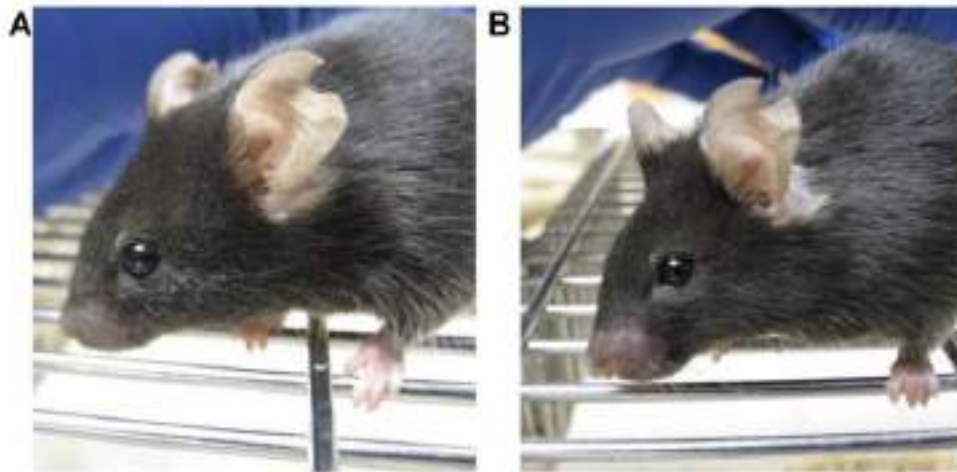
Figure 41. Representative images of spontaneous eye closure in a CD11c-DTR mouse before (A) and 48h after (B) PBS injection.
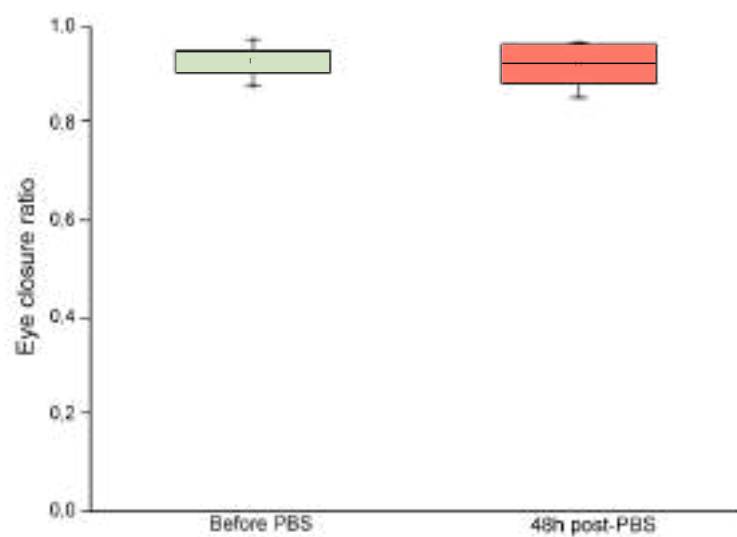
Figure 42. Eye closure ratio before and 48h after PBS injection. N=11 mice, p=0.614. Before and after differences using Paired-test.
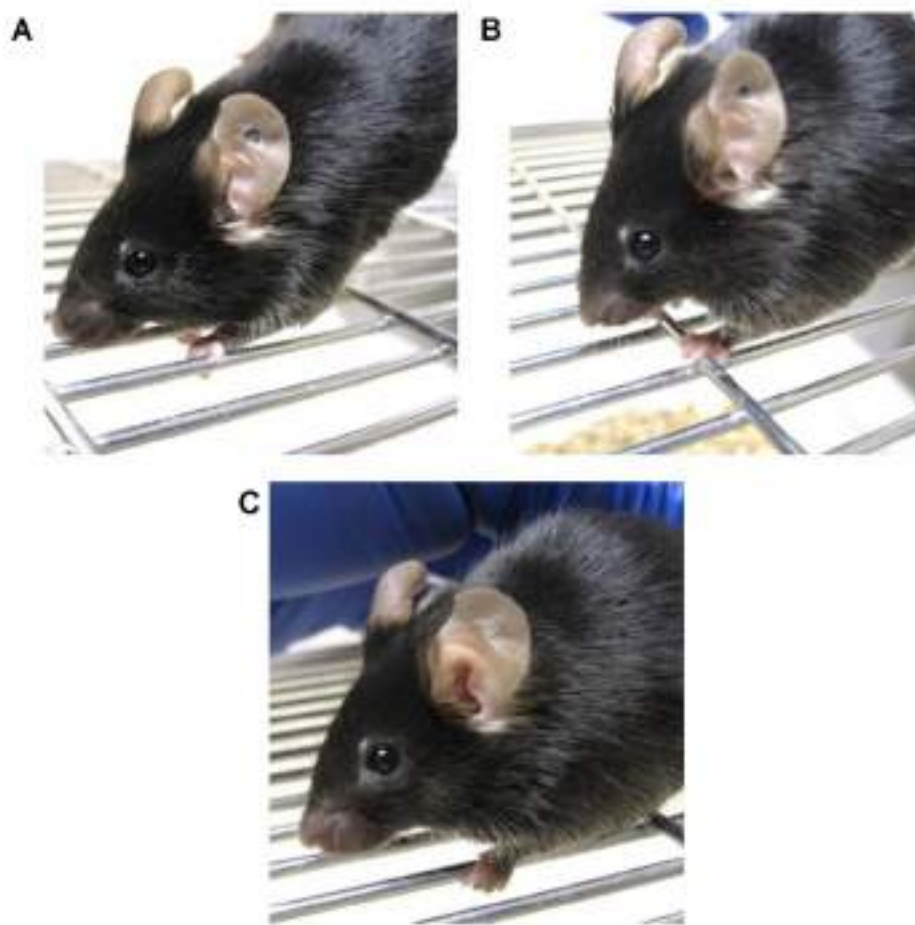
Figure 43. Representative images of spontaneous eye closure in a CD11c-DTR mouse before (A), and 2 days (B) and 8 days (C) after subconjunctival PBS injections.
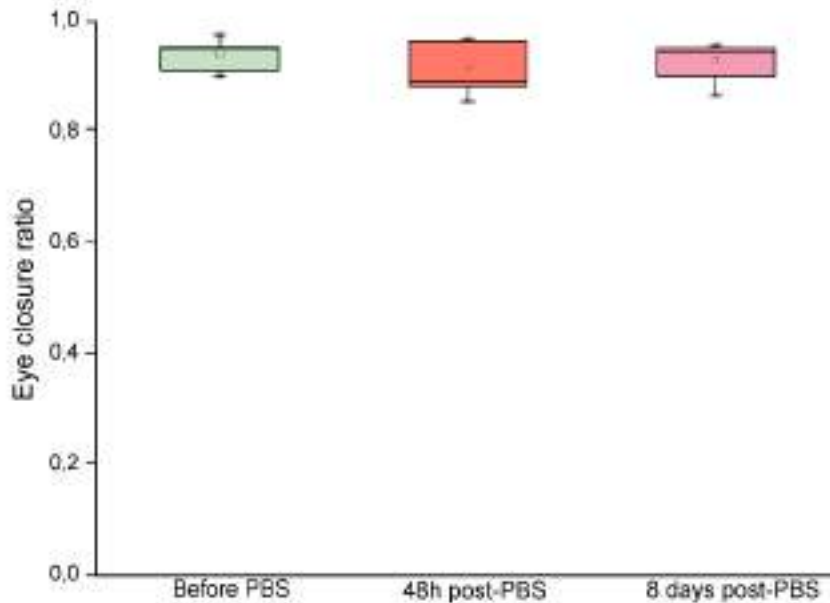
Figure 44. Eye closure ratio before and 2 and 8 days after PBS subconjunctival injection. N=6 mice, p=0.477. Repeated measures differences using One Way Repeated Measures Analysis of Variance.

2.3 Signs of pain behaviour after DC repopulation of DC-depleted corneas

In animals in which DC had been repopulated 8 days after their initial depletion, we observed an almost completed recovery of naïve nerve activity (see above). However, when we measured the signs of spontaneous eye pain in these animals, we continued to observe a significant reduction in the eye closure ratio (RC: 0.95 ±0.01 before DT injection to induce DC depletion *vs*. 0.45±0.05, 8 days afterwards, n=4, p=0.002, **Figures 45, 46**), being the eye closure ratio value very similar to that observed under long-term depletion conditions(LTDT: 0.45±0.04 at day 8, n=5).

These data reflect that pain persisted in animals allowed to recover corneal DC repopulation. As there was an almost normal cold thermoreceptor nerve terminal activity under this condition, pain experienced by the animals could be attributable to changes in the activity of other corneal sensory receptors such as polymodal nociceptors, or to changes of neural activity at other levels of the nervous system that take to recover longer than DC repopulation.
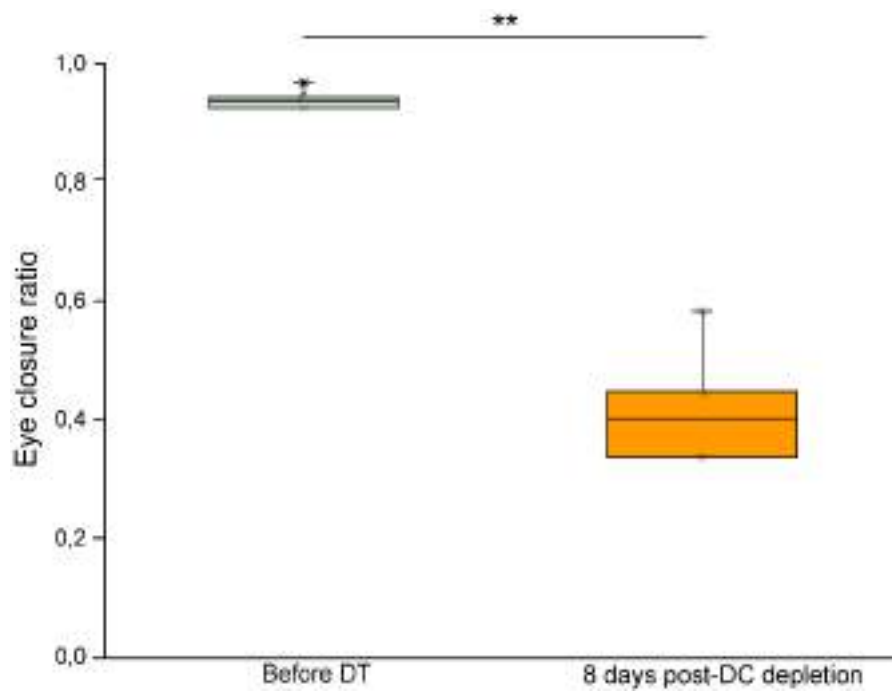
Figure 45. Eye closure ratio before and 8 days post-DC depletion induced by DT subconjunctival injection. N=4 mice, **p≤0.005. Before and after differences using Paired-test.
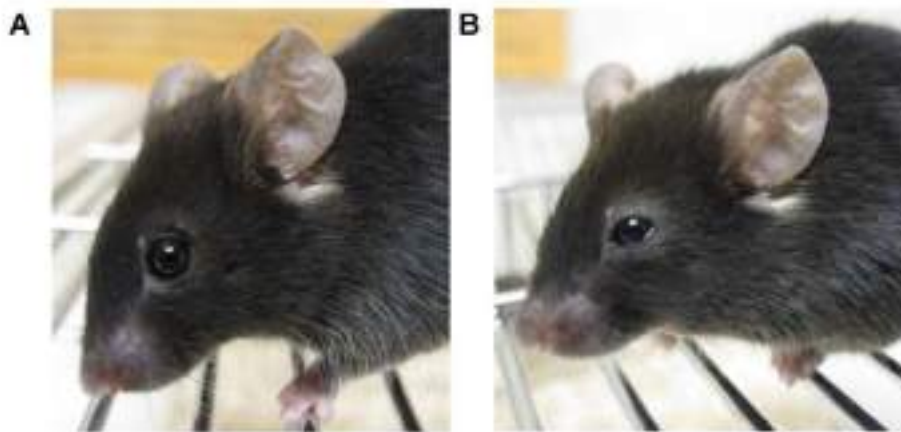
Figure 46. Representative images of spontaneous eye closure in a CD11c-DTR mouse before (A) and 8 days post-DC depletion by subconjunctival DT injection (B).

3. Basal tearing

3.1 Basal tearing rate under DC depletion conditions

TRPM8-dependent activity of corneal cold thermoreceptors is responsible for the regulation of basal tear flow by the central nervous system (Parra 2010). This prompted us to investigate if the changes in nerve activity observed in cold thermoreceptors under short-term and long-term DC depletion conditions had an impact in basal tearing.

We found that short-term DC depletion produced a significant reduction of basal tearing to almost the half of the initial value (STDT: 2.5±0,3mm before DT injection *vs* 1.3±0,2mm at 2 days post DT, n=18, p≤0.001, **Figure 47**). However, after 8 days of repetitive DT injections, the basal tearing value had almost returned to normal values (LTDT: 1.7±0.3mm before DT injection *vs*. 0.8±0.2mm at 2 days after DT *vs*. 1.03±0.6mm at 8 days after DT, n=3, p=0.272, **Figure 48**).
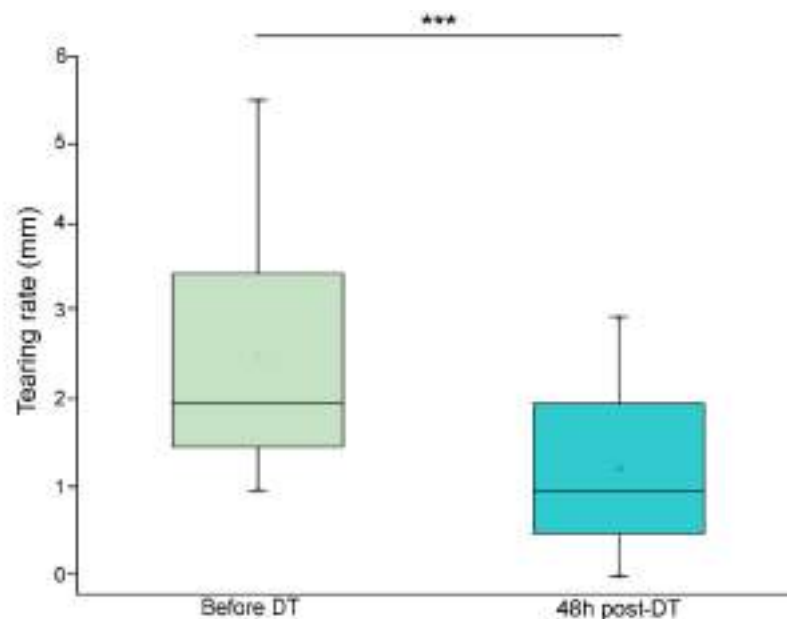
Figure 47. Basal tearing before and 48h after subconjunctival injection of DT. N=18 mice, ***p≤0.001. Before and after differences using Wilcoxon Signed Rank Test.
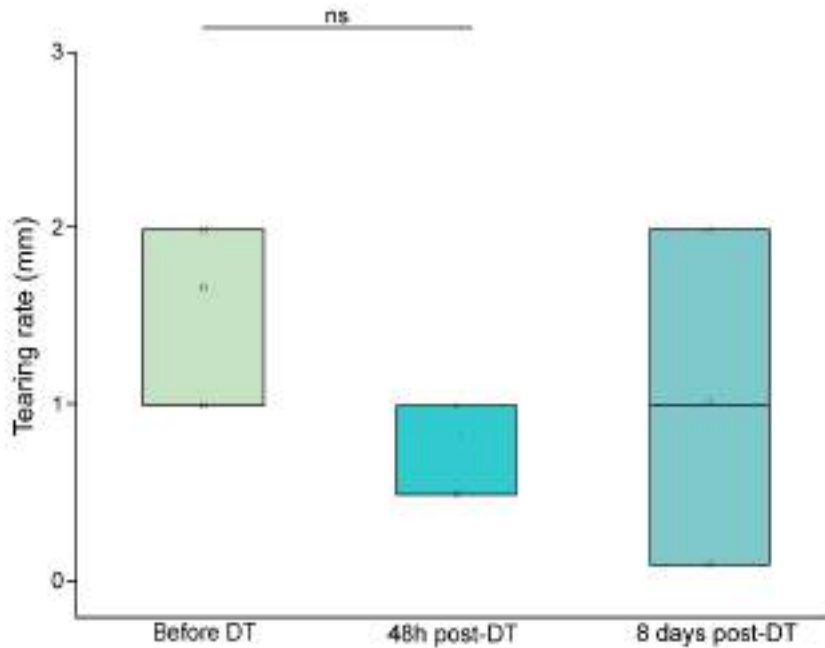
Figure 48. Basal tearing before, 2 days and 8 days after subconjunctival DT injection. N=3 mice, p=0.272, One Way Repeated Measures Analysis of Variance.

3.2 Basal tearing rate after subconjunctival saline injection

We also wanted to check if the slight changes in nerve activity produced by PBS injections altered or not the basal tearing. We found that neither short-term nor long-term PBS injections had any effect on it (STPBS: 3.1±0,4mm before PBS *vs*. 3.1±0,3mm at 2 days, n=6, p=0.950, paired t-test; LTPBS: 2.9±0.5mm before PBS injections *vs*. 2.7±0.2mm at 2 days after PBS *vs*. 3.7±1.5mm at day 8 after PBS, n=3, p=0.701, RM One-way ANOVA, **Figures 49, 50**). The absence of effects of subconjunctival injections in tearing rate support the idea that the changes in basal tearing found under short-term DC depletion are specific and not due to the injection itself.
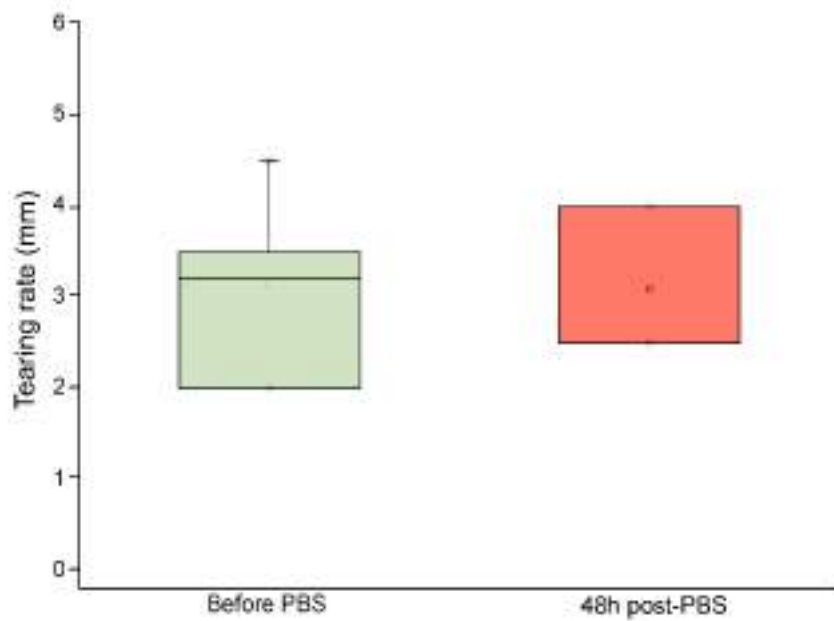
Figure 49. Basal tearing volume measured before and 2 days after PBS subconjunctival injections. N=6 mice, p=0.950. Before and after differences using Paired-test.
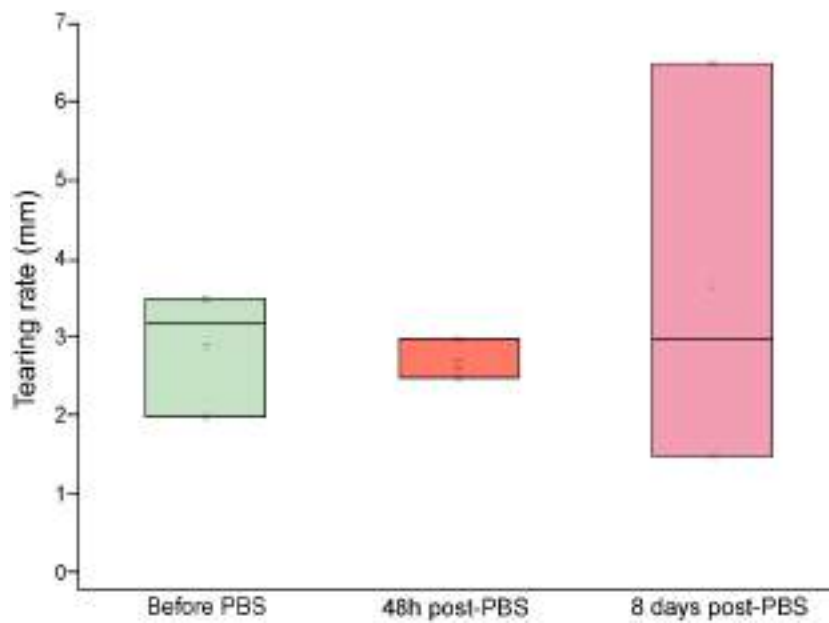
Figure 50. Basal tearing volume measured before and 2 days and 8 days after PBS injections. N=3 mice, p=0.701. Repeated measures differences using One Way Repeated Measures Analysis of Variance.

3.3 Basal tearing rate after corneal DC repopulation

In RC animals, we observed a slight decrease in the basal tearing volume, although it was not statically significant (RC: 2.4±0.6mm before DT injection *vs.* 0.9±0.3mm, 8 days after DT, n=4, p=0.104, **Figure 51**), confirming the idea of an almost total recovery of the phenotype after corneal DC repopulation.
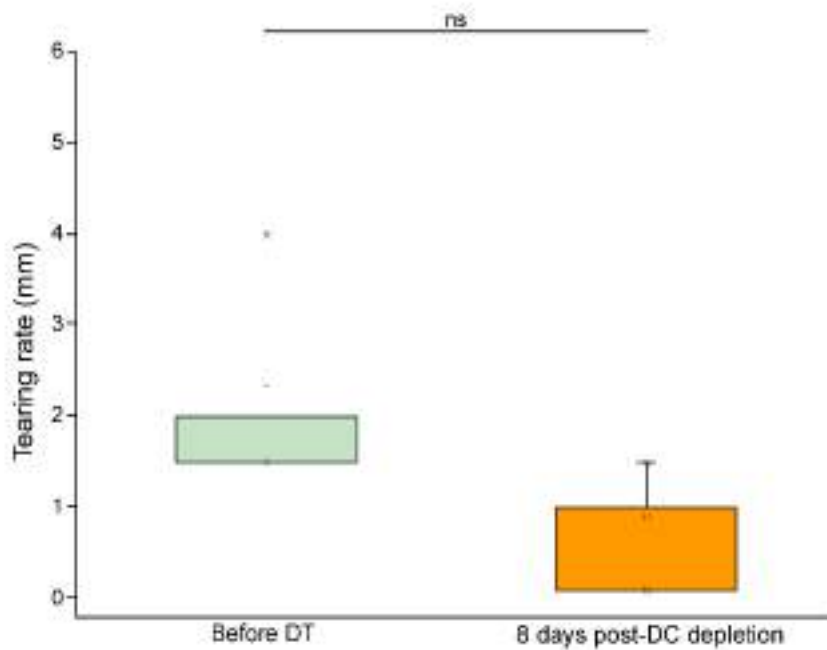
Figure 51. Basal tearing volume measured before and after corneal DC repopulation (8 days after a single subconjunctival DT injection). N=4 mice, p=0.104. Before and after differences using Paired-test.

4. Corneal DC distribution under different experimental conditions

4.1 Short- and long-term DC depletion

Corneal whole-mount preparations were used to assess changes in DC distribution and morphology under the different experimental conditions. In naïve animals two morphologically different DCs, dendritiform and round-shaped cells, were found within the cornea (**Figure 52**). The density of dendritiform DCs was higher near the limbus and decreased from the periphery to the central cornea. As expected, no DCs were found in the cornea under both STDT and LTDT conditions (**Figures 53, 54**), although in both cases some DCs could be observed at the limbal area.
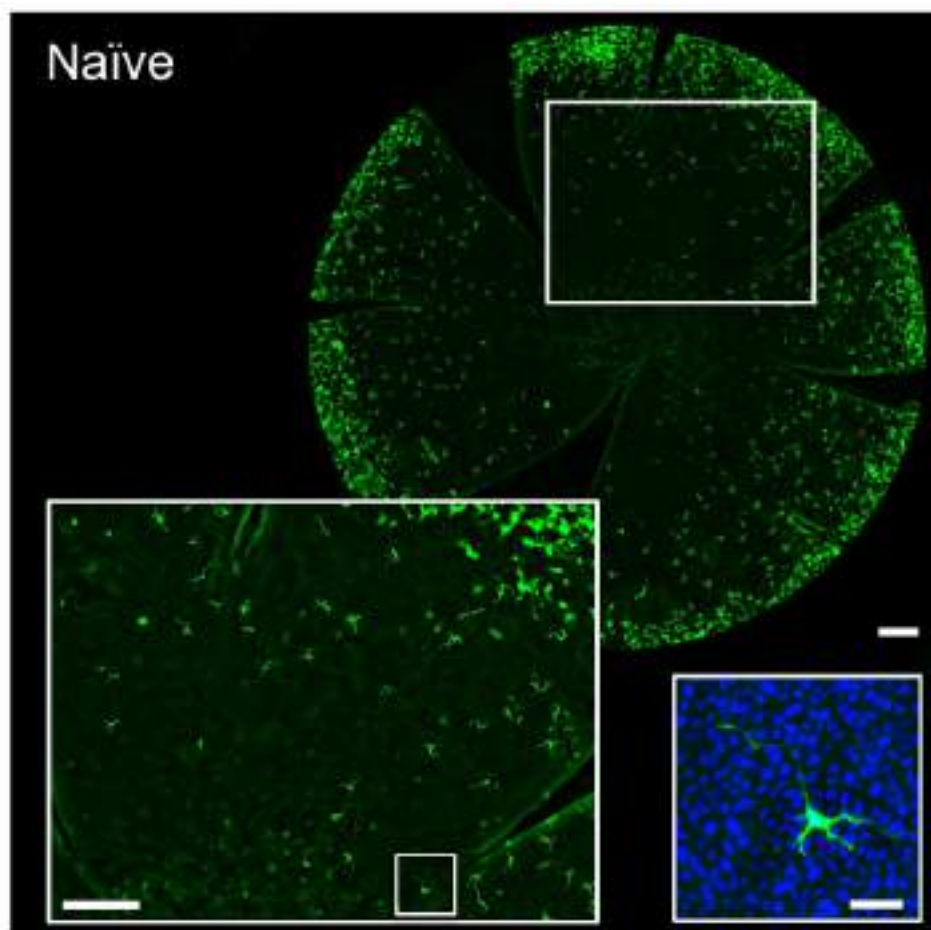
Figure 52. Whole-mount cornea of a CD11c-DTR mouse in naïve conditions. The mosaic image of the cornea showing the endogenous GFP expression in DC (green) and DAPI staining of cell nuclei (blue, bottom right panel) was captured using a Leica THUNDER 3D Tissue Imager (after computational clearing) provided with x10 and x40 objectives. Scale bars: 250 µm for the x10 whole cornea image and

x10 zoom image (bottom left panel); 25 μm for x40 image (bottom right panel). This image shows a representative naif cornea.
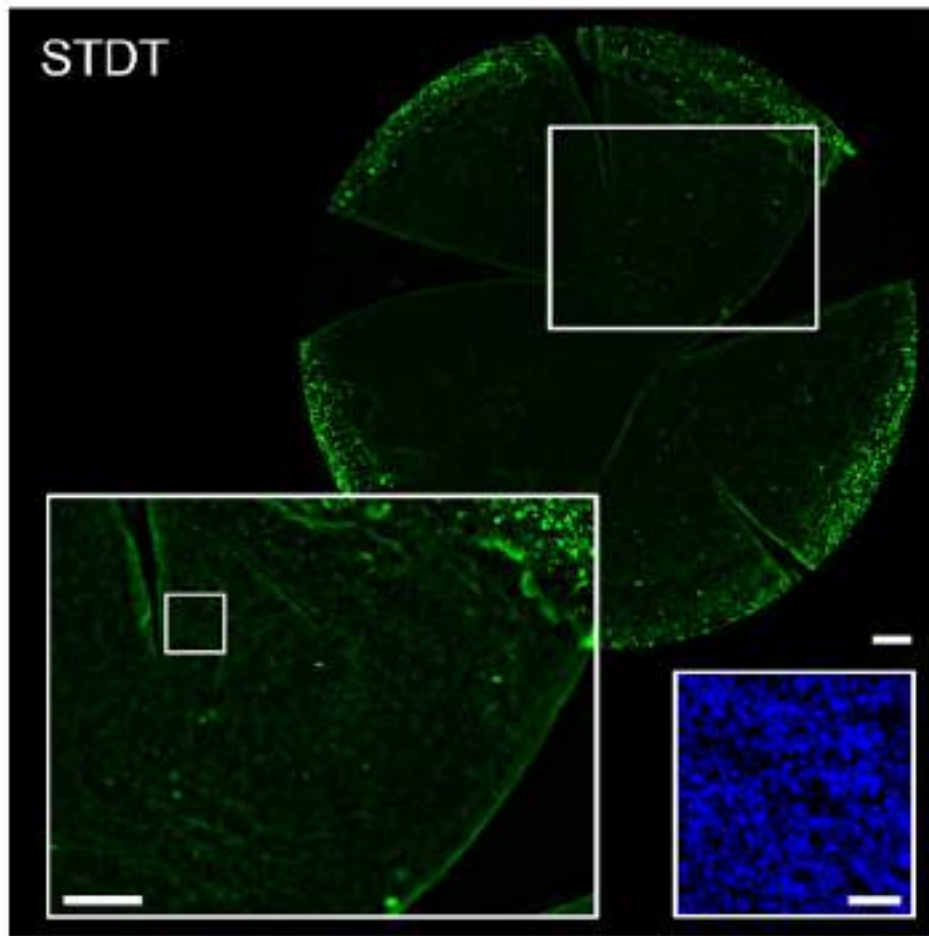
Figure 53. Whole-mount cornea of a CD11c-DTR mouse under short-term DC depletion conditions (STDT). GFP expression in DC (green) and nuclei DAPI staining (blue, only at x40 images). The mosaic image was captured using Leica THUNDER Imager Tissue (after computational clearing) with x10 and x40 objectives. Scale bar: 250 μm for x10 image and x10 zoom image (left panel); 25 μm for x40 image (right panel). This image shows a representative cornea of the STDT experimental group.
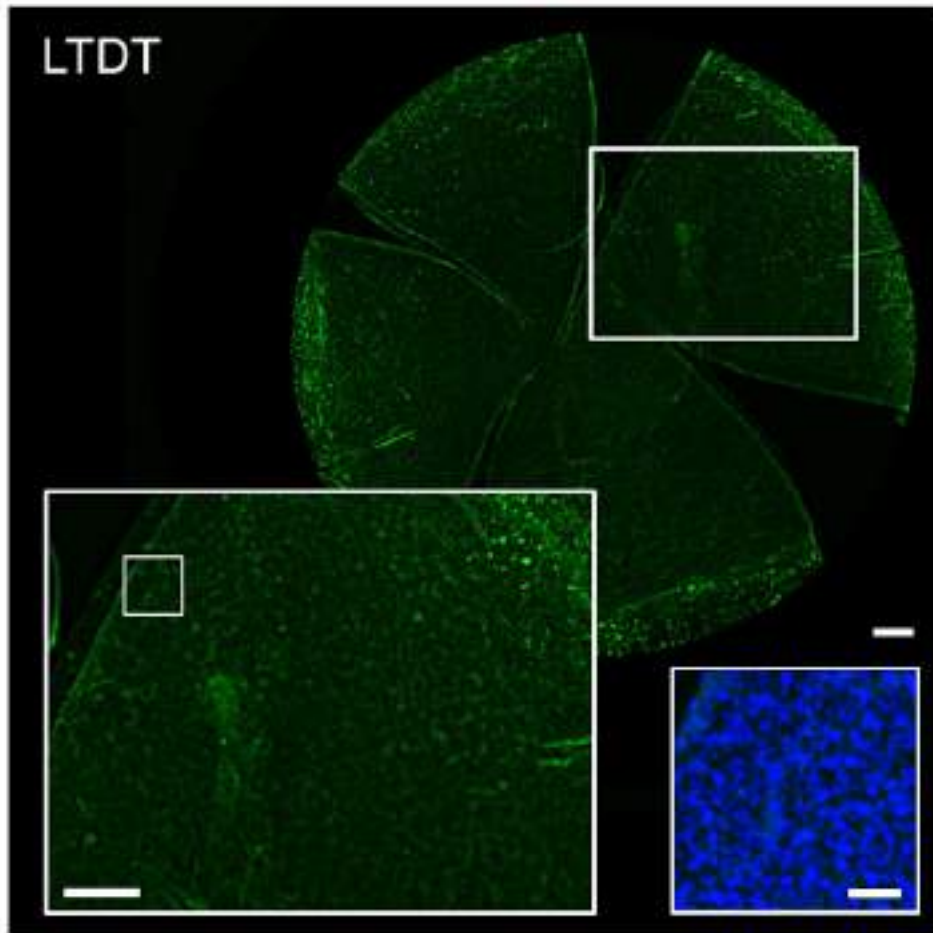
Figure 54. Flat whole-mount cornea of a CD11c-DTR mouse under long-term DC depletion conditions (LTDT). GFP expression in DC (green) and nuclei DAPI staining (blue, only at x40 images). The mosaic image was captured using Leica THUNDER Imager Tissue (after computational clearing) with x10 and x40 objectives. Scale bar: 250 μm for x10 image and x10 zoom image (left panel); 25 μm for x40 image (right panel). This image shows a representative cornea in the LTDT experimental group.

4.2. Saline subconjunctival injections

When studying the effect of subconjunctival injections of PBS on corneal DC, we observed the same as in naïve animals. A slightly higher DC density was observed in the limbus of STPBS and LTPBS corneas with respect to the naïve (**Figures 55, 56**), mostly of DCs with few dendritic processes.
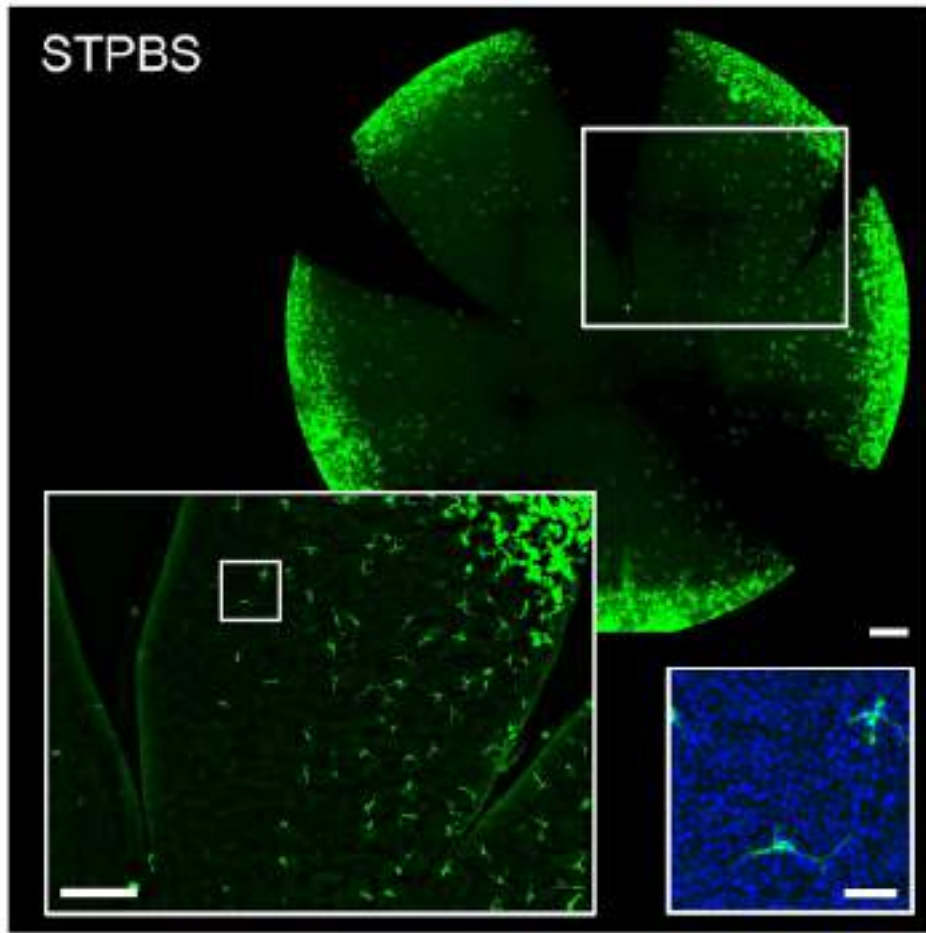
Figure 55. Flat whole-mount cornea of a CD11c-DTR mouse under short-term PBS injection conditions (STPBS). GFP expression in DC (green) and nuclei DAPI staining (blue, only at x40 images). The mosaic image was captured using Leica THUNDER Imager Tissue (after computational clearing) with x10 and x40 objectives. Scale bar: 250 μm for x10 image and x10 zoom image (left panel); 25 μm for x40 image (right panel). This image shows a representative cornea in the STPBS experimental group.
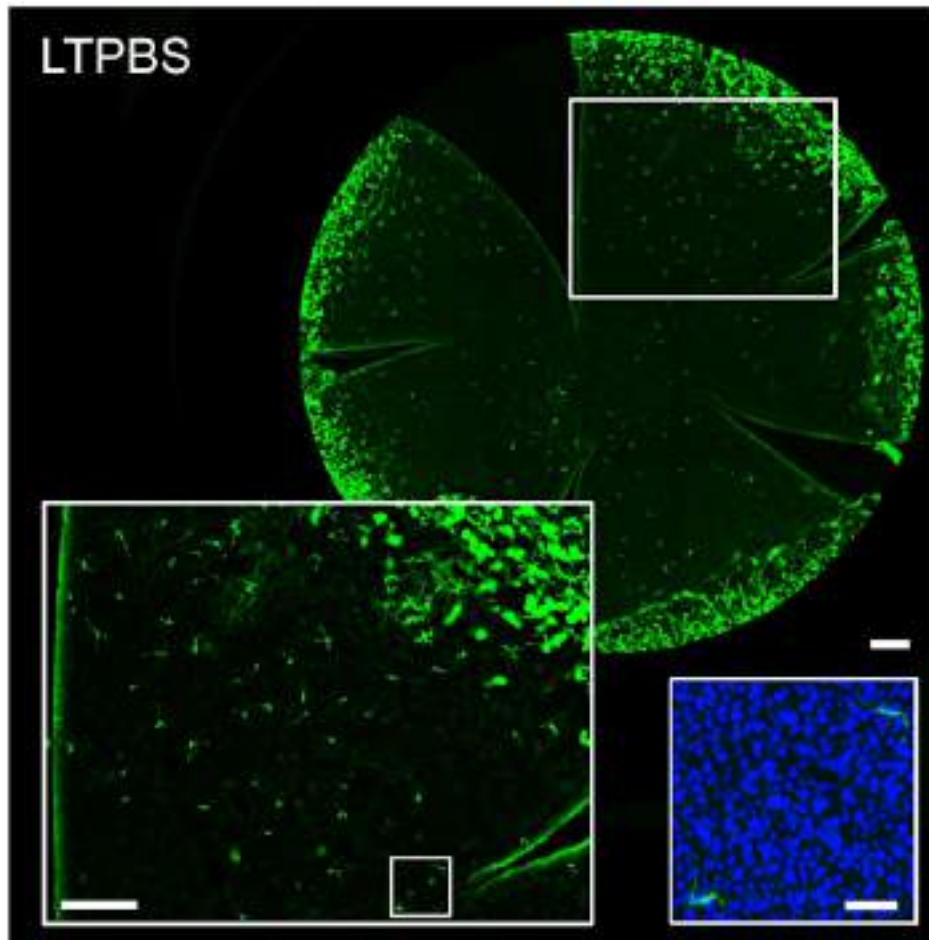
Figure 56. Flat whole-mount cornea of a CD11c-DTR mouse under long-term PBS injection conditions (LTPBS). GFP expression in DC (green) and nuclei DAPI staining (blue, only at x40 images). The mosaic image was captured using Leica THUNDER Imager Tissue (after computational clearing) with x10 and x40 objectives. Scale bar: 250 μm for x10 image and x10 zoom image (left panel); 25 μm for x40 image (right panel). This image shows a representative cornea in the LTPBS experimental group.

4.3. DC repopulation of previously depleted corneas

In recovery group animals, most DCs present in the cornea were round-shaped, while a low proportion were provided with few dendritic processes **(Figure 57)**. Most DCs were located in the peripheral cornea.
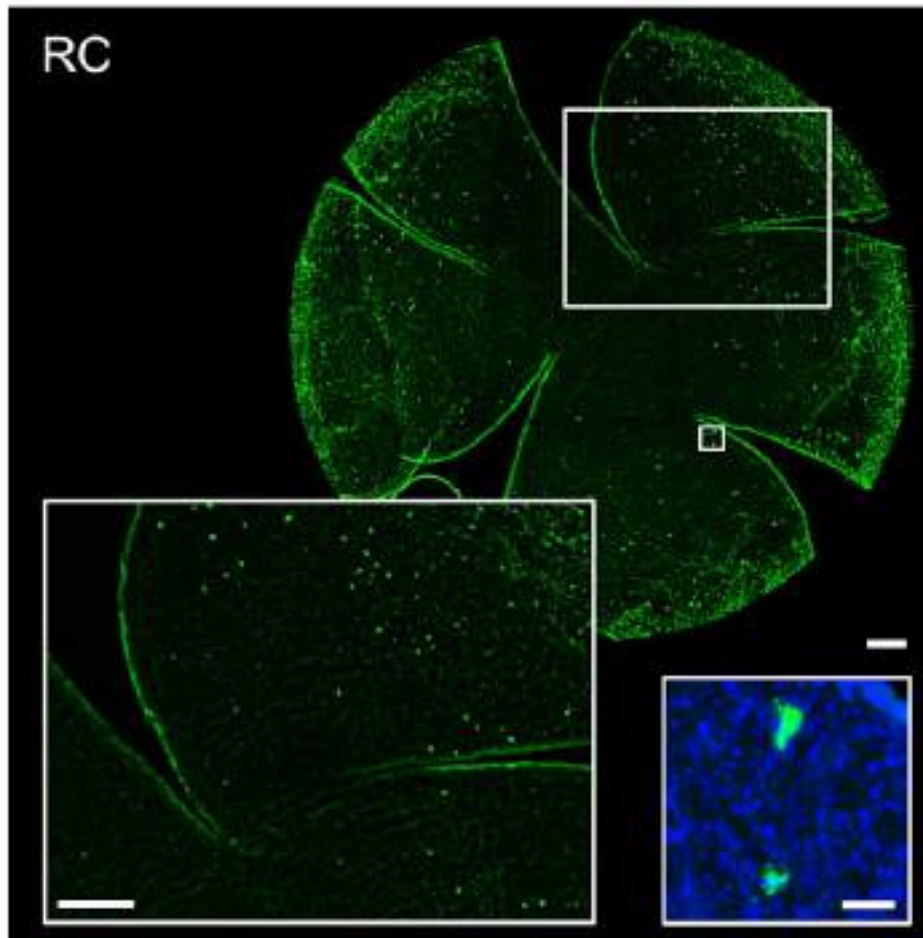
Figure 57. Flat whole-mount cornea of a CD11c-DTR mouse under DC repopulation conditions (RC).
GFP expression in DC (green) and nuclei DAPI staining (blue, only at x40 images). The mosaic image was captured using Leica THUNDER Imager Tissue (after computational clearing) with x10 and x40 objectives. Scale bar: 250 μm for x10 image and x10 zoom image (left panel); 25 μm for x40 image (right panel). This image shows a representative cornea in the RC experimental group.

4.4. Development of a mouse model to ascertain morphological neuroimmune interactions in the living mice

As part of the last objective of this work, we have generated a transgenic mouse model in which somatosensory sensory axons and DC were constitutively labelled with fluorescent proteins of different colours. We successfully developed it by doing the following steps:

- First of all, to generate a mouse where the corneas have the sensory axons labelled with tdTomato, we crossed Advillin-Cre$^{tg/+}$ (Tg(Avil-cre)1Phep) mice ((Zurborg et al., 2011); MGI:5292346) with Ai14$^{fl/fl}$ (Gt(ROSA)26Sor$^{tm14(CAG-tdTomato)Hze}$) mice ((Madisen et al., 2010); MGI:3809524) (**Figure 58A**). Advillin is an actin-binding protein expressed by all somatosensory neurons; this way, the peripheral axons of the somatosensory neurons innervating the transparent cornea will finally express a red fluorescent protein.

- Then, the first offspring generation (F1) was back-crossed with Ai14$^{fl/fl}$ mice to obtain Advillin-Cre$^{tg/+}$ Ai14$^{fl/fl}$ offspring (F2 generation) (**Figure 58B**).

- After generating the mice with tdTomato-labelled sensory nerves, we wanted to obtain GFP-labelled DCs. For this purpose, Advillin-Cre$^{tg/+}$ Ai14$^{fl/fl}$ mice were crossed with CD11c-DTR/GFP$^{tg/tg}$ (1700016L21Rik$^{Tg(Itgax-DTR/EGFP)57Lan}$) mice ((Jung et al., 2002); MGI:3057163) to obtain Advillin-Cre$^{tg/+}$Ai14$^{fl/+}$CD11c-DTR/GFP$^{tg/+}$ offspring (F3 generation) (**Figure 58C**), in which somatosensory axons will constitutively express a red fluorescent protein and DCs will be sensitive to diphtheria toxin and constitutively express a green fluorescent protein.
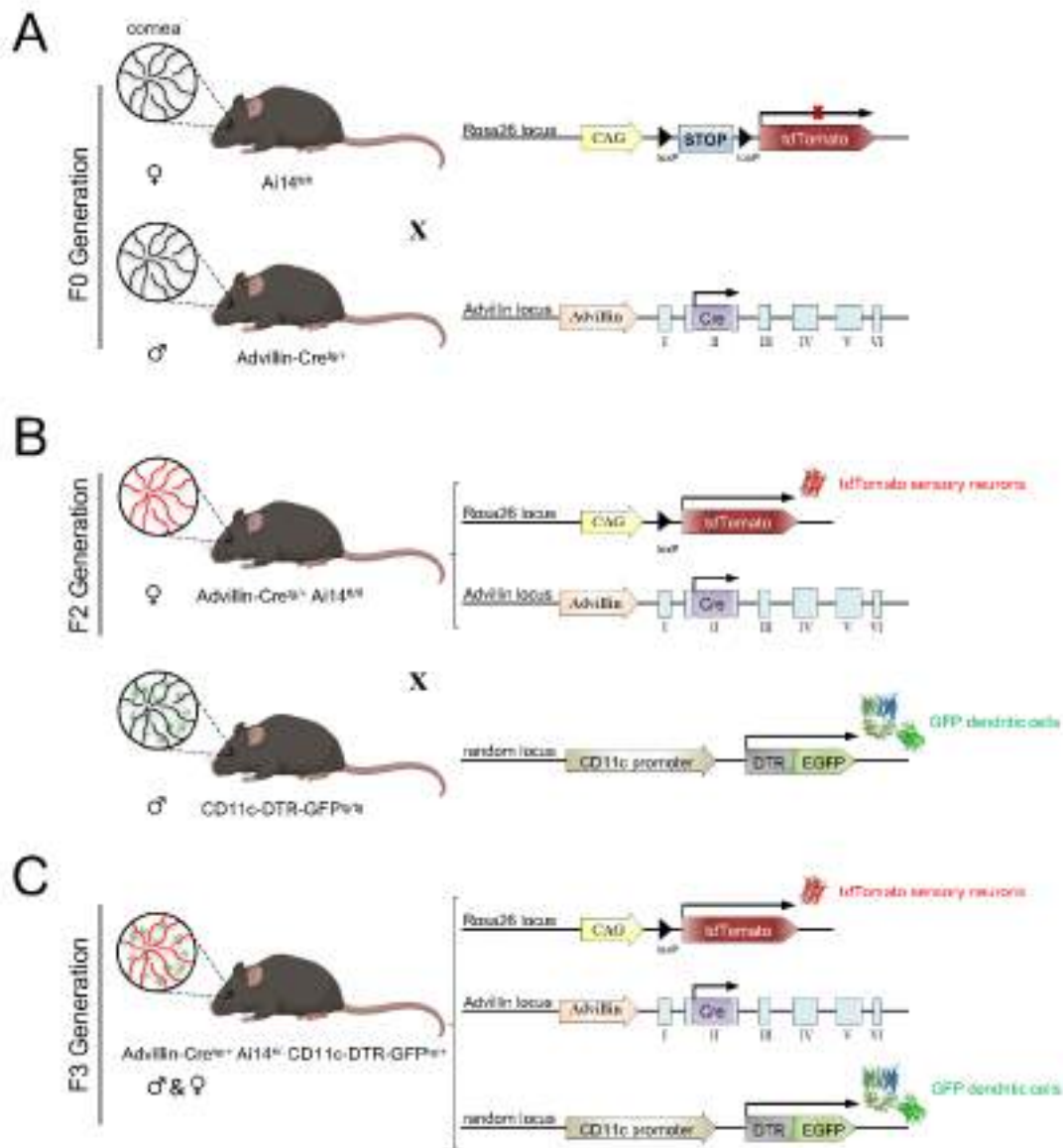
Figure 58. Scheme of the generation of the Advillin-Cretg/+ Ai14fl/- CD11c-DTR-GFPtg/+ mouse model. Ai14fl/fl females were crossed with Avidillin-Cretg/+ males to produce the F1 generation (A). To obtain a F2 generation of Advillin-Cretg/+ Ai14fl/fl mice (B), F1 females were crossed with Ai14fl/fl males (which have corneal sensory nerves framed with tdTomato). To generate the animal model of interest (C), F2 females were crossed with male CD11c-DTR-GFPtg/tg mice that express diphtheria toxin receptor (DTR) and GFP in DCs.

Figure 59 is a representative image of the cornea of a Advillin-Cre$^{tg/+}$Ai14$^{fl/+}$CD11c-DTR/GFP$^{tg/+}$ mouse showing DCs in green and sensory nerves in red. Although a more in-depth study is needed, the images obtained both *in vivo* and *ex vivo* processed corneas suggest that there is not a close relationship between DCs and corneal subbasal nerves.
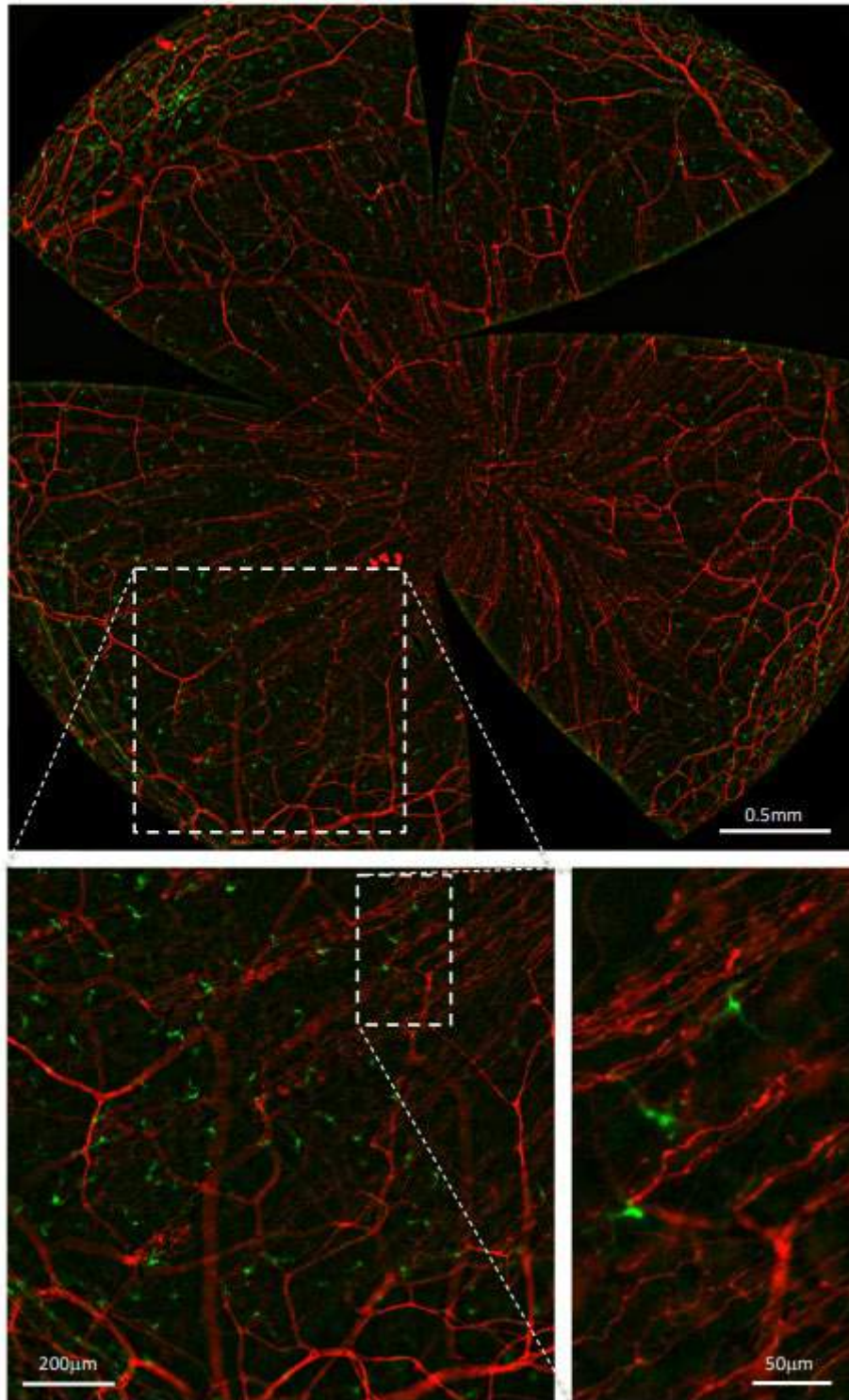
Figure 59. Nerves and DCs in the advillin-Cretg/+ Ai14fl/- CD11c-DTR-GFPtg/+ mouse cornea. All panels are maximal intensity z-projection stacks (30μm) performed with a Leica THUNDER Imager Tissue provided with a 20x objective. **A**. Flat mount overview of a whole-mount cornea (64 tiles merged) showing tdTomato (red) expression in corneal sensory nerves and GFP (green) expression in DCs after computational clearing of the out-of-focus blur. **B-C**. Higher magnification images showing nerve fibres and DCs endogenously expressing tdTomato and GFP respectively. Scale bars: A, 500 μm; B, 200 μm; C, 50 μm.

5. Summary of results

1. Short-term DC depletion increased the percentage of cold thermoreceptors responding to heat stimulation. The mean discharge rate in response to heating ramps was increased and the heating threshold is lower than in naïve corneas (control). Cold responses were similar to control, while mechanical responsiveness was lower.

2. In LTDT corneas there was an increase in both the cooling threshold and the temperature needed to reach the maximum response during cooling ramps. No significant differences in mechanical or heat responsiveness were found.

3. A significant decrease in the maximum rate of voltage change during the impulse downstroke and a significant increase of impulse duration, result of longer depolarization and repolarization times, was found under long-term DC depletion. This suggests the inactivation or downregulation of repolarization and/or background K+ channels under this condition.

4. The different results obtained after subconjunctival injections of PBS and diphtheria toxin suggest that the effects on cold nerve activity and nerve impulse shape we observed in our experimental groups were not due to the injection procedure itself but to the DC depletion produced by the toxin. The changes in nerve activity and nerve impulse shape observed under short and long-term DC depletion are suggestive of a certain degree of ocular inflammation and damage associated with DC depletion that alters the activity of transducing and coding ion channels.

5. When DCs are allowed to repopulate the cornea after short-term DC depletion, parameters defining responsiveness to stimulation and nerve terminal impulse shape are similar to those of cold thermoreceptor terminals recorded in naïve corneas thus suggesting that DCs are crucial for the normal functioning of corneal cold sensory neurons.

6. Signs of spontaneous pain were observed even in the RC group, when cold nerve terminal activity had returned to normal. This prompts us to think that not only cold thermoreceptors but also nociceptors are sensitised under DC depletion. Polymodal nociceptors take longer to recover normal activity than cold thermoreceptors, whose activity is normalised in DC repopulated corneas. The possibility also exists that neural changes induced by DC depletion are also being produced at upper levels of the nervous system sites other than the corneal nerve terminals and produce central sensitization, which takes longer to disappear.

7. The reduced basal tear volume found under short-term depletion is probably a consequence of the reduction of corneal cold thermoreceptors nerve activity under this condition. This reduced activity of cold thermoreceptors was still present under long-term DC depletion, although it could be compensated by other mechanisms such as an increased activity of polymodal nociceptors, which is known to evoke reflex tearing.

8. No DCs were observed in the corneas of DT-injected animals, which present a few DCs at the corneoscleral limbus. In the DC recovery group, round-shaped DCs were distributed throughout the cornea at 8 days after DT injection. There seems to be a correlation between the distribution of DCs and active cold thermoreceptor terminals, as almost no active cold thermoreceptors were found in the central cornea in short-term and long-term DC depleted corneas. PBS subconjunctival injections did not significantly affect DC distribution and morphology.

9. In addition to allowing the functional study of the activity of the corneal sensory nerves, the developed mouse model will allow a deeper understanding of the neuro-immune crosstalk under inflammatory and steady-state conditions of the eye.

V. DISCUSSION

1. Methodological considerations.

In the present work, we carried out bilateral subconjunctival injections of 30 ng of DT in 10µl of PBS (5 µl nasal and 5 µl temporal) once or repeated every two days for 8 days) to induce corneal short-term or long-term depletion of DCs, respectively.

Unexpectedly, some LTDT animals died between the second and the third DT injection, regardless of the litter or the toxin stock. The unexpected deaths of some mice after chronic injections of DT are the reason why the number of mice in the LTDT group is slightly lower than in other groups. It has been described that repetitive systemic DT application resulted in DTR-transgenic mice lethality (Jung 2002), but local depletion such as the one we were performing in our experiments was not expected to present this problem. Our first explanation was that unexpected deaths were a consequence of the repetitive general anaesthesia needed to perform each subconjunctival injection. Nevertheless, we wondered if the toxin was being absorbed systemically through the abundant blood vessels of the conjunctiva, thus causing the death. To confirm or exclude this possibility, we injected subconjunctivally 10 µl of 9 mg/ml of Evans blue (EB) dye in PBS (5 µl nasal and 5 µl temporal) in only one eye of three mice to fluorescently label their intact vasculature (Honeycutt and O'Brien, 2020). If the injected solution was absorbed systemically, we would expect to see the fundus of the contralateral eye bluish as EB is visible to the naked eye when filling the blood vessels, appearing in a deep blue colour. Twenty-four hours after the injection, we observed that 1 out of 3 injected mice had a slightly blue fundus, confirming that part of the solution injected subconjunctivally in the contralateral eye reached the systemic circulation. Also, the cumulative effects of repetitive anaesthesia and the possible infections resulting from the absence of DCs cannot be ruled out.

2. Cold thermoreceptors' responses to thermal and mechanical stimulation.

Cold thermoreceptor ongoing activity at basal temperature (34ºC) was similar under corneal DC depletion, sham subconjunctival injections and naïve animals. On the contrary, response to stimulation changed under different conditions. Under short-term DC depletion, cold thermoreceptors' response to cold was slightly increased and the response to heat was significantly altered. Cold thermoreceptor activity decreases when heating and eventually gets silent (nerve activity goes to zero), although some of them have a paradoxical response to heat (Gallar et al., 1993; Acosta et al., 2013, 2014, Gonzalez-Gonzalez et al., 2017). In our study, short-term DC depletion led to a sensitisation of cold thermoreceptor response to heat, as reflected by their significant decrease in the heating thresholds and increasing firing response to the heating ramp. The number of units responding to heat stimulus was also increased under STDT conditions.

Changes in the sensitivity to heat of cold thermoreceptors has been described during ocular surface inflammation, where the percentage of cold thermoreceptor terminals responding to heat is also increased as in the present experiments (Acosta et al., 2013, 2014). Inflammatory agents released by immune cells during inflammation acts on specific receptors at nociceptive nerve terminals producing post-translational changes that ultimately lead to an increased insertion of these channels into the membrane altering thresholds (Hucho and Levine, 2007). The sensitization to heat we found in cold thermoreceptor terminals may be mediated through TRPV1 channels (Basbaum et al., 2009), a temperature transducing channel present in a fraction of cold thermoreceptors (Okazawa et al., 2004), together with the cold transducing channel TRPM8, whose activity is inhibited by inflammatory agents (Zhang, 2015). Based on that, our results would be perfectly explained by an increased number of TRPV1 channels in the nerve ending membrane and/or by a reduction of their threshold induced by inflammatory substances like bradykinin (Chuang et al., 2001), NGF (Zhang et al., 2005), IL-6 (Fang et al., 2015) or ATP (Moriyama et al., 2003) among others.

Mechanical threshold was not accomplished for cold thermoreceptors as our mechanical stimulation by displacement of the recording pipette doesn't allow us to quantify the response to the mechanical stimulus, only to ascertain if the terminal responded or not to the pressure exerted by the pipette. Under short-term DC depletion

conditions, the proportion of cold terminals responding to mechanical stimulation was significantly lower compared to naïve animals, which we interpreted as a decrease in their mechanical sensitivity. This result is in line with the *in vivo* previous studies showing that corneal DC depletion produces a significant decrease in corneal mechanical sensitivity measured with the Cochet-Bonnet aesthesiometer in unanaesthetised mice (Gao et al 2016a).

On the other hand, long-term corneal DC depletion seems to reduce the response of cold thermoreceptors to cold stimulation, while response to heat is only slightly affected. Under long-term absence of DCs, there was an increase in both the cooling threshold and the temperature to reach the maximum firing frequency during the cooling ramp, being necessary larger temperature decreases to elicit responses to cold. These changes in cold thermoreceptor activity are similar to those expected under an inflammatory process. Inflammatory conditions produce an inhibition of the cold-transducing channel TRPM8 (Zhang et al., 2012), thus reducing the stimulus-evoked activity of cold thermoreceptors (Zhang et al., 2012; Acosta et al., 2013, 2014).

To rule out that these changes in cold thermoreceptor activity were not produced by the subconjunctival injection itself, we studied cold thermoreceptor activity after injecting PBS instead of DT. Short-term and long-term PBS injections produced an increase in the cooling response and in the peak frequency during the cooling ramp (being more prominent under STPBS conditions). These changes are the opposite of those expected under inflammatory conditions (Acosta et al., 2013, 2014) and closer to those associated with corneal nerve injury (Kovacs et al., 2016). Thus, it seems that performance of subconjunctival injections did not produce a significant inflammatory reaction. Despite this, as DCs are present in the corneas of PBS-injected animals, several pro-inflammatory cytokines could be released by them as an innate immune response to the injection, thus exerting unknown effects on cold thermoreceptor activity that may be different to that of bradykinin (Zhang et al., 2012). Another possible explanation of these changes could be an increase in neutrophil recruitment in the cornea, as neutrophilia has been described in DT intraperitoneal injected animals of this same strain (Van Blijswijk et al., 2013). However, other authors did not observe the presence of polymorphonuclear (PMNs) neutrophils in unwounded corneas regardless of PBS or DT subconjunctival injections (Gao et al., 2011). Finally, a mild lesion of corneal nerves due to the repetitive subconjunctival injections and the reduced blink during the anaesthesia cannot be

discarded. This would explain the increase in cold nerve activity we obtained in the sham group (Kovacs et al., 2016). This would also explain the lower success rate in finding nerve activity in both STPBS and LTPBS corneas, with part of the cold thermoreceptors showing no activity and part showing increased responses to cold, depending on the degree of the lesion.

These results suggest that, if present, the effects of subconjunctival injection are mild and masked or overcomed by the effects of DC depletion. Depending on the degree of inflammation and injury during an ocular pathology, different changes in corneal sensory nerves activity (sensitisation/desensitisation) are induced and subsequently the experienced sensations (pain/dryness/freshness) also differ (Belmonte et al., 2015, 2019). According to that, the different degrees of injury/inflammation associated with the subconjunctival injections and the DC depletion would explain the different changes in cold thermoreceptors' activity.

Regarding the response to mechanical stimulation, a slight decrease in the percentage of terminals with response to mechanical stimulus was also found in PBS injected animals, especially under LTPBS conditions. Although there is a large variability in the percentage of the mechanical responsiveness between our experimental groups, the variable degree of inflammation/injury mentioned above could explain, at least in part, the decrease in the mechanical response possibly due to a reduction in the ability of our mechanical stimulus to stimulate the terminal adequately.

We also wondered whether the diphtheria toxin itself might influence corneal cold nerve activity. Searching the literature, we found no previous reports on the direct effects of DT on nerve activity, and a few references supporting that there were almost no differences between CD11c-DTR animals injected with PBS and WT C57BL6 animals injected with DT in any of the parameters on corneal nerve morphology analysed by the authors (Gao et.al 2016a). Besides, it has been demonstrated that non-genetically modified murine cells are insensitive to killing by DT, unlike primate cells (Pappenheimer et al., 1982).

Considering all the above, and due to the almost complete functional recovery observed in DC repopulated animals (RC group), our results suggest that the presence of DCs in corneal tissue is necessary for the "normal" functioning of the corneal cold

sensory nerves, while their long-term absence produce nerve activity changes similar to that induced by an inflammatory environment.

3. Cold thermoreceptor nerve terminal impulse shape.

At basal temperature (that is, without any intended thermal stimuli), cold thermoreceptors have a background activity initiated when the electrotonic generator potential of the nerve terminal passively invade the spike initiation site of the axon (Brock et al., 2001; Carr et al., 2002; Goldstein et al., 2019). In addition to transduction channels such as the Transient Receptor Potential Channel families (TRP channels) and their importance in determining cooling and heating responsiveness, other codifying channels such as Na^+ and K^+ channels are important for sensory nerve activity. For instance, K^+ and Na^+ currents are thought to be critical in specifying cold activation threshold of $TRPM8^+$ neurons (Thut et al., 2003; Zimmermann et al., 2007; Zhang, 2015). Voltage-gated Na^+ and K^+ channels are crucial not only in NTI generation but also to define the shape of impulses recorded by focal electrophysiological recording (Brock et al., 2001, 2006; Carr et al., 2002), the technique used in the present work.

The changes of membrane potential recorded extracellularly using this technique are proportional to the net membrane current, being the shape of the recorded NTI the first derivative of the membrane voltage change, which is predominantly outward during the spike depolarization (thus generating a positive peak in our NTI recording) and inward during the spike repolarization (thus recorded as a negative peak) (Smith, 1988; Brock et al., 2006) (see **Figure 23** in Methods). Na^+ channels seem to have a very low contribution to the background NTI activity of cold thermoreceptor terminals at basal temperature because most of these channels are inactivated due to the relatively low membrane potential of the nerve terminals (Carr et al., 2002). According to that, activity of voltage-activated (and probably other types of) K^+ channels should be on the basis of the variations over time of background NTI in cold thermoreceptors. Indeed, blockade of K^+ channels speeds the initial phase of the repolarization, reduces the maximum amplitude of the negative peak component (inward current) and increases the NTI duration (Brock et al., 2006), although its effects on NTI frequency or patterning at the basal temperature are small (Brock et al., 2006) and limited to those drugs acting specifically on HCN channels (Quirce, 2020).

Although no significant changes were found under short-term corneal DC depletion, the maximum rate of voltage change during the downstroke was significantly decreased and the duration of NTI was significantly increased (with longer upstroke and downstroke times) under long-term DC depletion. The changes of NTI shape observed in cold NTI under LTDT conditions are in concordance with the changes observed after using K^+ channel blockers (Brock et al., 2006) so it could be speculated that the DC depletion induces inactivation and/or downregulation of K^+ channels. Further studies are necessary to establish the channels altered under this condition.

The pharmacological blockade of K^+ channels responsible for the action potential repolarization produces a slowing in this phase (Brock et al., 2006), fully in accordance with our results regarding the slowing in the downstroke and in the longer repolarization time. The longer depolarization time would be also explained, at least in part, by the inactivation or downregulation of background K^+ channels. Blockade of K^+ channels results in an increase of the terminal membrane resistance and therefore of the membrane time constant (Brock et al., 2006), which may result in slowing the action potential depolarization, primarily determined by passive membrane properties (Brock et al., 2006), and would explain our longer and the NTI upstroke times. The downregulation of K^+ currents and/or K^+ channel expression is a general phenomenon in peripheral nociceptive fibres as a main mechanism of sensitization and is a causative factor in the development of chronic pain (reviewed by (Du and Gamper, 2013). This altered expression/activity of Na^+ and K^+ channels is also present in cold thermoreceptor neurons, where chronic tear deficiency alters morpho-functionally corneal nerves and induces an increase in Na^+ and a decrease in K^+ currents of cultured TG cold-sensitive neurons (Kovacs et al., 2016). If those changes in ion channel expression or activity induced by nerve damage are also present at the nerve terminals, they might explain the changes of both cold nerve terminal activity and shape found in the present work.

Finally, when DCs repopulated the cornea after a short-term DC depletion, cold thermoreceptor NTI shape was similar to that found in naïve corneas, further supporting the importance of DCs in cold thermoreceptor functioning.

4. Signs of pain.

We found clear signs of pain in both short-term and long-term DC depletion conditions. However, this pain was much more prominent in acute conditions, which is consistent with the development of an inflammatory condition produced by DC depletion that resolves partially over time. Under inflammation, corneal nerve activity of corneal cold thermoreceptor and nociceptor nerves is altered, as well as under our experimental conditions. Like in other tissues, corneal polymodal nociceptors would be sensitised during inflammation (Gallar et al., 2004, 2007; Acosta et al., 2013, 2014; Kovács et al., 2016; Belmonte, 2019; Luna et al., 2021), being this nociceptor sensitization on the basis of spontaneous pain and hyperalgesia experienced during ocular surface inflammation. Besides, the increased activity of polymodal nociceptors triggers the local release of pro-inflammatory neuropeptides as Substance-P (Müller et al., 2003; Murata and Masuko, 2006; Yang et al., 2021) and produces the subsequent neurogenic inflammation (Gonzalez et al., 1993; Vitar et al., 2021) worsening the inflammatory condition. Similar signs of spontaneous pain were observed in the LTDT and RC animals despite the functional recovery of cold nerve terminal activity in DC repopulated corneas. This suggests that pain experienced by the animals under these conditions may also depend on the activity of corneal polymodal nociceptors. The possibility exists that either polymodal nociceptor activity takes longer to recover after DC repopulation than cold thermoreceptor activity, or the nerve activity changes and pain sensation induced by DC depletion are result of changes transferred to sites other than the nerve terminals, such as the central nervous system, inducing s state of central sensitisation that take longer to disappear (Woolf, 2011; Belmonte et al., 2015). Neither short- nor long-term PBS injections produce pain behaviour, suggesting the idea of an inflammatory ambient caused by the absence of DCs.

Corneal DC depletion produces epithelial defects (Gao et al., 2011). Together with the changes induced by DC absence on cold thermoreceptor activity, an altered epithelial integrity is also expected. Intraepithelial DCs are in physical contact with epithelial cells through their dendritic processes, extending or retracting them in response to different external stimuli as thermal injury (Ward et al., 2007). DCs migrate along the epithelial sheet during epithelial wound repair, being determinant in this process (Gao et al., 2011). Corneal epithelial cells have been proposed to function as surrogate Schwann cells to

support intraepithelial nerve terminals (Stepp et al., 2017) surrounding them (Müller et al., 2003), phagocytizing axon fragments (Stepp et al., 2017) and modulating the immune response to injury (Fleiszig and Evans, 2002). In turn, the tonic release of neuropeptides and other trophic factors by corneal nerves are supposed to supply molecules essential to maintain corneal epithelial cells differentiation and proliferation (Stepp et al., 2017). Taking all of this into account, it is very likely that the inflammatory conditions produced by DC depletion may be due to a disruption in the functional interaction between nerves, and dendritic and epithelial cells.

5. Basal tearing.

When we analysed the basal tearing rate in animals with no resident DCs, we observed that the tearing rate was significantly reduced under short-term depletion only. This reduction in tear volume can be explained by the reduced activity of cold thermoreceptors seen in these mice. TRPM8-dependent activity of corneal cold thermoreceptors contributes to regulating the basal tear flow and the deletion of TRPM8 channel in mice eliminates cold responsiveness and reduces basal tearing (Parra et al 2010).

According to that, we would expect to find changes also under long-term DC depletion conditions, as reduced cooling responses were observed in cold thermoreceptors of these animals. However, the tearing rate at 8 days under DC depletion was similar to that observed before the depletion. We cannot fully exclude that the absence of statistical significance is due, at least in part, to the high variability of data. It is also possible that polymodal sensitization induces reflex tearing (Acosta et al., 2004) that compensate for the decrease of basal tearing associated with the lower cold thermoreceptor input produced by DC depletion. Nevertheless, it should be noted that, due to the loss of animals over the 8 days of treatment, the number of animals in which the tearing rate was measured before DT injections and at 2 and 8 days under long-term DC depletion was very low (n=3), thus limiting the possibility to draw solid conclusions. The absence of changes in tearing rate in PBS-injected animals further support that the changes observed in DT-injected animals are due to the absence of the DCs.

6. DC distribution and morphology.

In naïve animals two morphologically different DC, dendritiform and round-shaped, were found within the cornea. Their number decreased from the corneal periphery to the centre as previously described (Yamagami et al., 2005; Hattori et al., 2016). As expected, no DCs were found in the cornea neither in short-term nor in long-term DC depletion conditions. However, in both cases, scarce DCs were present near the corneoscleral limbus. DC depletion impairs nerve regeneration in wounded corneas because DCs are the main source of ciliary neurotrophic factor (CNTF) in this tissue (Gao et al., 2016b). Also, DCs could be participating in corneal epithelium innervation by accompanying sensory nerve fibres in crossing the basement membrane and in branching into nerve endings (Gao et al., 2016a). Less nerve density has been reported both in the centre and in the periphery of the cornea of DT-injected animals (Gao et al., 2016a). The possible reduction of nerve terminal branching and density may explain the little changes observed in the cold thermoreceptor distribution over the cornea in the long-term DC depleted corneas. Under this condition, the probability of finding active cold thermoreceptors was reduced in the central cornea but not in the peripheral area. This may be due to close proximity to the limbus, where newly recruited DCs coming from the blood vessels are present and the effects of DC depletion are not so prominent. Indeed, the location of active cold thermoreceptors seems to be somehow related to DC distribution, as there was an increased probability of recording them at the mid-peripheral and peripheral cornea in short-term and long-term DC depleted corneas respectively, being this reversed when allowing DCs to repopulate the cornea.

In PBS-injected animals we also found the two morphologically types of DCs present in the cornea of naïve animals (dendritiform and round-shaped), although a higher density of DCs with less dendritic processes were observed near the limbus, suggesting they are immature DCs concentrated around the limbal blood vessels. The presence of more DCs near the limbus in both short-term and long-term PBS injected animals in comparison with naïve corneas may also explain the increased nerve activity found in the corneal periphery of PBS-injected mice. The lower number of dendritic processes observed may be also associated with a slightly higher release of cytokines from DCs due to the injection. The level of cytokine IL-1β in tears is inversely proportional with the

number of dendrites of corneal DCs (Yamaguchi et al., 2014) and this could be one of the causes behind the slight changes in DC morphology.

When animals are allowed to recover corneal DCs (RC group), most DCs are clearly round-shaped and are preferentially located in the periphery. The round-shaped DCs found in RC corneas suggest that they are immature DCs (Kim and Kim, 2019) that have recently arrived to the cornea after their depletion. Besides, as round-shaped DCs are supposed to be helping in nerve branching (Gao et al., 2016a), their presence in RC corneas would also contribute to explain the normalisation of the nerve activity and distribution of active cold thermoreceptor over the cornea.

7. A mouse model allowing morphological study of the neuro-immune interactions in the cornea

The use of whole mount cornea preparations and the *in vivo* confocal imaging of CD11C-DTR mice cornea made it possible to visualise the endogenously GFP-labelled DCs present in this transparent tissue. However, this mouse strain does not allow to see corneal nerves *in vivo*, being necessary to perform immunofluorescent staining against beta-III tubulin to visualise corneal innervation. Uniformity in labelling is critical and sometimes this is not achieved with immunofluorescence techniques. This is the reason why we decided to create a mouse model in which not only DCs were endogenously labelled but also corneal sensory nerves.

Although our main objective has been to analyse the functional changes induced in cold nerve activity under different experimental conditions, to describe the possible morphological interactions between DCs and nerves is also of interest. The developed mouse model allows us to study in the living mice their morphological interactions, as DCs and epithelial nerves are located in close proximity. We confirmed that dendrites of DCs cross one or several subbasal nerve fibres or intraepithelial nerve endings, although there does not seem to be any type of physical union between them. However, this is an aspect of the study in which we intend to deepen in the future. Similarly, to complete the present work, it would be interesting to study in depth other pending questions such as the effects of DCs repopulation after their depletion for longer than 8 days. This would allow us to see if there is a complete recovery of the nerve activity phenotype and pain

behaviour. Besides, it would also be interesting to carry out an exhaustive and quantitative study on the morphology of the corneal nerves under short-term and long-term DC depletion and DC recovery conditions, in order to determine whether the changes observed in cold nerve activity are associated with changes in nerve morphology.

8.Concluding remarks.

Despite the abundant literature on neuro-immune interactions in the cornea, most of the previous experimental studies were done under pathological conditions, including viral infection, and did not explore functionally corneal nerve activity (Veiga-Fernandes and Mucida, 2016). This PhD Thesis shows by the first time, performing *ex vivo* electrophysiological recordings and pain behavioural experiments, that a functional interaction between immune DC and sensory nerves also occurs at basal tissue conditions and that this interaction is crucial in maintaining a normal cold sensory nerve activity in the cornea and allowing ocular surface homeostasis.

Understanding how important the presence of DCs is for the maintenance of corneal health (and particularly its influence on corneal nerve activity in steady state conditions) is essential to better understand the pathophysiology of several diseases and to better guide the possible therapeutic options. Furthermore, since the association between DCs and nerves not only occurs in the cornea, but also occurs in other tissues such as the skin (Riol-Blanco et al., 2014; Kashem et al., 2015), the lung (Kradin et al., 1997; Veres et al., 2007) or the gut (Yoo and Mazmanian, 2017) maybe this discovery will allow us to better know the homeostatic mechanisms maintaining tissue health and how neuro-immunity disruption is behind the pathophysiology of several diseases. This new role for DCs, somehow beyond their canonical immune function, opens a new paradigm in understanding neuroimmune interactions and can lead to a better knowledge and management of many diseases.

VI. CONCLUSIONS

1. Activity of corneal cold thermoreceptors depends on the presence or absence of resident dendritic cells. Under short-term corneal DC depletion, cold thermoreceptor responsiveness to heat is increased and mechanical responsiveness is decreased. However, their responsiveness to cold is not altered compared with steady-state conditions.

2. Under long-term DC depletion responsiveness of cold thermoreceptors to cooling is reduced in comparison with steady-state conditions.

3. The shape of cold nerve terminal impulses is altered under corneal long-term DC depletion, suggesting the inactivation or downregulation of background and/or repolarization K^+ channels under this condition.

4. The changes in nerve activity and nerve impulse shape observed under short and long-term DC depletion are suggestive of a certain degree of ocular inflammation and damage associated with DC depletion that affects the activity of transducing and coding ion channels.

5. When DCs are allowed to repopulate the cornea after short-term DC depletion, parameters defining responsiveness to stimulation and nerve terminal impulse shape are similar to those of cold thermoreceptor terminals recorded in naïve corneas, further supporting the idea that DCs are crucial for the normal functioning of corneal cold sensory neurons.

6. The absence of DCs caused pain, the magnitude of which decreased over time after DC depletion although it did not fully disappear after DCs repopulated the cornea, suggesting the development of a sensitised state of corneal sensory nerves.

7. Basal tearing rate is reduced under short-term DC depletion but recover normal values under long-term DC depletion conditions.

8. Corneal tissue is free of DCs after subconjunctival injections of diphtheria toxin. Distribution of DCs is normal at 8 days after a single diphtheria toxin subconjunctival injection.

9. There is a functional interaction between resident DCs and corneal sensory nerves at steady-state conditions. The developed mouse model will also allow a deeper understanding of the neuro-immune crosstalk under inflammatory conditions of the eye.

CONCLUSIONES

1. La actividad de los termorreceptores de frío de la córnea depende de la presencia o ausencia de las células dendríticas residentes. Bajo condiciones de depleción de las CD corneales a corto plazo, la respuesta de los termorreceptores de frío al calor está aumentada y la respuesta a la estimulación mecánica está disminuida. Sin embargo, su respuesta a frío no está alterada en comparación con la que se da en condiciones basales.

2. Bajo condiciones de depleción de CD a largo plazo, la respuesta de los termorreceptores de frío al enfriamiento se reduce en comparación con lo que ocurre en condiciones basales.

3. La forma de los impulsos nerviosos de las terminaciones de los termorreceptores de frío está alterada en condiciones de depleción de CD corneales a largo plazo, lo que sugiere la inactivación o regulación a la baja de los canales de K+ de fondo y/o de repolarización en estas condiciones.

4. Los cambios en la actividad y la forma de los impulsos nerviosos de las terminaciones de los termorreceptores de frío observados bajo las condiciones de depleción de CD tanto a corto como a largo plazo sugieren cierto grado de inflamación y daño ocular asociados a la depleción de las CD que afecta a la actividad de los canales iónicos transductores y codificadores.

5. Cuando se produce la repoblación de las CD en la córnea tras su depleción a corto plazo, los parámetros que definen la respuesta a la estimulación y la forma de los impulsos nerviosos de los termorreceptores de frío son similares a los que se registran corneas naif, apoyando aún más la idea de que las CD son cruciales para el funcionamiento normal de las neuronas sensoriales de frío corneales.

6. La ausencia de CD produce dolor, cuya magnitud disminuye con el tiempo tras la depleción de las CD, aunque no desaparece por completo después de que las CD repueblen la córnea, sugiriendo el desarrollo de un estado de sensibilización de los nervios sensoriales corneales.

7. La tasa de lagrimeo basal se reduce bajo condiciones de depleción de las CD a corto plazo, pero recupera valores normales bajo condiciones de depleción de las CD a largo plazo.

8. La córnea está libre de CD tras las inyecciones subconjuntivales de toxina diftérica. La distribución de las CD es normal 8 días después de una única inyección subconjuntival de toxina diftérica.

9. Existe una interacción funcional entre las CD residentes y los nervios sensoriales corneales en condiciones basales. El modelo de ratón desarrollado permitirá una comprensión más profunda de las interacciones neuro-inmunes en condiciones inflamatorias del ojo.

VII. BIBLIOGRAPHY

Acosta, M. C., Belmonte, C., and Gallar, J. (2001). Sensory experiences in humans and single-unit activity in cats evoked by polymodal stimulation of the cornea. J. Physiol. 534, 511–25. Available at: http://www.ncbi.nlm.nih.gov/pubmed/11454968.

Acosta, M. C., Luna, C., Quirce, S., Belmonte, C., and Gallar, J. (2013). Changes in sensory activity of ocular surface sensory nerves during allergic keratoconjunctivitis. Pain 154, 2353–2362. doi:10.1016/j.pain.2013.07.012.

Acosta, M. C., Luna, C., Quirce, S., Belmonte, C., and Gallar, J. (2014). Corneal sensory nerve activity in an experimental model of UV keratitis. Investig. Ophthalmol. Vis. Sci. 55, 3403–3412. doi:10.1167/iovs.13-13774.

Acosta, M. C., Peral, A., Luna, C., Pintor, J., Belmonte, C., and Gallar, J. (2004). Tear secretion induced by selective stimulation of corneal and conjunctival sensory nerve fibers. Invest. Ophthalmol. Vis. Sci. 45, 2333–6. Available at: http://www.ncbi.nlm.nih.gov/pubmed/15223813.

Al-Aqaba, M. A., Dhillon, V. K., Mohammed, I., Said, D. G., and Dua, H. S. (2019). Corneal nerves in health and disease. Prog. Retin. Eye Res. 73, 100762. doi:10.1016/j.preteyeres.2019.05.003.

Al-Aqaba, M. A., Fares, U., Suleman, H., Lowe, J., and Dua, H. S. (2010). Architecture and distribution of human corneal nerves. Br. J. Ophthalmol. 94, 784–789. doi:10.1136/bjo.2009.173799.

Alcalde I, Íñigo-Portugués A, González-González O, Almaraz L, Artime E, Morenilla-Palao C, Gallar J, Viana F, Merayo-Lloves J, Belmonte C. (2018). Morphological and functional changes in TRPM8-expressing corneal cold thermoreceptor neurons during aging and their impact on tearing in mice. J Comp Neurol. 526(11):1859-1874. doi: 10.1002/cne.24454.

Alamri, A. S., Wood, R. J., Ivanusic, J. J., and Brock, J. A. (2018). The neurochemistry and morphology of functionally identified corneal polymodal nociceptors and cold thermoreceptors. PLoS One 13, e0195108. doi:10.1371/journal.pone.0195108.

Almubrad, T., and Akhtar, S. (2011). Structure of corneal layers, collagen fibrils, and proteoglycans of tree shrew cornea. Mol. Vis. 17, 2283–2291. Available at: /pmc/articles/PMC3171502/.

Ambati, B. K., Nozaki, M., Singh, N., Takeda, A., Jani, P. D., Suthar, T., et al. (2006). Corneal avascularity is due to soluble VEGF receptor-1. Nature 443, 993–997. doi:10.1038/nature05249.

Amsen, D., Blander, J. M., Lee, G. R., Tanigaki, K., Honjo, T., and Flavell, R. A. (2004). Instruction of distinct CD4 T helper cell fates by different notch ligands on antigen-presenting cells. Cell 117, 515–526. doi:10.1016/S0092-8674(04)00451-9.

Argüeso, P., and Gipson, I. K. (2001). Epithelial mucins of the ocular surface: Structure, biosynthesis and function. Exp. Eye Res. 73, 281–289. doi:10.1006/exer.2001.1045.

Bachem, A., Güttler, S., Hartung, E., Ebstein, F., Schaefer, M., Tannert, A., et al. (2010). Superior antigen cross-presentation and XCR1 expression define human CD11c+CD141+ cells as homologues of mouse CD8+ dendritic cells. J. Exp. Med. 207, 1273–1281. doi:10.1084/jem.20100348.

Bailey, S. L., Schreiner, B., McMahon, E. J., and Miller, S. D. (2007). CNS myeloid DCs presenting endogenous myelin peptides "preferentially" polarize CD4+ TH-17 cells in relapsing EAE. Nat. Immunol. 8, 172–180. doi:10.1038/ni1430.

Bakri, Y., Sarrazin, S., Mayer, U. P., Tillmanns, S., Nerlov, C., Boned, A., et al. (2005). Balance of MafB and PU.1 specifies alternative macrophage or dendritic cell fate. Blood 105, 2707–2716. doi:10.1182/blood-2004-04-1448.

Bamboat, Z. M., Stableford, J. A., Plitas, G., Burt, B. M., Nguyen, H. M., Welles, A. P., et al. (2009). Human Liver Dendritic Cells Promote T Cell Hyporesponsiveness. J. Immunol. 182, 1901–1911. doi:10.4049/jimmunol.0803404.

Banchereau, J., Briere, F., Caux, C., Davoust, J., Lebecque, S., Liu, Y. J., et al. (2000). Immunobiology of dendritic cells. Annu. Rev. Immunol. 18, 767–811. doi:10.1146/annurev.immunol.18.1.767.

Basbaum AI, Bautista DM, Scherrer G, Julius D (2009) Cellular and Molecular Mechanisms of Pain. Cell 139:267–284 Available at: /pmc/articles/PMC2852643/?report=abstract.

Belmonte, C. (2019). Pain, Dryness, and Itch Sensations in Eye Surface Disorders Are Defined By a Balance Between Inflammation and Sensory Nerve Injury. Cornea 38 Suppl 1, S11–S24. doi:10.1097/ICO.0000000000002116.

Belmonte, C., Acosta, M. C., and Gallar, J. (2004a). Neural basis of sensation in intact and injured corneas. Exp. Eye Res. 78, 513–25. Available at: http://www.ncbi.nlm.nih.gov/pubmed/15106930.

Belmonte C, Acosta MC, Merayo-Lloves J, Gallar J (2015) What Causes Eye Pain? Curr Ophthalmol Rep 3:111–121 Available at: http://dx.doi.org/10.1007/s40135-015-0073-9.

Belmonte, C., Aracil, A., Acosta, M. C., Luna, C., and Gallar, J. (2004b). Nerves and sensations from the eye surface. Ocul. Surf. 2, 248–53. Available at: http://www.ncbi.nlm.nih.gov/pubmed/17216099.

Belmonte, C., and Gallar, J. (2011). Cold thermoreceptors, unexpected players in tear production and ocular dryness sensations. Invest. Ophthalmol. Vis. Sci. 52, 3888–3892. doi:10.1167/iovs.09-5119.

Belmonte, C., Gallar, J., Pozo, M. A., and Rebollo, I. (1991). Excitation by irritant chemical substances of sensory afferent units in the cat's cornea. J. Physiol. 437, 709–725. doi:10.1113/jphysiol.1991.sp018621.

Belmonte C, Garcia-Hirschfeld J, Gallar J. (1997). Neurobiology of ocular pain. Progr Ret Eye Res. 16, 117–156.

Belmonte, C., and Giraldez, F. (1981). Responses of cat corneal sensory receptors to mechanical and thermal stimulation. J. Physiol. 321, 355–68. Available at: http://www.ncbi.nlm.nih.gov/pubmed/7338816.

Belmonte, C., Tervo, T.T., and Gallar, J. (2011). "Sensory Innervation of the Eye", in Adler's Physiology of the Eye, ed. Levin, L.A., (Elsevier), 16, 363-384.

Bendriss-Vermare, N., Barthélémy, C., Durand, I., Bruand, C., Dezutter-Dambuyant, C., Moulian, N., et al. (2001). Human thymus contains IFN-α-producing CD11c-, myeloid CD11c+, and mature interdigitating dendritic cells. J. Clin. Invest. 107, 835–844. doi:10.1172/JCI11734.

Bessou, P., and Perl, E. R. (1969). Response of cutaneous sensory units with unmyelinated fibers to noxious stimuli. J. Neurophysiol. 32, 1025–1043. doi:10.1152/jn.1969.32.6.1025.

Birbeck, M. S., Breathnach, A. S., and Everall, J. D. (1961). An Electron Microscope Study of Basal Melanocytes and High-Level Clear Cells (Langerhans Cells) in Vitiligo**From the Chester Beatty Research Institute, Royal Cancer Hospital, London, S.W. 3, and the Departments of Anatomy, and Dermatology, St. Mary's Hospital Medical School (University of London) London, W. 2, England. J. Invest. Dermatol. 37, 51–64. doi:10.1038/jid.1961.80.

Boor, P. P. C., Bosma, B. M., Tran, K. T. C., Van Derlaan, L. J. W., Hagenaars, H., IJzermans, J. N. M., et al. (2019). Characterization of antigen-presenting cell subsets in human liver-draining lymph nodes. Front. Immunol. 10. doi:10.3389/fimmu.2019.00441.

Brissette-Storkus, C. S., Reynolds, S. M., Lepisto, A. J., and Hendricks, R. L. (2002). Identification of a novel macrophage population in the normal mouse corneal stroma. Investig. Ophthalmol. Vis. Sci. 43, 2264–2271. Available at: /pmc/articles/PMC3253392/?report=abstract.

Brock J, Acosta MC, Abed A Al, Pianova S, Belmonte C (2006) Barium ions inhibit the dynamic response of guinea-pig corneal cold receptors to heating but not to cooling. J Physiol 5752:573–581.

Brock JA, Pianova S, Belmonte C (2001) Differences between nerve terminal impulses of polymodal nociceptors and cold sensory receptors of the guinea-pig cornea. J Physiol 533:493–501.

Bron, R., Wood, R. J., Brock, J. A., and Ivanusic, J. J. (2014). Piezo2 expression in corneal afferent neurons. J. Comp. Neurol. 522, 2967–2979. doi:10.1002/cne.23560.

Cabeza-Cabrerizo, M., Cardoso, A., Minutti, C. M., Pereira da Costa, M., and Reis Sousa, C. (2021). Annual Review of Immunology Dendritic Cells Revisited. doi:10.1146/annurev-immunol-061020.

Carr RW, Pianova S, Brock JA (2002) The effects of polarizing current on nerve terminal impulses recorded from polymodal and cold receptors in the guinea-pig cornea. J Gen Physiol 120:395–405 Available at: http://www.ncbi.nlm.nih.gov/pubmed/12198093.

Carr, R. W., Pianova, S., Fernandez, J., Fallon, J. B., Belmonte, C., and Brock, J. A. (2003). Effects of heating and cooling on nerve terminal impulses recorded from cold-sensitive receptors in the guinea-pig cornea. J. Gen. Physiol. 121, 427–439. doi:10.1085/jgp.200308814.

Chan-Ling, T. (1989). Sensitivity and neural organization of the cat cornea. Investig. Ophthalmol. Vis. Sci. 30, 1075–1082. Available at: https://iovs.arvojournals.org/article.aspx?articleid=2178300.

Chen, X., Gallar, J., and Belmonte, C. (1997). Reduction by antiinflammatory drugs of the response of corneal sensory nerve fibers to chemical irritation. Investig. Ophthalmol. Vis. Sci. 38, 1944–1953. doi:10.1016/s0002-9394(99)80127-5.

Chistiakov, D. A., Orekhov, A. N., Sobenin, I. A., and Bobryshev, Y. V. (2014). Plasmacytoid dendritic cells: Development, functions, and role in atherosclerotic inflammation. Front. Physiol. 5 JUL. doi:10.3389/fphys.2014.00279.

Chopin, M., Seillet, C., Chevrier, S., Wu, L., Wang, H., Morse, H. C., et al. (2013). Langerhans cells are generated by two distinct PU.1-dependent transcriptional networks. J. Exp. Med. 210, 2967–2980. doi:10.1084/jem.20130930.

Chuang HH, Prescott ED, Kong H, Shields S, Jordt SE, Basbaum AI, Chao M V., Julius D (2001) Bradykinin and nerve growth factor release the capsaicin receptor from PtdIns(4,5)P2-mediated inhibition. Nature 411:957–962 Available at: http://www.ncbi.nlm.nih.gov/pubmed/11418861.

Constant, S., Pfeiffer, C., Woodard, A., Pasqualini, T., and Bottomly, K. (1995). Extent of T cell receptor ligation can determine the functional differentiation of naive cd4+ T cells. J. Exp. Med. 182, 1591–1596. doi:10.1084/jem.182.5.1591.

Contractor, N., Louten, J., Kim, L., Biron, C. A., and Kelsall, B. L. (2007). Cutting Edge: Peyer's Patch Plasmacytoid Dendritic Cells (pDCs) Produce Low Levels of Type I Interferons: Possible Role for IL-10, TGFβ, and Prostaglandin E 2 in Conditioning a Unique Mucosal pDC Phenotype . J. Immunol. 179, 2690–2694. doi:10.4049/jimmunol.179.5.2690.

Cruzat, A., Schrems, W. A., Schrems-Hoesl, L. M., Cavalcanti, B. M., Baniasadi, N., Witkin, D., et al. (2015). Contralateral clinically unaffected eyes of patients with unilateral infectious keratitis demonstrate a sympathetic immune response. Investig. Ophthalmol. Vis. Sci. 56, 6612–6620. doi:10.1167/iovs.15-16560.

Cruzat, A., Witkin, D., Baniasadi, N., Zheng, L., Ciolino, J. B., Jurkunas, U. V., et al. (2011). Inflammation and the Nervous System: The Connection in the Cornea in Patients with Infectious Keratitis. Investig. Opthalmology Vis. Sci. 52, 5136. doi:10.1167/iovs.10-7048.

Cursiefen, C., Chen, L., Saint-Geniez, M., Hamrah, P., Jin, Y., Rashid, S., et al. (2006). Nonvascular VEGF receptor 3 expression by corneal epithelium maintains avascularity and vision. Proc. Natl. Acad. Sci. U. S. A. 103, 11405–11410. doi:10.1073/pnas.0506112103.

Dawson, D.G., Ubels, J.L., and Edelhauser, H.F. (2011). "Cornea and Sclera," in Adler's Physiology of the Eye, ed. Levin, L.A., (Elsevier), 4, 71-130.

Delgado, M., and Ganea, D. (2013). Vasoactive intestinal peptide: A neuropeptide with pleiotropic immune functions. Amino Acids 45, 25–39. doi:10.1007/s00726-011-1184-8.

DelMonte, D. W., and Kim, T. (2011). Anatomy and physiology of the cornea. J. Cataract Refract. Surg. 37, 588–598. doi:10.1016/j.jcrs.2010.12.037.

Donnenberg, V. S., and Donnenberg, A. D. (2003). Identification, rare-event detection and analysis of dendritic cell subsets in broncho-alveolar lavage fluid and peripheral blood by flow cytometry. Front. Biosci. 8. doi:10.2741/1185.

Du X, Gamper N (2013) Potassium Channels in Peripheral Pain Pathways: Expression, Function and Therapeutic Potential. Curr Neuropharmacol 11:621–640.

Dua, H. S., Watson, N. J., Mathur, R. M., and Forrester, J. V. (1993). Corneal epithelial cell migration in humans: 'hurricane and blizzard keratopathy.' Eye 7, 53–58. doi:10.1038/eye.1993.12.

Dvorscak, L., and Marfurt, C. F. (2008). Age-related changes in rat corneal epithelial nerve density. *Investig. Ophthalmol. Vis. Sci.* 49, 910–916. doi:10.1167/iovs.07-1324.

Ehinger, B. (1966). Connections between Adrenergic Nerves and other Tissue Components in the Eye. *Acta Physiol. Scand.* 67, 57–64. doi:10.1111/j.1748-1716.1966.tb03287.x.

Facchetti, F., De Wolf-Peeters, C., Mason, D. Y., Pulford, K., Van den Oord, J. J., and Desmet, V. J. (1988). Plasmacytoid T cells. Immunohistochemical evidence for their monocyte/macrophage origin. Am. J. Pathol. 133, 15–21. Available at: /pmc/articles/PMC1880653/?report=abstract.

Fainaru, O., Woolf, E., Lotem, J., Yarmus, M., Brenner, O., Goldenberg, D., et al. (2004). Runx3 regulates mouse TGF-β-mediated dendritic cell function and its absence results in airway inflammation. EMBO J. 23, 969–979. doi:10.1038/sj.emboj.7600085.

Fang D, Kong LY, Cai J, Li S, Liu XD, Han JS, Xing GG (2015) Interleukin-6-mediated functional upregulation of TRPV1 receptors in dorsal root ganglion neurons through the activation of JAK/PI3K signaling pathway: Roles in the development of bone cancer pain in a rat model. Pain 156:1124–1144 Available at: http://www.ncbi.nlm.nih.gov/pubmed/25775359.

Fernández-Trillo, J., Florez-Paz, D., Íñigo-Portugués, A., González-González, O., del Campo, A. G., González, A., et al. (2020). Piezo2 mediates low-threshold mechanically evoked pain in the cornea. J. Neurosci. 40, 8976–8993. doi:10.1523/JNEUROSCI.0247-20.2020.

Fleiszig SMJ, Evans DJ (2002) The pathogenesis of bacterial keratitis: Studies with Pseudomonas aeruginosa. Clin Exp Optom 85:271–278.

Forrester, J. V., and Xu, H. (2012). Good news-bad news: The Yin and Yang of immune privilege in the eye. Front. Immunol. 3, 338. doi:10.3389/fimmu.2012.00338.

Forrester, J. V. (2009). Privilege revisited: An evaluation of the eye's defence mechanisms. Eye 23, 756–766. doi:10.1038/eye.2008.259.

Foulsham, W., Coco, G., Amouzegar, A., Chauhan, S. K., and Dana, R. (2018). When Clarity Is Crucial: Regulating Ocular Surface Immunity. Trends Immunol. 39, 288–301. doi:10.1016/j.it.2017.11.007.

Francisco, L. M., Sage, P. T., and Sharpe, A. H. (2010). The PD-1 pathway in tolerance and autoimmunity. Immunol. Rev. 236, 219–242. doi:10.1111/j.1600-065X.2010.00923.x.

Gallar, J., Acosta, M. C., Gutiérrez, A. R., and Belmonte, C. (2007). Impulse activity in corneal sensory nerve fibers after photorefractive keratectomy. Invest. Ophthalmol. Vis. Sci. 48, 4033–4037. doi:10.1167/iovs.07-0012.

Gallar, J., Acosta, M. C., Moilanen, J. A. O., Holopainen, J. M., Belmonte, C., and Tervo, T. M. T. (2004). Recovery of corneal sensitivity to mechanical and chemical stimulation after laser in situ keratomileusis. J. Refract. Surg. 20, 229–235. Available at: http://www.ncbi.nlm.nih.gov/pubmed/15188899.

Gallar, J., Pozo, M. A., Tuckett, R. P., and Belmonte, C. (1993). Response of sensory units with unmyelinated fibers to mechanical, thermal and chemical stimulation of the cat's cornea. J. Physiol. 468, 609–22. Available at: http://www.ncbi.nlm.nih.gov/pubmed/8254527.

Gao, N., Lee, P., and Yu, F.-S. (2016a). Intraepithelial dendritic cells and sensory nerves are structurally associated and functional interdependent in the cornea. Sci. Rep. 6, 36414. doi:10.1038/srep36414.

Gao, N., Yan, C., Lee, P., Sun, H., and Yu, F. S. (2016b). Dendritic cell dysfunction and diabetic sensory neuropathy in the cornea. J. Clin. Invest. 126, 1998–2011. doi:10.1172/JCI85097.

Gao N, Yin J, Yoon GS, Mi Q-S, Yu F-SX (2011) Dendritic cell-epithelium interplay is a determinant factor for corneal epithelial wound repair. Am J Pathol 179:2243–2253 Available at: http://www.ncbi.nlm.nih.gov/pubmed/21924232.

Geissmann, F., Manz, M. G., Jung, S., Sieweke, M. H., Merad, M., and Ley, K. (2010). Development of monocytes, macrophages, and dendritic cells. Science. 327, 656–661. doi:10.1126/science.1178331.

Goldstein RH, Barkai O, Íñigo-Portugués A, Katz B, Lev S, Binshtok AM (2019) Location and Plasticity of the Sodium Spike Initiation Zone in Nociceptive Terminals In Vivo. Neuron 102:801-812.e5 Available at: https://pubmed.ncbi.nlm.nih.gov/30926280/.

Gonzalez, G. G., Garcia de la Rubia, P., Gallar, J., and Belmonte, C. (1993). Reduction of capsaicin-induced ocular pain and neurogenic inflammation by calcium antagonists. Invest. Ophthalmol. Vis. Sci. 34, 3329–3335. Available at: https://pubmed.ncbi.nlm.nih.gov/8225868/.

González-González, O., Bech, F., Gallar, J., Merayo-Lloves, J., and Belmonte, C. (2017). Functional properties of sensory nerve terminals of the mouse cornea. Investig. Ophthalmol. Vis. Sci. 58, 404–415. doi:10.1167/iovs.16-20033.

Hacker, C., Kirsch, R. D., Ju, X. S., Hieronymus, T., Gust, T. C., Kuhl, C., et al. (2003). Transcriptional profiling identifies Id2 function in dendritic cell development. Nat. Immunol. 4, 380–386. doi:10.1038/ni903.

Halim, T. Y. F., Hwang, Y. Y., Scanlon, S. T., Zaghouani, H., Garbi, N., Fallon, P. G., et al. (2016). Group 2 innate lymphoid cells license dendritic cells to potentiate memory TH2 cell responses. Nat. Immunol. 17, 57–64. doi:10.1038/ni.3294.

Hambleton, S., Salem, S., Bustamante, J., Bigley, V., Boisson-Dupuis, S., Azevedo, J., et al. (2011). IRF8 Mutations and Human Dendritic-Cell Immunodeficiency. N. Engl. J. Med. 365, 127–138. doi:10.1056/NEJMoa1100066.

Hamrah, P., Seyed-Razavi, Y., and Yamaguchi, T. (2016). Translational Immunoimaging and Neuroimaging Demonstrate Corneal Neuroimmune Crosstalk. *Cornea* 35, S20–S24. doi:10.1097/ICO.0000000000001014.

Hamrah, P., Huq, S. O., Liu, Y., Zhang, Q., and Dana, M. R. (2003a). Corneal immunity is mediated by heterogeneous population of antigen-presenting cells. J. Leukoc. Biol. 74, 172–178. doi:10.1189/jlb.1102544.

Hamrah, P., Liu, Y., Zhang, Q., and Dana, M. R. (2003b). Alterations in corneal stromal dendritic cell phenotype and distribution in inflammation. Arch. Ophthalmol. 121, 1132–1140. doi:10.1001/archopht.121.8.1132.

Hamrah, P., Liu, Y., Zhang, Q., and Dana, M. R. (2003c). The Corneal Stroma Is Endowed with a Significant Number of Resident Dendritic Cells. Investig. Opthalmology Vis. Sci. 44, 581. doi:10.1167/iovs.02-0838.

Hamrah, P., Zhang, Q., Liu, Y., and Dana, M. R. (2002). Novel characterization of MHC class II-negative population of resident corneal Langerhans cell-type dendritic cells. Investig. Ophthalmol. Vis. Sci. 43, 639–646. Available at: https://pubmed.ncbi.nlm.nih.gov/11867578/.

Haniffa, M., Collin, M., and Ginhoux, F. (2013). "Ontogeny and Functional Specialization of Dendritic Cells in Human and Mouse," in Advances in Immunology (Academic Press Inc.), 1–49. doi:10.1016/B978-0-12-417028-5.00001-6.

Haniffa, M., Shin, A., Bigley, V., McGovern, N., Teo, P., See, P., et al. (2012). Human Tissues Contain CD141 hi Cross-Presenting Dendritic Cells with Functional Homology to Mouse CD103 + Nonlymphoid Dendritic Cells. Immunity 37, 60–73. doi:10.1016/j.immuni.2012.04.012.

Hanna, C., Bicknell, D. S., and O'brien, J. E. (1961). Cell Turnover in the Adult Human Eye. Arch. Ophthalmol. 65, 695–698. doi:10.1001/archopht.1961.01840020697016.

Hassell, J. R., and Birk, D. E. (2010). The molecular basis of corneal transparency. Exp. Eye Res. 91, 326–335. doi:10.1016/j.exer.2010.06.021.

Hattori, T., Takahashi, H., and Dana, R. (2016). Novel insights into the immunoregulatory function and localization of dendritic cells. Cornea 35, S49–S54. doi:10.1097/ICO.0000000000001005.

Haustein, J. (1983). On the ultrastructure of the developing and adult mouse corneal stroma. *Anat. Embryol. (Berl).* 168, 291–305. doi:10.1007/BF00315823.

Hawiger, D., Inaba, K., Dorsett, Y., Guo, M., Mahnke, K., Rivera, M., et al. (2001). Dendritic cells induce peripheral T cell unresponsiveness under steady state conditions in vivo. J. Exp. Med. 194, 769–779. doi:10.1084/jem.194.6.769.

Hazlett LD (1993) Corneal and Ocular Surface Histochemistry. Prog Histochem Cytochem 25:3–6 Available at: https://pubmed.ncbi.nlm.nih.gov/8456177/.

Henriksson, J. T., McDermott, A. M., and Bergmanson, J. P. G. (2009). Dimensions and morphology of the cornea in three strains of mice. *Investig. Ophthalmol. Vis. Sci.* 50, 3648–3654. doi:10.1167/iovs.08-2941.

He, J., Bazan, N. G., and Bazan, H. E. P. (2010). Mapping the entire human corneal nerve architecture. Exp. Eye Res. 91, 513–523. doi:10.1016/j.exer.2010.07.007.

Hildner, K., Edelson, B. T., Purtha, W. E., Diamond, M., Matsushita, H., Kohyama, M., et al. (2008). Batf3 deficiency reveals a critical role for CD8α+ dendritic cells in cytotoxic T cell immunity. Science. 322, 1097–1100. doi:10.1126/science.1164206.

Honeycutt SE, O'Brien LL (2020) Injection of Evans blue dye to fluorescently label and image intact vasculature. Biotechniques 70:181 Available at: /pmc/articles/PMC7983036/.

Hori, J., Vega, J. L., and Masli, S. (2010). Review of ocular immune privilege in the year 2010: Modifying the immune privilege of the eye. Ocul. Immunol. Inflamm. 18, 325–333. doi:10.3109/09273948.2010.512696.

Huang, G., Wang, Y., and Chi, H. (2012). Regulation of TH17 cell differentiation by innate immune signals. Cell. Mol. Immunol. 9, 287–295. doi:10.1038/cmi.2012.10.

Hu, K., Harris, D. L., Yamaguchi, T., Von Andrian, U. H., and Hamrah, P. (2015). A dual role for corneal dendritic cells in herpes simplex keratitis: Local suppression of corneal damage and promotion of systemic viral dissemination. PLoS One 10. doi:10.1371/journal.pone.0137123.

Hu, K., Harris, D., Yamaguchi, T., Ghiasi, H., Von Andrian, U., and Hambrah, P. (2013). The role of corneal plasmacytoid dendritic cells in acute herpes simplex virus infection. Investig. Ophthalmol. Vis. Sci. 54 (15), 2158. ARVO Abstract.

Hucho T, Levine JD (2007) Signaling Pathways in Sensitization: Toward a Nociceptor Cell Biology. Neuron 55:365–376 Available at: http://www.ncbi.nlm.nih.gov/pubmed/17678851.

Inaba, K., Inaba, M., Romani, N., Aya, H., Deguchi, M., Ikehara, S., et al. (1992). Generation of large numbers of dendritic cells from mouse bone marrow cultures supplemented with granulocyte/macrophage colony-stimulating factor. J. Exp. Med. 176, 1693–1702. doi:10.1084/jem.176.6.1693.

Ivanusic, J. J., Wood, R. J., and Brock, J. A. (2013). Sensory and sympathetic innervation of the mouse and guinea pig corneal epithelium. J. Comp. Neurol. 521, 877–93. doi:10.1002/cne.23207.

Jamali, A., Hu, K., Sendra, V. G., Blanco, T., Lopez, M. J., Ortiz, G., et al. (2020). Characterization of Resident Corneal Plasmacytoid Dendritic Cells and Their Pivotal Role in Herpes Simplex Keratitis. Cell Rep. 32, 108099. doi:10.1016/j.celrep.2020.108099.

Jamali, A., Harris, D. L., Blanco, T., Lopez, M. J., and Hamrah, P. (2020). Resident plasmacytoid dendritic cells patrol vessels in the naïve limbus and conjunctiva. *Ocul. Surf.* 18, 277–285. doi:10.1016/j.jtos.2020.02.005.

Jamali, A., Kenyon, B., Ortiz, G., Abou-Slaybi, A., Sendra, V. G., Harris, D. L., et al. (2021). Plasmacytoid dendritic cells in the eye. Prog. Retin. Eye Res. 80, 100877. doi:10.1016/j.preteyeres.2020.100877.

Jenkins, S. J., Perona-Wright, G., Worsley, A. G. F., Ishii, N., and MacDonald, A. S. (2007). Dendritic Cell Expression of OX40 Ligand Acts as a Costimulatory, Not Polarizing, Signal for

Optimal Th2 Priming and Memory Induction In Vivo. J. Immunol. 179, 3515–3523. doi:10.4049/jimmunol.179.6.3515.

Jung, S., Unutmaz, D., Wong, P., Sano, G.-I., De los Santos, K., Sparwasser, T., et al. (2002). In vivo depletion of CD11c+ dendritic cells abrogates priming of CD8+ T cells by exogenous cell-associated antigens. Immunity 17, 211–20. Available at: http://www.ncbi.nlm.nih.gov/pubmed/12196292.

Kadowaki, N. (2007). Dendritic cells - A conductor of T cell differentiation. Allergol. Int. 56, 193–199. doi:10.2332/allergolint.R-07-146.

Kashem SW, Riedl MS, Yao C, Honda CN, Vulchanova L, Kaplan DH (2015) Nociceptive Sensory Fibers Drive Interleukin-23 Production from CD301b+ Dermal Dendritic Cells and Drive Protective Cutaneous Immunity. Immunity 43:515–526.

Kashiwada, M., Pham, N. L. L., Pewe, L. L., Harty, J. T., and Rothman, P. B. (2011). NFIL3/E4BP4 is a key transcription factor for CD8α+ dendritic cell development. Blood 117, 6193–6197. doi:10.1182/blood-2010-07-295873.

Khandelwal, P., Blanco-Mezquita, T., Emami, P., Lee, H. S., Reyes, N. J., Mathew, R., et al. (2013). Ocular Mucosal CD11b+ and CD103+ Mouse Dendritic Cells under Normal Conditions and in Allergic Immune Responses. PLoS One 8. doi:10.1371/journal.pone.0064193.

Kim MK, Kim J (2019) Properties of immature and mature dendritic cells: phenotype, morphology, phagocytosis, and migration. RSC Adv 9:11230–11238.

Klechevsky, E., Morita, R., Liu, M., Cao, Y., Coquery, S., Thompson-Snipes, L. A., et al. (2008). Functional Specializations of Human Epidermal Langerhans Cells and CD14+ Dermal Dendritic Cells. Immunity 29, 497–510. doi:10.1016/j.immuni.2008.07.013.

Kovács I, Luna C, Quirce S, Mizerska K, Callejo G, Riestra A, Fernández-Sánchez L, Meseguer VM, Cuenca N, Merayo-Lloves J, Acosta MC, Gasull X, Belmonte C, Gallar J (2016) Abnormal activity of corneal cold thermoreceptors underlies the unpleasant sensations in dry eye disease. Pain 157:399–417 Available at: http://www.ncbi.nlm.nih.gov/pubmed/26675826.

Kradin R, MacLean J, Duckett S, Schneeberger EE, Waeber C, Pinto C (1997) Pulmonary response to inhaled antigen: neuroimmune interactions promote the recruitment of dendritic cells to the lung and the cellular immune response to inhaled antigen. Am J Pathol 150:1735–1743 Available at: http://www.ncbi.nlm.nih.gov/pubmed/9137097 [Accessed March 14, 2018].

Leal Rojas, I. M., Mok, W. H., Pearson, F. E., Minoda, Y., Kenna, T. J., Barnard, R. T., et al. (2017). Human blood cD1c+ dendritic cells promote Th1 and Th17 effector function in memory cD4+ T cells. Front. Immunol. 8, 971. doi:10.3389/fimmu.2017.00971.

Lee, D. J., and Taylor, A. W. (2013). Both MC5r and A2Ar Are Required for Protective Regulatory Immunity in the Spleen of Post–Experimental Autoimmune Uveitis in Mice. J. Immunol. 191, 4103–4111. doi:10.4049/jimmunol.1300182.

Lehtonen, A., Veckman, V., Nikula, T., Lahesmaa, R., Kinnunen, L., Matikainen, S., et al. (2005). Differential Expression of IFN Regulatory Factor 4 Gene in Human Monocyte-Derived Dendritic Cells and Macrophages. J. Immunol. 175, 6570–6579. doi:10.4049/jimmunol.175.10.6570.

Leppin, K., Behrendt, A. K., Reichard, M., Stachs, O., Guthoff, R. F., Baltrusch, S., et al. (2014). Diabetes mellitus leads to accumulation of dendritic cells and nerve fiber damage of the subbasal nerve plexus in the cornea. *Investig. Ophthalmol. Vis. Sci.* 55, 3603–3615. doi:10.1167/iovs.14-14307.

Li, Z., Burns, A. R., Rumbaut, R. E., and Smith, C. W. (2007). γδ T cells are necessary for platelet and neutrophil accumulation in limbal vessels and efficient epithelial repair after corneal abrasion. Am. J. Pathol. 171, 838–845. doi:10.2353/ajpath.2007.070008.

Lin, H., Li, W., Dong, N., Chen, W., Liu, J., Chen, L., et al. (2010). Changes in corneal epithelial layer inflammatory cells in aqueous tear-deficient dry eye. Investig. Ophthalmol. Vis. Sci. 51, 122–128. doi:10.1167/iovs.09-3629.

Liu, J., and Cao, X. (2015). Regulatory dendritic cells in autoimmunity: A comprehensive review. J. Autoimmun. 63, 1–12. doi:10.1016/j.jaut.2015.07.011.

Liu, Q., Smith, C. W., Zhang, W., Burns, A. R., and Li, Z. (2012). NK cells modulate the inflammatory response to corneal epithelial abrasion and thereby support wound healing. Am. J. Pathol. 181, 452–462. doi:10.1016/j.ajpath.2012.04.010.

Luna, C., Mizerska, K., Quirce, S., Belmonte, C., Gallar, J., Acosta, M. del C., et al. (2021). Sodium channel blockers modulate abnormal activity of regenerating nociceptive corneal nerves after surgical lesion. Invest. Ophthalmol. Vis. Sci. 62. doi:10.1167/IOVS.62.1.2.

Lund, J. M., Linehan, M. M., Iijima, N., and Iwasaki, A. (2006). Cutting Edge: Plasmacytoid Dendritic Cells Provide Innate Immune Protection against Mucosal Viral Infection In Situ. J. Immunol. 177, 7510–7514. doi:10.4049/jimmunol.177.11.7510.

Madisen, L., Zwingman, T. A., Sunkin, S. M., Oh, S. W., Zariwala, H. A., Gu, H., et al. (2010).

A robust and high-throughput Cre reporting and characterization system for the whole mouse brain. *Nat. Neurosci.* 13, 133–140. doi:10.1038/nn.2467.

Manicassamy, S., and Pulendran, B. (2011). Dendritic cell control of tolerogenic responses. Immunol. Rev. 241, 206–227. doi:10.1111/j.1600-065X.2011.01015.x.

Marfurt, C.F. (2000). "Nervous control of the cornea," in Nervous Control of the Eye, (Amsterdam: Harwood Academic Publishers), 41.

Marfurt, C. F., Cox, J., Deek, S., and Dvorscak, L. (2010). Anatomy of the human corneal innervation. Exp. Eye Res. 90, 478–492. doi:10.1016/j.exer.2009.12.010.

Marfurt, C. F., Kingsley, R. E., and Echtenkamp, S. E. (1989). Sensory and sympathetic innervation of the mammalian cornea. A retrograde tracing study. Investig. Ophthalmol. Vis. Sci. 30, 461–472. Available at: https://iovs.arvojournals.org/article.aspx?articleid=2160253.

Marfurt, C. F., and Ellis, L. C. (1993). Immunohistochemical localization of tyrosine hydroxylase in corneal nerves. *J. Comp. Neurol.* 336, 517–531. doi:10.1002/cne.903360405.

Maruoka, S., Inaba, M., and Ogata, N. (2018). Activation of Dendritic Cells in Dry Eye Mouse Model. Invest. Ophthalmol. Vis. Sci. 59, 3269–3277. doi:10.1167/IOVS.17-22550.

Matsui, T., Connolly, J. E., Michnevitz, M., Chaussabel, D., Yu, C.-I., Glaser, C., et al. (2009). CD2 Distinguishes Two Subsets of Human Plasmacytoid Dendritic Cells with Distinct Phenotype and Functions. J. Immunol. 182, 6815–6823. doi:10.4049/jimmunol.0802008.

Maurice, D.M. (1957). The structure and transparency of the cornea. J. Physiol. 136, 263–286. doi:10.1113/jphysiol.1957.sp005758.

Maurice, D. M. (1970). The transparency of the corneal stroma. Vision Res. 10, 107–108. doi:10.1016/0042-6989(70)90068-4.

Mayer, W.J., Irschick, U.M., Moser, P., Wurm, M., Huemer, H. P., Romani, N., et al. (2007). Characterization of antigen-presenting cells in fresh and cultured human corneas using novel dendritic cell markers. Investig. Ophthalmol. Vis. Sci. 48, 4459–4467. doi:10.1167/iovs.06-1184.

McCarey, B.E., Edelhauser, H.F., and Lynn, M.J. (2008). Review of corneal endothelial specular microscopy for FDA clinical trials of refractive procedures, surgical devices, and new intraocular drugs and solutions. Cornea 27, 1–16. doi:10.1097/ICO.0b013e31815892da.

Mckenna, C.C., and Lwigale, P.Y. (2011). Innervation of the mouse cornea during development. Investig. Ophthalmol. Vis. Sci. 52, 30–35. doi:10.1167/iovs.10-5902.

Medawar, P.B. (1948). Immunity to homologous grafted skin; the fate of skin homografts. Br. J. Exp. Pathol. 29, 58–69. Available at: https://www.ncbi.nlm.nih.gov/pmc/articles/PMC2073079/.

Meyer, R.A., Ringkamp, M., Campbell, J.N., and Raja, S.N. (2008). "Peripheral mechanisms of cutaneous nociception," in Wall and Melzack's Textbook of Pain, ed. McMahon, S.B., and. Koltzenburg, M., (Philadelphia: Elsevier), 3–34

Miranda-Saksena, M., Armati, P., Boadle, R. A., Holland, D. J., and Cunningham, A. L. (2000). Anterograde Transport of Herpes Simplex Virus Type 1 in Cultured, Dissociated Human and Rat Dorsal Root Ganglion Neurons. J. Virol. 74, 1827–1839. doi:10.1128/jvi.74.4.1827-1839.2000.

Morelli, A. E., and Thomson, A. W. (2007). Tolerogenic dendritic cells and the quest for transplant tolerance. Nat. Rev. Immunol. 7, 610–621. doi:10.1038/nri2132.

Morgan, C., DeGroat, W. C., and Jannetta, P.J. (1987). Sympathetic innervation of the cornea from the superior cervical ganglion. An HRP study in the cat. *J. Auton. Nerv. Syst.* 20, 179–183. doi:10.1016/0165-1838(87)90115-9.

Moriyama T, Iida T, Kobayashi K, Higashi T, Fukuoka T, Tsumura H, Leon C, Suzuki N, Inoue K, Gachet C, Noguchi K, Tominaga M (2003) Possible involvement of P2Y2 metabotropic receptors in ATP-induced transient receptor potential vanilloid receptor 1-mediated thermal hypersensitivity. J Neurosci 23:6058–6062.

Müller, L. J., Marfurt, C. F., Kruse, F., and Tervo, T. M. T. (2003). Corneal nerves: Structure, contents and function. Exp. Eye Res. 76, 521–542. doi:10.1016/S0014-4835(03)00050-2.

Murata, Y., and Masuko, S. (2006). Peripheral and central distribution of TRPV1, substance P and CGRP of rat corneal neurons. Brain Res. 1085, 87–94. doi:10.1016/j.brainres.2006.02.035.

Murphy, T. L., Grajales-Reyes, G. E., Wu, X., Tussiwand, R., Briseño, C. G., Iwata, A., et al. (2016). Transcriptional Control of Dendritic Cell Development. Annu. Rev. Immunol. 34, 93–119. doi:10.1146/annurev-immunol-032713-120204.

Nagasaki, T., and Zhao, J. (2003). Centripetal Movement of Corneal Epithelial Cells in the Normal Adult Mouse. Invest. Ophthalmol. Vis. Sci. 44, 558–566. doi:10.1167/IOVS.02-0705.

Nakano, H., Yanagita, M., and Gunn, M. D. (2001). CD11c+B220+Gr-1+ cells in mouse lymph nodes and spleen display characteristics of plasmacytoid dendritic cells. J. Exp. Med. 194, 1171–1178. doi:10.1084/jem.194.8.1171.

Nestle, F. O., Conrad, C., Tun-Kyi, A., Homey, B., Gombert, M., Boyman, O., et al. (2005). Plasmacytoid predendritic cells initiate psoriasis through interferon-α production. J. Exp. Med. 202, 135–143. doi:10.1084/jem.20050500.

Niederkorn, J. Y. (2019). The eye sees eye to eye with the immune system: The 2019 Proctor lecture. Investig. Ophthalmol. Vis. Sci. 60, 4489–4495. doi:10.1167/iovs.19-28632.

Okazawa M, Inoue W, Hori A, Hosokawa H, Matsumura K, Kobayashi S (2004) Noxious heat receptors present in cold-sensory cells in rats. Neurosci Lett 359:33–36 Available at: http://www.ncbi.nlm.nih.gov/pubmed/15050705.

O'Keeffe, M., Mok, W. H., and Radford, K. J. (2015). Human dendritic cell subsets and function in health and disease. Cell. Mol. Life Sci. 72, 4309–4325. doi:10.1007/s00018-015-2005-0.

Palomar, A. P. del, Montolío, A., Cegoñino, J., Dhanda, S. K., Lio, C. T., and Bose, T. (2019). The Innate Immune Cell Profile of the Cornea Predicts the Onset of Ocular Surface Inflammatory Disorders. J. Clin. Med. 8, 2110. doi:10.3390/jcm8122110.

Parra, A., Gonzalez-Gonzalez, O., Gallar, J., and Belmonte, C. (2014). Tear fluid hyperosmolality increases nerve impulse activity of cold thermoreceptor endings of the cornea. Pain 155, 1481–1491. doi:10.1016/j.pain.2014.04.025.

Pappenheimer AM, Harper AA, Moynihan M, Brockes JP (1982) Diphtheria toxin and related proteins: effect of route of injection on toxicity and the determination of cytotoxicity for various cultured cells. J Infect Dis 145:94–102 Available at: https://pubmed.ncbi.nlm.nih.gov/6798133/.

Parra, A., Madrid, R., Echevarria, D., del Olmo, S., Morenilla-Palao, C., Acosta, M. C., et al. (2010). Ocular surface wetness is regulated by TRPM8-dependent cold thermoreceptors of the cornea. Nat. Med. 16, 1396–1399. doi:10.1038/nm.2264.

Patel, D. V., and McGhee, C. N. J. (2005). Mapping of the normal human corneal sub-basal nerve plexus by in vivo laser scanning confocal microscopy. Investig. Ophthalmol. Vis. Sci. 46, 4485–4488. doi:10.1167/iovs.05-0794.

Patente, T. A., Pinho, M. P., Oliveira, A. A., Evangelista, G. C. M., Bergami-Santos, P. C., and Barbuto, J. A. M. (2019). Human dendritic cells: Their heterogeneity and clinical application potential in cancer immunotherapy. Front. Immunol. 10, 3176. doi:10.3389/fimmu.2018.03176.

Plantinga, M., Guilliams, M., Vanheerswynghels, M., Deswarte, K., Branco-Madeira, F., Toussaint, W., et al. (2013). Conventional and Monocyte-Derived CD11b+ Dendritic Cells

Initiate and Maintain T Helper 2 Cell-Mediated Immunity to House Dust Mite Allergen. *Immunity* 38, 322–335. doi:10.1016/j.immuni.2012.10.016.

Postole, A. S., Knoll, A. B., Auffarth, G. U., and Mackensen, F. (2016). In vivo confocal microscopy of inflammatory cells in the corneal subbasal nerve plexus in patients with different subtypes of anterior uveitis. Br. J. Ophthalmol. 100, 1551–1556. doi:10.1136/bjophthalmol-2015-307429.

Quallo, T., Vastani, N., Horridge, E., Gentry, C., Parra, A., Moss, S., et al. (2015). TRPM8 is a neuronal osmosensor that regulates eye blinking in mice. Nat. Commun. 6, 7150. doi:10.1038/ncomms8150.

Quirce, S. (2020). Actividad de los nervios sensoriales de la córnea durante la deficiencia lagrimal crónica y su modulación farmacológica. https://hdl.handle.net/11000/25635

Raker, V. K., Domogalla, M. P., and Steinbrink, K. (2015). Tolerogenic dendritic cells for regulatory T cell induction in man. Front. Immunol. 6, 569. doi:10.3389/fimmu.2015.00569.

Randolph, G. J., Beaulieu, S., Lebecque, S., Steinman, R. M., and Muller, W. A. (1998). Differentiation of monocytes into dendritic cells in a model of transendothelial trafficking. Science. 282, 480–483. doi:10.1126/science.282.5388.480.

Rehbinder, C. (1978). Fine structure of the mouse cornea. Z. Versuchstierk. 20:28.

Reis E Sousa, C. (2006). Dendritic cells in a mature age. Nat. Rev. Immunol. 6, 476–483. doi:10.1038/nri1845.

Reizis, B., Bunin, A., Ghosh, H. S., Lewis, K. L., and Sisirak, V. (2011). Plasmacytoid dendritic cells: Recent progress and open questions. Annu. Rev. Immunol. 29, 163–183. doi:10.1146/annurev-immunol-031210-101345.

Rescigno, M. (2014). Dendritic cell-epithelial cell crosstalk in the gut. Immunol. Rev. 260, 118–128. doi:10.1111/imr.12181.

Reynolds, G., and Haniffa, M. (2015). Human and mouse mononuclear phagocyte networks: A tale of two species? Front. Immunol. 6, 25. doi:10.3389/fimmu.2015.00330.

Rincón-Frutos, L. Dendritic cell depletion modifies corneal nerve activity and mice nociceptive bahavior. Acta Ophthalmol. (in press). EVER Abstract.

Riol-Blanco L, Ordovas-Montanes J, Perro M, Naval E, Thiriot A, Alvarez D, Paust S, Wood JN, Von Andrian UH (2014) Nociceptive sensory neurons drive interleukin-23-mediated psoriasiform

skin inflammation. Nature 510:157–161 Available at: http://www.ncbi.nlm.nih.gov/pubmed/24759321.

Rózsa, A. J., and Beuerman, R. W. (1982). Density and organization of free nerve endings in the corneal epithelium of the rabbit. Pain 14, 105–120. doi:10.1016/0304-3959(82)90092-6.

Rüfer, F., Schröder, A., and Erb, C. (2005). White-to-white corneal diameter: Normal values in healthy humans obtained with the Orbscan II topography system. Cornea 24, 259–261. doi:10.1097/01.ico.0000148312.01805.53.

Ruskell, G. L. (1974). Ocular fibers of the maxillary nerve in monkeys. J. Anat. 118, 195–203. Available at: https://www.ncbi.nlm.nih.gov/pmc/articles/PMC1231500/ [Accessed September 8, 2021].

Sallusto, F., and Lanzavecchi, A. (1994). Efficient presentation of soluble antigen by cultured human dendritic cells is maintained by granulocyte/macrophage colony-stimulating factor plus iuterleukin 4 and downregulated by tumor necrosis factor α. J. Exp. Med. 179, 1109–1118. doi:10.1084/jem.179.4.1109.

Saude, T. (1993). Ocular anatomy and physiology, Oxford: Blackwell Science Ltd.

Sawai, C. M., Sisirak, V., Ghosh, H. S., Hou, E. Z., Ceribelli, M., Staudt, L. M., et al. (2013). Transcription factor Runx2 controls the development and migration of plasmacytoid dendritic cells. J. Exp. Med. 210, 2151–2159. doi:10.1084/jem.20130443.

Schaible, H. G., and Schmidt, R. F. (1985). Effects of an experimental arthritis on the sensory properties of fine articular afferent units. J. Neurophysiol. 54, 1109–1122. doi:10.1152/jn.1985.54.5.1109.

Schiavoni, G., Mattei, F., Sestili, P., Borghi, P., Venditti, M., Morse, H. C., et al. (2002). ICSBP Is Essential for the Development of Mouse Type I Interferon-producing Cells and for the Generation and Activation of CD8α+ Dendritic Cells. J. Exp. Med. 196, 1415–1425. doi:10.1084/JEM.20021263.

Schimmelpfennig, B. (1982). Nerve structures in human central corneal epithelium. Graefe's Arch. Clin. Exp. Ophthalmol. 218, 14–20. doi:10.1007/BF02134093.

Schlitzer, A., McGovern, N., Teo, P., Zelante, T., Atarashi, K., Low, D., et al. (2013). IRF4 Transcription Factor-Dependent CD11b+ Dendritic Cells in Human and Mouse Control Mucosal IL-17 Cytokine Responses. Immunity 38, 970–983. doi:10.1016/j.immuni.2013.04.011.

Segura, E., Touzot, M., Bohineust, A., Cappuccio, A., Chiocchia, G., Hosmalin, A., et al. (2013). Human Inflammatory Dendritic Cells Induce Th17 Cell Differentiation. Immunity 38, 336–348. doi:10.1016/j.immuni.2012.10.018.

Segura, E., Valladeau-Guilemond, J., Donnadieu, M. H., Sastre-Garau, X., Soumelis, V., and Amigorena, S. (2012). Characterization of resident and migratory dendritic cells in human lymph nodes. J. Exp. Med. 209, 653–660. doi:10.1084/jem.20111457.

Sendra, V.G., Jamali, A., Lopez, MJ., Harris, D.L., Hamrah, P. (2017). Plasmacytoid dendritic cells modulate corneal inflammation through transforming growth factor (TGF)-β1. Invest. Ophthalmol. Vis. Sci. 58 (8), 3618-3618. ARVO Abstract.

Sendra, V., Jamali, A., Lopez, MJ., Hamrah, P. (2016). Plasmacytoid dendritic cells mediate T cell responses by direct interaction in lymph nodes during herpes simplex virus-1 keratitis. Invest. Ophthalmol. Vis. Sci. 57 (12), 331-331. ARVO Abstract.

Sendra, V.G., Jamali, A., Harris, D.L. and Hamrah, P. (2014). Role of plasmacytoid dendritic cell in the immune regulation in sutured inflamed cornea. Invest. Ophthalmol. Vis. Sci. 55 (13), 1694-1694. ARVO Abstract.

Seyed-Razavi, Y., Chinnery, H. R., and McMenamin, P. G. (2014). A novel association between resident tissue macrophages and nerves in the peripheral stroma of the murine cornea. *Investig. Ophthalmol. Vis. Sci.* 55, 1313–1320. doi:10.1167/iovs.13-12995.

Smith DO (1988) Determinants of nerve terminal excitability. Neurol Neurobiol 35:411–438.

Smith, R.S., Sundberg, J.P., and John. S.W.M. (2002). "The Anterior Segment and Ocular Adnexae," in Systematic Evaluation of the MOUSE EYE. Anatomy, Pathology and Biomethods, ed. Smith, R.S., (CRC PRESS), 1, 3-23.

Soumelis, V., Reche, P. A., Kanzler, H., Yuan, W., Edward, G., Homey, B., et al. (2002). Human epithelial cells trigger dendritic cell-mediated allergic inflammation by producing TSLP. Nat. Immunol. 3, 673–680. doi:10.1038/ni805.

Sozzani, S., Vermi, W., Del Prete, A., and Facchetti, F. (2010). Trafficking properties of plasmacytoid dendritic cells in health and disease. Trends Immunol. 31, 270–277. doi:10.1016/j.it.2010.05.004.

Springer, J., Geppetti, P., Fischer, A., and Groneberg, D. A. (2003). Calcitonin gene-related peptide as inflammatory mediator. Pulm. Pharmacol. Ther. 16, 121–130. doi:10.1016/S1094-5539(03)00049-X.

Steinman, R. M. (2012). Decisions about dendritic cells: Past, present, and future. Annu. Rev. Immunol. 30, 1–22. doi:10.1146/annurev-immunol-100311-102839.

Steinman, R. M., and Cohn, Z. A. (1973). Identification of a novel cell type in peripheral lymphoid organs of mice: I. Morphology, quantitation, tissue distribution. J. Exp. Med. 137, 1142–1162. doi:10.1084/jem.137.5.1142.

Steinman, R. M., Hawiger, D., Liu, K., Bonifaz, L., Bonnyay, D., Mahnke, K., et al. (2003). Dendritic cell function in Vivo during the steady state: A role in peripheral tolerance. in Annals of the New York Academy of Sciences (New York Academy of Sciences), 15–25. doi:10.1111/j.1749-6632.2003.tb06029.x.

Steinman, R. M., and Swanson, J. (1995). The endoeytie activity of dendritic cells. J. Exp. Med. 182, 283–288. doi:10.1084/jem.182.2.283.

Stepp, M. A., Tadvalkar, G., Hakh, R., and Pal-Ghosh, S. (2017). Corneal epithelial cells function as surrogate Schwann cells for their sensory nerves. Glia 65, 851–863. doi:10.1002/glia.23102.

Stramer, B, M., Zieske, J.D., Jung, J-C., Austin, J.S., and Fini, E. (2003). Molecular Mechanisms Controlling the Fibrotic Repair Phenotype in Cornea: Implications for Surgical Outcomes. Investig. Ophthalmol. Vis. Sci. 44, 4237-4246. doi:https://doi.org/10.1167/iovs.02-1188.

Tamoutounour, S., Guilliams, M., MontananaSanchis, F., Liu, H., Terhorst, D., Malosse, C., et al. (2013). Origins and functional specialization of macrophages and of conventional and monocyte-derived dendritic cells in mouse skin. *Immunity* 39, 925–938. doi:10.1016/j.immuni.2013.10.004.

Taylor, A. W. (2016). Ocular Immune Privilege and Transplantation. Front. Immunol. 7, 37. doi:10.3389/fimmu.2016.00037.

Thoft, R.A., and Friend, J. (1983). The X, Y, Z hypothesis of corneal epithelial maintenance. Invest. Ophthalmol. Vis. Sci. 24, 1442-1443.

Thut PD, Wrigley D, Gold MS (2003) Cold transduction in rat trigeminal ganglia neurons in vitro. Neuroscience 119:1071–1083 Available at: http://www.ncbi.nlm.nih.gov/pubmed/12831865.

Toivanen, M., Tervo, T., Partanen, M., Vannas, A., and Hervonen, A. (1987). Histochemical demonstration of adrenergic nerves in the stroma of human cornea. *Investig. Ophthalmol. Vis. Sci.* 28, 398–400. Available at: https://iovs.arvojournals.org/article.aspx?articleid=2160260.

Trombetta, E. S., and Mellman, I. (2005). Cell biology of antigen processing in vitro and in vivo. Annu. Rev. Immunol. 23, 975–1028. doi:10.1146/annurev.immunol.22.012703.104538.

Tuisku, I. S., Konttinen, Y. T., Konttinen, L. M., and Tervo, T. M. (2008). Alterations in corneal sensitivity and nerve morphology in patients with primary Sjögren's syndrome. Exp. Eye Res. 86, 879–885. doi:10.1016/j.exer.2008.03.002.

Van Blijswijk J, Schraml BU, Sousa CR e. (2013) Advantages and limitations of mouse models to deplete dendritic cells. Eur J Immunol 43:22–26 Available at: http://www.ncbi.nlm.nih.gov/pubmed/23322690.

Varol, C., Landsman, L., Fogg, D. K., Greenshtein, L., Gildor, B., Margalit, R., et al. (2007). Monocytes give rise to mucosal, but not splenic, conventional dendritic cells. *J. Exp. Med.* 204, 171–180. doi:10.1084/jem.20061011.

Veiga-Fernandes H, Mucida D (2016) Neuro-Immune Interactions at Barrier Surfaces. Cell 165:801–811 Available at: http://www.ncbi.nlm.nih.gov/pubmed/27153494.

Veres TZ, Rochlitzer S, Shevchenko M, Fuchs B, Prenzler F, Nassenstein C, Fischer A, Welker L, Holz O, Müller M, Krug N, Braun A (2007) Spatial interactions between dendritic cells and sensory nerves in allergic airway inflammation. Am J Respir Cell Mol Biol 37:553–561 Available at: http://www.ncbi.nlm.nih.gov/pubmed/17600312.

Villani, E., Baudouin, C., Efron, N., Hamrah, P., Kojima, T., Patel, S. V., et al. (2014). In vivo confocal microscopy of the ocular surface: From bench to bedside. Curr. Eye Res. 39, 213–231. doi:10.3109/02713683.2013.842592.

Villani, E., Galimberti, D., Papa, N. Del, Nucci, P., and Ratiglia, R. (2013). Inflammation in dry eye associated with rheumatoid arthritis: Cytokine and in vivo confocal microscopy study. Innate Immun. 19, 420–427. doi:10.1177/1753425912471692.

Vitar, R. M. L., Barbariga, M., Fonteyne, P., Bignami, F., Rama, P., and Ferrari, G. (2021). Modulating Ocular Surface Pain Through Neurokinin-1 Receptor Blockade. Invest. Ophthalmol. Vis. Sci. 62. doi:10.1167/IOVS.62.3.26.

Vonderahe, A. R. (1928). Corneal and scleral anesthesia of the lower hale of the eye in a case of trauma of the superior maxillary nerve. Arch. Neurol. Psychiatry 20, 836–837. doi:10.1001/archneurpsyc.1928.02210160177016.

Wang, C., Fu, T., Xia, C., and Li, Z. (2012). Changes in mouse corneal epithelial innervation with age. Investig. Ophthalmol. Vis. Sci. 53, 5077–5084. doi:10.1167/iovs.12-9704.

Wang, J., Dai, X., Hsu, C., Ming, C., He, Y., Zhang, J., et al. (2017). Discrimination of the heterogeneity of bone marrow-derived dendritic cells. Mol. Med. Rep. 16, 6787–6793. doi:10.3892/mmr.2017.7448.

Ward BR, Jester J V., Nishibu A, Vishwanath M, Shalhevet D, Kumamoto T, Petroll WM, Cavanagh HD, Takashima A (2007) Local thermal injury elicits immediate dynamic behavioural responses by corneal Langerhans cells. Immunology 120:556–572.

Watchmaker, P. B., Lahl, K., Lee, M., Baumjohann, D., Morton, J., Kim, S. J., et al. (2014). Comparative transcriptional and functional profiling defines conserved programs of intestinal DC differentiation in humans and mice. Nat. Immunol. 15, 98–108. doi:10.1038/ni.2768.

Watsky, M. A. (1995). Keratocyte gap junctional communication in normal and wounded rabbit corneas and human corneas. Investig. Ophthalmol. Vis. Sci. 36, 2568–2576. Available at: https://iovs.arvojournals.org/article.aspx?articleid=2179796.

Weiss, E.-M., Schmidt, A., Vobis, D., Garbi, N., Lahl, K., Mayer, C. T., et al. (2011). Foxp3-Mediated Suppression of CD95L Expression Confers Resistance to Activation-Induced Cell Death in Regulatory T Cells. J. Immunol. 187, 1684–1691. doi:10.4049/jimmunol.1002321.

Woolf CJ (2011) Central sensitization: Implications for the diagnosis and treatment of pain. Pain 152:S2 Available at: /pmc/articles/PMC3268359/.

Worbs, T., Hammerschmidt, S. I., and Förster, R. (2017). Dendritic cell migration in health and disease. Nat. Rev. Immunol. 17, 30–48. doi:10.1038/nri.2016.116.

Wu, L., D'Amico, A., Winkel, K. D., Suter, M., Lo, D., and Shortman, K. (1998). RelB is essential for the development of myeloid-related CD8α- dendritic cells but not of lymphoid-related CD8α+ dendritic cells. Immunity 9, 839–847. doi:10.1016/S1074-7613(00)80649-4.

Yamagami, S., Yokoo, S., Usui, T., Yamagami, H., Amano, S., and Ebihara, N. (2005). Distinct populations of dendritic cells in the normal human donor corneal epithelium. Investig. Ophthalmol. Vis. Sci. 46, 4489–4494. doi:10.1167/iovs.05-0054.

Yamaguchi, T., Calvacanti, B. M., Cruzat, A., Qazi, Y., Ishikawa, S., Osuka, A., et al. (2014). Correlation Between Human Tear Cytokine Levels and Cellular Corneal Changes in Patients With Bacterial Keratitis by In Vivo Confocal Microscopy. Investig. Opthalmology Vis. Sci. 55, 7457. doi:10.1167/iovs.14-15411.

Yang, L. Y., Mehta, J., and Liu, Y.-C. (2021). Corneal neuromediator profiles following laser refractive surgery. Neural Regen. Res. 16, 2177. doi:10.4103/1673-5374.308666.

Yates, S. F., Paterson, A. M., Nolan, K. F., Cobbold, S. P., Saunders, N. J., Waldmann, H., et al. (2007). Induction of Regulatory T Cells and Dominant Tolerance by Dendritic Cells Incapable of Full Activation. J. Immunol. 179, 967–976. doi:10.4049/jimmunol.179.2.967.

Yoo BB, Mazmanian SK (2017) The Enteric Network: Interactions between the Immune and Nervous Systems of the Gut. Immunity 46:910–926 Available at: http://www.ncbi.nlm.nih.gov/pubmed/28636959.

Zander, E., and Weddell, G. (1951). Observations on the innervation of the cornea. J. Anat. 85, 68–99. Available at: https://www.ncbi.nlm.nih.gov/pmc/articles/PMC1273614/.

Zhang X (2015) Molecular sensors and modulators of thermoreception. Channels 9:73–81.

Zhang X, Huang J, McNaughton PA (2005) NGF rapidly increases membrane expression of TRPV1 heat-gated ion channels. EMBO J 24:4211–4223 Available at: http://www.ncbi.nlm.nih.gov/pubmed/16319926.

Zhang, X., Mak, S., Li, L., Parra, A., Denlinger, B., Belmonte, C., et al. (2012). Direct inhibition of the cold-activated TRPM8 ion channel by Gαq. Nat. Cell Biol. 14, 851–858. doi:10.1038/ncb2529.

Zhivov, A., Stave, J., Vollmar, B., and Guthoff, R. (2007). In Vivo Confocal Microscopic Evaluation of Langerhans Cell Density and Distribution in the Corneal Epithelium of Healthy Volunteers and Contact Lens Wearers. Cornea 26, 47–54. doi:10.1097/ICO.0b013e31802e3b55.

Zhu, X. J., Yang, Z. F., Chen, Y., Wang, J., and Rosmarin, A. G. (2012). PU.1 Is Essential for CD11c Expression in CD8+/CD8- Lymphoid and Monocyte-Derived Dendritic Cells during GM-CSF or FLT3L-Induced Differentiation. PLoS One 7. doi:10.1371/journal.pone.0052141.

Zimmermann K, Leffler A, Babes A, Cendan CM, Carr RW, Kobayashi JI, Nau C, Wood JN, Reeh PW (2007) Sensory neuron sodium channel Nav1.8 is essential for pain at low temperatures. Nature 447:855–858.

Zurborg, S., Piszczek, A., Martínez, C., Hublitz, P., Al Banchaabouchi, M., Moreira, P., et al. (2011). Generation and characterization of an Advillin-Cre driver mouse line. *Mol. Pain* 7. doi:10.1186/1744-8069-7-66.

ANNEX

Quality indicators

Review

An Experimental Model of Neuro–Immune Interactions in the Eye: Corneal Sensory Nerves and Resident Dendritic Cells

Laura Frutos-Rincón [1,2], José Antonio Gómez-Sánchez [1,*], Almudena Íñigo-Portugués [1], M. Carmen Acosta [1,2] and Juana Gallar [1,2,3]

1 Instituto de Neurociencias, Universidad Miguel Hernández—Consejo Superior de Investigaciones Científicas, 03550 San Juan de Alicante, Spain; l.frutos@umh.es (L.F.-R.); ainigo@umh.es (A.Í.-P.); mcarmen.acosta@umh.es (M.C.A.); juana.gallar@umh.es (J.G.)
2 The European University of Brain and Technology-NeurotechEU, 03550 San Juan de Alicante, Spain
3 Instituto de Investigación Biomédica y Sanitaria de Alicante, 03010 Alicante, Spain
* Correspondence: j.gomez@umh.es; Tel.: +34-965-91-9594

Abstract: The cornea is an avascular connective tissue that is crucial, not only as the primary barrier of the eye but also as a proper transparent refractive structure. Corneal transparency is necessary for vision and is the result of several factors, including its highly organized structure, the physiology of its few cellular components, the lack of myelinated nerves (although it is extremely innervated), the tightly controlled hydration state, and the absence of blood and lymphatic vessels in healthy conditions, among others. The avascular, immune-privileged tissue of the cornea is an ideal model to study the interactions between its well-characterized and dense sensory nerves (easily accessible for both focal electrophysiological recording and morphological studies) and the low number of resident immune cell types, distinguished from those cells migrating from blood vessels. This paper presents an overview of the corneal structure and innervation, the resident dendritic cell (DC) subpopulations present in the cornea, their distribution in relation to corneal nerves, and their role in ocular inflammatory diseases. A mouse model in which sensory axons are constitutively labeled with tdTomato and DCs with green fluorescent protein (GFP) allows further analysis of the neuro-immune crosstalk under inflammatory and steady-state conditions of the eye.

Keywords: corneal nerves; dendritic cells; neuro-immune interactions; ocular inflammation; ocular pain; animal models

1. Introduction

Several studies have determined the influence of the nervous system on the immune system, but conversely, the influence of immune cells on the nervous system, besides their protective role, has not been so widely studied. The various functions of resident immune cells have been assessed in many ocular pathological conditions and diseases, however, their contribution to the maintenance of corneal tissue and sensitivity remains elusive. Corneal DC depletion during steady-state produces a reduction in the nerve ending density in the center of the cornea, as well as epithelial defects and delayed nerve regeneration [1]. Although previous results suggest that intraepithelial DCs and sensory nerves have intimate connections and are functionally interdependent, no functional or behavioral studies have been done so far to confirm this functional neuro–immune interaction.

2. The Cornea

The cornea and the conjunctiva constitute the eye tissues exposed to the environment. The cornea is an avascular connective tissue that is crucial, not only as the primary barrier for the eye but also as a powerful refractive structure. As a barrier, the cornea provides structural integrity to the ocular globe and protects its inner components from infectious agents and physical injury or chemical insults. On the other hand, as a refractive structure,

it has two key properties: refractive power (for light refraction) and transparency (for light transmission) [2].

The shape of the human cornea is prolate, which creates an aspheric optical system [3]. The human cornea has a refractive index of 1.376 and a dioptric power higher than 40 dioptres, about 2/3 of the total ocular power [4]. It is 540–700 μm thick, being thinner in the center and thicker in the periphery [2]. The human cornea measures about 11 mm vertically and 12 mm horizontally [5] covering the anterior 1/6th of the ocular surface and is organized into 5 layers (Figure 1): epithelium, Bowman's layer, stroma, Descemet's membrane, and endothelium. Among species, the cornea keeps the same general structure, with differences in thickness and presence or absence of Bowman's layer.
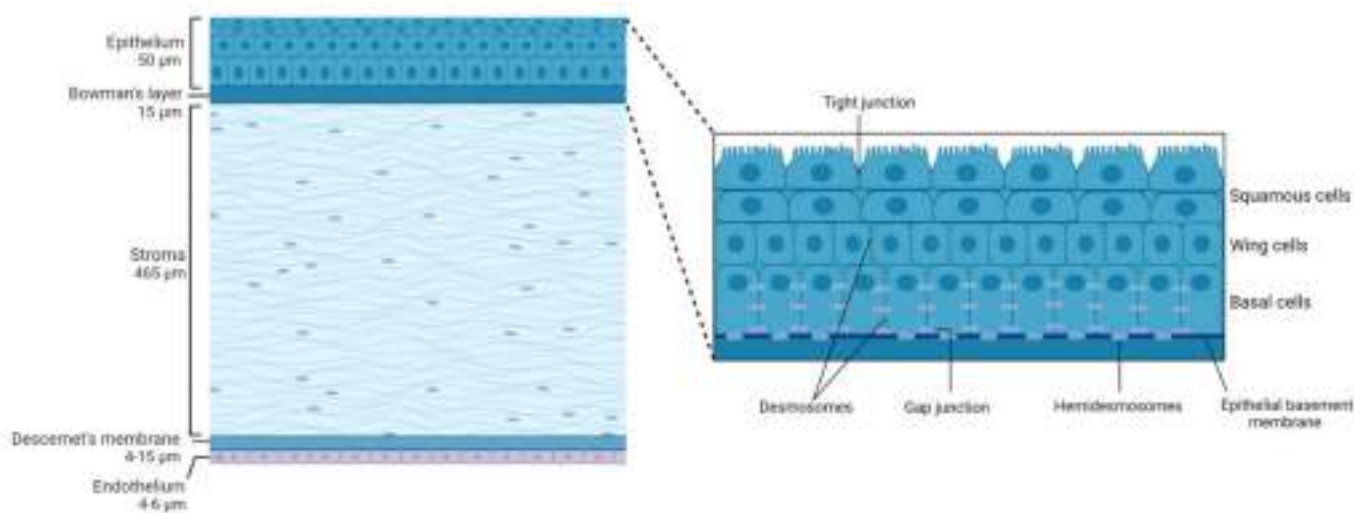
Figure 1. Schematic representation of the corneal structure, showing its five main layers and their thickness. Inset: diagram of the corneal epithelium, showing its different cell layers and details on the different types of cell-cell junctions contributing to corneal epithelium impermeability.

Transparency of all ocular structures is crucial for vision. Transparency of the cornea is the result of many factors including its highly organized anatomical structure, the physiology of its cellular components, the lack of myelination of nerves inside the cornea, its tightly controlled (de)hydration state and the absence of blood and lymphatic vessels, among others. Since vision plays a critical role in obtaining information from the external environment, the cornea also has specific characteristics that ensure its own protection against injury. One of the most important features in this regard is the high sensitivity of the cornea to external insults provided by its extremely rich sensory innervation.

Taking all the corneal characteristics into account, it is clear that the cornea is an ideal model for studying the interactions between corneal nerves and the few cell types present in this quite simple structure. Particularly, the cornea represents a perfect scenario to study neuro–immune interactions for different reasons: the cornea is densely innervated [6,7] with sensory nerves easily accessible for electrophysiological recordings whose functional properties have been described in detail [8,9]; the cornea is fully transparent [10,11], which means that fluorescence data could be gathered at high resolution for both in vivo and ex vivo experiments and finally, the cornea is avascular [12,13], which allows distinguishing the contribution of resident immune cells from that of immune cells migrating from blood vessels.

2.1. Corneal Structure

2.1.1. Epithelium

The corneal epithelium composed of a single layer of basal cells and several stratified and non-keratinized cell layers (Figure 1, inset), constitutes the first protective ocular barrier

against external threats. In humans, it is 50 μm thick, representing around 8% of the total thickness of the cornea [14].

The outermost corneal epithelium constitutes 2–3 layers of squamous cells [3] (Figure 1, inset). These cells are flat and polygonal and have apical microvilli which, in turn, are covered by a fine glycocalyx consisting of membrane-associated mucins, including MUC1, MUC4, and MUC16 [15]. These squamous cells maintain tight junctions with their neighbors, which is essential for their function as a barrier to prevent large molecules or microbes from entering the deeper corneal layers. Beneath the superficial layers of squamous cells are the mid-epithelial layers of wing cells (Figure 1, inset). Wing cells are less flattened but have tight lateral junctions with their neighbors very similar to those observed in the squamous cells [3]. Finally, basal cells constitute the deepest cell layer of the corneal epithelium (Figure 1, inset). This layer, around 20 μm thick, constitutes a single layer of columnar epithelial cells that are connected through gap junctions and desmosomes and are attached to the underlying basement membrane by hemidesmosomes, preventing the epithelium from separating from the other corneal layers [3].

In mice, the epithelium contributes approximately 30% to the total corneal thickness. The stratified layout of the murine corneal epithelium is consistent with the description of this epithelium in the mammalian cornea. However, the mouse corneal epithelium consists of approximately twice the layers of cells compared with the human epithelium, with a higher number of squamous cells [16].

Corneal epithelial cell layers turn over every 7–10 days [17] following a delicate balance between superficial cell shedding and cell proliferation and migration from basal cells. Basal progenitor epithelial cells from the limbus (limbal stem cells) migrate towards the center of the cornea where they differentiate into transient amplifying cells (TA). TA basal cells, which are two horizontal progenies from the stem cells, migrate from the limbus to the periphery of the cornea to reach the center and undergo mixed proliferation (one daughter cell is retained in the basal cell layer, and the other moves into the middle layers of the epithelium). Once TA cells reach the end of their proliferative capacity, they become basal epithelial cells. Basal epithelial cells undergo vertical proliferation in two daughter cells resulting in two wing cells and eventually into two squamous cells that will be later shed by blinking. This concept was coined the X, Y, Z hypothesis of Thoft and Friend [18] where X is the basal corneal epithelial cell horizontal migration and vertical terminal proliferation, Y is the limbal cell proliferation and migration and Z is the squamous corneal epithelial cell shedding.

Between the corneal epithelium and the next corneal layer, the stroma, there is the epithelial basement membrane synthesized by epithelium basal cells. This membrane, also called the basal lamina, is approximately 0.05 μm thick and comprises laminin, type IV collagen, heparan sulfate, and fibronectin. Basal lamina serves as a scaffold for epithelial cell movement and attachment, and it is composed of two distinct layers when observed by electron microscopy: the more external *Lamina lucida* and a thicker more internal *Lamina densa* [2].

2.1.2. Bowman's Layer

Bowman's layer in the human cornea is an acellular condensate of collagen types IV, V, VI, and VII arranged randomly [4] that help the cornea to maintain its shape [3]. This layer is approximately 15 μm thick and is associated with the basal lamina of the epithelium and continues with the stroma. Different roles have been ascribed to this layer of the cornea that is not present in all species, such as that it provides some kind of barrier function against the passage of macromolecules, such as medium and large size proteins, or that it is responsible for a substantial portion of the biomechanical rigidity of the cornea. However, there are also studies that conclude the opposite and the exact function of this layer remains unclear (see Wilson 2020 for a review [19]). It has been hypothesized that Bowman's layer develops because of cytokine-mediated interactions occurring between corneal epithelial cells and the underlying keratocytes, including negative chemotactic and apoptotic effects

on the keratocytes by low levels of cytokines, such as interleukin-1α [20]. Bowman's layer is highly resistant to damage, but it cannot regenerate after injury and may result in a scar [21].

It is worth mentioning that in mice, subepithelial collagen fibers are also arranged randomly forming what would be a thin Bowman's layer. However, some authors believe that this is not a true layer [22] but an adaptation of the stromal tissue [16].

2.1.3. Stroma

Corneal stroma comprises 90% of the total corneal thickness [2]. It is mainly composed of water (78%), an organized structural network of types I and V collagen fibers (80% of corneal stroma's dry weight), keratocytes, and extracellular matrix.

The stromal collagen fibers are arranged in parallel bundles (fibrils) that are packed in parallel arranged layers (lamellae). In turn, each of these layers is arranged at right angles relative to fibers in adjacent lamellae, and this precise organization results in stromal transparency as it reduces forward light scatter [23].

Keratocytes, the major cell type of corneal stroma, are sandwiched between collagenous lamellae, mostly in the anterior stroma. These stellate-shaped cells are connected to each other through gap junctions present on their numerous dendritic processes [24]. Keratocytes are involved in maintaining the extracellular matrix environment and stromal composition as they are able to synthesize glycosaminoglycans, collagen molecules, and matrix metalloproteases (MMPs) [3]. As a first response to stromal injury, keratocytes are activated and migrate taking on a fibroblast-like appearance [25] and within 1–2 weeks of the initial insult, myofibroblasts enter the injured area and become involved in the stromal remodeling which can take months or even years to complete [3].

In mice, the corneal stroma accounts for two-thirds of the total corneal thickness. In these animals, stromal collagen fibers have a diameter of 29 ± 4 nm [26] with keratocytes arranged parallel to the collagen bundles.

In the posterior part of the human corneal stroma, there is a distinct region that constitutes the separation between the stroma and the Descemet's membrane. This pre-Descemet or Dua's layer is acellular and composed of 5 to 8 lamellae of predominantly type-1 collagen bundles arranged in transverse, longitudinal, and oblique directions [27].

2.1.4. Descemet's Membrane

Descemet's membrane is primarily composed of types IV and VIII collagen fibrils as well as the glycoproteins fibronectin, laminin, and thrombospondin. It is less strong and stiff than the posterior stroma and is secreted by endothelial cells since the 8th gestation week [3]. Descemet's membrane has a thickening rate of approximately 1 μm per decade of life: its thickness is around 4 μm at birth, while at the end of the normal lifespan Descemet's membrane is around 10–15 μm thick [2]. In addition, this thickness can also increase focally or diffusely with injury (trauma or surgery) or disease, due to abnormal collagen deposition.

Descemet's membrane in mice is more homogeneous and granular on the anterior chamber side, resembling a typical basal lamina, and it also becomes thicker with age [28].

2.1.5. Endothelium

The corneal endothelium is a monolayer of hexagonal cells whose density and topography change continuously throughout life [3]. At birth, corneal endothelium is 10 μm thick and its cell density is approximately 3500 cells/mm^2, however, this number decreases at approximately 0.6% per year [3]. Corneal endothelium maintains its continuity by migration and expansion of survival cells to cover the defect surface, so the percentage of hexagonal cells decreases (*pleomorphism*, that is, endothelial cells become different from each other in shape), while the coefficient of variation in cell area increases (*polymegathism*, that is, endothelial cells become different from each other in size, appearing large cells) [2].

The main function of the corneal endothelium is to maintain corneal transparency and health by regulating its hydration and nutrition [2]. Adjacent endothelial cells share extensive lateral interdigitations and possess tight and gap junctions along their apical and lateral borders, respectively, forming an incomplete barrier with a preference for the diffusion of small molecules [2]. The endothelium acts as a "leaky" barrier that allows passive fluid flow from the hypotonic corneal stroma to hypertonic aqueous humor through the osmotic gradient, maintaining the relatively dehydrated state of the stroma. Nevertheless, although this passive movement does not require energy, endothelial cells maintain the osmotic gradient by active transport of ions. In this context, the major transport protein found to be essential is Na^+/K^+-ATPase, present in the basolateral membranes of endothelial cells.

2.2. Corneal Innervation

The cornea is supplied by both sensory and autonomic nerves, being one of the most densely innervated tissues in the body [6]. The trigeminal nerve, the major sensory nerve of the head, has three different sensory branches: ophthalmic (V1), maxillary (V2), and mandibular (V3) [29,30]. Most nerves supplying the cornea are sensory nerves, and most of them have their origin in the ophthalmic branch of the trigeminal ganglion (TG). Furthermore, a little innervation from the maxillary branch has also been reported in the inferior cornea and the conjunctiva [31,32].

V1 branches into the frontal, the lachrymal, and the nasociliary nerves. In turn, the nasociliary nerve branches into two long ciliary nerves and a connecting branch with the ciliary ganglion, a parasympathetic ganglion that sends 5–10 short ciliary nerves carrying both trigeminal sensory nerve fibers from the nasociliary nerve and parasympathetic and sympathetic axons, the last from the superior cervical ganglion. The density of the sympathetic nerves varies significantly among different species [33], being higher in the cat and rabbit cornea [34–36] and very sparse in humans and other primates [34,37].

Short and long ciliary nerves enter the posterior globe medially and laterally to the optic nerve [30,38], penetrating the sclera. After that, they form a ring around the optic nerve and travel anteriorly in the suprachoroidal space towards the anterior segment of the eye [30], undergoing repetitive branching. When reaching the limbal area, some fibers innervate the ciliary body and the iris, while most fibers form a dense ring-like network that encircles the limbus around the cornea, giving rise to the limbal plexus [39]. The majority of nerve fibers in this plexus are believed to be vasomotor nerves innervating limbal blood vessels, while a variable number of nerve trunks enter the corneal stroma unrelated to blood vessels [40].

2.2.1. Corneal Nerve Architecture

The architecture of corneal innervation has been studied for many years by a wide variety of methods, including light and electron microscopy, immunohistochemistry, and IVCM, among others. Moreover, it has been described among different species such as human [6,38], cat [36,41], guinea pig [42,43], and mouse [44,45]. Corneal innervation is anatomically organized into four levels from the penetrating stromal nerve trunks to the nerve terminals in the epithelium.

Stromal Nerves

Corneal stromal nerves enter the cornea radially through the corneoscleral limbus in the middle third of the stroma. In addition, other small nerve bundles enter the cornea more superficially in the episcleral and conjunctival planes, innervating the superficial stroma and the periphery of the corneal epithelium, respectively [39,41,42].

When entering the stroma at a depth of approximately 293 μm, myelinated axons (about 20%) lose their perineurium and myelin sheath [6] and run within the stroma as fascicles enclosed by a basal lamina and Remak Schwann cells (the non-myelinating Schwann cells) [30]. The distal branches of this arborization anastomose extensively form the anterior stromal nerve plexus, a complex network of nerve bundles and individual

axons. The posterior half of the stroma and endothelium, on the contrary, are devoid of sensory nerve fibers [30].

In mice, stromal nerves do not enter the cornea radially at regular intervals as in humans. Stromal innervation is provided by nerve bundles entering into the cornea from four quadrants and branching irregularly to cover the entire cornea (Figure 2A,B).

In humans and higher mammals, the most superficial layer of the anterior stromal nerve plexus, immediately beneath Bowman's layer, is referred to as the corneal subepithelial nerve plexus. The subepithelial plexus has a very high nerve density, but in general, it is denser in the peripheral and intermediate cornea, and less dense in the central cornea [38].

Anatomically, in the subepithelial plexus, there are two distinct types of nerve bundles [30,38]. One form a complex anastomotic meshwork of single axons and thin tortuous fascicles that do not penetrate Bowman's membrane, while the second type consists of about 400–500 medium-sized, curvilinear bundles that turn 90° and penetrate Bowman's layer and basal lamina mainly in the peripheral and intermediate cornea [6,38]. These nerve bundles terminate in bulb-like structures and divide into smaller ones in groups up to 20 subbasal nerve fibers, known as epithelial leashes [6,38]. These leashes, which are parallel to the ocular surface, anastomose extensively to form a dense subbasal nerve plexus (see below).

It is worth mentioning that while unmyelinated nerves maintain their Remak Schwann cell coating in the stroma, they shed them before penetrating the basal lamina. In this regard, it has been suggested that corneal epithelial cells function as surrogate Schwann cells for the subbasal and intraepithelial nerves in healthy conditions and after injury [46].

Subbasal Nerve Plexus

The corneal epithelium receives sensory nerve fibers either from the subepithelial plexus or directly from the conjunctival nerves [39,40]. The subbasal nerve plexus constitutes epithelial leashes from subepithelial nerves that anastomose extensively and interconnect repeatedly with one another such that they are no longer recognizable as individual leashes (Figure 2C,D), although leashes are less numerous and separated in the periphery [38]. The term "epithelial leash" was defined as a group of subbasal nerves that derive from the same parent anterior stromal nerve trunk [41,47,48], being a unique neuroanatomical structure only found in the cornea of most species, including humans.

The subbasal nerve plexus is a dense, homogenous nerve plexus situated between the basal epithelial cells and the basal lamina. In humans, it is formed by 5000–7000 nerve fascicles in an area of about 90 mm^2 [49], with a total number of axons estimated to vary between 20,000 and 44,000 [6]. Morphologically, each leash consists of a variable number of straight nerve fibers, each containing 3–10 individual axons traveling up to several millimeters. Subbasal nerve fibers converge on a spiral whose center is called the vortex [50,51]. This vortex is also present in other species, including mice [43,44] and rats [52], and the mechanisms underlying its formation remain unclear. The most extended hypothesis is that nerves and basal epithelial cells advance in the same direction and velocity in a whorl-like pattern in response to chemotropic guidance, electromagnetic cues, and/or to population pressures [53,54].

Intraepithelial Nerve Terminals

Single nerve fibers arising from the subbasal plexus split off and turn 90° vertically as a profusion of terminal axons ascending between the epithelial cells, often with a modest amount of additional branching (Figure 2E–I) [30]. The term intraepithelial nerve terminal was defined by Carl Marfurt as the entire epithelial axon distal to its point of origin from a subbasal nerve and all its collateral branches and terminal expansions (the so-called nerve endings) [38]. Corneal epithelium innervation is extremely dense. It is estimated that the human central cornea contains around 5000–7000 nerve terminals per square millimeter, although this number changes throughout life and in ocular pathologies.

The intraepithelial nerve terminals innervate the corneal epithelium through all its layers. Those running between the basal and wing epithelium cells run in a horizontal direction and branch relatively infrequently [38], while intraepithelial nerve terminals that terminate within the more superficial cell layers are generally more complex (Figure 2E,G–I). Intraepithelial nerve terminals can be classified into three different types: simple, ramifying, and complex [29]. Simple terminals do not branch after leaving the subbasal plexus and end with a bulbar swelling within or below the superficial squamous cells [29,43] (Figure 2G). Simple terminals are more abundant in the central cornea. Ramifying terminals branch within the squamous cell layer into 3–4 branches that run horizontally for a hundred microns and that end in a single bulbar swelling like the simple terminals [29,43] (Figure 2H), being more numerous in the peripheral cornea [43]. Finally, axons forming the complex terminals start to branch within the wing cells layer and terminate with multiple larger bulbous endings within the wing and squamous cell layers (Figure 2I). Complex terminals are found in the central and the peripheral cornea, but their complexity and size are higher in the periphery [43].

Intraepithelial nerve terminals seem to be functionally different as immunocytochemical staining reveals differences in the expression of neuropeptides and neurotransmitters. In mice and guinea pigs, nerves that terminate in the basal epithelium and the outermost cell layers have simple endings immunopositive for Calcitonin Gene-Related Peptide (CGRP) and substance P (SP), suggesting that peptidergic simple nerve terminals correspond functionally to polymodal nociceptor nerve terminals [43]. On the other hand, complex nerve terminals are immunoreactive to TRPM8 (Transient receptor potential channel subfamily M member 8), supporting the idea that complex terminals correspond to cold thermoreceptor terminals [43]. More recent studies in guinea pig corneas also suggest that these intraepithelial nerve terminals can be distinguished morphologically as TRPM8-positive terminals are more complex than TRPV1-positive terminals [55].

2.2.2. Functional Types of Corneal Nerves

Electrophysiological recordings of sensory nerve fibers innervating the cornea have revealed the existence of different functional types of ocular sensory nerves, classically classified depending on the modality of stimulus by which they are activated [7,56]. Most corneal sensory nerves are the peripheral branches of medium or small trigeminal neurons with thin myelinated (A-delta) or unmyelinated (C) axons [56]. The external stimuli are transduced by their intraepithelial nerve terminals into a discharge of nerve impulses that encode the stimulus' spatial and temporal characteristics. The impulse discharge is conducted by trigeminal neurons to the central nervous system, where sensory input is processed to finally evoke a sensation and is also used to regulate protective functions, such as tearing and blinking. Depending on the variable activation of the different classes of corneal sensory neurons, different sensations are evoked [7,57].

Mechanonociceptors

About 15% of corneal nerve fibers are mechanonociceptors, which express Piezo2 channels [58,59] and are activated exclusively by mechanical forces (Figure 3). Mechanonociceptors are usually A-delta fibers and produce a short-lasting impulse discharge in response to a sustained mechanical stimulus, therefore signaling the presence and velocity of change in the mechanical force, rather than its intensity or duration [60,61]. These relatively rapidly adapting mechanosensitive fibers contribute to the pain experienced when a foreign body touches the ocular surface [57].
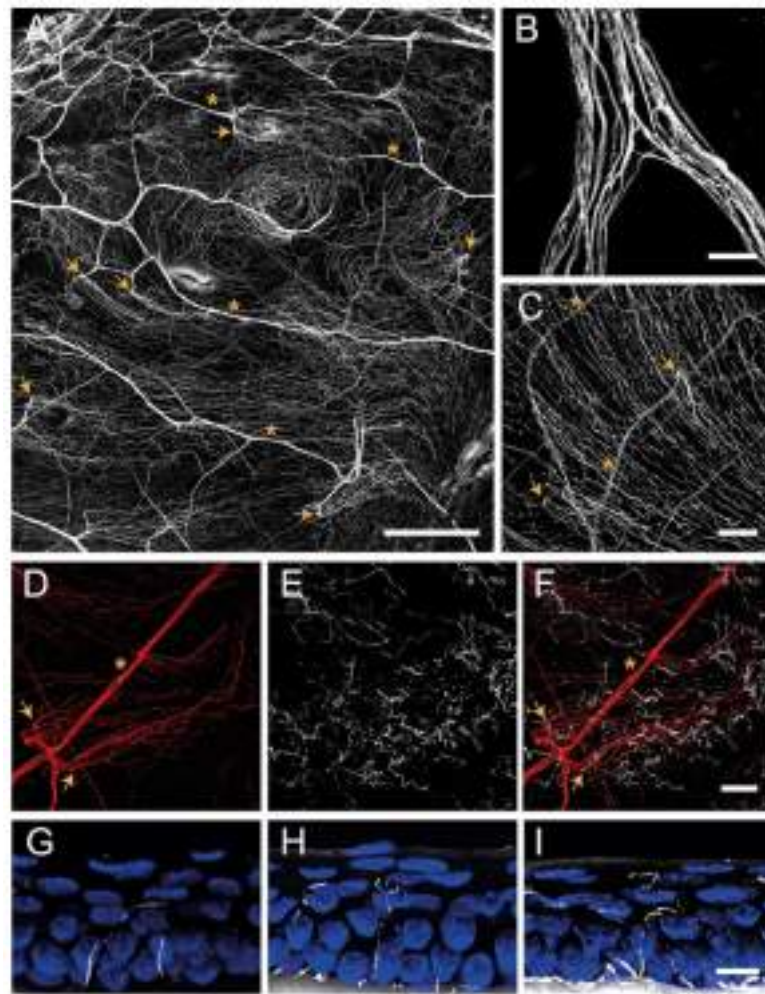
Figure 2. Confocal images of sensory nerves immunostained with anti–β tubulin III antibody in mouse cornea. (**A**) Sensory nerve trunks enter from the limbus into the stroma of the cornea where they ramify, giving rise to a dense subepithelial plexus (asterisks). (**B**) Detail of a stromal nerve trunk branching. (**C**,**D**) From the stroma, nerve fibers penetrate through the basal lamina (arrowheads) and form the subbasal plexus. Subbasal nerve fibers run parallel for a long distance within the epithelium basal cell layer. (**E–I**) Subbasal nerves give rise to terminal branches that ascend along their trajectory through the epithelial cells. According to the number of branches, three morphological types of corneal nerve terminals are identified: simple (**G**), ramified (**H**), and complex (**I**) nerve terminals. Scale bars: (**A**) 250 μm; (**B**) 25 μm; (**C–F**) 50 μm; (**G–I**) 10 μm. Methods: C57BL/6J eyes were fixed for 2 h at RT in methanol and DMSO (4:1), incubated 5 min at −20 °C in methanol, rehydrated, and washed in PBS. (**A–F**) Corneas were dissected, incubated 2 h at RT in blocking solution (5% goat normal serum, 1% BSA and 0.1%Triton X–100 in PBS) and 48 h at 4 °C with anti–β tubulin III antibody (1:500 in blocking solution; #801201, BioLegend, CA, San Diego, USA), rinsed and then incubated for 2 h at RT with AF555 (1:500 in PBS; #A32727, ThermoFisher Scientific, OR, Waltham, USA), washed in PBS and mounted with Fluoromount-G (ThermoFisher Scientific). (**G–I**) Eyes were cryoprotected (30% sucrose in PBS overnight at 4 °C), embedded in OCT, frozen in liquid nitrogen, cut on a cryostat in serial 15 mm thick sections, and mounted in slides. Tissue sections were rinsed in 0.03% Triton X–100 in PBS and then for 30 min in blocking solution followed by overnight incubation at 4 °C with anti–β tubulin III antibody in blocking solution, washing with PBS and incubation with AF555 in PBS for 2 h at RT. Afterward, slides were rinsed with PBS, incubated with Hoechst 33342 (10 μm/mL; #H1399, ThermoFisher Scientific), and coverslipped with Fluoromount–G. Images were collected using a laser scanning confocal microscope Zeiss LSM 880 (Oberkochen, DEU).
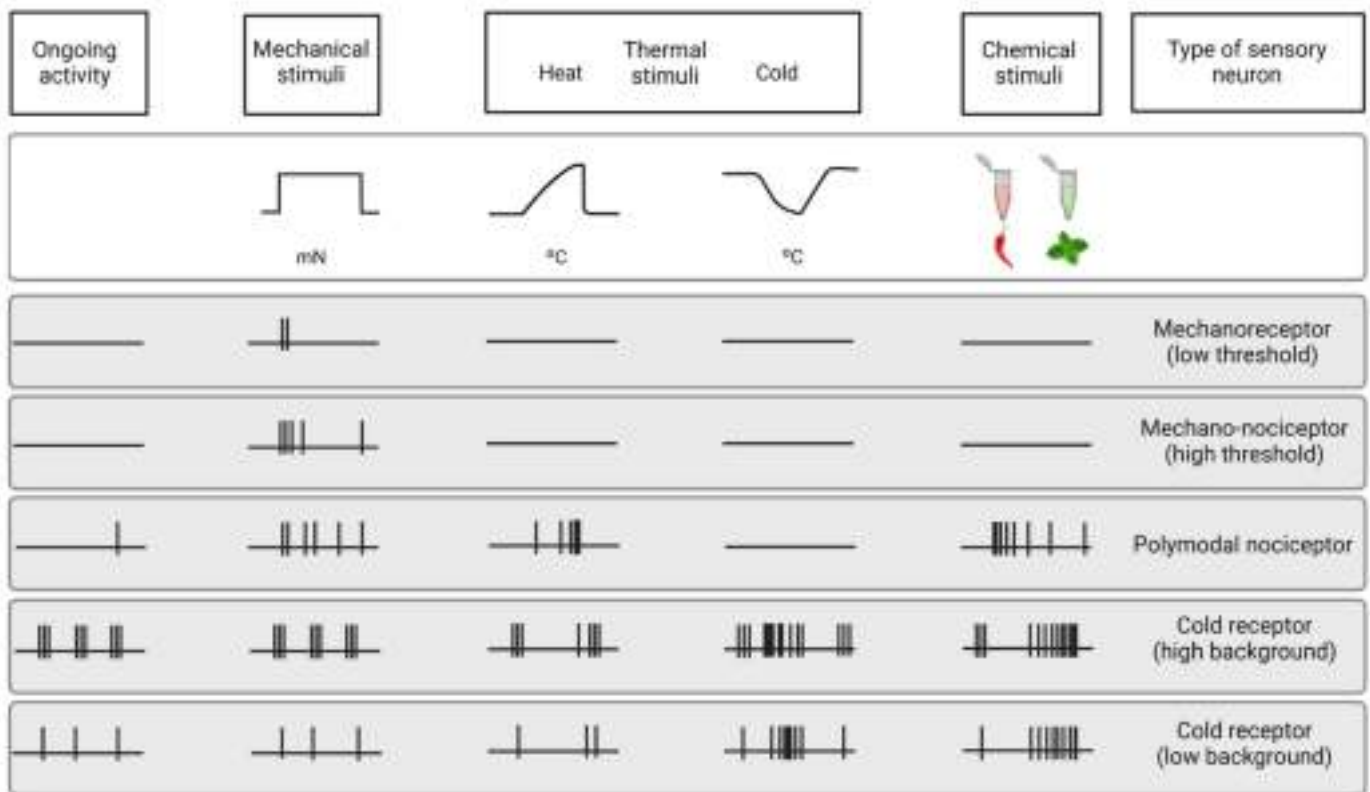
Figure 3. Functional types of sensory neurons innervating the cornea. Schematic representation of the spontaneous and stimulus-evoked nerve impulse activity of the different functional types of sensory nerves innervating the cornea. Based on the characteristics of the impulse discharge in absence of intended stimulation (ongoing activity) and response to different types of stimuli (upper part of the figure), the peripheral terminals of primary sensory neurons innervating the cornea are classified into five different functional types of sensory neurons.

Polymodal Nociceptors

The majority of corneal sensory fibers (around 70%) are polymodal nociceptors, which express a diversity of transducing ion channels in their nerve terminals, such as TRPA1, TRPV1, ASIC, and Piezo2, that allow them to be activated by noxious mechanical forces, heat (temperatures over 39 °C) and a wide variety of exogenous and endogenous chemicals (protons, ATP, prostaglandins, cytokines, etc.) [8,62] (Figure 3).

Polymodal nociceptors produce an irregular and repetitive discharge as long as the stimulus is maintained that is proportional to its intensity [8,63]. Moreover, under certain circumstances, polymodal nociceptors can be sensitized, developing an irregular low frequency long after the stimulus has disappeared [64]. In addition, sensitization produces a decrease in threshold and an increase in the firing frequency in response to a new stimulus [60,65]. Most corneal polymodal nociceptors are slow-conducting C-type fibers and are the origin of the ocular discomfort and pain sensations developed under pathological conditions, local inflammation, or injury [64,66].

Cold Thermoreceptors

The third class of corneal sensory fibers is cold thermoreceptors (10–15%), associated with A-delta and C nerve fibers. Cold thermoreceptors have spontaneous discharge and increase their firing rate in response to temperature reduction and osmolality increases [63,67,68] (Figure 3). Cold thermoreceptors are transiently silenced upon warming, although some of them restart firing in response to high temperatures (paradoxical response to heat) [7,69]. Cold thermoreceptors firing increases proportionally to the speed and magnitude of the corneal temperature reduction, as well as to the final static temperature [7].

When enough cold thermoreceptors are recruited with augmented tear evaporation, a conscious sensation of dryness is expected [56]. Cooling sensations with temperature reductions are increasingly unpleasant when higher temperature decreases are applied [57].

The activity of corneal cold thermoreceptors expressing TRPM8 is crucial in different mechanisms protecting the eye, such as lacrimation and blinking [7,70–72]. The deletion of TRPM8 channels produces both a decrease in basal tearing [71] and blinking [72] in mice, supporting the idea that sensory input of cold thermoreceptors is used by the CNS to regulate blinking and tearing. Aging induces changes in TRPM8 expression and activity, which correlates with the changes in tearing developed with age [73].

2.2.3. Changes of Nerve Activity under Inflammation and after Injury

After inflammation or lesion, corneal sensory nerve activity is altered. Like in other tissues, corneal nociceptors (specially polymodal nociceptors) are sensitized [64,69,74–79], a functional state characterized by an increase in spontaneous activity, a reduction in the response threshold, and an increased response to stimulation. Sensitization constitutes the basis of spontaneous pain and hyperalgesia experienced during inflammation. Additionally, corneal nociceptors also contribute to the inflammatory processes of the ocular surface (a process known as neurogenic inflammation) [80,81] by releasing pro-inflammatory neuropeptides, such as SP and CGRP [6,82,83]. After injury, regenerating nociceptors present increased spontaneous activity due to the increased expression of specific types of Na^+ channels by regenerating neurons [79].

Contrarily, cold thermoreceptors' activity is decreased under inflammation [69,76] because the activity of TRPM8 channels is inhibited by inflammatory mediators, such as bradykinin through a G-protein [84]. During chronic tear deficiency, the activity of cold thermoreceptors is increased due to the increase in Na^+ currents and the decrease in K^+ currents [77].

2.3. The Cornea: An Immune-Privileged Tissue

The ocular surface is a mucosal surface in which the optical properties are critically important and where immune-mediated inflammation should not cause collateral damage [85]. Most of our current knowledge about the ocular surface immune-privileged arises from studies with corneal allografts, whose benefits have been widely described [86,87]. The cornea should perform an important balance between fighting infections and maintaining transparency in order to preserve vision. This immune-privileged tissue can be exposed to antigens, allergens, and pathogens without eliciting significant immune responses. The concept of '*immune privilege*' was first coined by Medawar decades ago [88], however, it has been extensively reviewed since its initial conception [89,90]. Traditionally, the corneal immune privilege was ascribed to the lack of lymphatic and blood vessels and the lack of resident antigen-presenting cells (APCs) at basal conditions. Nevertheless, until today, different studies have demonstrated that the cornea is endowed with a significant number of resident APCs, such as macrophages and dendritic cells (DCs) [91–95]. In this regard, immune privilege means that even if immune cell activity is present, it is driven towards anti-inflammatory and tolerogenic immune responses [86].

Cells in the cornea, mostly epithelial cells, express and secrete different molecules that confer a tolerogenic profile upon DCs [85] or that promote regulatory activity or apoptosis in the T cells [86]. Among these molecules, the immunoregulatory factor Decay Accelerating Factor (DAF, also known as CD55) [96] or the apoptosis-inducing ligands FasL (FasLigand) and Programmed Death Ligand-1 (PDL-1) [85] seem to be crucial. In addition to suppressing T cell effector responses by producing their apoptosis, these ligands also allow regulatory T cells (Tregs) to function since Tregs are more resistant to FasL-induced apoptosis [97] and are activated by PDL-1 [98,99].

Along with the previously described mechanisms that contribute to the cornea's immune privilege, there is also a neuroregulation of ocular surface immunity by corneal nerves [85]. Different neuropeptides released by corneal nerves are involved in this process.

Vasoactive intestinal polypeptide (VIP) downregulates TLRs, inhibits chemokine expression, induces tolerogenic DCs, and limits the release of pro-inflammatory cytokines [100], while CGRP inhibits the production of inflammatory cytokines by macrophages and also the maturation of DCs [101].

3. Dendritic Cells

3.1. An Overview of Dendritic Cells

First discovered in mouse spleen in the 1970s [102], DCs are a heterogeneous group of professional APCs that induce naïve T cell activation and T effector differentiation [93,103], playing an important role between innate and adaptive immune responses. DCs include members of different lineages that can be found in two different functional states: mature and immature [93,103]. Immature DCs are characterized by a high antigen-capture ability due to their high endocytic capacity, but a low T cell-stimulatory capability due to their low surface expression of co-stimulatory molecules and chemokine receptors [104,105]. DC maturation, which is triggered by tissue homeostasis disturbances, leads to a decrease in their endocytic activity but an increase in the expression of major histocompatibility complex class II (MHC-II) and co-stimulatory molecules, such as CD40, CD80, and CD86 [105–108], becoming powerful T cell stimulators in secondary lymphoid organs [109,110].

Mature DCs can induce specific CD8+ and CD4+ T cell responses [111]. When interacting with CD4+ T cells, DCs can induce their differentiation into different T helper (Th) subsets, such as Th1, required for immunity against intracellular pathogens and cancer [103,111–114], Th2, essential for driving immune responses against parasitic infections [111,112,115,116], or Th17, important for neutralizing bacterial and fungal pathogens [117,118]. T cell differentiation in each subtype is a complex phenomenon that can be influenced by the cytokines in the DC tissue of origin [119] or their maturation state [107].

In addition to their role in inducing specific CD8+ and CD4+ T cells responses, DCs are also able to induce and maintain immune tolerance at basal conditions [103,120–122]. These "tolerogenic DCs" are immature DCs that express less co-stimulatory molecules, upregulate the expression of inhibitory molecules, and secrete anti-inflammatory cytokines [123,124], being essential to preventing responses against healthy tissues [109,120,125].

In both humans and mice, DCs are identified by their high expression of MHC-II and CD11c [103]. However, DCs express other molecules that allow their classification into different subtypes that differ from their phenotypic markers and genetic profile. Overall, these subtypes are types 1 and 2 conventional DCs (cDCs), plasmacytoid DCs (pDCs), Langerhans cells (LCs), and monocyte-derived DCs (MCs).

DCs arise from CD34+ hematopoietic stem cells (HSCs) that give rise to lymphoid (LPs) and myeloid precursors (MPs) (Figure 4). MPs differentiate into monocyte and DC precursors (MDPs), which, in turn, give rise to monocytes and the common DC precursors (CDPs). CDPs can differentiate into the preclassical DCs (pre-cDCs), which are the progenitors of the two major cDC subpopulations, cDC1 and cDC2, or into pDCs [103,126] (Figure 4), although recent studies suggest that mouse pDCs predominantly originate from a distinct progenitor from cDCs [111,127]. LPs can also give rise to pDCs, however, this ontogenic pathway is not completely elucidated (Figure 4). Once in the blood, pDCs and cDCs can migrate to lymphoid and nonlymphoid tissues.

LCs derive primarily from fetal liver monocytes that colonize the skin during embryogenesis [128] and maintain themselves by local proliferation in response to macrophage growth factors and IL-32 [109].

Finally, MCs are cells with DC-like features that can be generated by mouse monocytes during steady-state in skin and mucosal tissues [129,130] and during inflammation [130,131]. In vitro, mouse MCs can be also produced by bone marrow precursor stimulation with granulocyte-macrophage colony-stimulating factor (GM-CSF) [132]. Human MCs are produced in vitro by culturing human monocytes in the presence of GM-CSF and IL-4 [133].
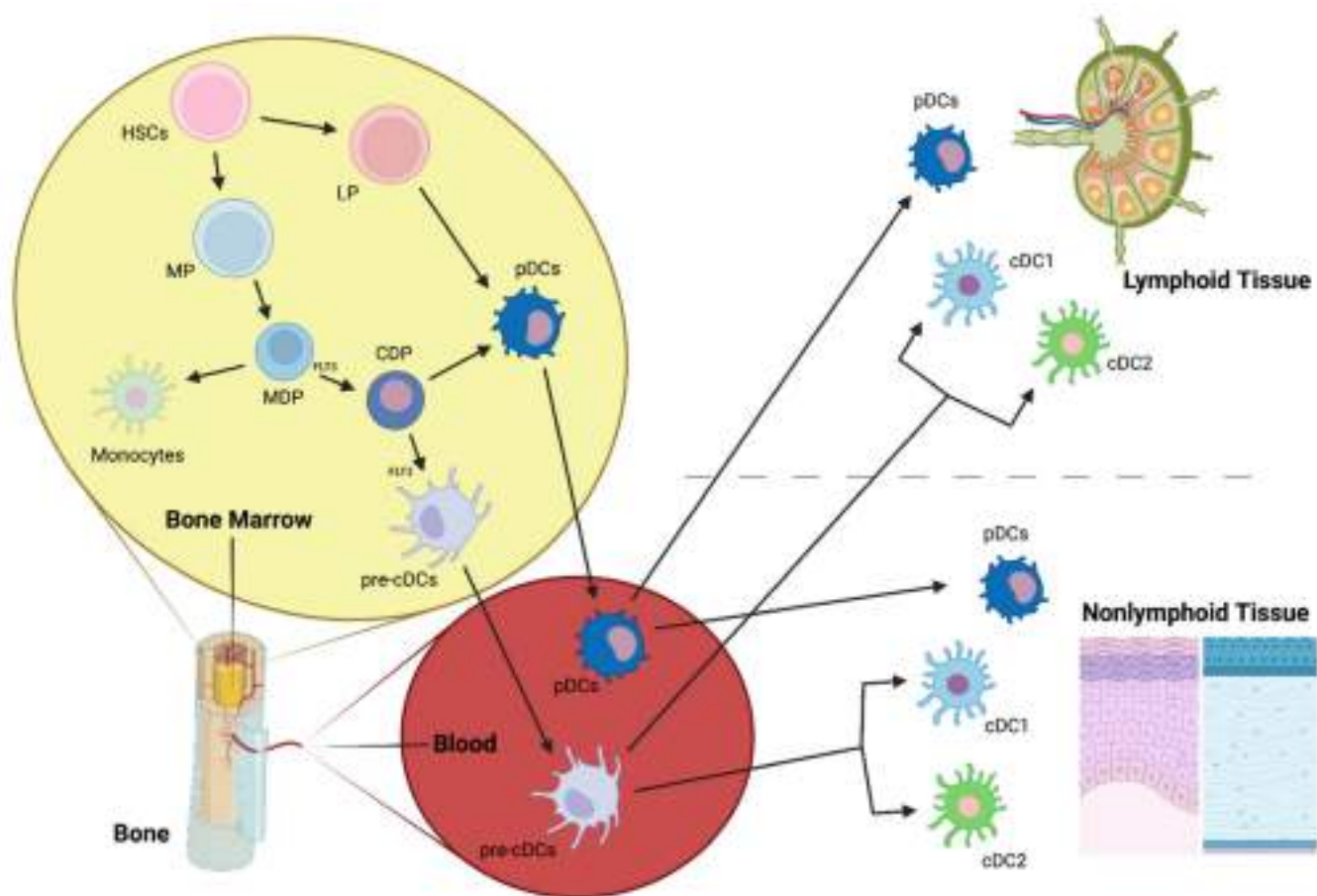
Figure 4. cDC1 and cDC2, main conventional dendritic cell subtypes; CDP, common DC precursor; FLT3, Fms-Related Tyrosine Kinase 3; HSCs, hematopoietic stem cells; LP, lymphoid precursor; MDP, macrophage-DC precursor; MP, myeloid precursor; pre-cDCs, pre-classical dendritic cells; pDCs, plasmacytoid dendritic cells.

3.2. Dendritic Cell Subpopulations

3.2.1. Conventional DCs (cDCs)

cDC1

cDC1 is a cDC subpopulation that efficiently primes CD8+ T cells by performing antigen cross-presentation [134]. cDC1can be found both in the periphery (where they represent 30% of cDC) and in lymphoid organs (where they account for 40%).

In humans and mice, cDC1s express CD141, the chemokine receptor XCR1, C-type lectin CLEC9A, and the cell adhesion molecule CADM1 [135] (Figure 5). Moreover, in mice, cDC1s are identified by the expression of CD8α in the spleen and CD103 in non-lymphoid tissues [135] (Figure 5) and can be also characterized by the expression of other C-type lectin receptors, such as CD205 and CD207 [136].

For the generation of cDC1s, the main transcription factors (TFs) are the basic leucine zipper transcriptional factor ATF-like 3 (BATF3) [137] and IFN-regulatory factor 8 (IRF8) [138]. In mice, in addition to BATF3 and IRF8, other TFs are also essential for cDC1s generation [135,139,140], such as DNA binding protein inhibitor ID2 and nuclear factor interleukin-3-regulated protein (NFIL3).

Figure 5. The different DC subtypes express specific surface markers in humans and mice.

cDC2

cDC2 is a more heterogeneous DC subset than cDC1 that has been shown to induce Th1, Th2, and Th17 responses from CD4+ helper T cells (Th) [141,142] and that has different regulatory roles by inducing regulatory T cells (Tregs) in some tissues, such as intestine or liver [143,144]. cDC2s can be found in lymphoid, non-lymphoid tissues, and blood [103,145] where they are more abundant than cDC1s.
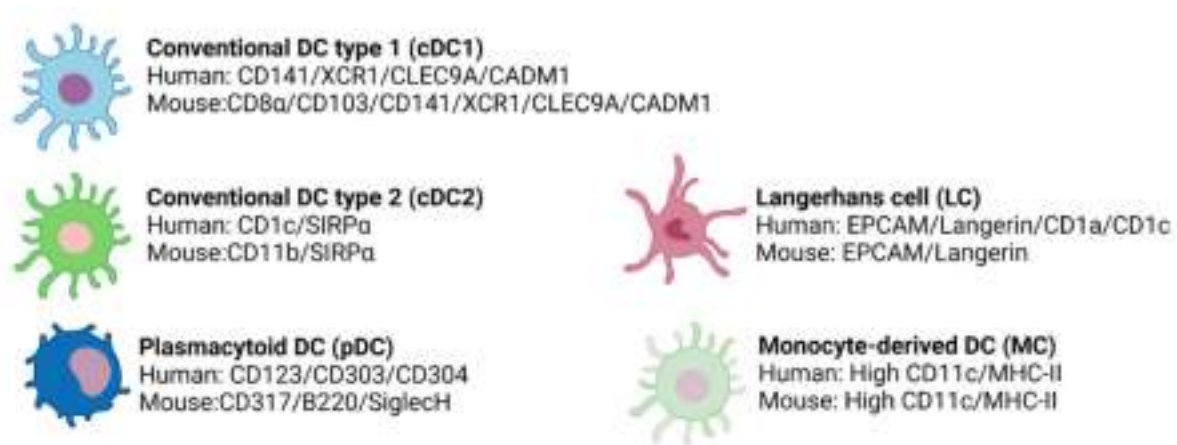
This subpopulation is characterized by the expression of SIRPα in both humans and mice and CD1c or CD11b in humans or mice, respectively [111,135] (Figure 5). Moreover, cDC2s can express other markers according to their location, which produces their great heterogeneity [103].

For cDC2 differentiation, different TFs are involved, with IRF4 traditionally considered the most important [146]. However, more recent studies suggest that IRF4 is more essential for cDC2 function regulation rather than for cDC2 development [147]. Other TFs shown to be associated with cDC2 differentiation are PU.1 and RelB [148,149] in mice and IRF8 [150] in humans.

3.2.2. Plasmacytoid DCs (pDCs)

pDC1 is a DC subpopulation that secretes high levels of IFN-α after TLR7/9 stimulation and has a pivotal role in viral infections [151]. In addition, these cells have also been associated with immune tolerance [152]. pDCs are continuously generated in the bone marrow and subsequently enter the bloodstream (where they constitute less than 1% of mononuclear cells) [153,154] to then home primary and secondary lymphoid tissues in steady-state [155–158]. During microbial infections or autoimmune diseases, these cells are recruited to peripheral tissues where they are typically absent [159,160]. However, although in low densities, few peripheral tissues host pDC during steady-state, such as the lung or the vagina [161,162].

Phenotypically, pDCs are distinct in mice and humans. In humans, pDCs are identified by their expression of CD123, CD303 (BDCA2), and CD304, while in mice, pDCs express CD307, B220, and SiglecH [135] (Figure 5). Importantly, human pDCs do not express CD11c [152,163] and can be divided into two subsets based on their levels of DC2 expression [164].

Regarding TFs for pDC generation, in both humans and mice, E2.2 seems to be the most important [103,111,135].

3.2.3. Langerhans Cells (LCs)

LCs are a subset of cells located in epidermal surfaces, being the most numerous antigen-presenting cells in human skin [111,135]. LCs can induce several immune responses by

stimulating CD4+ T cell proliferation and polarization towards the Th2 phenotype[111,165], and particularly in humans, these cells can also stimulate naïve CD8+T cells [165].

Human and murine LCs express EPCAM, low CD11c, and langerin, which act as a receptor for microbial pathogens [135] (Figure 5). Furthermore, in both humans and mice, LCs present Birbeck granules [166], a type of organelle whose function still remains unclear. Additionally, in humans, LCs are also CD1a+ and CD1c+ [135,167].

The development of LCs is mainly dependent on Runx3 and PU.1 [168,169].

3.2.4. Monocyte-Derived DCs (MCs)

MCs have contributed significantly to the knowledge about DCs in humans. Due to their potential, they are currently being studied for the treatment and monitoring of different human diseases, mainly cancer [103]. Ontogeny data suggest that inflammatory DCs (another DC subpopulation that expresses high levels of CD11c and MHC-II) are the in vivo counterparts of MCs [135,170] (Figure 5).

PU.1 and IRF4 act as TFs for human monocyte differentiation into MCs in vitro [171,172].

3.3. Resident Dendritic Cell Distribution in the Cornea

Traditionally, the cornea has been considered a tissue devoid of resident immune cells. However, heretofore many studies in humans and mice have shown the presence of macrophages [91,93,173] and the major DC subsets (Figure 6) in this tissue [174,175]. In addition, other immune cells, such as γδ T lymphocytes [176] or NK cells [177], have been reported in the limbus.
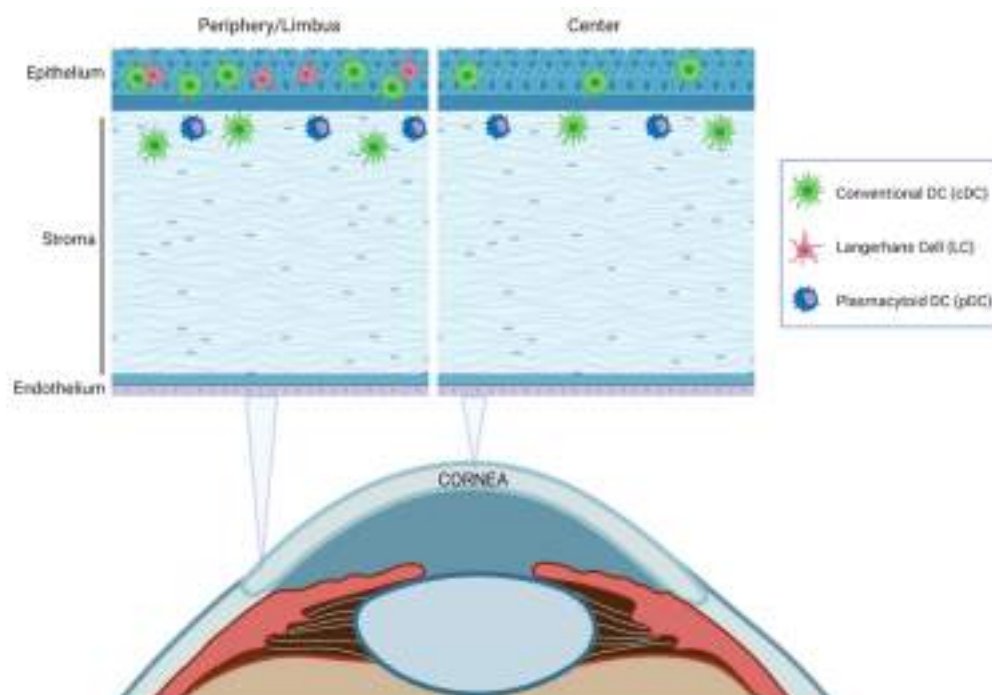
Figure 6. Schematic illustration of the distribution of resident DCs in the cornea at steady-state. Most DC subtypes are preferentially distributed in the epithelium and the anterior stroma and are more abundant in the peripheral cornea and limbal area than in the central cornea.

The density of DCs decreases from the limbus towards the center of the cornea [174,175] and correlates with ocular inflammation [173]. DC localization throughout corneal layers depends on the DC subpopulation [92,94,173] (Figure 6). cDCs were traditionally thought to be confined to the peripheral cornea and the limbus. Nevertheless, it was later demonstrated that these cells are also located in the central corneal epithelium and stroma, especially during inflammation [173]. Immature cDCs are more numerous in the periphery, but in response to an inflammatory stimulus, they increase and mature throughout the

cornea, with higher levels of MHC-II and co-stimulatory molecules [85,173]. LCs have been reported only in the peripheral epithelium [92] with a distribution pattern very similar to that in skin [178] and pDC are located in the anterior stroma, immediately below the basal epithelium both in the central and peripheral cornea [152].

3.4. Dendritic Cells in Ocular Diseases

3.4.1. Humans

DCs are the major immune cells involved in the most common ocular surface diseases [179]. In humans, most of the current investigations into corneal DCs are done by using In Vivo Confocal Microscopy (IVCM), which allows the study of subbasal and stromal corneal nerves. IVCM has been more and more used for the diagnosis and management of different corneal diseases because it is minimally invasive and has a high resolution [180]. In this context, the in vivo dynamic assessment of corneal inflammatory cell density seems to be a good indicator of the disease severity. An inverse correlation between corneal nerve density and density of DCs has been described in patients with long COVID, especially those with neurological symptoms [181], and also in patients with infectious keratitis including fungal, bacterial, and *Acanthamoeba* keratitis [182] Moreover, the reduction in corneal nerves and the increase in DC density was bilateral even after unilateral infectious keratitis [183]. Along the same lines, an increase in corneal DC density has also been observed by IVCM in patients with herpetic uveitis [184], aqueous-deficient dry eye disease (DED) [185], Sjögren's syndrome (SS) [186], and in contact lens wearers [187].

In this vein, other clinical studies have postulated a connection between the patient's tear cytokines and corneal DCs. A significant correlation between proinflammatory cytokines and increased DC density, and reduction in corneal subbasal nerve density has been described in bacterial keratitis [188]. Significantly higher levels of IL-1β, IL-6, and IL-8 cytokines were found in tears of the affected eyes compared with healthy controls, as well as higher levels of CCL-2, IL-10, and IL-17a cytokines in the contralateral eyes [188]. However, this is not the only study that correlates proinflammatory tear cytokines with corneal DC density. In patients with rheumatoid arthritis after systemic therapy [189] a decrease in tear IL-1 and IL-6 levels is accompanied by a decrease in DC density. Table 1 summarizes these examples of ocular pathologies in which DCs are involved.

Table 1. Changes in Dendritic Cells (DCs) in ocular pathologies.

Disease	Species	Corneal Changes	Reference
Long COVID	Human	Reduced corneal nerve density and increased DC density	[181]
Infectious keratitis (fungal, bacterial, or *Acanthamoeba*)	Human	Reduced corneal nerve density and increased DC density	[182]
Herpetic uveitis	Human	Increased DC density	[184]
Aqueous-deficient dry eye disease (DED)	Human	Increased DC density	[185]
Sjögren's syndrome (SS)	Human	Increased DC density	[186]
Contact lens wearing	Human	Increased DC density	[187]
Rheumatoid arthritis	Human	Decreased DC density	[189]
Herpes simplex virus (HSV) keratitis	Mouse	Increased DC density	[190]
Ocular allergy	Mouse	DC lead to allergic T cell responses	[191]
Diabetic sensory neuropathy	Mouse	Reduced corneal nerve and DC density	[192]
Dry eye disease (DED)	Mouse	More activated DCs in lymph nodes	[193]

3.4.2. Mice

Most of the current knowledge on the pathophysiology of DCs in ocular diseases arises from studies performed in mice. The implication of DCs in infectious keratitis and, particularly, in herpes simplex virus (HSV) keratitis, is one of the most characterized in models. As early as one day after HSV-1 inoculation, pDCs are increased in both peripheral and central cornea, and this increase progresses until 6 days post-inoculation [190]. Moreover, following HSV-1 inoculation, pDCs also increase in the draining lymph nodes (dLNs), with a major shift towards mature pDCs [194]. During primary herpes simplex keratitis, there is a neuro-invasion of sensory corneal nerves by HSV that remains latent in the TG. If there is a virus reactivation, that leads to chronic recurrent herpes stromal keratitis [195], it may eventually produce severe corneal scarring. In this context, it has been shown that pDC depletion prior to HSV-1 inoculation produces increased virus titers in the cornea and increased viral transmission to TG and dLNs [190,196], suggesting a protective role of these cells. This is the opposite of what is observed in the local depletion of cDCs, which produces a decreased corneal nerve infection and a decreased and delayed systemic viral transmission in TG and dLNs [197]. Nevertheless, in both cDC and pDC depleted-mice, a higher clinical keratitis severity was observed compared to sham-depleted animals, maybe due to the major influx of immune cells to the cornea. Further, depletion of corneal pDCs in BDCA-2-DTR mice prior to HSV-1 inoculation is accompanied by alterations in the dLN cytokine milieu, leading to decreased density of Tregs [196], as well as increased recruitment of ex-Tregs to the cornea and dLN in vivo [152].

DC immune responses in the cornea have been also widely studied in sterile models of inflammation. In ocular tissues, this sterile inflammation occurs in response to chemical and mechanical traumas, contact lens wear, or allergens. It has been shown that depletion of corneal pDCs prior to suture placement is accompanied by enhanced clinical opacity of the cornea, as well as augmented influx of inflammatory immune CD45+ cells [196,198]. Moreover, in a mouse model of ocular allergy, CD11b+ DC subset seems to play a dominant role in secondary allergic immune responses [191].

The implication of DCs in ocular diseases has also been described in diabetic sensory neuropathy in the cornea and DED. Sensory nerve density and DC populations were dramatically decreased in diabetic mice and DC decrease during wound healing results in the reduction in tissue levels of CNTF, which, in turn, impairs sensory nerve innervation and regeneration [192]. Furthermore, in an experimental model of DED induced by subcutaneous injections of scopolamine, DCs in dLNs were shown to be more activated than in control mice, suggesting that they may stimulate the T cells that participate in the onset and progression of the disease [193].

These examples (summarized in Table 1) are only a part of the huge number of results that are currently being obtained regarding the involvement of DCs in the pathophysiology of ocular diseases. However, we still have limited knowledge in many aspects of the immune response of DCs. Further studies need to be undertaken to define the molecular mechanisms behind DC immune responses and to elucidate the contribution of DCs in other ocular diseases.

4. Transgenic Mice to Study Neuro–Immune Interactions in the Cornea

Resident APCs in the cornea are located close to the corneal nerves [1,152,182,199–201]. Different studies have shown that the association between corneal nerves and APCs seems to have a potential role in corneal health and disease, with a reduced association under injury or pathological conditions [200]. In order to further analyze this neuro–immune crosstalk under pathological and steady-state conditions, our lab developed a mice model with C57BL/6J background in which sensory axons are labeled with tdTomato and DCs are labeled with green fluorescent protein (GFP) (Figures 7 and 8).
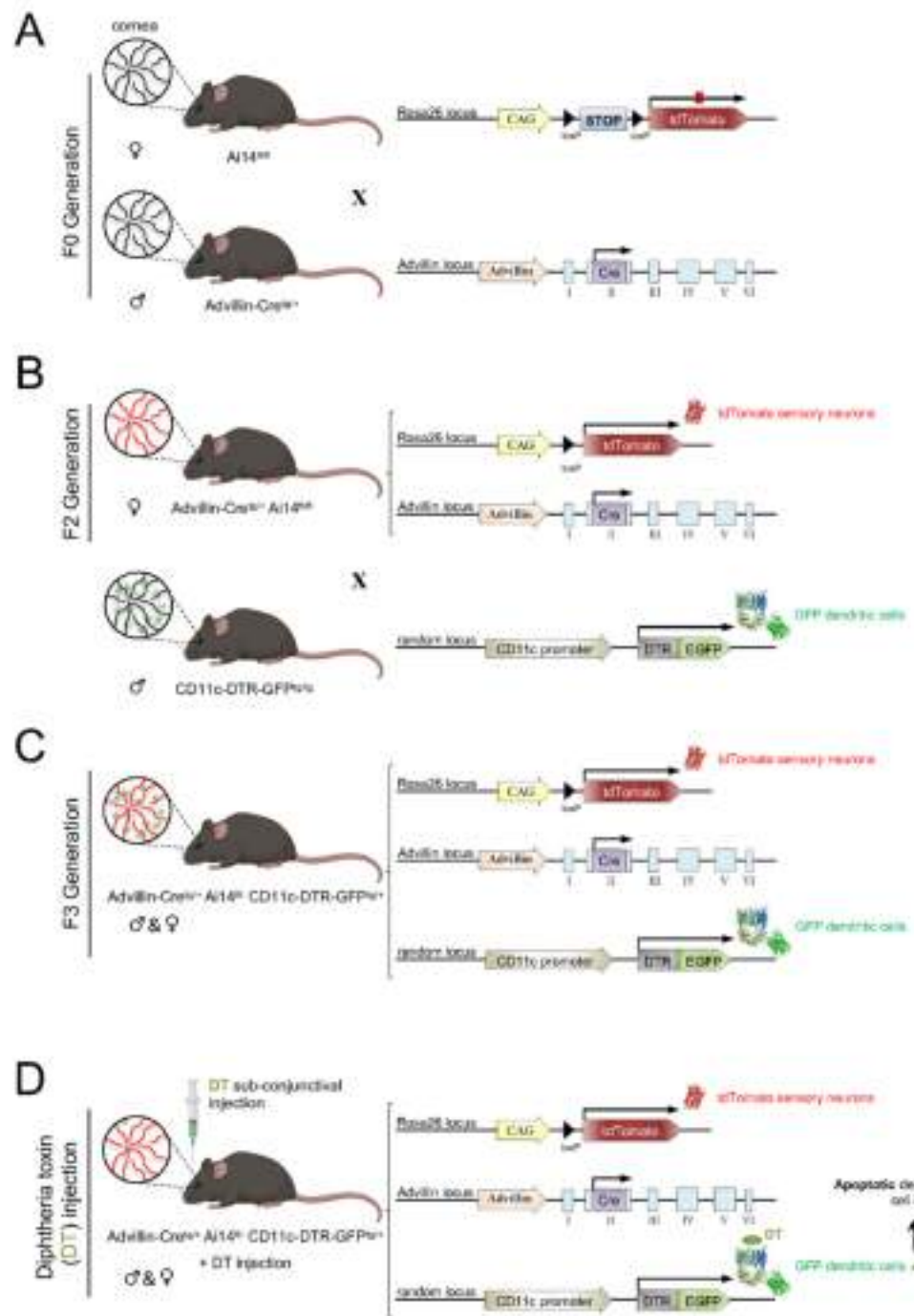
Figure 7. Scheme of the generation of the Advillin-Cretg/+ Ai14fl/- CD11c-DTR-GFPtg/+ mouse model. Ai14fl/fl females were crossed with Avidillin-Cretg/+ males to produce the F1 generation (**A**). To obtain a F2 generation of Advillin-Cretg/+ Ai14fl/fl mice (**B**), F1 females were crossed with Ai14fl/fl males (which had corneal sensory nerves framed with tdTomato). To generate the animal model of interest (**C**), F2 females were crossed with male CD11c-DTR-GFPtg/tg mice that expressed Diphtheria toxin Receptor (DTR) and GFP in DCs. Subconjunctival administration of DT to the resultant Advillin-Cretg/+ Ai14fl/− CD11c-DTR-GFPtg/+ mice caused apoptosis of corneal DCs (**D**).
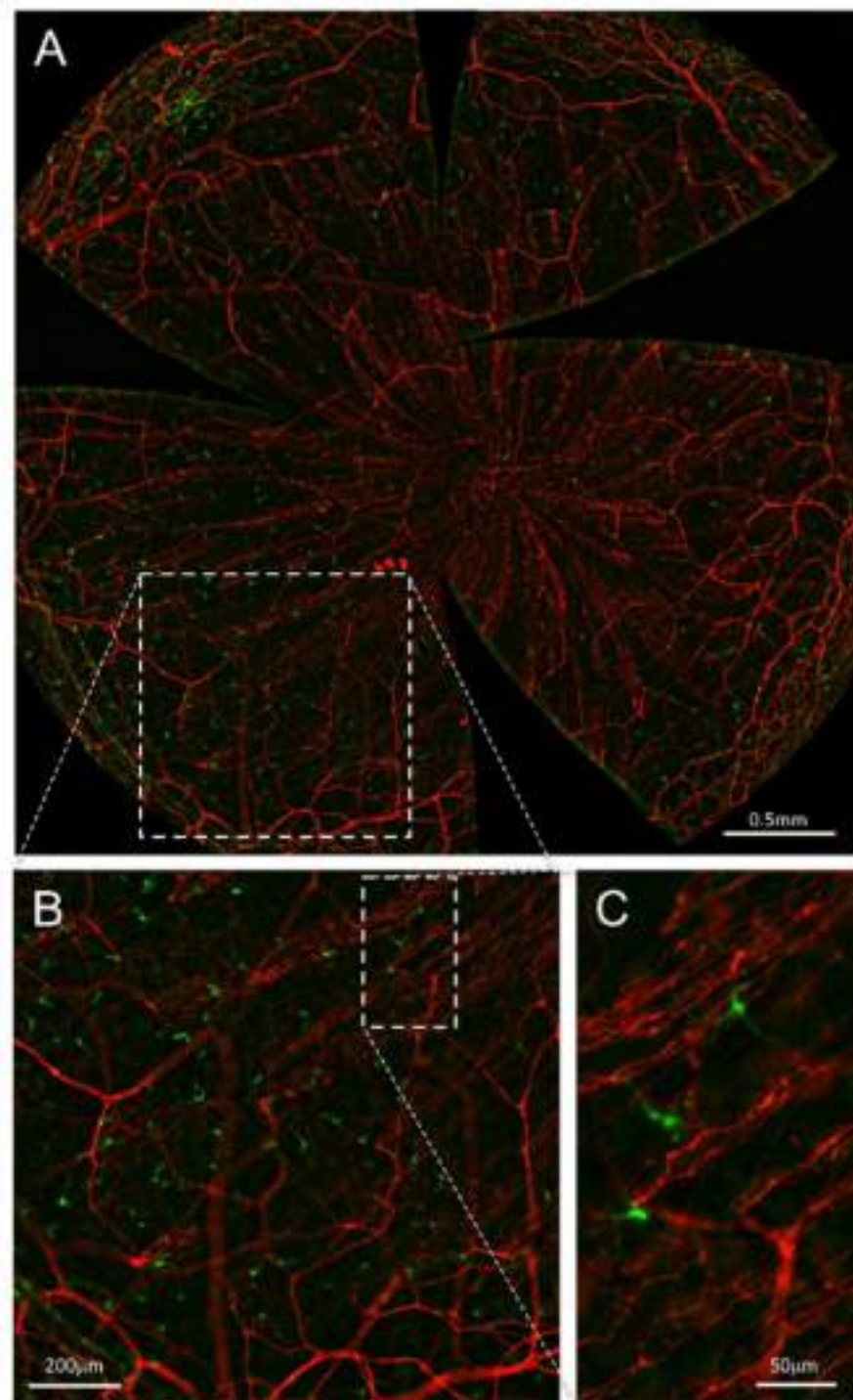
Figure 8. Nerves and DCs in the advillin-Cretg/+ Ai14fl/- CD11c-DTR-GFPtg/+ mouse cornea. All panels are maximal intensity z-projection stacks (30μm) performed with a Leica THUNDER Imager Tissue provided with a 20× objective. (**A**) Flat mount overview of a whole-mount cornea (64 tiles merged) showing tdTomato (red) expression in corneal sensory nerves and GFP (green) expression in DCs after computational clearing of the out-of-focus blur. (**B,C**) Higher magnification images showing nerve fibers and DCs endogenously expressing tdTomato and GFP, respectively. Scale bars: A, 500 μm; B, 200 μm; C, 50 μm. Methods: Ocular globes from 5-month-old mutant mice were fixed for 2 h at RT in 4% paraformaldehyde in PBS and then washed in PBS. After washing, corneas were dissected and flat-mounted with Fluoromount-G.

To generate a mouse where the corneas have sensory axons labeled with tdTomato, we crossed Advillin-Cre$^{tg/+}$ (Tg(Avil-cre)1Phep) mice ([202]; MGI:5292346) with Ai14$^{fl/fl}$ (Gt(ROSA)26Sor$^{tm14(CAG-tdTomato)Hze}$) mice ([203]; MGI:3809524) (Figure 7A). The F1 offspring was back-crossed with Ai14$^{fl/fl}$ mice to obtain Advillin-Cre$^{tg/+}$ Ai14$^{fl/fl}$ offspring (F2 generation) (Figure 7B).

After generating the mice with tdTomato-labeled sensory nerves, we wanted to add GFP-labeled DC. For this purpose, Advillin-Cre$^{tg/+}$ Ai14$^{fl/fl}$ mice were crossed with CD11c-DTR/GFP$^{tg/tg}$ (1700016L21Rik$^{Tg(Itgax-DTR/EGFP)57Lan}$) mice ([204]; MGI:3057163) to obtain Advillin-Cre$^{tg/+}$Ai14$^{fl/+}$CD11c-DTR/GFP$^{tg/+}$ offspring (F3 generation) (Figure 7C). CD11c-DTR mice, in addition, carry a transgene encoding for a simian diphtheria toxin (DT) receptor (DTR) plus a green fluorescent protein (GFP) fusion protein under the control of the murine CD11c promoter, which makes CD11c+ cells sensitive to DT (Figure 7D).

Ex vivo and in vivo imaging of the corneas of this mouse strain allowed a precise description of the interactions between nerve fibers and DCs, expressing tdTomato and GFP, respectively. Preliminary data on the influence of presence or absence of DCs on corneal nerve activity and nociceptive behavior of CD11c-DTR/GFP$^{tg/tg}$ mice have been reported elsewhere [205].

Institutional Review Board Statement: The animal study protocol was approved by the Universidad Miguel Hernandez de Elche Committee of Ethics and Integrity in Research, and Generalitat Valenciana (Reference number for the approved protocol was 2021VSCPEA0167, 7 July 2021).

Informed Consent Statement: Not applicable.

Data Availability Statement: Not applicable.

Conflicts of Interest: The authors declare that the research was conducted in the absence of any commercial or financial relationships that could be construed as a potential conflict of interest.

References

1. Gao, N.; Lee, P.; Yu, F.-S. Intraepithelial dendritic cells and sensory nerves are structurally associated and functional interdependent in the cornea. *Sci. Rep.* **2016**, *6*, 36414. [CrossRef] [PubMed]
2. Dawson, D.G.; Ubels, J.L.; Edelhauser, H.F. Cornea and sclera. In *Adler's Physiology of the Eye*, 11th ed.; Elsevier: Amsterdam, The Netherlands, 2011; Volume 4, pp. 71–130.
3. DelMonte, D.W.; Kim, T. Anatomy and physiology of the cornea. *J. Cataract Refract. Surg.* **2011**, *37*, 588–598. [CrossRef]
4. Saude, T. *Ocular Anatomy and Physiology*; Blackwell Science Ltd.: Oxford, UK, 1993.
5. Rüfer, F.; Schröder, A.; Erb, C. White-to-white corneal diameter: Normal values in healthy humans obtained with the Orbscan II topography system. *Cornea* **2005**, *24*, 259–261. [CrossRef] [PubMed]
6. Müller, L.J.; Marfurt, C.F.; Kruse, F.; Tervo, T.M.T. Corneal nerves: Structure, contents and function. *Exp. Eye Res.* **2003**, *76*, 521–542. [CrossRef]

7. Belmonte, C.; Gallar, J. Cold thermoreceptors, unexpected players in tear production and ocular dryness sensations. *Investig. Ophthalmol. Vis. Sci.* **2011**, *52*, 3888–3892. [CrossRef]

8. Belmonte, C.; Aracil, A.; Acosta, M.C.; Luna, C.; Gallar, J. Nerves and sensations from the eye surface. *Ocul. Surf.* **2004**, *2*, 248–253. [CrossRef]

9. González-González, O.; Bech, F.; Gallar, J.; Merayo-Lloves, J.; Belmonte, C. Functional properties of sensory nerve terminals of the mouse cornea. *Investig. Ophthalmol. Vis. Sci.* **2017**, *58*, 404–415. [CrossRef]

10. Maurice, D.M. The structure and transparency of the cornea. *J. Physiol.* **1957**, *136*, 263–286. [CrossRef]

11. Hassell, J.R.; Birk, D.E. The molecular basis of corneal transparency. *Exp. Eye Res.* **2010**, *91*, 326–335. [CrossRef]

12. Ambati, B.K.; Nozaki, M.; Singh, N.; Takeda, A.; Jani, P.D.; Suthar, T.; Albuquerque, R.J.C.; Richter, E.; Sakurai, E.; Newcomb, M.T.; et al. Corneal avascularity is due to soluble VEGF receptor-1. *Nature* **2006**, *443*, 993–997. [CrossRef]

13. Cursiefen, C.; Chen, L.; Saint-Geniez, M.; Hamrah, P.; Jin, Y.; Rashid, S.; Pytowski, B.; Persaud, K.; Wu, Y.; Streilein, J.W.; et al. Nonvascular VEGF receptor 3 expression by corneal epithelium maintains avascularity and vision. *Proc. Natl. Acad. Sci. USA* **2006**, *103*, 11405–11410. [CrossRef]

14. Almubrad, T.; Akhtar, S. Structure of corneal layers, collagen fibrils, and proteoglycans of tree shrew cornea. *Mol. Vis.* **2011**, *17*, 2283–2291.

15. Argüeso, P.; Gipson, I.K. Epithelial mucins of the ocular surface: Structure, biosynthesis and function. *Exp. Eye Res.* **2001**, *73*, 281–289. [CrossRef]

16. Henriksson, J.T.; McDermott, A.M.; Bergmanson, J.P.G. Dimensions and morphology of the cornea in three strains of mice. *Investig. Ophthalmol. Vis. Sci.* **2009**, *50*, 3648–3654. [CrossRef]

17. Hanna, C.; Bicknell, D.S.; O'brien, J.E. Cell Turnover in the Adult Human Eye. *Arch. Ophthalmol.* **1961**, *65*, 695–698. [CrossRef]

18. Thoft, R.A.; Friend, J. The X, Y, Z hypothesis of corneal epithelial maintenance. *Investig. Ophthalmol. Vis. Sci.* **1983**, *24*, 1442–1443.

19. Wilson, S.E. Bowman's layer in the cornea– structure and function and regeneration. *Exp. Eye Res.* **2020**, *195*, 108033. [CrossRef]

20. Wilson, S.E.; Hong, J.W. Bowman's layer structure and function: Critical or dispensable to corneal function? A Hypothesis. *Cornea* **2000**, *19*, 417–420. [CrossRef]

21. Lee, T. The ins and outs of corneal wound healing. *Rev. Optom.* **2016**, *153*, 44–56.

22. Hazlett, L.D. Corneal and Ocular Surface Histochemistry. *Prog. Histochem. Cytochem.* **1993**, *25*, 3–6. [CrossRef]

23. Maurice, D.M. The transparency of the corneal stroma. *Vision Res.* **1970**, *10*, 107–108. [CrossRef]

24. Watsky, M.A. Keratocyte gap junctional communication in normal and wounded rabbit corneas and human corneas. *Investig. Ophthalmol. Vis. Sci.* **1995**, *36*, 2568–2576.

25. Stramer, B.M.; Zieske, J.D.; Jung, J.C.; Austin, J.S.; Fini, M.E. Molecular mechanisms controlling the fibrotic repair phenotype in cornea: Implications for surgical outcomes. *Investig. Ophthalmol. Vis. Sci.* **2003**, *44*, 4237–4246. [CrossRef]

26. Haustein, J. On the ultrastructure of the developing and adult mouse corneal stroma. *Anat. Embryol.* **1983**, *168*, 291–305. [CrossRef]

27. Dua, H.S.; Faraj, L.A.; Said, D.G.; Gray, T.; Lowe, J. Human corneal anatomy redefined: A novel pre-Descemet's layer (Dua's layer). *Ophthalmology* **2013**, *120*, 1778–1785. [CrossRef]

28. Smith, R.S.; Sundberg, J.P.; John., S.W.M. The anterior segment and ocular adnexae. In *Systematic Evaluation of the Mouse Eye: Anatomy, Pathology and Biomethods*; Smith, R.S., Ed.; CRC Press: Boca Raton, FL, USA, 2002; Volume 1, pp. 3–23.

29. Al-Aqaba, M.A.; Dhillon, V.K.; Mohammed, I.; Said, D.G.; Dua, H.S. Corneal nerves in health and disease. *Prog. Retin. Eye Res.* **2019**, *73*, 100762. [CrossRef]

30. Belmonte, C.; Tervo, T.T.; Gallar, J. Sensory innervation of the eye. In *Adler's Physiology of the Eye*, 11th ed.; Elsevier: Amsterdam, The Netherlands, 2011; Volume 16, pp. 363–384.

31. Vonderahe, A.R. Corneal and scleral anesthesia of the lower hale of the eye in a case of trauma of the superior maxillary nerve. *Arch. Neurol. Psychiatry* **1928**, *20*, 836–837. [CrossRef]

32. Ruskell, G.L. Ocular fibers of the maxillary nerve in monkeys. *J. Anat.* **1974**, *118*, 195–203.

33. Marfurt, C.F.; Ellis, L.C. Immunohistochemical localization of tyrosine hydroxylase in corneal nerves. *J. Comp. Neurol.* **1993**, *336*, 517–531. [CrossRef]

34. Ehinger, B. Connections between Adrenergic Nerves and other Tissue Components in the Eye. *Acta Physiol. Scand.* **1966**, *67*, 57–64. [CrossRef]

35. Morgan, C.; DeGroat, W.C.; Jannetta, P.J. Sympathetic innervation of the cornea from the superior cervical ganglion. An HRP study in the cat. *J. Auton. Nerv. Syst.* **1987**, *20*, 179–183. [CrossRef]

36. Marfurt, C.F.; Kingsley, R.E.; Echtenkamp, S.E. Sensory and sympathetic innervation of the mammalian cornea. A retrograde tracing study. *Investig. Ophthalmol. Vis. Sci.* **1989**, *30*, 461–472.

37. Toivanen, M.; Tervo, T.; Partanen, M.; Vannas, A.; Hervonen, A. Histochemical demonstration of adrenergic nerves in the stroma of human cornea. *Investig. Ophthalmol. Vis. Sci.* **1987**, *28*, 398–400.

38. Marfurt, C.F.; Cox, J.; Deek, S.; Dvorscak, L. Anatomy of the human corneal innervation. *Exp. Eye Res.* **2010**, *90*, 478–492. [CrossRef] [PubMed]

39. He, J.; Bazan, N.G.; Bazan, H.E.P. Mapping the entire human corneal nerve architecture. *Exp. Eye Res.* **2010**, *91*, 513–523. [CrossRef] [PubMed]

40. Marfurt, C.F. Nervous control of the cornea. In *Nervous Control of the Eye*; Harwood Academic Publishers: Amsterdam, The Netherlands, 2000; p. 41.

41. Chan-Ling, T. Sensitivity and neural organization of the cat cornea. *Investig. Ophthalmol. Vis. Sci.* **1989**, *30*, 1075–1082.
42. Zander, E.; Weddell, G. Observations on the innervation of the cornea. *J. Anat.* **1951**, *85*, 68–99.
43. Ivanusic, J.J.; Wood, R.J.; Brock, J.A. Sensory and sympathetic innervation of the mouse and guinea pig corneal epithelium. *J. Comp. Neurol.* **2013**, *521*, 877–893. [CrossRef]
44. Mckenna, C.C.; Lwigale, P.Y. Innervation of the mouse cornea during development. *Investig. Ophthalmol. Vis. Sci.* **2011**, *52*, 30–35. [CrossRef]
45. Wang, C.; Fu, T.; Xia, C.; Li, Z. Changes in mouse corneal epithelial innervation with age. *Investig. Ophthalmol. Vis. Sci.* **2012**, *53*, 5077–5084. [CrossRef]
46. Stepp, M.A.; Tadvalkar, G.; Hakh, R.; Pal-Ghosh, S. Corneal epithelial cells function as surrogate Schwann cells for their sensory nerves. *Glia* **2017**, *65*, 851–863. [CrossRef]
47. Rózsa, A.J.; Beuerman, R.W. Density and organization of free nerve endings in the corneal epithelium of the rabbit. *Pain* **1982**, *14*, 105–120. [CrossRef]
48. Schimmelpfennig, B. Nerve structures in human central corneal epithelium. *Graefe's Arch. Clin. Exp. Ophthalmol.* **1982**, *218*, 14–20. [CrossRef]
49. Belmonte, C.; Garcia-Hirschfeld, J.; Gallar, J. Neurobiology of ocular pain. *Progr. Ret. Eye Res.* **1997**, *16*, 117–156. [CrossRef]
50. Dua, H.S.; Watson, N.J.; Mathur, R.M.; Forrester, J.V. Corneal epithelial cell migration in humans: 'hurricane and blizzard keratopathy'. *Eye* **1993**, *7*, 53–58. [CrossRef]
51. Al-Aqaba, M.A.; Fares, U.; Suleman, H.; Lowe, J.; Dua, H.S. Architecture and distribution of human corneal nerves. *Br. J. Ophthalmol.* **2010**, *94*, 784–789. [CrossRef]
52. Dvorscak, L.; Marfurt, C.F. Age-related changes in rat corneal epithelial nerve density. *Investig. Ophthalmol. Vis. Sci.* **2008**, *49*, 910–916. [CrossRef]
53. Nagasaki, T.; Zhao, J. Centripetal Movement of Corneal Epithelial Cells in the Normal Adult Mouse. *Investig. Ophthalmol. Vis. Sci.* **2003**, *44*, 558–566. [CrossRef]
54. Patel, D.V.; McGhee, C.N.J. Mapping of the normal human corneal sub-basal nerve plexus by in vivo laser scanning confocal microscopy. *Investig. Ophthalmol. Vis. Sci.* **2005**, *46*, 4485–4488. [CrossRef]
55. Alamri, A.S.; Wood, R.J.; Ivanusic, J.J.; Brock, J.A. The neurochemistry and morphology of functionally identified corneal polymodal nociceptors and cold thermoreceptors. *PLoS ONE* **2018**, *13*, e0195108. [CrossRef]
56. Belmonte, C.; Acosta, M.C.; Gallar, J. Neural basis of sensation in intact and injured corneas. *Exp. Eye Res.* **2004**, *78*, 513–525. [CrossRef]
57. Acosta, M.C.; Belmonte, C.; Gallar, J. Sensory experiences in humans and single-unit activity in cats evoked by polymodal stimulation of the cornea. *J. Physiol.* **2001**, *534*, 511–525. [CrossRef]
58. Bron, R.; Wood, R.J.; Brock, J.A.; Ivanusic, J.J. Piezo2 expression in corneal afferent neurons. *J. Comp. Neurol.* **2014**, *522*, 2967–2979. [CrossRef]
59. Fernández-Trillo, J.; Florez-Paz, D.; Íñigo-Portugués, A.; González-González, O.; del Campo, A.G.; González, A.; Viana, F.; Belmonte, C.; Gomis, A. Piezo2 mediates low-threshold mechanically evoked pain in the cornea. *J. Neurosci.* **2020**, *40*, 8976–8993. [CrossRef]
60. Belmonte, C.; Giraldez, F. Responses of cat corneal sensory receptors to mechanical and thermal stimulation. *J. Physiol.* **1981**, *321*, 355–368. [CrossRef]
61. Belmonte, C.; Gallar, J.; Pozo, M.A.; Rebollo, I. Excitation by irritant chemical substances of sensory afferent units in the cat's cornea. *J. Physiol.* **1991**, *437*, 709–725. [CrossRef]
62. Chen, X.; Gallar, J.; Belmonte, C. Reduction by antiinflammatory drugs of the response of corneal sensory nerve fibers to chemical irritation. *Investig. Ophthalmol. Vis. Sci.* **1997**, *38*, 1944–1953. [CrossRef]
63. Gallar, J.; Pozo, M.A.; Tuckett, R.P.; Belmonte, C. Response of sensory units with unmyelinated fibres to mechanical, thermal and chemical stimulation of the cat's cornea. *J. Physiol.* **1993**, *468*, 609–622. [CrossRef]
64. Gallar, J.; Acosta, M.C.; Gutiérrez, A.R.; Belmonte, C. Impulse activity in corneal sensory nerve fibers after photorefractive keratectomy. *Investig. Ophthalmol. Vis. Sci.* **2007**, *48*, 4033–4037. [CrossRef]
65. Bessou, P.; Perl, E.R. Response of cutaneous sensory units with unmyelinated fibers to noxious stimuli. *J. Neurophysiol.* **1969**, *32*, 1025–1043. [CrossRef]
66. Meyer, R.A.; Ringkamp, M.; Campbell, J.N.; Raja, S.N. Peripheral mechanisms of cutaneous nociception. In *Wall & Melzack's Textbook of Pain*; Elsevier: Amsterdam, The Netherlands, 2006; pp. 3–34. [CrossRef]
67. Carr, R.W.; Pianova, S.; Fernandez, J.; Fallon, J.B.; Belmonte, C.; Brock, J.A. Effects of heating and cooling on nerve terminal impulses recorded from cold-sensitive receptors in the guinea-pig cornea. *J. Gen. Physiol.* **2003**, *121*, 427–439. [CrossRef] [PubMed]
68. Parra, A.; Gonzalez-Gonzalez, O.; Gallar, J.; Belmonte, C. Tear fluid hyperosmolality increases nerve impulse activity of cold thermoreceptor endings of the cornea. *Pain* **2014**, *155*, 1481–1491. [CrossRef] [PubMed]
69. Acosta, M.C.; Luna, C.; Quirce, S.; Belmonte, C.; Gallar, J. Changes in sensory activity of ocular surface sensory nerves during allergic keratoconjunctivitis. *Pain* **2013**, *154*, 2353–2362. [CrossRef] [PubMed]
70. Acosta, M.C.; Peral, A.; Luna, C.; Pintor, J.; Belmonte, C.; Gallar, J. Tear secretion induced by selective stimulation of corneal and conjunctival sensory nerve fibers. *Investig. Ophthalmol. Vis. Sci.* **2004**, *45*, 2333–2336. [CrossRef]

71. Parra, A.; Madrid, R.; Echevarria, D.; del Olmo, S.; Morenilla-Palao, C.; Acosta, M.C.; Gallar, J.; Dhaka, A.; Viana, F.; Belmonte, C. Ocular surface wetness is regulated by TRPM8-dependent cold thermoreceptors of the cornea. *Nat. Med.* **2010**, *16*, 1396–1399. [CrossRef]

72. Quallo, T.; Vastani, N.; Horridge, E.; Gentry, C.; Parra, A.; Moss, S.; Viana, F.; Belmonte, C.; Andersson, D.A.; Bevan, S. TRPM8 is a neuronal osmosensor that regulates eye blinking in mice. *Nat. Commun.* **2015**, *6*, 7150. [CrossRef]

73. Alcalde, I.; Íñigo-Portugués, A.; González-González, O.; Almaraz, L.; Artime, E.; Morenilla-Palao, C.; Gallar, J.; Viana, F.; Merayo-Lloves, J.; Belmonte, C. Morphological and functional changes in TRPM8-expressing corneal cold thermoreceptor neurons during aging and their impact on tearing in mice. *J. Comp. Neurol.* **2018**, *526*, 1859–1874. [CrossRef]

74. Gallar, J.; Acosta, M.C.; Moilanen, J.A.O.; Holopainen, J.M.; Belmonte, C.; Tervo, T.M.T. Recovery of corneal sensitivity to mechanical and chemical stimulation after laser in situ keratomileusis. *J. Refract. Surg.* **2004**, *20*, 229–235. [CrossRef]

75. Luna, C.; Quirce, S.; Aracil-Marco, A.; Belmonte, C.; Gallar, J.; Acosta, M.C. Unilateral Corneal Insult Also Alters Sensory Nerve Activity in the Contralateral Eye. *Front. Med.* **2021**, *8*, 2079. [CrossRef]

76. Acosta, M.C.; Luna, C.; Quirce, S.; Belmonte, C.; Gallar, J. Corneal sensory nerve activity in an experimental model of UV keratitis. *Investig. Ophthalmol. Vis. Sci.* **2014**, *55*, 3403–3412. [CrossRef]

77. Kovács, I.; Luna, C.; Quirce, S.; Mizerska, K.; Callejo, G.; Riestra, A.; Fernández-Sánchez, L.; Meseguer, V.M.; Cuenca, N.; Merayo-Lloves, J.; et al. Abnormal activity of corneal cold thermoreceptors underlies the unpleasant sensations in dry eye disease. *Pain* **2016**, *157*, 399–417. [CrossRef]

78. Belmonte, C. Pain, Dryness, and Itch Sensations in Eye Surface Disorders Are Defined by a Balance between Inflammation and Sensory Nerve Injury. *Cornea* **2019**, *38*, S11–S24. [CrossRef]

79. Luna, C.; Mizerska, K.; Quirce, S.; Belmonte, C.; Gallar, J.; del Carmen Acosta, M.; Meseguer, V. Sodium Channel Blockers Modulate Abnormal Activity of Regenerating Nociceptive Corneal Nerves After Surgical Lesion. *Investig. Opthalmol. Vis. Sci.* **2021**, *62*, 2. [CrossRef]

80. Gonzalez, G.G.; De la Rubia, P.G.; Gallar, J.; Belmonte, C. Reduction of capsaicin-induced ocular pain and neurogenic inflammation by calcium antagonists. *Investig. Ophthalmol. Vis. Sci.* **1993**, *34*, 3329–3335.

81. Vitar, R.M.L.; Barbariga, M.; Fonteyne, P.; Bignami, F.; Rama, P.; Ferrari, G. Modulating ocular surface pain through neurokinin-1 receptor blockade. *Investig. Ophthalmol. Vis. Sci.* **2021**, *62*, 26. [CrossRef]

82. Murata, Y.; Masuko, S. Peripheral and central distribution of TRPV1, substance P and CGRP of rat corneal neurons. *Brain Res.* **2006**, *1085*, 87–94. [CrossRef]

83. Yang, L.; Mehta, J.; Liu, Y.C. Corneal neuromediator profiles following laser refractive surgery. *Neural Regen. Res.* **2021**, *16*, 2177–2183.

84. Zhang, X.; Mak, S.; Li, L.; Parra, A.; Denlinger, B.; Belmonte, C.; McNaughton, P.A. Direct inhibition of the cold-Activated TRPM8 ion channel by Gα q. *Nat. Cell Biol.* **2012**, *14*, 850–858. [CrossRef]

85. Foulsham, W.; Coco, G.; Amouzegar, A.; Chauhan, S.K.; Dana, R. When Clarity Is Crucial: Regulating Ocular Surface Immunity. *Trends Immunol.* **2018**, *39*, 288–301. [CrossRef]

86. Taylor, A.W. Ocular Immune Privilege and Transplantation. *Front. Immunol.* **2016**, *7*, 37. [CrossRef]

87. Niederkorn, J.Y. The eye sees eye to eye with the immune system: The 2019 Proctor lecture. *Investig. Ophthalmol. Vis. Sci.* **2019**, *60*, 4489–4495. [CrossRef]

88. Medawar, P.B. Immunity to homologous grafted skin; the fate of skin homografts. *Br. J. Exp. Pathol.* **1948**, *29*, 58–69.

89. Forrester, J.V. Privilege revisited: An evaluation of the eye's defence mechanisms. *Eye* **2009**, *23*, 756–766. [CrossRef]

90. Hori, J.; Vega, J.L.; Masli, S. Review of ocular immune privilege in the year 2010: Modifying the immune privilege of the eye. *Ocul. Immunol. Inflamm.* **2010**, *18*, 325–333. [CrossRef]

91. Brissette-Storkus, C.S.; Reynolds, S.M.; Lepisto, A.J.; Hendricks, R.L. Identification of a novel macrophage population in the normal mouse corneal stroma. *Investig. Ophthalmol. Vis. Sci.* **2002**, *43*, 2264–2271.

92. Hamrah, P.; Zhang, Q.; Liu, Y.; Dana, M.R. Novel characterization of MHC class II-negative population of resident corneal Langerhans cell-type dendritic cells. *Investig. Ophthalmol. Vis. Sci.* **2002**, *43*, 639–646.

93. Hamrah, P.; Huq, S.O.; Liu, Y.; Zhang, Q.; Dana, M.R. Corneal immunity is mediated by heterogeneous population of antigen-presenting cells. *J. Leukoc. Biol.* **2003**, *74*, 172–178. [CrossRef]

94. Hamrah, P.; Liu, Y.; Zhang, Q.; Dana, M.R. The corneal stroma is endowed with a significant number of resident dendritic cells. *Investig. Ophthalmol. Vis. Sci.* **2003**, *44*, 581–589. [CrossRef]

95. Jamali, A.; Hu, K.; Sendra, V.G.; Blanco, T.; Lopez, M.J.; Ortiz, G.; Qazi, Y.; Zheng, L.; Turhan, A.; Harris, D.L.; et al. Characterization of Resident Corneal Plasmacytoid Dendritic Cells and Their Pivotal Role in Herpes Simplex Keratitis. *Cell Rep.* **2020**, *32*, 108099. [CrossRef] [PubMed]

96. Forrester, J.V.; Xu, H. Good news-bad news: The Yin and Yang of immune privilege in the eye. *Front. Immunol.* **2012**, *3*, 338. [CrossRef] [PubMed]

97. Weiss, E.-M.; Schmidt, A.; Vobis, D.; Garbi, N.; Lahl, K.; Mayer, C.T.; Sparwasser, T.; Ludwig, A.; Suri-Payer, E.; Oberle, N.; et al. Foxp3-Mediated Suppression of CD95L Expression Confers Resistance to Activation-Induced Cell Death in Regulatory T Cells. *J. Immunol.* **2011**, *187*, 1684–1691. [CrossRef] [PubMed]

98. Francisco, L.M.; Sage, P.T.; Sharpe, A.H. The PD-1 pathway in tolerance and autoimmunity. *Immunol. Rev.* **2010**, *236*, 219–242. [CrossRef] [PubMed]

99. Lee, D.J.; Taylor, A.W. Both MC5r and A2Ar Are Required for Protective Regulatory Immunity in the Spleen of Post–Experimental Autoimmune Uveitis in Mice. *J. Immunol.* **2013**, *191*, 4103–4111. [CrossRef]

100. Delgado, M.; Ganea, D. Vasoactive intestinal peptide: A neuropeptide with pleiotropic immune functions. *Amino Acids* **2013**, *45*, 25–39. [CrossRef]

101. Springer, J.; Geppetti, P.; Fischer, A.; Groneberg, D.A. Calcitonin gene-related peptide as inflammatory mediator. *Pulm. Pharmacol. Ther.* **2003**, *16*, 121–130. [CrossRef]

102. Steinman, R.M.; Cohn, Z.A. Identification of a novel cell type in peripheral lymphoid organs of mice: I. Morphology, quantitation, tissue distribution. *J. Exp. Med.* **1973**, *137*, 1142–1162. [CrossRef]

103. Patente, T.A.; Pinho, M.P.; Oliveira, A.A.; Evangelista, G.C.M.; Bergami-Santos, P.C.; Barbuto, J.A.M. Human dendritic cells: Their heterogeneity and clinical application potential in cancer immunotherapy. *Front. Immunol.* **2019**, *10*, 3176. [CrossRef]

104. Steinman, R.M.; Swanson, J. The endoeytie activity of dendritic cells. *J. Exp. Med.* **1995**, *182*, 283–288. [CrossRef]

105. Trombetta, E.S.; Mellman, I. Cell biology of antigen processing in vitro and in vivo. *Annu. Rev. Immunol.* **2005**, *23*, 975–1028. [CrossRef]

106. Banchereau, J.; Briere, F.; Caux, C.; Davoust, J.; Lebecque, S.; Liu, Y.J.; Pulendran, B.; Palucka, K. Immunobiology of dendritic cells. *Annu. Rev. Immunol.* **2000**, *18*, 767–811. [CrossRef]

107. Reis, E.; Sousa, C. Dendritic cells in a mature age. *Nat. Rev. Immunol.* **2006**, *6*, 476–483. [CrossRef] [PubMed]

108. Steinman, R.M. Decisions about dendritic cells: Past, present, and future. *Annu. Rev. Immunol.* **2012**, *30*, 1–22. [CrossRef] [PubMed]

109. Hawiger, D.; Inaba, K.; Dorsett, Y.; Guo, M.; Mahnke, K.; Rivera, M.; Ravetch, J.V.; Steinman, R.M.; Nussenzweig, M.C. Dendritic cells induce peripheral T cell unresponsiveness under steady state conditions in vivo. *J. Exp. Med.* **2001**, *194*, 769–779. [CrossRef] [PubMed]

110. Worbs, T.; Hammerschmidt, S.I.; Förster, R. Dendritic cell migration in health and disease. *Nat. Rev. Immunol.* **2017**, *17*, 30–48. [CrossRef]

111. O'Keeffe, M.; Mok, W.H.; Radford, K.J. Human dendritic cell subsets and function in health and disease. *Cell. Mol. Life Sci.* **2015**, *72*, 4309–4325. [CrossRef]

112. Constant, S.; Pfeiffer, C.; Woodard, A.; Pasqualini, T.; Bottomly, K. Extent of T cell receptor ligation can determine the functional differentiation of naive cd4+ T cells. *J. Exp. Med.* **1995**, *182*, 1591–1596. [CrossRef]

113. Amsen, D.; Blander, J.M.; Lee, G.R.; Tanigaki, K.; Honjo, T.; Flavell, R.A. Instruction of distinct CD4 T helper cell fates by different notch ligands on antigen-presenting cells. *Cell* **2004**, *117*, 515–526. [CrossRef]

114. Kadowaki, N. Dendritic cells—A conductor of T cell differentiation. *Allergol. Int.* **2007**, *56*, 193–199. [CrossRef]

115. Soumelis, V.; Reche, P.A.; Kanzler, H.; Yuan, W.; Edward, G.; Homey, B.; Gilliet, M.; Ho, S.; Antonenko, S.; Lauerma, A.; et al. Human epithelial cells trigger dendritic cell-mediated allergic inflammation by producing TSLP. *Nat. Immunol.* **2002**, *3*, 673–680. [CrossRef]

116. Jenkins, S.J.; Perona-Wright, G.; Worsley, A.G.F.; Ishii, N.; MacDonald, A.S. Dendritic Cell Expression of OX40 Ligand Acts as a Costimulatory, Not Polarizing, Signal for Optimal Th2 Priming and Memory Induction In Vivo. *J. Immunol.* **2007**, *179*, 3515–3523. [CrossRef]

117. Bailey, S.L.; Schreiner, B.; McMahon, E.J.; Miller, S.D. CNS myeloid DCs presenting endogenous myelin peptides "preferentially" polarize CD4+ TH-17 cells in relapsing EAE. *Nat. Immunol.* **2007**, *8*, 172–180. [CrossRef]

118. Huang, G.; Wang, Y.; Chi, H. Regulation of TH17 cell differentiation by innate immune signals. *Cell. Mol. Immunol.* **2012**, *9*, 287–295. [CrossRef]

119. Rescigno, M. Dendritic cell-epithelial cell crosstalk in the gut. *Immunol. Rev.* **2014**, *260*, 118–128. [CrossRef]

120. Steinman, R.M.; Hawiger, D.; Liu, K.; Bonifaz, L.; Bonnyay, D.; Mahnke, K.; Iyoda, T.; Ravetch, J.; Dhodapkar, M.; Inaba, K.; et al. Dendritic cell function in Vivo during the steady state: A role in peripheral tolerance. *Ann. N. Y. Acad. Sci.* **2003**, *987*, 15–25. [CrossRef]

121. Liu, J.; Cao, X. Regulatory dendritic cells in autoimmunity: A comprehensive review. *J. Autoimmun.* **2015**, *63*, 1–12. [CrossRef]

122. Raker, V.K.; Domogalla, M.P.; Steinbrink, K. Tolerogenic dendritic cells for regulatory T cell induction in man. *Front. Immunol.* **2015**, *6*, 569. [CrossRef]

123. Morelli, A.E.; Thomson, A.W. Tolerogenic dendritic cells and the quest for transplant tolerance. *Nat. Rev. Immunol.* **2007**, *7*, 610–621. [CrossRef]

124. Manicassamy, S.; Pulendran, B. Dendritic cell control of tolerogenic responses. *Immunol. Rev.* **2011**, *241*, 206–227. [CrossRef]

125. Yates, S.F.; Paterson, A.M.; Nolan, K.F.; Cobbold, S.P.; Saunders, N.J.; Waldmann, H.; Fairchild, P.J. Induction of Regulatory T Cells and Dominant Tolerance by Dendritic Cells Incapable of Full Activation. *J. Immunol.* **2007**, *179*, 967–976. [CrossRef]

126. Geissmann, F.; Manz, M.G.; Jung, S.; Sieweke, M.H.; Merad, M.; Ley, K. Development of monocytes, macrophages, and dendritic cells. *Science* **2010**, *327*, 656–661. [CrossRef]

127. Wang, J.; Dai, X.; Hsu, C.; Ming, C.; He, Y.; Zhang, J.; Wei, L.; Zhou, P.; Wang, C.Y.; Yang, J.; et al. Discrimination of the heterogeneity of bone marrow-derived dendritic cells. *Mol. Med. Rep.* **2017**, *16*, 6787–6793. [CrossRef] [PubMed]

128. Halim, T.Y.F.; Hwang, Y.Y.; Scanlon, S.T.; Zaghouani, H.; Garbi, N.; Fallon, P.G.; Mckenzie, A.N.J. Group 2 innate lymphoid cells license dendritic cells to potentiate memory TH2 cell responses. *Nat. Immunol.* **2016**, *17*, 57–64. [CrossRef] [PubMed]

129. Varol, C.; Landsman, L.; Fogg, D.K.; Greenshtein, L.; Gildor, B.; Margalit, R.; Kalchenko, V.; Geissmann, F.; Jung, S. Monocytes give rise to mucosal, but not splenic, conventional dendritic cells. *J. Exp. Med.* **2007**, *204*, 171–180. [CrossRef] [PubMed]

130. Tamoutounour, S.; Guilliams, M.; MontananaSanchis, F.; Liu, H.; Terhorst, D.; Malosse, C.; Pollet, E.; Ardouin, L.; Luche, H.; Sanchez, C.; et al. Origins and functional specialization of macrophages and of conventional and monocyte-derived dendritic cells in mouse skin. *Immunity* **2013**, *39*, 925–938. [CrossRef]

131. Plantinga, M.; Guilliams, M.; Vanheerswynghels, M.; Deswarte, K.; Branco-Madeira, F.; Toussaint, W.; Vanhoutte, L.; Neyt, K.; Killeen, N.; Malissen, B.; et al. Conventional and Monocyte-Derived CD11b+ Dendritic Cells Initiate and Maintain T Helper 2 Cell-Mediated Immunity to House Dust Mite Allergen. *Immunity* **2013**, *38*, 322–335. [CrossRef]

132. Inaba, K.; Inaba, M.; Romani, N.; Aya, H.; Deguchi, M.; Ikehara, S.; Muramatsu, S.; Steinman, R.M. Generation of large numbers of dendritic cells from mouse bone marrow cultures supplemented with granulocyte/macrophage colony-stimulating factor. *J. Exp. Med.* **1992**, *176*, 1693–1702. [CrossRef]

133. Sallusto, F.; Lanzavecchi, A. Efficient presentation of soluble antigen by cultured human dendritic cells is maintained by granulocyte/macrophage colony-stimulating factor plus iuterleukin 4 and downregulated by tumor necrosis factor α. *J. Exp. Med.* **1994**, *179*, 1109–1118. [CrossRef]

134. Bachem, A.; Güttler, S.; Hartung, E.; Ebstein, F.; Schaefer, M.; Tannert, A.; Salama, A.; Movassaghi, K.; Opitz, C.; Mages, H.W.; et al. Superior antigen cross-presentation and XCR1 expression define human CD11c+CD141+ cells as homologues of mouse CD8+ dendritic cells. *J. Exp. Med.* **2010**, *207*, 1273–1281. [CrossRef]

135. Reynolds, G.; Haniffa, M. Human and mouse mononuclear phagocyte networks: A tale of two species? *Front. Immunol.* **2015**, *6*, 25. [CrossRef]

136. Cabeza-Cabrerizo, M.; Cardoso, A.; Minutti, C.M.; Pereira da Costa, M.; Reis e Sousa, C. Dendritic cells revisited. *Annu. Rev. Immunol.* **2021**, *39*, 131–166. [CrossRef]

137. Hildner, K.; Edelson, B.T.; Purtha, W.E.; Diamond, M.; Matsushita, H.; Kohyama, M.; Calderon, B.; Schraml, B.U.; Unanue, E.R.; Diamond, M.S.; et al. Batf3 deficiency reveals a critical role for CD8α+ dendritic cells in cytotoxic T cell immunity. *Science* **2008**, *322*, 1097–1100. [CrossRef]

138. Schiavoni, G.; Mattei, F.; Sestili, P.; Borghi, P.; Venditti, M.; Morse, H.C.; Belardelli, F.; Gabriele, L. ICSBP Is Essential for the Development of Mouse Type I Interferon-producing Cells and for the Generation and Activation of CD8α+ Dendritic Cells. *J. Exp. Med.* **2002**, *196*, 1415–1425. [CrossRef]

139. Hacker, C.; Kirsch, R.D.; Ju, X.S.; Hieronymus, T.; Gust, T.C.; Kuhl, C.; Jorgas, T.; Kurz, S.M.; Rose-John, S.; Yokota, Y.; et al. Transcriptional profiling identifies Id2 function in dendritic cell development. *Nat. Immunol.* **2003**, *4*, 380–386. [CrossRef]

140. Kashiwada, M.; Pham, N.L.L.; Pewe, L.L.; Harty, J.T.; Rothman, P.B. NFIL3/E4BP4 is a key transcription factor for CD8α+ dendritic cell development. *Blood* **2011**, *117*, 6193–6197. [CrossRef]

141. Segura, E.; Valladeau-Guilemond, J.; Donnadieu, M.H.; Sastre-Garau, X.; Soumelis, V.; Amigorena, S. Characterization of resident and migratory dendritic cells in human lymph nodes. *J. Exp. Med.* **2012**, *209*, 653–660. [CrossRef]

142. Leal Rojas, I.M.; Mok, W.H.; Pearson, F.E.; Minoda, Y.; Kenna, T.J.; Barnard, R.T.; Radford, K.J. Human blood cD1c+ dendritic cells promote Th1 and Th17 effector function in memory cD4+ T cells. *Front. Immunol.* **2017**, *8*, 971. [CrossRef]

143. Bamboat, Z.M.; Stableford, J.A.; Plitas, G.; Burt, B.M.; Nguyen, H.M.; Welles, A.P.; Gonen, M.; Young, J.W.; DeMatteo, R.P. Human Liver Dendritic Cells Promote T Cell Hyporesponsiveness. *J. Immunol.* **2009**, *182*, 1901–1911. [CrossRef]

144. Watchmaker, P.B.; Lahl, K.; Lee, M.; Baumjohann, D.; Morton, J.; Kim, S.J.; Zeng, R.; Dent, A.; Ansel, K.M.; Diamond, B.; et al. Comparative transcriptional and functional profiling defines conserved programs of intestinal DC differentiation in humans and mice. *Nat. Immunol.* **2014**, *15*, 98–108. [CrossRef]

145. Haniffa, M.; Collin, M.; Ginhoux, F. Ontogeny and functional specialization of dendritic cells in human and mouse. In *Advances in Immunology*; Academic Press Inc.: Cambridge, MA, USA, 2013; Volume 120, pp. 1–49.

146. Schlitzer, A.; McGovern, N.; Teo, P.; Zelante, T.; Atarashi, K.; Low, D.; Ho, A.W.S.; See, P.; Shin, A.; Wasan, P.S.; et al. IRF4 Transcription Factor-Dependent CD11b+ Dendritic Cells in Human and Mouse Control Mucosal IL-17 Cytokine Responses. *Immunity* **2013**, *38*, 970–983. [CrossRef]

147. Murphy, T.L.; Grajales-Reyes, G.E.; Wu, X.; Tussiwand, R.; Briseño, C.G.; Iwata, A.; Kretzer, N.M.; Durai, V.; Murphy, K.M. Transcriptional Control of Dendritic Cell Development. *Annu. Rev. Immunol.* **2016**, *34*, 93–119. [CrossRef]

148. Wu, L.; D'Amico, A.; Winkel, K.D.; Suter, M.; Lo, D.; Shortman, K. RelB is essential for the development of myeloid-related CD8α- dendritic cells but not of lymphoid-related CD8α+ dendritic cells. *Immunity* **1998**, *9*, 839–847. [CrossRef]

149. Zhu, X.J.; Yang, Z.F.; Chen, Y.; Wang, J.; Rosmarin, A.G. PU.1 Is Essential for CD11c Expression in CD8+/CD8- Lymphoid and Monocyte-Derived Dendritic Cells during GM-CSF or FLT3L-Induced Differentiation. *PLoS ONE* **2012**, *7*, e52141. [CrossRef] [PubMed]

150. Hambleton, S.; Salem, S.; Bustamante, J.; Bigley, V.; Boisson-Dupuis, S.; Azevedo, J.; Fortin, A.; Haniffa, M.; Ceron-Gutierrez, L.; Bacon, C.M.; et al. *IRF8* Mutations and Human Dendritic-Cell Immunodeficiency. *N. Engl. J. Med.* **2011**, *365*, 127–138. [CrossRef] [PubMed]

151. Reizis, B.; Bunin, A.; Ghosh, H.S.; Lewis, K.L.; Sisirak, V. Plasmacytoid dendritic cells: Recent progress and open questions. *Annu. Rev. Immunol.* **2011**, *29*, 163–183. [CrossRef]

152. Jamali, A.; Kenyon, B.; Ortiz, G.; Abou-Slaybi, A.; Sendra, V.G.; Harris, D.L.; Hamrah, P. Plasmacytoid dendritic cells in the eye. *Prog. Retin. Eye Res.* **2021**, *80*, 100877. [CrossRef]

153. Sawai, C.M.; Sisirak, V.; Ghosh, H.S.; Hou, E.Z.; Ceribelli, M.; Staudt, L.M.; Reizis, B. Transcription factor Runx2 controls the development and migration of plasmacytoid dendritic cells. *J. Exp. Med.* **2013**, *210*, 2151–2159. [CrossRef]

154. Chistiakov, D.A.; Orekhov, A.N.; Sobenin, I.A.; Bobryshev, Y.V. Plasmacytoid dendritic cells: Development, functions, and role in atherosclerotic inflammation. *Front. Physiol.* **2014**, *5*, 279. [CrossRef]

155. Bendriss-Vermare, N.; Barthélémy, C.; Durand, I.; Bruand, C.; Dezutter-Dambuyant, C.; Moulian, N.; Berrih-Aknin, S.; Caux, C.; Trinchieri, G.; Brière, F. Human thymus contains IFN-α-producing CD11c-, myeloid CD11c+, and mature interdigitating dendritic cells. *J. Clin. Investig.* **2001**, *107*, 835–844. [CrossRef]

156. Nakano, H.; Yanagita, M.; Gunn, M.D. CD11c+B220+Gr-1+ cells in mouse lymph nodes and spleen display characteristics of plasmacytoid dendritic cells. *J. Exp. Med.* **2001**, *194*, 1171–1178. [CrossRef]

157. Contractor, N.; Louten, J.; Kim, L.; Biron, C.A.; Kelsall, B.L. Cutting Edge: Peyer's Patch Plasmacytoid Dendritic Cells (pDCs) Produce Low Levels of Type I Interferons: Possible Role for IL-10, TGFβ, and Prostaglandin E 2 in Conditioning a Unique Mucosal pDC Phenotype. *J. Immunol.* **2007**, *179*, 2690–2694. [CrossRef]

158. Boor, P.P.C.; Bosma, B.M.; Tran, K.T.C.; Van Derlaan, L.J.W.; Hagenaars, H.; IJzermans, J.N.M.; Metselaar, H.J.; Kwekkeboom, J. Characterization of antigen-presenting cell subsets in human liver-draining lymph nodes. *Front. Immunol.* **2019**, *10*, 441. [CrossRef]

159. Nestle, F.O.; Conrad, C.; Tun-Kyi, A.; Homey, B.; Gombert, M.; Boyman, O.; Burg, G.; Liu, Y.J.; Gilliet, M. Plasmacytoid predendritic cells initiate psoriasis through interferon-α production. *J. Exp. Med.* **2005**, *202*, 135–143. [CrossRef]

160. Sozzani, S.; Vermi, W.; Del Prete, A.; Facchetti, F. Trafficking properties of plasmacytoid dendritic cells in health and disease. *Trends Immunol.* **2010**, *31*, 270–277. [CrossRef]

161. Donnenberg, V.S.; Donnenberg, A.D. Identification, rare-event detection and analysis of dendritic cell subsets in broncho-alveolar lavage fluid and peripheral blood by flow cytometry. *Front. Biosci.* **2003**, *8*, s1175–s1180. [CrossRef]

162. Lund, J.M.; Linehan, M.M.; Iijima, N.; Iwasaki, A. Cutting Edge: Plasmacytoid Dendritic Cells Provide Innate Immune Protection against Mucosal Viral Infection In Situ. *J. Immunol.* **2006**, *177*, 7510–7514. [CrossRef]

163. Facchetti, F.; De Wolf-Peeters, C.; Mason, D.Y.; Pulford, K.; Van den Oord, J.J.; Desmet, V.J. Plasmacytoid T cells. Immunohisto-chemical evidence for their monocyte/macrophage origin. *Am. J. Pathol.* **1988**, *133*, 15–21.

164. Matsui, T.; Connolly, J.E.; Michnevitz, M.; Chaussabel, D.; Yu, C.-I.; Glaser, C.; Tindle, S.; Pypaert, M.; Freitas, H.; Piqueras, B.; et al. CD2 Distinguishes Two Subsets of Human Plasmacytoid Dendritic Cells with Distinct Phenotype and Functions. *J. Immunol.* **2009**, *182*, 6815–6823. [CrossRef]

165. Klechevsky, E.; Morita, R.; Liu, M.; Cao, Y.; Coquery, S.; Thompson-Snipes, L.A.; Briere, F.; Chaussabel, D.; Zurawski, G.; Palucka, A.K.; et al. Functional Specializations of Human Epidermal Langerhans Cells and CD14+ Dermal Dendritic Cells. *Immunity* **2008**, *29*, 497–510. [CrossRef]

166. Birbeck, M.S.; Breathnach, A.S.; Everall, J.D. An Electron Microscope Study of Basal Melanocytes and High-Level Clear Cells (Langerhans Cells) in Vitiligo**From the Chester Beatty Research Institute, Royal Cancer Hospital, London, S.W. 3, and the Departments of Anatomy, and Dermatology, St. Mary's Hospital Medical School (University of London) London, W. 2, England. *J. Investig. Dermatol.* **1961**, *37*, 51–64. [CrossRef]

167. Haniffa, M.; Shin, A.; Bigley, V.; McGovern, N.; Teo, P.; See, P.; Wasan, P.S.; Wang, X.N.; Malinarich, F.; Malleret, B.; et al. Human Tissues Contain CD141 hi Cross-Presenting Dendritic Cells with Functional Homology to Mouse CD103 + Nonlymphoid Dendritic Cells. *Immunity* **2012**, *37*, 60–73. [CrossRef]

168. Fainaru, O.; Woolf, E.; Lotem, J.; Yarmus, M.; Brenner, O.; Goldenberg, D.; Negreanu, V.; Bernstein, Y.; Levanon, D.; Jung, S.; et al. Runx3 regulates mouse TGF-β-mediated dendritic cell function and its absence results in airway inflammation. *EMBO J.* **2004**, *23*, 969–979. [CrossRef] [PubMed]

169. Chopin, M.; Seillet, C.; Chevrier, S.; Wu, L.; Wang, H.; Morse, H.C.; Belz, G.T.; Nutt, S.L. Langerhans cells are generated by two distinct PU.1-dependent transcriptional networks. *J. Exp. Med.* **2013**, *210*, 2967–2980. [CrossRef]

170. Segura, E.; Touzot, M.; Bohineust, A.; Cappuccio, A.; Chiocchia, G.; Hosmalin, A.; Dalod, M.; Soumelis, V.; Amigorena, S. Human Inflammatory Dendritic Cells Induce Th17 Cell Differentiation. *Immunity* **2013**, *38*, 336–348. [CrossRef]

171. Bakri, Y.; Sarrazin, S.; Mayer, U.P.; Tillmanns, S.; Nerlov, C.; Boned, A.; Sieweke, M.H. Balance of MafB and PU.1 specifies alternative macrophage or dendritic cell fate. *Blood* **2005**, *105*, 2707–2716. [CrossRef]

172. Lehtonen, A.; Veckman, V.; Nikula, T.; Lahesmaa, R.; Kinnunen, L.; Matikainen, S.; Julkunen, I. Differential Expression of IFN Regulatory Factor 4 Gene in Human Monocyte-Derived Dendritic Cells and Macrophages. *J. Immunol.* **2005**, *175*, 6570–6579. [CrossRef]

173. Hamrah, P.; Liu, Y.; Zhang, Q.; Dana, M.R. Alterations in corneal stromal dendritic cell phenotype and distribution in inflammation. *Arch. Ophthalmol.* **2003**, *121*, 1132–1140. [CrossRef]

174. Yamagami, S.; Yokoo, S.; Usui, T.; Yamagami, H.; Amano, S.; Ebihara, N. Distinct populations of dendritic cells in the normal human donor corneal epithelium. *Investig. Ophthalmol. Vis. Sci.* **2005**, *46*, 4489–4494. [CrossRef]

175. Hattori, T.; Takahashi, H.; Dana, R. Novel insights into the immunoregulatory function and localization of dendritic cells. *Cornea* **2016**, *35*, S49–S54. [CrossRef]

176. Li, Z.; Burns, A.R.; Rumbaut, R.E.; Smith, C.W. γδ T cells are necessary for platelet and neutrophil accumulation in limbal vessels and efficient epithelial repair after corneal abrasion. *Am. J. Pathol.* **2007**, *171*, 838–845. [CrossRef] [PubMed]

177. Liu, Q.; Smith, C.W.; Zhang, W.; Burns, A.R.; Li, Z. NK cells modulate the inflammatory response to corneal epithelial abrasion and thereby support wound healing. *Am. J. Pathol.* **2012**, *181*, 452–462. [CrossRef] [PubMed]

178. Mayer, W.J.; Irschick, U.M.; Moser, P.; Wurm, M.; Huemer, H.P.; Romani, N.; Irschick, E.U. Characterization of antigen-presenting cells in fresh and cultured human corneas using novel dendritic cell markers. *Investig. Ophthalmol. Vis. Sci.* **2007**, *48*, 4459–4467. [CrossRef]

179. Del Palomar, A.P.; Montolío, A.; Cegoñino, J.; Dhanda, S.K.; Lio, C.T.; Bose, T. The Innate Immune Cell Profile of the Cornea Predicts the Onset of Ocular Surface Inflammatory Disorders. *J. Clin. Med.* **2019**, *8*, 2110. [CrossRef]

180. Villani, E.; Baudouin, C.; Efron, N.; Hamrah, P.; Kojima, T.; Patel, S.V.; Pflugfelder, S.C.; Zhivov, A.; Dogru, M. In vivo confocal microscopy of the ocular surface: From bench to bedside. *Curr. Eye Res.* **2014**, *39*, 213–231. [CrossRef]

181. Bitirgen, G.; Korkmaz, C.; Zamani, A.; Ozkagnici, A.; Zengin, N.; Ponirakis, G.; Malik, R.A. Corneal confocal microscopy identifies corneal nerve fibre loss and increased dendritic cells in patients with long COVID. *Br. J. Ophthalmol.* **2021**. [CrossRef]

182. Cruzat, A.; Witkin, D.; Baniasadi, N.; Zheng, L.; Ciolino, J.B.; Jurkunas, U.V.; Chodosh, J.; Pavan-Langston, D.; Dana, R.; Hamrah, P. Inflammation and the nervous system: The connection in the cornea in patients with infectious keratitis. *Investig. Ophthalmol. Vis. Sci.* **2011**, *52*, 5136–5143. [CrossRef]

183. Cruzat, A.; Schrems, W.A.; Schrems-Hoesl, L.M.; Cavalcanti, B.M.; Baniasadi, N.; Witkin, D.; Pavan-Langston, D.; Dana, R.; Hamrah, P.; Hamrah, P. Contralateral clinically unaffected eyes of patients with unilateral infectious keratitis demonstrate a sympathetic immune response. *Investig. Ophthalmol. Vis. Sci.* **2015**, *56*, 6612–6620. [CrossRef]

184. Postole, A.S.; Knoll, A.B.; Auffarth, G.U.; Mackensen, F. In vivo confocal microscopy of inflammatory cells in the corneal subbasal nerve plexus in patients with different subtypes of anterior uveitis. *Br. J. Ophthalmol.* **2016**, *100*, 1551–1556. [CrossRef]

185. Lin, H.; Li, W.; Dong, N.; Chen, W.; Liu, J.; Chen, L.; Yuan, H.; Geng, Z.; Liu, Z. Changes in corneal epithelial layer inflammatory cells in aqueous tear-deficient dry eye. *Investig. Ophthalmol. Vis. Sci.* **2010**, *51*, 122–128. [CrossRef]

186. Tuisku, I.S.; Konttinen, Y.T.; Konttinen, L.M.; Tervo, T.M. Alterations in corneal sensitivity and nerve morphology in patients with primary Sjögren's syndrome. *Exp. Eye Res.* **2008**, *86*, 879–885. [CrossRef]

187. Zhivov, A.; Stave, J.; Vollmar, B.; Guthoff, R. In vivo confocal microscopic evaluation of langerhans cell density and distribution in the corneal epithelium of healthy volunteers and contact lens wearers. *Cornea* **2007**, *26*, 47–54. [CrossRef]

188. Yamaguchi, T.; Calvacanti, B.M.; Cruzat, A.; Qazi, Y.; Ishikawa, S.; Osuka, A.; Lederer, J.; Hamrah, P. Correlation Between Human Tear Cytokine Levels and Cellular Corneal Changes in Patients with Bacterial Keratitis by In Vivo Confocal Microscopy. *Investig. Opthalmol. Vis. Sci.* **2014**, *55*, 7457. [CrossRef]

189. Villani, E.; Galimberti, D.; Del Papa, N.; Nucci, P.; Ratiglia, R. Inflammation in dry eye associated with rheumatoid arthritis: Cytokine and in vivo confocal microscopy study. *Innate Immun.* **2013**, *19*, 420–427. [CrossRef]

190. Hu, K.; Harris, D.; Yamaguchi, T.; Ghiasi, H.; Von Andrian, U.; Hambrah, P. The role of corneal plasmacytoid dendritic cells in acute herpes simplex virus infection. *Investig. Ophthalmol. Vis. Sci.* **2013**, *54*, 2158.

191. Khandelwal, P.; Blanco-Mezquita, T.; Emami, P.; Lee, H.S.; Reyes, N.J.; Mathew, R.; Huang, R.; Saban, D.R. Ocular Mucosal CD11b+ and CD103+ Mouse Dendritic Cells under Normal Conditions and in Allergic Immune Responses. *PLoS ONE* **2013**, *8*, e64193. [CrossRef]

192. Gao, N.; Yan, C.; Lee, P.; Sun, H.; Yu, F.S. Dendritic cell dysfunction and diabetic sensory neuropathy in the cornea. *J. Clin. Investig.* **2016**, *126*, 1998–2011. [CrossRef]

193. Maruoka, S.; Inaba, M.; Ogata, N. Activation of Dendritic Cells in Dry Eye Mouse Model. *Investig. Ophthalmol. Vis. Sci.* **2018**, *59*, 3269–3277. [CrossRef]

194. Sendra, V.; Jamali, A.; Lopez, M.J.; Hamrah, P. Plasmacytoid Dendritic Cells Mediate T cell Responses by Direct Interaction in Lymph Nodes during Herpes Simplex Virus-1 Keratitis. *Investig. Ophthalmol. Vis. Sci.* **2016**, *57*, 331.

195. Miranda-Saksena, M.; Armati, P.; Boadle, R.A.; Holland, D.J.; Cunningham, A.L. Anterograde Transport of Herpes Simplex Virus Type 1 in Cultured, Dissociated Human and Rat Dorsal Root Ganglion Neurons. *J. Virol.* **2000**, *74*, 1827–1839. [CrossRef] [PubMed]

196. Sendra, V.G.; Jamali, A.; Lopez, M.J.; Harris, D.L.; Hamrah, P. Plasmacytoid dendritic cells modulate corneal inflammation through transforming growth factor (TGF)-beta1. *Investig. Ophthalmol. Vis. Sci.* **2017**, *58*, 3618.

197. Hu, K.; Harris, D.L.; Yamaguchi, T.; Von Andrian, U.H.; Hamrah, P. A dual role for corneal dendritic cells in herpes simplex keratitis: Local suppression of corneal damage and promotion of systemic viral dissemination. *PLoS ONE* **2015**, *10*, e0137123. [CrossRef] [PubMed]

198. Sendra, V.G.; Jamali, A.; Harris, D.L.; Hamrah, P. Role of plasmacytoid dendritic cell in the immune regulation in sutured inflamed cornea. *Investig. Ophthalmol. Vis. Sci.* **2014**, *55*, 1694.

199. Leppin, K.; Behrendt, A.K.; Reichard, M.; Stachs, O.; Guthoff, R.F.; Baltrusch, S.; Eule, J.C.; Vollmar, B. Diabetes mellitus leads to accumulation of dendritic cells and nerve fiber damage of the subbasal nerve plexus in the cornea. *Investig. Ophthalmol. Vis. Sci.* **2014**, *55*, 3603–3615. [CrossRef]

200. Seyed-Razavi, Y.; Chinnery, H.R.; McMenamin, P.G. A novel association between resident tissue macrophages and nerves in the peripheral stroma of the murine cornea. *Investig. Ophthalmol. Vis. Sci.* **2014**, *55*, 1313–1320. [CrossRef]

201. Hamrah, P.; Seyed-Razavi, Y.; Yamaguchi, T. Translational Immunoimaging and Neuroimaging Demonstrate Corneal Neuroimmune Crosstalk. *Cornea* **2016**, *35*, S20–S24. [CrossRef]

202. Zurborg, S.; Piszczek, A.; Martínez, C.; Hublitz, P.; Al Banchaabouchi, M.; Moreira, P.; Perlas, E.; Heppenstall, P.A. Generation and characterization of an Advillin-Cre driver mouse line. *Mol. Pain* **2011**, *7*, 1744–8069. [CrossRef]

203. Madisen, L.; Zwingman, T.A.; Sunkin, S.M.; Oh, S.W.; Zariwala, H.A.; Gu, H.; Ng, L.L.; Palmiter, R.D.; Hawrylycz, M.J.; Jones, A.R.; et al. A robust and high-throughput Cre reporting and characterization system for the whole mouse brain. *Nat. Neurosci.* **2010**, *13*, 133–140. [CrossRef]

204. Jung, S.; Unutmaz, D.; Wong, P.; Sano, G.-I.; De los Santos, K.; Sparwasser, T.; Wu, S.; Vuthoori, S.; Ko, K.; Zavala, F.; et al. In vivo depletion of CD11c+ dendritic cells abrogates priming of CD8+ T cells by exogenous cell-associated antigens. *Immunity* **2002**, *17*, 211–220. [CrossRef]

205. Rincon Frutos, L.; Luna, C.; Antonio Gómez Sánchez, J.; Carmen Acosta, M.; Belmonte, C.; Seyed-Razavi, Y.; Hamrah, P.; Gallar, J. Dendritic cell depletion modifies corneal nerve activity and mice nociceptive behaviour. *Acta Ophthalmol.* **2022**, *100*. [CrossRef]

AGRADECIMIENTOS

A lo largo de mis años de Doctorado han sido tantas, TANTÍSIMAS las personas que han contribuido a mi crecimiento personal que sería injusto enumerarlas aquí a riesgo de olvidar alguna. Haré pues unos agradecimientos generales, que, aunque más fríos, los considero más justos.

- A mis directoras de Tesis por haberme dado la oportunidad de llevar a cabo este trabajo. Por haber depositado su confianza en la "niña" que llegó al laboratorio y haberla convertido en una científica con mayúsculas.

- A mis compañeros de laboratorio, compañeros *en la rutina y en los bostezos* como dice Ismael Serrano en una de sus canciones. Especialmente a esos me han ayudado en lo profesional y en lo personal y que, a día de hoy, tengo la suerte de llamar amigos.

- A mis amigos, a esos que siempre estuvieron y a todos los que han aparecido por el camino. Qué verdad aquello de que sois la familia que se elige. Gracias por confiar en mi más que yo misma.

- For all those people and friends that I have met during my stays and travels abroad. Thank you for making me feel at home.

- A mi "Virus" particular, por ser mi mayor apoyo y mi mundo desde que *dejé mi habitación en tus pupilas.*

- A mi familia, porque me hacéis conocer el significado del amor incondicional cada día de mi vida. En especial a mi madre, por ser las huellas sobre las que camino dentro y fuera de la ciencia.

- A todas aquellas personas que se han ido, en lo real y en lo figurado.

"Tus ojos son la luz de tu cuerpo; de manera que,

si tus ojos están sanos, todo tu cuerpo tendrá

luz. Pero si tus ojos están enfermos, todo tu

cuerpo tendrá oscuridad".